

**EFFECT OF WORKING TEMPERATURE ON  
RHEOLOGICAL PROPERTIES OF CRUMB RUBBER  
MODIFIED BINDERS WITH WARM MIX ADDITIVES**

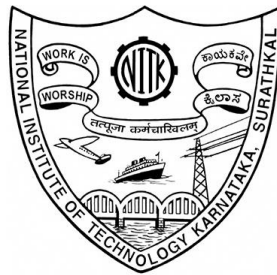
**Thesis**

Submitted in partial fulfilment of the requirements for the degree of

**DOCTOR OF PHILOSOPHY**

By

**HEMANTH KUMAR V**



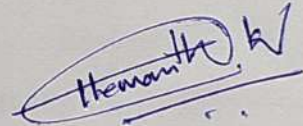
**DEPARTMENT OF CIVIL ENGINEERING  
NATIONAL INSTITUTE OF TECHNOLOGY KARNATAKA  
SURATHKAL, MANGALORE-575 025**

**MAY 2022**

## DECLARATION

*By the Ph.D. Research Scholar*

I hereby *declare* that the Research Thesis entitled “**EFFECT OF WORKING TEMPERATURE ON RHEOLOGICAL PROPERTIES OF CRUMB RUBBER MODIFIED BINDERS WITH WARM MIX ADDITIVES**” which is being submitted to the **National Institute of Technology Karnataka, Surathkal** in partial fulfilment of the requirements for the award of the Degree of **Doctor of Philosophy** in the **Department of Civil Engineering** is a *bonafide report of the research work carried out by me*. The material contained in this Research Thesis has not been submitted to any University or Institution for the award of any degree.



HEMANTH KUMAR V

165103CV16F08

Department of Civil Engineering

NITK, Surathkal – 575025

Place: NITK, Surathkal

Date: 10/05/2022

## CERTIFICATE

This is to *certify* that the Research Thesis entitled “**EFFECT OF WORKING TEMPERATURE ON RHEOLOGICAL PROPERTIES OF CRUMB RUBBER MODIFIED BINDERS WITH WARM MIX ADDITIVES**” submitted by Mr. **HEMANTH KUMAR V (Register number 165103CV16F08)**, as the record of the research work carried out by him, *is accepted as the Research Thesis submission* in partial fulfilment of the requirements for the award of degree of **Doctor of Philosophy**.



*Suresha S.N.* 17/05/2022

**Dr. SURESHA S. N.**

Research Guide

(Signature with Date and Seal)

*Jayalekshmi* 17/05/2022

**Dr. B. R. JAYALEKSHMI**

Chairperson-DRPC

(Signature with Date and Seal)

**Chairman (DRPC)**

**Department of Civil Engineering**

**National Institute of Technology Karnataka, Surathkal  
Mangalore - 575 025, Karnataka, INDIA**

## *Dedication*

I dedicate this thesis to my teachers, beloved parents  
and my country for their eternal love

&

*Along with those close to my heart*

**Visvesvaraya Iron and Steel Limited (VISL),**

*sisters, brother and friends*

## ACKNOWLEDGEMENTS

With deep sense of gratitude, I express my heartfelt thanks to my research supervisor Dr. Suresha S N, Associate Professor, Department of Civil Engineering, NITK for his invaluable guidance, encouragement, and motivation throughout my research work. I am indebted to him for his wholehearted interest and keenness in every phase of research work. His moral support, guidance, interactions, discussions and precious suggestions have greatly helped me to complete this research work. It has been my greatest opportunity and pleasure to work under him. His crucial comments have guided me to publish my research work in acclaimed International Journals. I would also like to convey my sincere thanks to my Research Progress Assessment Committee (RPAC) members, Dr. Gangadhar Mahesh, Department of Civil Engineering and Dr. Vadivuchezhian Kaliveeran, Department of Water Resources and Ocean Engineering, and the former RPAC member Dr. Gowri Asaithambi, Department of Civil Engineering, IIT Tirupati for providing valuable suggestions, comments and encouragement at various stages of this research work.

I would like to express my special appreciation and thanks to Indian Referee members Dr. Rajan Choudhary, Professor, IIT Guwahati and Dr. Devesh Tiwari, Chief scientist, CSIR-CRRI, New Delhi for evaluating my Ph.D. Thesis and providing a detailed constructive comments and suggestions on the topic. I would also like to convey my heartfelt thanks to DTAC members Dr. B R Jayalekshmi (Professor and Head), Dr. A. U. Ravi Shankar (Department of Civil Engineering) and Dr. Ramesh M.R (Department of Mechanical Engineering) for providing valuable comments and suggestions.

I would like to thank Prof. B R Jayalekshmi, Head of the Department of Civil Engineering and the former Head Prof. D. Venkat Reddy, Prof. Varghese George, and Prof. K. Swaminathan for all the support throughout my stay. I sincerely express thanks to the Director of the Institute (NITK), for the financial support provided and for extending the facilities for the research.

I also like to acknowledge the financial support extended by the Department of Science and Technology, Government of India under the scheme 'Fund for Improvement of Science & Technology Infrastructure' (No.SR/FST/ETI-356/2013) for the creation of required research facilities at the Advanced Asphalt Characterisation and Rheology Laboratory, Department of Civil Engineering, National Institute of Technology Karnataka, India.

I am also thankful to the suppliers of asphalt binders, M/s MRPL, Mangalore, India, and M/s Tiki Tar, Mangalore, India. Acknowledgments to Balakrishna Gatty, Nevil D'Souza, Padma Engineering works, Bunder, and Baikampadi, Mangalore, Karnataka, India, for their help in fabricating the aluminum tube for a given design for my research work. My best regards to Indrajeet Upadhyay of AkzoNobel specialty chemicals for supplying WMA additives Rediset and Spectrum Chemicals for supplying Sasobit for research purposes.

A special thanks to my family. Words cannot express how grateful I am to my brothers and sisters for all the sacrifices you have made for me. I am forever thankful to my father, Sri. Veeraiah V, mother Smt. Rajeshwari S provided me the best available education and encouraged me in all my endeavours. My heartfelt respect to my friend Biswajit for your encouragement all the time; you were my great source of inspiration.

I appreciate the co-operation and help rendered by the staff of laboratories and the office of the Civil Engineering Department. My heartfelt thanks to Mr. Purushotham Vamanjoor and Mr. Ramesh, who helped me complete my laboratory studies safely and smoothly.

I lovingly acknowledge the moral support and help extended by my best friends and colleagues during this journey. Their informal support and encouragement have been very crucial. I am grateful to everybody who helped and encouraged me during this research work.

**Place: NITK, Surathkal**

**(Hemanth Kumar V)**

**Date: 10/05/2022**

## ABSTRACT

Despite the extensive use of rolling thin film oven (RTFO) for short-term aging of asphalt binders, there is a concern in understanding the rheology of short-term aging characteristics of the crumb rubber modified asphalt binders. Crumb rubber modified binder (CRMB) mixed with warm mix asphalt (WMA) additives Sasobit (S) and Rediset (R) to investigate their short-term aging temperature based on equiviscous principle, i.e., the temperature corresponding to  $0.17\pm 0.02$  Pa.s viscosity. This temperature is implemented during RTFO aging process to investigate its effect on rutting performance parameters. Rheological tests such as frequency sweep test, temperature sweep test, time-temperature superposition (TTS), high-temperature performance grading (PG grading), and multiple stress creep recovery (MSCR) are studied to understand the influence of RTFO aging temperature on CRMB. The same RTFO aged samples were subjected to pressure aging vessel (PAV) to investigate the fatigue performance parameters using intermediate performance grading, linear amplitude sweep (LAS), thixotropic behaviour. The Fourier transform infrared (FT-IR) spectroscopy and field emission scanning electron microscopy (FE-SEM) are also applied to justify the effects of the WMA additives on the CRM binders in terms of chemically and morphological properties on an RTFO and PAV aged conditions. Finally, the storage stability of CRMB was investigated using a separation tube test.

The high-temperature rheological properties revealed that due to an increase in RTFO aging temperature, the critical thermo-rheological behaviour of CRMB in the presence of WMA additives is significantly affected. It was found that CRMB with sasobit additives greatly enhanced visco-elastic properties at  $177^{\circ}\text{C}$  RTFO aging conditions than rediset additives. However, fatigue performance properties indicated that CRMB with rediset additives experienced lower viscosity behaviour at intermediate pavement temperature than sasobit for  $177^{\circ}\text{C}$  RTFO aged followed by PAV aging conditions. Moreover, FE-SEM and FT-IR analysis proved that asphaltene formation was directly dependent on the aging conditions, which helps conserve the rheological properties of base binder present in the CRMB. Finally, storage stability showed a significant phase

separation in CRMB binder in the presence of WMA due to aging temperature expect stored at 177°C.

**Keywords:** Crumb rubber modified binder (CRMB); Short-term aging; long-term aging; rutting parameter; fatigue parameter; thixotropy; rolling thin film oven (RTFO); dynamic shear rheometer (DSR); Sasobit; Rediset; storage stability; mixing temperature



# TABLE OF CONTENTS

Sl. No	TITLE	Page. No.
	<b>DECLARATION</b>	<b>i</b>
	<b>CERTIFICATE</b>	<b>ii</b>
	<b>ACKNOWLEDGEMENT</b>	<b>iv</b>
	<b>ABSTRACT</b>	<b>vi</b>
	<b>TABLE OF CONTENTS</b>	<b>viii</b>
	<b>LIST OF FIGURES</b>	<b>xi</b>
	<b>LIST OF TABLES</b>	<b>xvii</b>
	<b>NOMENCLATURE</b>	<b>xix</b>
	<b>CHAPTER 1: INTRODUCTION</b>	<b>1-8</b>
1.1	BACKGROUND	1
1.2	STATEMENT OF RESEARCH PROBLEM	5
1.3	RESEARCH OBJECTIVES AND SCOPE	6
1.4	ORGANIZATION OF THE THESIS	7
	<b>CHAPTER 2: LITERATURE REVIEW</b>	<b>9-28</b>
2.1	GENERAL	9
2.2	WORKING TEMPERATURE OF CRMB	9
2.3	VISCOSITY BEHAVIOUR OF CRMB	13
2.4	VISCOELASTIC PROPERTIES OF CRMB	15
2.4.1	Rutting performance of CRMB	15
2.4.2	Fatigue performance of CRMB	19
2.5	MORPHOLOGICAL PROPERTIES OF CRMB	21
2.6	MODIFICATION IN CHEMICAL BOND OF CRMB	21
2.7	SUMMARY	23
	<b>CHAPTER 3: MATERIALS AND METHODOLOGY</b>	<b>29-44</b>
3.1	MATERIALS	29
3.1.1	Asphalt binders	29
3.1.2	Warm Mix Asphalt Additives	30
3.2	ROTATIONAL VISCOMETER	31
3.3	SHORT-TERM AND LONG-TERM AGING PROCESS	32

3.4	DYNAMIC SHEAR RHEOMETER	33
3.4.1	Frequency Sweep Test	34
3.4.2	Temperature Sweep test	34
3.4.3	Time-Temperature Superposition Test	35
3.4.4	Performance Grade Test	36
3.4.5	Multiple Stress Creep Recovery Test	36
3.4.6	Linear Amplitude Sweep Test	37
3.4.7	Thixotropy Test	39
3.4.8	Storage Stability Test	40
3.4.9	Short and Long-term Aging Simulation of asphalt binder	41
3.4.10	Scanning Electronic Microscopic and Fourier transform infrared spectroscopy Test	42
	<b>CHAPTER 4: SELECTION OF OPTIMUM WORKING TEMPERATURE OF CRMB</b>	<b>45-66</b>
4.1	GENERAL	45
4.2	LABORATORY EXPERIMENTAL PLAN	45
4.3	RESULTS AND DISCUSSIONS	49
4.3.1	Equiviscous temperature Method	49
4.3.2	Steady Shear Flow Method	51
4.3.3	Phase Angle Method	53
4.3.4	Effect of working temperature on Mass Loss of asphalt binder	56
4.3.5	Correlation Study	61
4.4	SUMMARY	66
	<b>CHAPTER 5: INFLUENCE OF WORKING TEMPERATURE ON RUTTING PERFORMANCE OF CRMB WITH WMA ADDITIVES</b>	<b>67-98</b>
5.1	GENERAL	67
5.2	EXPERIMENTAL PLAN FOR RUTTING PERFORMANCE OF CRMB	67
5.3	RESULTS AND DISCUSSION	69
5.3.1	Frequency Sweep Test	69

5.3.2	Temperature Sweep Test	75
5.3.3	Time Temperature Superposition Test	80
5.3.4	High-Temperature performance Test	83
5.3.5	Multiple Stress Creep recovery Test	87
5.3.6	Scanning electron micrographs	90
5.3.7	Storage Stability test	96
5.4	SUMMARY	97

**CHAPTER 6: INFLUENCE OF WORKING  
TEMPERATURE ON FATIGUE PERFORMANCE OF  
CRMB** **99-132**

6.1	GENERAL	99
6.2	EXPERIMENTAL PLAN FOR STUDIES ON FATIGUE PERFORMANCE OF CRMB	99
6.3	RESULTS AND DISCUSSION	100
6.3.1	Intermediate Performance grade test	100
6.3.2	Linear Amplitude Sweep test	101
6.3.3	Thixotropic behaviour	110
6.3.4	Scanning Electronic Microscopic test	116
6.3.5	Fourier Transform Infrared Spectroscopy test	123
6.4	SUMMARY	130

**CHAPTER 7: CONCLUSIONS AND  
RECOMMENDATIONS** **133-140**

7.1	CONCLUSIONS	133
7.1.1	Working Temperature of CRMB	133
7.1.2	Rutting behaviour of CRMB	134
7.1.3	Fatigue performance of CRMB	136
7.2	RECOMMENDATIONS AND LIMITATIONS	137
7.3	SUGGESTIONS FOR FUTURE RESEARCH	139
	REFERENCES	141
	BIO-DATA	165

## LIST OF FIGURES

<b>Figure No.</b>	<b>Figure caption</b>	<b>Page No.</b>
1.1	Temperature maintained at different stages of asphalt mixture production	5
2.1	Effect of an increased working temperature on rubber particles	11
2.2	Schematic representation of asphaltene behaviour with different aging conditions	15
3.1	Warm mix asphalt additives (WMA); Sasobit and Rediset	31
3.2	Rotational viscometer apparatus	32
3.3	Determining the viscosity of CRMB using spindle no. 27	32
3.4	RTFO Apparatus	33
3.5	Samples placed on cooling rack after short-term aging	33
3.6	DSR Apparatus (MCR-502)	33
3.7	Silicone mould holding 25mm dia. Sample	33
3.8	25mm dia. parallel plate geometry	33
3.9	PAV apparatus and samples	34
3.10	The characteristic curve of asphalt binder's thixotropic behavior in dynamic mode	40
3.11	Aluminium tube used for storage stability test	41
3.12	SEM Specimens	42
3.13	FTIR Specimens	42
3.14	Specimens for SEM image analysis	43
3.15	Experimental flow chart	44
4.1	Flowchart for experimental research plan of working temperature	48
4.2	Equiviscous temperature test results	50
4.3	Steady shear flow test results	52
4.4	Phase angle method test results of CRMB-55	54

4.5	Phase angle method test results of CRMB-55+S	54
4.6	Phase angle method test results of CRMB-55+R	55
4.7	Interaction plot of working temperature with type of binders and methods	55
4.8	Mass loss of VG-30	57
4.9	Mass loss of VG-40	57
4.10	Mass loss of CRMB-55	58
4.11	Mass loss of CRMB-55+R	58
4.12	Mass loss of CRMB-55+S	59
4.13	Interaction plot of percentage mass loss with RTFO aging temperature and type of binders	60
4.14	Correlation between mass loss and softening point of VG-30	63
4.15	Correlation between mass loss and softening point of VG-40	63
4.16	Correlation between mass loss and softening point of CRMB-55	64
4.17	Correlation between mass loss and softening point of CRMB-55+S	64
4.18	Correlation between mass loss and softening point of CRMB-55+R	65
4.19	Interaction plot of softening point with RTFO aging temperature and type of binders	65
5.1	Flowchart for experimental plan of visco-elastic and rutting studies on modified binders	68
5.2	Effect of frequency on $G^*$ and $\delta$ for unaged conditions	70
5.3	Effect of frequency on $G^*$ and $\delta$ for 163°C RTFO aging conditions	71
5.4	Effect of frequency on $G^*$ and $\delta$ for 177°C RTFO aging conditions	71
5.5	Effect of frequency on $G^*$ and $\delta$ for 195°C RTFO aging conditions	72

5.6	Comparison of frequency effect on $G^*$ and $\delta$ between 163°C of CRMB with rediset and sasobit with 195°C RTFO aging conditions	73
5.7	Comparison of frequency effect on $G^*$ and $\delta$ between 177°C of CRMB with rediset and sasobit with 195°C RTFO aging conditions	74
5.8	Interaction plot of $G^*$ with working temperature and type of binders	74
5.9	Effect of temperature sweep on $G^*$ and $\delta$ for unaged	76
5.10	Effect of temperature sweep on $G^*$ and $\delta$ for 163°C RTFO aging conditions	77
5.11	Effect of temperature sweep on $G^*$ and $\delta$ for 177°C RTFO aging conditions	77
5.12	Effect of temperature sweep on $G^*$ and $\delta$ for 195°C aging conditions	78
5.13	Effect of temperature on $G^*$ and $\delta$ for CRMB-55+S and CRMB-55+R at 163°C and 195°C RTFO aging conditions	79
5.14	Comparison of temperature sweep effect on $G^*$ and $\delta$ for Effect of temperature on $G^*$ and $\delta$ for CRMB-55+S and CRMB-55+R at 177°C and 195°C RTFO aging conditions	80
5.15	Interaction plot between $G^*$ and working temperature, binder type, test temperature	80
5.16	Comparison of TTS effect on $G^*$ master curve data at a 30°C reference temperature between CRMB-55 with sasobit and CRMB-55 at 163°C, 195°C	81
5.17	Comparison of TTS effect on $G^*$ master curve data at a 30°C reference temperature between CRMB-55 with sasobit and CRMB-55 at 177°C, 195°C	82
5.18	Comparison of TTS effect on $G^*$ master curve data at a 30°C reference temperature between CRMB-55 with rediset and CRMB-55 at 163°C, 195°C	82

5.19	Comparison of TTS effect on $G^*$ master curve data at a 30°C reference temperature between CRMB-55 with sasobit and CRMB-55 at 177°C, 195°C	83
5.20	$G^*/\sin\delta$ value of VG-30 for 163°C, 177°C, and 195°C RTFO aging conditions	84
5.21	$G^*/\sin\delta$ value of VG-40 for 163°C, 177°C, and 195°C RTFO aging conditions	85
5.22	$G^*/\sin\delta$ value of CRMB-55 for 163°C, 177°C, and 195°C RTFO aging conditions	85
5.23	$G^*/\sin\delta$ value of CRMB-55+R for 163°C, 177°C, and 195°C RTFO aging conditions	86
5.24	$G^*/\sin\delta$ value of CRMB-55+S for 163°C, 177°C, and 195°C RTFO aging conditions	86
5.25	Effect of working temperature on Jnr values at 64°C	88
5.26	Effect of working temperature on %R values at 64°C	89
5.27	The plot between Jnr and %R for asphalt binders	90
5.28	SEM image of VG-30 for RTFO aged at 163°C	92
5.29	SEM image of VG-30 for RTFO aged at 195°C	93
5.30	EDAX analysis of VG-30 elemental mapping	93
5.31	SEM image of CRMB-55 for RTFO aged at 163°C	94
5.32	SEM image of CRMB-55 for RTFO aged at 195°C	94
5.33	SEM image of CRMB-55+S for RTFO aged at 177°C	95
5.34	SEM image of CRMB-55+R for RTFO aged at 177°C	95
5.35	Comparison between softening point of one-third top and bottom of aluminium tube	96
6.1	Flowchart for experimental plan of fatigue performance of CRMB-55 with WMA additives	100
6.2	Performance grade at intermediate service temperature	101
6.3	Effective shear stress versus strain response of binders RTFO aged at 163°C and PAV aged	103
6.4	Effective shear stress versus strain response of binders RTFO aged at 177°C and PAV aged	104

6.5	Effective shear stress versus strain response of binders RTFO aged at 195°C and PAV aged	104
6.6	Variation of integrity parameter with damage intensity of binders RTFO aged at 163°C and PAV aged	107
6.7	Variation of integrity parameter with damage intensity of binders RTFO aged at 177°C and PAV aged	107
6.8	Variation of integrity parameter with damage intensity of binders RTFO aged at 195°C and PAV aged	108
6.9	Fatigue Life of binders RTFO aged at 163°C, 177°C, 195°C and PAV aged for 2.5% stress level	109
6.10	Fatigue Life of binders RTFO aged at 163°C, 177°C, 195°C and PAV aged for 5% stress level	109
6.11	Thixotropic behaviour of VG-30 for RTFO aged at 163°C and PAV aged	111
6.12	Thixotropic behaviour of VG-30 for RTFO aged at 177°C and PAV aged	112
6.13	Thixotropic behaviour of CRMB-55 for RTFO aged at 163°C and PAV aged	112
6.14	Thixotropic behaviour of CRMB-55 for RTFO aged at 195°C and PAV aged	113
6.15	Thixotropic behaviour of CRMB-55+S for RTFO aged at 177°C and PAV aged	113
6.16	Thixotropic behaviour of CRMB-55+R for RTFO aged at 177°C and PAV aged	114
6.17	Exponential fit model for the first part of the thixotropic curve “formation of the structure” at 0.1 (s <sup>-1</sup> ) shear rate of binders.	114
6.18	Bigaussian fit model for the third part of the thixotropic curve “reaching to equilibrium” at 0.1 (s <sup>-1</sup> ) shear rate of binders.	115
6.19	FE-SEM images of CRMB-55 for unaged conditions	117
6.20	FE-SEM images of CRMB-55 for 163°C RTFO aging followed by PAV conditions	117



6.21	FE-SEM images of CRMB-55 for 177°C RTFO aging followed by PAV conditions	118
6.22	FE-SEM images of CRMB-55 for 195°C RTFO aging followed by PAV conditions	118
6.23	EDAX analysis of CRMB-55 elemental mapping for RTFO and PAV aging conditions	119
6.24	FE-SEM images of CRMB-55+S for 163°C RTFO aging followed by PAV conditions	119
6.25	FE-SEM images of CRMB-55+R for 163°C RTFO aging followed by PAV conditions	120
6.26	FE-SEM images of CRMB-55+S for 177°C RTFO aging followed by PAV conditions	121
6.27	FE-SEM images of CRMB-55+R for 177°C RTFO aging followed by PAV conditions	121
6.28	FE-SEM images of CRMB-55+S for 195°C RTFO aging followed by PAV conditions	122
6.29	FE-SEM images of CRMB-55+R for 195°C RTFO aging followed by PAV conditions	122
6.30	Observation of FTIR spectra of VG-30 for RTFO (163°C) and PAV aging conditions	124
6.31	Observation of FTIR spectra of CRMB-55 for RTFO (195°C) followed by PAV aging conditions	126
6.32	Observation of FTIR spectra of CRMB-55+R for RTFO (177°C) followed by PAV aging conditions	126
6.33	Observation of FTIR spectra of CRMB-55+S for RTFO (177°C) followed by PAV aging conditions	127

## **LIST OF TABLES**

<b>Table No.</b>	<b>CONTENT</b>	<b>Page No.</b>
1.1	Summary on effect of working temperature on rheological properties of CRMB	25
1.2	Summary on viscosity test temperature and rheological properties of CRMB	26
1.3	Summary on effect of working temperature on rutting and fatigue performance of CRMB	27
3.1	Physical properties of asphalt binder	29
3.2	Physical properties of CRMB	30
3.3	Physical properties of WMA additives	31
4.1	Non-linear curve fit parameters	50
4.2	One-Way ANOVA significance test results of viscosity	51
4.3	One-Way ANOVA significance test results of % mass loss	60
4.4	Regression constant and coefficient of determination for linear, exponential, and power models	62
5.1	Details on different binder's matrix for the rutting performance study	68
6.1	Details on different matrix for analysing the fatigue performance study	99
6.2	Different coefficients obtained from VECD Analysis	106
6.3	Exponential fit parameters values of the first part of the curve for different short-term aging temperatures	115
6.4	Biguassian fit parameters values of the third part of the thixotropic curve for different short-term aging temperatures.	116

6.5	The characteristics of molecular structures at different wavenumbers	123
6.6	Structural indexes of the CRMB-55 with and without WMA additives	129
6.7	Variation of structural indexes of the CRMB-55 with and without WMA additives after aging for VG-30	130
6.8	One -Way Anova significance test results structural indexes	130

## NOMENCLATURE

AASHTO	American Association of State Highway and Transportation Officials
ASTM	American Society for Testing and Materials
CRMB	Crumb Rubber Modified Binder
CRMB-55+S	Crumb Rubber Modified Binder with Sasobit
CRMB-55+R	Crumb Rubber Modified Binder With Rediset
DSR	Dynamic Shear Rheometer
EDX	Electron Dispersion X-ray
FE-SEM	Field Emission Scanning Electron Microscope
FT-IR	Fourier transform infrared spectroscopy
HMA	Hot Mix Asphalt
IS	Indian Standard
LVER	Linear Visco Elastic Region
LAS	Linear Amplitude Sweep
MSCR	Multiple Stress Creep and Recovery
MRPL	Mangalore Refinery and Petrochemical Limited
NCHRP	National Cooperative Highway Research Program
PG	Performance Grading
PAV	Pressure Aging Vessel
PMB	Polymer Modified Binder
RV	Rotational Viscometer
RTFO	Rolling Thin Film Oven
TTSP	Time Temperature Superposition Principle
TFO	Thin Film Oven
VECD	Visco Elastic Continuum Damage
VG	Viscosity Grade
WMA	Warm Mix Asphalt

# CHAPTER 1

## INTRODUCTION

### 1.1. BACKGROUND

Globally, one billion waste tyres are generated annually from the vehicles, in which the US alone produces 290 million compared to China and India (Association Rubber Manufacturers 2006). However, only 7% of waste tyre rubber was recycled, 11% were used as fuel, 5% were exported, and 77% were unused, equivalent to 765 million tyres. Whereas, in India, 6-7% of waste tyres are generated annually, with a growth of 12% yearly by a local tyre industry. In 2016, over 1,00,000 km of road were constructed by adding recycled rubber to asphalt binder, in which 5,00,000 tonnes of crumb rubber modified bitumen (CRMB) was used (Mishra 2016). Therefore, to improve the binder properties in terms of longer pavement serviceability, the crumb rubber modifier (CRM) was initiated in the mid-1950s (Shen and Amirkhanian 2005). In recent years, the US has increased CRM usage in asphalt mixtures, which reported a significant improvement in pavement service compared to a conventional binder. Also, Places like California, Florida, and Arizona reported that CRMB is a cost-effective material, while some oppose the implementation (Ching 2007; Hicks et al. 1995; Maupin Jr 1996; Ruth 1992).

The behaviour of CRMB has been studied extensively in recent years. The main areas of studies such as concentration, depolymerisation, particles size, type of base binder used, and compatibility between the type of asphalt binder and particle size of CRM (Ghaly 1999; Kim et al. 2001; Kuennen 2005; Macleod et al. 2007; Mehta et al. 2004; Navarro et al. 2005; Tayebali et al. 1997; Zanzotto and Kennepohl 1996). According to (Ching and Wing-gun 2007; Lougheed, T.J., and Papagiannakis 1996), the underperformance of CRMB is due to the lack of understanding of volume changes during the swelling phenomenon of crumb rubber (CR) at mixing and handling temperature. However, CRMB is necessary to counter the permanent deformation

(rutting) due to traffic loading, especially under the high pavement temperature conditions, and preserve the pavement structure from the damaging (Palit et al. 2004). Moreover, the mix design concerns are due to dynamic action like gel nature of CRMB and to fit into the voids of mineral aggregates with minimum interference with aggregate contact (Attia and Abdelrahman 2009; Heitzman 1992). CRMB also changes its binding properties with method and degree of processing control such as mixing time and temperature (Attia and Abdelrahman 2009; Chehovits et al. 1982; Pavlovich et al. 1979).

Furthermore, the incompatibility of asphalt binder type and CRM leads to premature damages such as rutting and fatigue due to improper aging and loss of binder properties such as adhesion (Attia and Abdelrahman 2009; Stroup-Gardiner et al. 1993). Therefore, the aging process for a CRM binder is a prime concern in determining the Superpave specification requirement (Attia and Abdelrahman 2009; Branthaver et al. 1993; Lexington 1993). (McGennis 1995) also reported that the rolling thin film oven test (RTFO) treatment depends on the type of asphalt binders such as base asphalt or CRMB to accept the Superpave testing parameters.

As CRM asphalt mixture is workable with high mixing and compaction temperature during the construction, there are possibilities of increasing the base binder's aging, degradation of rubber particles and asphalt binders, which will lead to higher fuel consumptions and emission of harmful gases (Bocoum et al. 2014; Habal and Singh 2016; Rühl et al. 2007; Stienss et al. 2018; Zapata and Gambatese 2005). To reduce these effects, warm mix asphalt (WMA) additives improved the compatibility of mixes and reduced the air voids under laboratory conditions using a Superpave gyratory compactor (Hurley and Prowell 2006). Furthermore, asphalt binder mixture with sasobit additives, compacted at 90°C and 70°C temperature, reported high resistance towards moisture-induced damages, rutting, and fatigue, compared to 130°C compaction temperature (Shiva Kumar and Suresha 2017). It was also evident that asphalt binder mixture with sasobit additives resulted in lower compaction densification index (CDI) and higher traffic densification index (TDI), which indicates less energy consumption during compaction and higher resistance towards traffic loading, irrespective of compaction temperature (Suresha and Kumar 2018).

Warm mix asphalt (WMA) technology offers a significant reduction of mixing and compaction temperature of CRMB by lowering its viscosity without damaging the base binder performance properties at the pavement service temperature (Sun and Li 2010). This range of reduced mixing temperature depends upon the nature, type, and concentration of modifiers used, and viscosity of the base binder used. Therefore, all these factors are reliable in deciding the modified binders' ideal mixing and compaction temperature. Moreover, to simulate the same mixing temperature in the laboratory known as short-term aging, a rolling thin film oven (RTFO) test is performed. A literature review has shown that most researchers still perform short-term aging at 163°C (ASTM D2872-12 2012) for the modified binders in the presence of WMA additives and determine their rheological characteristics using a dynamic shear rheometer (DSR).

The warm-mix asphalt (WMA) additives in CRMB reduces the mixing and compaction temperatures of asphalt mixture, which can help reduce fuel consumption and conserve environmental fuel pollution and avoid waste tyre rubber disposal problems (Ma et al. 2017), (Oliveira et al. 2013), (Wen et al. 2018), (Wasiuddin et al. 2007), (Lakshmi Roja et al. 2018), (Wang et al. 2020). Furthermore, the rheological properties of CRMB were found to be improved at various stages of the pavement service temperature and have been proven to be more flexible at low pavement temperature and also more elastic at higher pavement temperature compared to conventional binder (Akisetty et al. 2010). The NCHRP 459 report has recommended modified binder's viscosity to be 0.30 to 0.40 Pa.s for mixing and 1.00 to 1.20 Pa.s for compaction (Bahia et al. 2001). When the CRMB is mixed with aggregates at high temperatures, i.e., greater than 195°C (Nivitha and Krishnan 2018), the properties of the base binder used in production CRMB may deteriorate soon, and this effect can be reflected in terms of rutting and fatigue performances in the pavement. However, according to ASTM D6925-15, preparing the specimen using a Superpave gyratory compactor specifies a mixing temperature range of viscosity for unaged asphalt binder to be  $0.17 \pm 0.02$  Pa.s and a compaction temperature range of  $0.28 \pm 0.03$  Pa.s

The short-term and long-term aging behavior of virgin and modified asphalt binder in the presence of layered materials have been recognized using rheological

properties, which improves aging resistance (Pang et al. 2014; Xu et al. 2015). In the case of intrinsic healing properties of asphalt binder, the fraction of stiffness gained during the healing process slightly decreases with aging and increases with high temperature (Bhasin et al., 2011). However, to investigate the effect of short-term aging on asphalt binder in the laboratory, many researchers implement a thin film oven (TFO) and rolling thin film oven (RTFO) test. The viscosity of CRM binders was increased compared to unmodified binders after the short-term aging process (Liang and Lee 1996).

The selection of short-term aging temperature in the laboratory is still one of the most operational methods to select the asphalt binder for road construction. Many researchers have focused on enhancing the rheological properties of asphalt binders by adding varieties of modifiers to CRMB and have proposed numerous evaluation test methods for ranking the different asphalt binders. And the addition of modifiers to CRMB such as warm mix additives (WMA), rejuvenating agent, water activation of CR, and aging behavior has been widely studied (Akisetty et al. 2011a; Liang and Lee 1996; Shatanawi et al. 2009; Shen et al. 2005; Wang et al. 2012a).

In the presence of WMA additives, the rheological performance of CRMB has a close relationship after the short-term aging process (Wang et al., 2012a). Rodriguez-Alloza et al. (2014) analyzed the high and low-temperature properties of CRMB by reducing its viscosity in the presence of WMA. Yang et al. (2017) discussed the effect of Evotherm on the mechanical and environmental performance of CRMB. However, Xiao et al. (2009) analyzed the relationship between the long-term performance of crumb rubber-modified pavement and conventional asphalt pavement due to WMA additives. While Gallego et al. (2016) and Yu et al. (2014) discussed the effect of WMA additives on mechanical response and chemical composition using a DSR and FTIR.

The study of rheological and chemical behaviour on a short-term aged asphalt binder has practical significance in guiding the selection of various binders for road construction. In this study, the rheological properties of optimized short-term aged binders are investigated through laboratory tests. The storage stability was used to obtain the separation tendency of CRM particles to analyze the effect of storage temperature in the presence of WMA additives using the modified aluminum tube. It



was also discussed that changing the short-term aging temperatures followed by long-term aging has an impact on morphological and chemical composition as reflected on rheological properties.

## **1.2. STATEMENT OF RESEARCH PROBLEM**

RTFO test method simulates the asphalt binder aging during the manufacture and construction of HMA pavements (Roberts et al. 1991). If the mixing temperature differs appreciably from 163°C, a significant effect on binder properties will be occurred (ASTM D2872-12, 2013). However, working temperature (WT) is broad range of temperature experienced by the asphalt binder, aggregate in various stages of work i.e., mixing plant, laying site, and rolling at laying site. According to Morth specification, the working temperature varies with viscosity grade for unmodified asphalt binder. Therefore, the working temperature for CRMB will be higher than conventional asphalt binder. As shown in Figure 1.1, the range of working temperature under three scenarios i.e., working temperature of unmodified binder ( $WT_{UB}$ ), working temperature of CRMB ( $WT_{CRMB}$ ), lower working temperature of CRMB with WMA ( $LWT_{CRMB+WMA}$ ), and Ideal working temperature of CRMB with WMA ( $IWT_{CRMB+WMA}$ ) are hypothesized to understand WT of binder at mixing stage of the work.

To understand effect of WT using short-term aging process on viscosity of modified binders, and how these aging temperature affects the rheological, morphological and chemical composition, it is necessary to bridge the gap between mixing temperatures and rheological properties. Therefore, using viscosity behaviour of binders in the presence of WMA additives, as hypothesized in Figure 1.1 understanding of the mixing temperature as a function of viscosity is important in selection of suitable asphalt binder for road construction.

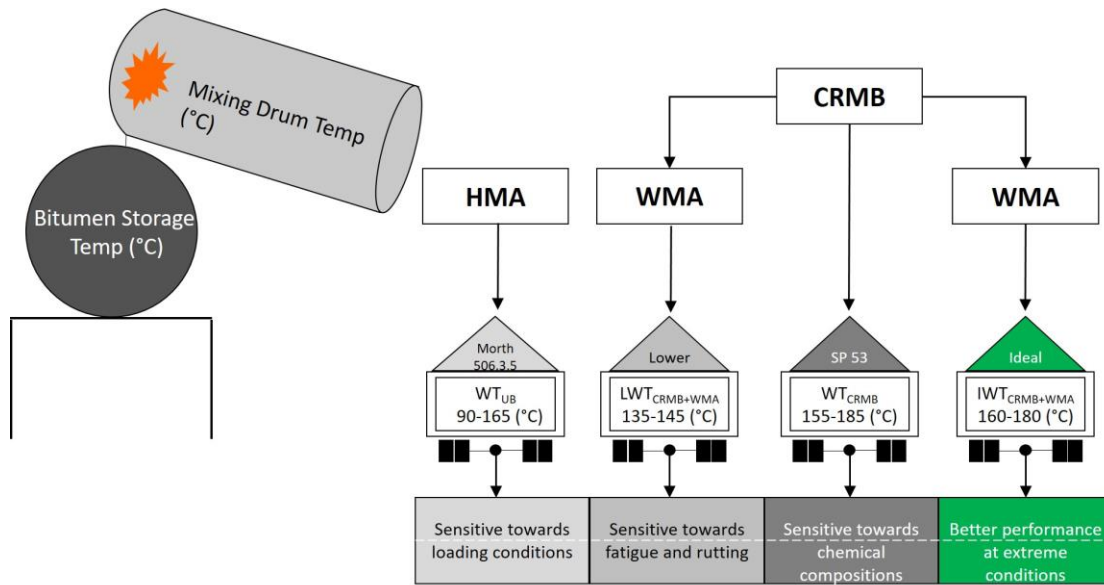


Figure 1.1 Temperature maintained at different stages of asphalt mixture production

### 1.3. RESEARCH OBJECTIVES AND SCOPE

The main objective of this study was to characterize the rheological properties of CRMB-55 binder with WMA additives sasobit and rediset, subjected to short-term aged at optimized temperature using RTFO (ASTM D2872-12 2012) procedure.

The specific objectives of the present research are as follows:

1. To determine the RTFO working temperature of CRMB-55 with WMA additives and compare with base binder
2. To assess the effect of short-term aging temperature on rutting resistance of CRMB-55 under the influence of various doses of WMA in comparison with base binder
3. To study the fatigue performance of CRMB-55 under the effect of multiple doses of WMA with selected working temperature followed by long-term aging.
4. To study the thixotropy, morphology, and chemical properties of CRMB-55 with WMA additives compared to base binders.

## 1.4. ORGANIZATION OF THE THESIS

This thesis is organized into seven chapters, followed by a list of references. The background on the selection of suitable working temperature for CRMB with WMA additives for characterization of visco-elastic, rutting and fatigue properties, and morphology and chemical properties of CRMB under the laboratory conditions, and its importance in the asphaltic industry during the road construction, statement of a research problem, research objectives and scope, and thesis organization of this research are presented in the Chapter 1.

Chapter 2 of this study presents a comprehensive review of the research findings and the impact of working temperature selection on CRMB in the presence of WMA additives during the investigation of visco-elastic behaviour, rutting and fatigue performance, morphology and morphology chemical behaviour, and storage stability characteristics. Also, a discussion on thixotropic behaviour and storage stability were evaluated using a DSR and aluminum tube.

The details of various materials used during the laboratory investigation, physical properties of base and CRMB, WMA additives, the method used to determine the working temperature, **the details of different laboratory tests, and altered aluminum tube** are provided in Chapter 3.

Chapter 4 presents a method used to determine the optimum working temperature of CRMB in the presence of WMA additives. In this study, the **objective-1** was to evaluate the ideal operating temperature by equiviscous temperature method, steady shear flow, and phase angle method using rotational viscometer and DSR as recommended by NCHRP 648 (West et al. 2010). The temperature corresponding to  $0.17 \pm 0.02$  Pa.s viscosity was included as criteria per AASHTO T312 in determining the mixing temperature. By extrapolating the high shear rate viscosity, i.e.,  $490 \text{ s}^{-1}$  for  $76^\circ\text{C}$ ,  $82^\circ\text{C}$ ,  $88^\circ\text{C}$ , and  $94^\circ\text{C}$  temperature till it intercepts  $0.17 \pm 0.02$  Pa.s viscosity criteria were used to find the mixing temperature. Finally, in the phase angle method using the phase angle master curve at  $80^\circ\text{C}$  reference temperature, the frequency corresponding to  $86^\circ$  phase angle is used in a power-law regression equation established by Casola.

Chapter 5 of this dissertation is in the form of a technical paper submitted for the journal of Construction Building and Materials, entitled "**Effect of optimized short-term aging temperature on rheological properties of rubberized binders containing warm mix additives.**" This study aims to assess and analyse **objective-2** visco-elastic and rutting performance properties of unmodified and modified binder subjected to different short-term aging conditions. The behaviour of complex shear modulus ( $G^*$ ) is determined by conducting the frequency sweep test, temperature sweep test, time-temperature superposition (TTS), high-performance grading, multiple stress creep recovery (MSCR) test on CRMB. In addition, SEM image analysis and storage stability were observed for different short-term aging conditions. The findings observed from rheological SEM images and storage stability investigation of CRMB with WMA additives in this study can successfully describe the rutting performance behaviour.

Chapter 6 of this dissertation evaluated resistance to fatigue distress of CRMB with WMA additives by conducting performance grade at intermediate temperature, linear amplitude sweep test as mentioned in objective-3, and thixotropic behaviour on short and long-term aging conditions as specified in **objective-4**. In addition, the aging effect on morphological and chemical components of the unmodified and modified binder was evaluated in terms of fatigue parameter  $G^* \cdot \sin \delta$ , strain dependency, structural recovery, and chemical elements. Conclusion and recommendations drawn based on the present investigation are given in Chapter 7.

## **CHAPTER 2**

### **LITERATURE REVIEW**

#### **2.1. GENERAL**

The primary purpose of the comprehensive review was to present the effect of laboratory aging temperature explicitly used during the short-term aging procedure by various researchers to investigate the viscoelastic behaviour, rutting, fatigue, morphological and chemical behaviour of CRMB in the presence of WMA additives. However, there is less research available regarding selecting suitable working temperatures regarding the CRMB with WMA additives and findings on CRMB rutting and fatigue properties using DSR methodology, which is a promising test method. This review consists of i) effect of working temperature on CRMB, ii) Viscosity behaviour of CRMB iii) Rutting and fatigue characterisation, iv) Morphological behaviour of CRMB, v) chemical structural behaviour of CRMB.

#### **2.2. WORKING TEMPERATURE OF CRMB**

The CRMB was identified as a better-modified binder in recent years due to its enhanced fatigue and rutting performance (Palit et al. 2004; Wang et al. 2012). The usage of CRMB in many countries leads to resolving the disposal of rubber tires (Oliveira et al. 2013; Palit et al. 2004; Wang et al. 2012). However, the higher working temperature during CRMB production at the site was challenging concerning quality aspects (Habal and Singh 2016; Liu et al. 2013; Rühl et al. 2007; Zapata and Gambatese 2005). It is known that due to higher working temperature, the crumb rubber particles and asphalt binder results in disintegrations (Ghavibazoo et al. 2013; Huang et al. 2017; Ren et al. 2021; Tang et al. 2016). In the perspective of micro-level, many researchers identified that due to this degradations, it significantly affects the rheological properties (Abdelrahman and Carpenter 1999; Billiter et al. 1997b; Ghavibazoo et al. 2013; Zanzotto and Kennepohl 1996), which is major occurred due to changes in molecular

weight distributions and molecular structure (Billiter et al. 1997b; Ghavibazoo et al. 2013).

To solve the storage stability problem, terminal blend (TB) of rubberized asphalt technology came into existence in recent years. In this method, the working temperature of TB was 220 to 260°C without shearing action as rubber particles fully digest into asphalt (Huang et al. 2017; Li et al. 2017; Tang et al. 2016). Using the popular method FTIR, it was found that components from rubber particles are released into asphalt binder (Ghavibazoo et al. 2013; Ragab et al. 2013; Tang et al. 2016). In addition, CRMB consists of complex components due to natural and synthetic rubber, sulfur, and carbon black, which are cross-linked and composed of hydrocarbons (Ghavibazoo et al. 2013; Mark et al. 2013). However, according to (Abdelrahman and Carpenter 1999; Zanzotto and Kennepohl 1996) study, rubber particles are partially disintegrated into asphalt binder due to their cross-linked structure, but changes in its structure occur during the application of working temperature.

Many studies showed that CRM particles capture asphalt binder's light oil components and increase its size by five times at 160°C interaction temperature (Ghavibazoo et al. 2013). Therefore, the swelling phenomenon and light-oil fractions of asphalt binder play a vital role in the rheological properties of CRMB (Putman and Amirkhanian 2010). Hence, stiffness properties of CRMB are enhanced during the swelling phenomenon and decreased when partially disintegrate into asphalt binder (Abdelrahman and Carpenter 1999; Billiter et al. 1997b). Therefore, depolymerization naturally occurs at higher working temperatures as it decreases the molecular weight of CRM (Billiter et al. 1997b). Hence, the combination of swelling phenomenon and disintegration of CRM is dependent upon the complex nature of CRM and asphalt binders at a given working temperature (Billiter et al. 1997a). In addition, the swelling and rate of degradation of CRM depend on working temperature, time, particles size, and type of asphalt binder used (Ren et al. 2021; Wang et al. 2019). Overall, the rheological properties of CRMB is depended on the following factors particle size, surface texture of CR, working temperature, phenomenon of CR degradation, type of asphalt binder (Bahia and Davies 1994; Lee et al. 2008; Navarro et al. 2004; Xiang et al. 2009; Yildirim 2007).

Furthermore, during the aging process of CRMB, the asphalt binder components alter their proportions due to the volatilization of light oil fractions. This leads to the conversion of micro-molecule to macromolecules (Lu and Isacson 2002; Ruan et al. 2003; Siddiqui and Ali 1999). Therefore, the components of asphalt binder determine the properties of CRMB (Pang et al. 2014; Wu et al. 2009). Using an advanced characterisation technique, a laboratory asphalt stability test (LAST) found that rubber particles' size and concentration have a more negligible effect on storage stability and binder degradation (Kim et al. 2001).

Previous studies on CRMB indicated that rubber particles release their components into asphalt binder for a given working temperature, which resists the ingress of oxygen molecules into asphalt binder and retards the aging process (Gawel et al. 2006; Ghavibazoo and Abdelrahman 2013; Wang et al. 2020). According to (Xiang et al. 2009), due to the swelling of rubber particles, it begins to form a gel-like structure and forms cross-linked bonds, which improves the binder properties physically and mechanically. However, the cross-linked network of CRMB may lead to degrading into asphalt binder at a higher working temperature 240°C (Wang et al. 2017; Yao et al. 2016b). Moreover, due to higher viscosity, CRMB requires higher working and compaction temperature (Oliveira et al. 2013; Rodríguez-Alloza et al. 2013), which increases the fuel consumption with toxic gas emission. The increase in working temperature of CRMB leads to swelling of rubber particles in the presence of asphalt binder in a stepwise process and leads to degradation as shown in Figure 2.1.

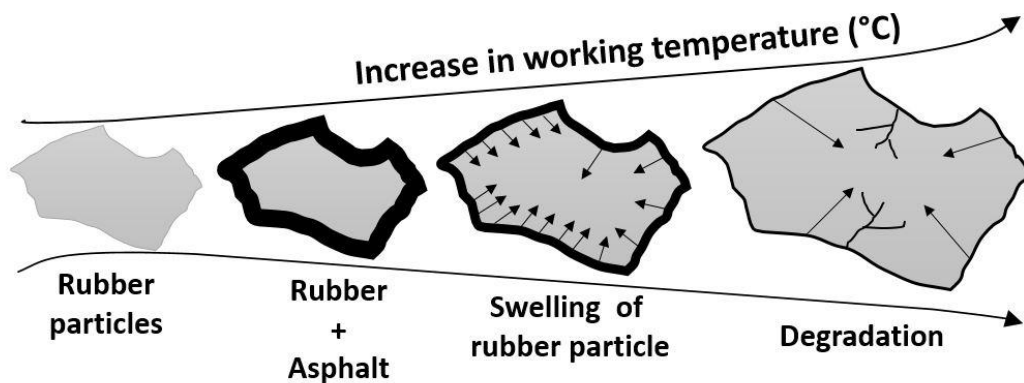


Figure 2.1 Effect of an increased working temperature on rubber particles (Abdelrahman 2006)

Therefore, to lower the working temperature of CRMB, the addition of WMA additives was found to be helpful, as it reduces the viscosity significantly (Wang et al. 2012). Initially, WMA was introduced in Europe (1990) and United States (2004) (Arega et al. 2011; D'Angelo et al. 2008). Since then, many researchers have investigated proper working and compaction temperature by adding WMA additives, which acquires lower temperature compared to hot mix asphalt (HMA) (Arega et al. 2011). The effect of reduced working temperature (143°C, 163°C) on viscosity, complex shear modulus ( $G^*$ ), rutting, and fatigue performance of asphalt binder was implemented by using the short-term aging process in the presence of WMA additives (Arega et al. 2011). A study on the selection of short-term aging temperature suggested that the complex shear modulus ( $G^*$ ) of PG-64-22 was highest when the RTFO test was conducted at a higher temperature (Banerjee et al. 2012).

The rheological properties for a lower RTFO aged condition indicated a lower impact on asphalt binder and suggested that standard 163°C temperature does not represent the proper mixing temperature as it depends on the grade of asphalt binder (Hofko et al. 2017b; Ragni et al. 2018). An extensive study on the impact of short-term aging temperature (123°C, 143°C, and 163°C) on the chemical structure of asphalt binder showed that it has a more substantial impact on the formation of sulfoxide structure, carbonyl structures (Hofko et al. 2018). The reduced short-term aging temperature (123°C, 143°C) by adding WMA additives to CRMB illustrated reduced stiffness and justify that it is no concern of susceptibility towards permanent deformation (Julaganti et al. 2018). Based on the reduced short-term aging temperature (143°C), PMB with Wax-S (2%) showed improved rutting and fatigue performance as well as a reduction in viscosity (Kataware and Singh 2017a).

The effect of WMA additives on the mixing and compaction temperature of AC-30 presented that it approximately reduced 20-29°C, respectively (Kataware and Singh 2018). A study influence of WMA additives on CRMB after being subjected to different working temperatures indicated that rheological properties depended on additives (Kataware and Singh 2017c). The short-term aging process entirely changed the mechanical behaviour of the asphalt binder with WMA additives compared to the base binder itself (Lakshmi Roja et al. 2018). A study on the impact of different working



temperatures on surface free energy (SFE) of asphalt binder was found to be statistically insignificant (Mishra and Singh 2019).

### **2.3. VISCOSITY BEHAVIOUR OF CRMB**

According to the Asphalt Institute, the viscosity of CRMB should be less than 3 Pas at 135°C (Asphalt Institute 1994; Thodesen et al. 2009). According to (Lougheed and Papagiannakis 1996), the viscosity of CRMB increases with an increase in rubber concentrations of any type. The factors affecting the consistency of CRMB are working temperature and duration (Akisetty et al. 2012; Bahia and Davies 1995; Billiter et al. 1997a; Roberts et al. 1989; Shuler et al. 1986), rubber concentration (Pavlovich et al. 1979; Thodesen et al. 2009), rubber particle shape and size (Heitzman 1992b; Pavlovich et al. 1979; West et al. 1998). Ultimately, the viscosity of CRMB is greatly affected by the grinding procedure of waste tires and the viscosity of neat binders (Thodesen et al. 2009). Handling the asphalt binder concerning viscosity is vital as it is usually stored at 150 to 180°C temperature (Corps 2000), therefore for CRMB, there is a concern in monitoring the viscosity (Stroup-Gardiner et al. 1993) as per the SHRP specifications. It was also observed that there is pronounced non-newtonian behaviour in CRMB (Lougheed and Papagiannakis 1996). From a regression and neural network analysis in predicting the viscosity of CRMB, it was noted that binder sources, rubber gradation, and its origin is insignificant (Thodesen et al. 2009).

According to (Heitzman 1992a), there is no chemical reaction between rubber particles and asphalt binder but the presence of diffusion phenomenon, i.e., ingress of light oil into rubber particles, which reduces the viscosity of CRMB (Lougheed and Papagiannakis 1996). Viscosity increases linearly with increased mixing time (80-90 min) (Roberts et al. 1989; Shuler et al. 1986). Many researchers reported that swelling of rubber particles leads to the formation of viscous gel-like structure and increases the viscosity of CRMB (Airey et al. 2002, 2007; Bahia and Davies 1994; Green and Tolonen 1977; Heitzman 1992a; Zanzotto and Kennepohl 1996). Some of the standard ways of reducing the viscosity of CRMB were the addition of WMA additives, biological substances, activating the rubber particles using furfural and polymeric treatment, devulcanization, using ultrasonic focusing apparatus (Cheng et al. 2011; Kedarisetty et al. 2016; Shatanawi et al. 2012; Shuler et al. 1986; Xu et al. 2015)

Various studies on the rutting performance of CRMB illustrated that it would be improved by increasing the viscosity of CRMB (Billiter et al. 1997c; Ching 2007; Huang 2008; Jorgenson 2003; Mohammadlouay and Gravesphilip 1994). Swelling and degradation of CRMB were mainly caused due to the higher interaction temperature and mixing conditions (Abdelrahman and Carpenter 1999; Zanzotto and Kennepohl 1996). According to (Sun and Li 2010), the impact of degraded CRM on the viscosity of CRMB is complicated. Still, the degraded CRM components alter the asphalt binder behaviour and improve the binder viscosity. The greater viscosity of CRMB is exhibited for the combination of ambient ground rubber particles and asphalt binder compared to cryogenically grounded (Shen et al. 2009). However, the size of rubber particles greatly influences the viscosity of CRMB (Shen et al. 2009; West et al. 1998). It was reported that the viscosity of the asphalt binder is responsible for the compatibility of the asphalt mixture (Celik and Atis 2008). The polymerization and depolymerization of CRMB lead to increased viscosity and enhance CR's phase separation from asphalt binder (Shatanawi et al. 2013). Therefore, the viscosity of CRMB could be expressed as the contribution of neat binder, the interaction between binder and rubber particles, the effect of rubber particle itself (Li et al. 2018). Based on the experimental investigation, lowering mixing and compaction were used as the modified binders viscosity showed low viscosity by the addition of oxidized polyethylene and propylene maleic Anhydride (Xu et al. 2016). According to (Heitzman 1992a) due to increased viscosity of CRMB, the coating of aggregate was found to be thicker, which results in sustaining the oxidation, rutting and fatigue distress. Viscosity of asphalt binder directly affects the swelling rate of CR, if asphalt binder is softer in nature greater the swelling rate (Lougheed and Papagiannakis 1996; Putman and Amirkhanian 2010).

A slight increase in viscosity of CRMB with 20 percent fine rubber particles, when tested from 175°C to 200°C using rotational viscometer, indicated that additional reaction between asphalt and rubber causing stiffness after viscosity is equilibrated with test temperature (McGennis 1995). According to (Wang et al. 2012), by increasing the rubber concentration by 15%, 20%, 25% to asphalt binder, the temperature required to obtain 3 Pas as per the SHRP specification showed 147°C, 162°C, and 174°C, respectively and this leads to increase mixing and compaction of CRMB. However, due

to the swelling of rubber particles, asphalt binder also undergoes phase change related to cross-linking within the materials. This mechanism could be seen as an elastic characteristic using phase angle measurement (Abdelrahman 2006). The viscosity of the asphalt binder is one of the main factors for the rate of settlement of crumb rubber particles during the separation process (Liu et al. 2009; Shen et al. 2012). The phenomenon of reduction in viscosity with an increase in shear rate explains the progressive breakdown of the internal structure of the binder and its build-up with a decrease of shear rate (Huang 2006). The behaviour of asphaltene content increases with aging conditions in asphalt binder, as shown in Figure 2.2

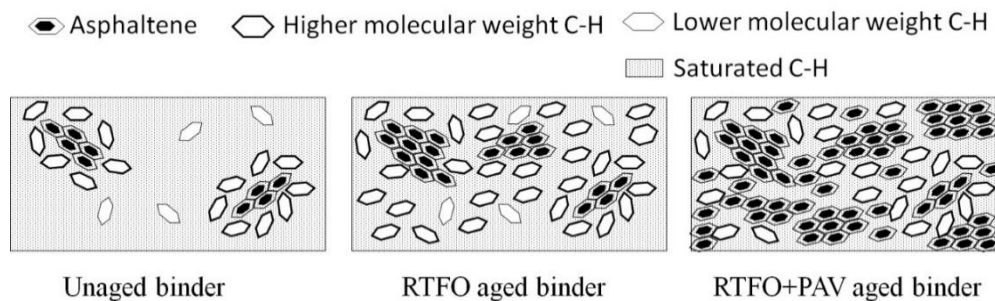


Figure 2.2 Schematic representation of asphaltene behaviour with different aging conditions (Girdler 1965)

## 2.4. VISCOELASTIC PROPERTIES OF CRMB

To evaluate the viscoelastic properties of modified asphalt binder under both strain/stress controlled at different frequency and temperature conditions DSR is used.

### 2.4.1. Rutting performance of CRMB

According to Superpave binders test criteria, the minimum recommended value of  $G^*/\sin\delta$  which is the viscous component at high temperature for unaged and short-term aged, must be at least 1 kPa and 2.2 kPa, respectively (Asphalt Institute 1994). Under extreme hot climatic conditions and traffic flow, flexible pavements are susceptible to rutting distresses (Wang et al. 2012). Therefore, these complex factors could be introduced using a DSR to understand the rutting behaviour; rheological parameters are investigated from intermediate to high temperature (Akisetty et al. 2011; Shatanawi et al. 2009; Xiao et al. 2012). To select a better rutting resistance asphalt binder, it should be highly susceptible to extreme temperature (Lee et al. 2008; Liu et

al. 2009; Xiao and Amirkhanian 2010). According to (Akisetty et al. 2007), the failure temperature of CRMB with WMA additives after RTFO aged was found to be high, which indicates better resistance towards the rutting. The performance grade analysis of non-foaming WMA additives showed that the source of asphalt binder plays a vital role in finding the failure temperature (Xiao et al. 2012). According to (Asphalt Institute 1994), a binder with a higher failure temperature demonstrate less susceptibility to rutting distresses at high pavement service temperature. The failure temperature of a long-term aging binder in the presence of WMA additives indicated a positive rutting resistance compared to the base binder with WMA additives (Lee et al. 2009). According to (Wasiuddin et al. 2007), the binder PG 64-22 with sasobit content (4%) increased the grading significantly by one grade bump, i.e., PG 69. The interaction effect of aged binder and sasobit increased the binder stiffness and made it more susceptible to fatigue performance at low temperatures (Shrum 2010). However, from the various study, it was recognized that  $G^*/\sin\delta$  does not reflect the actual binder recovery as it is challenging to identify the energy dissipated for permanent deformation (Bahia et al. 2001a).  $G^*/\sin\delta$  and creep compliance of an asphalt binder in the presence of sasobit was found to be increased, but it depends upon the aging conditions, binder type, and its sources (Biro et al. 2009; Cao and Ji 2011; Edwards et al. 2006; Jamshidi et al. 2012; Liu et al. 2011; Wasiuddin et al. 2011; Xiao et al. 2012). the performance grade of a modified binder for reduced RTFO aging temperature such as 150°C, 135°C in the presence of WMA additives couldn't meet the PG of the base binder, which shows poor rutting resistance (Hossain et al. 2012). Short-term aging condition was found to be highly affecting the failure temperature of warm asphalt additives sasobit and rediset with CRMB (Akisetty et al. 2007).

*Frequency sweep test:* To identify the linear viscoelastic properties of at various frequencies at 60°C frequency sweep test is useful, as it determines the behaviour of complex shear modulus ( $G^*$ ) and phase angle ( $\delta$ ) to analysis the rutting performance of asphalt binder (Anderson et al. 1994; Xiao et al. 2012). According to (Ferry 1980), the relationship between stress and strain is widely influenced by frequency alone than the magnitude of stress and strain within the linear viscoelastic region at 60°C. The frequency corresponding to 10 rad/s will simulate the shearing action by the traffic

movement corresponding to 88 kmph speed (Roberts et al. 1991). This shows that the binder with sasobit content at lower traffic speed present more elastic behaviour i.e., more stiffness than base binder (Biro et al. 2009). The mixing temperature could be determined using viscoelastic properties by frequency sweep at various temperatures and frequency corresponding to phase angle  $86^{\circ}\text{C}$  (West et al. 2010). The binder with sasobit content indicated a higher  $G^*$  with lower  $\delta$  at high test temperature over a wide range of frequencies, yielding better elastic properties similar to  $G^*/\sin\delta$  (Kheradmand et al. 2015). PMB and CRMB with sasobit content enhanced the elastic properties (Julaganti et al. 2017).

*Temperature sweep test:* According to (Biro et al. 2009), the complex shear modulus ( $G^*$ ) of the binder with WMA additives tends to be more elastic with a lower phase angle ( $\delta$ ), indicating the improved elasticity at a lower temperature, but there is less significant at a higher temperature. WMA additives in asphalt binder and their effect at low and high temperatures are necessary to determine the binder performance (Edwards et al. 2006). According to (Edwards and Isacson 2005), the crystallization of wax in asphalt binder depends on factors such as temperature, steric hardening, length of the carbon chain, and binders viscosity. (Edwards et al. 2006) also showed that temperature range between  $+25^{\circ}\text{C}$  and  $+90^{\circ}\text{C}$ , a binder with wax content resulted in higher stiffness effect, which depends upon the melting point of WMA additives. Temperature sensitivity of CRMB binder with Evotherm DAT showed less by measuring storage modulus and loss modulus, and if the slope is steeper, more sensitive towards the temperature (Yu et al. 2014)

*Multiple stress creeps recovery test:* The main reason for the rutting distress was the accumulation of strain induced by periodic traffic flow. Therefore, measuring dissipated energy is necessary to track this accumulation, known as loss compliance ( $J''$ ) (Ferry 1980). However, this parameter was suitable for neat binders compared to any polymer-modified binders (Anderson and Kennedy 1993; Bahia et al. 2001b; Bouldin et al. 2001; D'Angelo and Dongré 2002; Shenoy 2001). Therefore, to overcome the drawbacks of the  $G^*/\sin\delta$  parameter, MSCR methodology was extensively investigated (D'Angelo 2009; D Angelo 2009). The relationship between rutting performance of HMA and MSCR test parameters was found to be good (D

Angelo 2009; Masad et al. 2009; Wasage et al. 2011). The delayed strain response of CRMB from MSCR test results is depended on rubber size, base binder grade, applied stress level, and temperature (Zhang et al. 2016). The binder tends to behave as linear at a low-stress level, whereas its transit to a higher stress level it transit to non-linear behaviour (D Angelo 2009; Jafari et al. 2015). The lower  $J_{nr}$  value demonstrates the higher resistance against rutting distress for PMB at 60°C (Saboo et al. 2018). The main object of the MSCR test was to analyse the binder resistance towards the permanent deformation and its stress dependency for a given temperature (Domingos and Faxina 2015). Comparing the  $J_{nr}$  value and %R of CRMB-60 found to be low and moderate recovery, respectively compared to PMB 40, which showed more  $J_{nr}$  with reasonable level of %R indicating better performance than CRMB-60 (Kataware and Singh 2017b). Stiffness of CRMB found to be decreased as shown in MSCR test result  $J_{nr}$  value increased for lower RTFO aging temperature (Julaganti et al. 2018). Based on the MSCR test results, the chemical interaction between WMA additives and base binder plays a vital role on variation of stiffness and susceptibility towards rutting than by reducing a short-term aging temperature alone (Arega et al. 2011). In the presence of sasobit, asphalt binder decreases the strain accumulation compared to rediset additives regardless of base binder type and stress level (Jamshidi et al. 2015).

*Time-temperature superposition:* Based on the viscoelastic behaviour of CRMB, it was concluded that the TTS principle is applicable for master curve construction (Natu and Tayebali 2000). Master curve describes the interdependency of temperature and frequency using time-temperature superposition (TTS), which relates the time and temperature known to be thermo-rheologically simple (Gallego et al. 2016). However, CRMB with WMA additives was found to produce a significant inflection in the phase angle master curve, which is significantly affected by the presence of rubber (Rodríguez-Alloza et al. 2017). TTS principle could be used to the aging effect of asphalt binder using complex shear modulus or phase angle master curves (Huang 2008). The Master curve of the phase angle parameter explains the viscous and elastic behaviour of the asphalt binder (Yao et al. 2012). The smooth black curve could check the validity of the TTS principle curve without any disjoint if it occurs then indicates the breakdown of the TTS principle, which may be due to the

presence of a high percentage of wax and asphaltene content (Lesueur et al. 1996; Planche et al. 1996). According to (Palade et al. 2000), dynamic analyses indicated that TTSP is a rough calculation for asphalt binder only with high asphaltene content after aged conditions. However, if the measured rheological parameter shifts from linear-viscoelastic behaviour to non-linear, it distracts the thermo-rheological minimalism of the asphalt binder (Airey 2002). The complex shear modulus master curve asphalt binder modified with synthetic indicated thermo-rheologically simple at 25°C reference temperature (Airey and Mohammed 2008). The shift factor varies concerning the type of parameter used to construct the master curve, such as rheological parameters obtained from DSR and ductile failure energy measured using Double-edge-notched tension test (Andriescu and Hesp 2009). Moreover, according to (Nivitha et al. 2018), TTSP does not apply to unmodified and modified asphalt binder even for unaged and short-term aged conditions, as it does not behave thermo-rheologically simple even when the binder is subjected to small strain, because the binder in across temperature - 25°C to 75°C is a combination of viscoelastic fluid and solid.

#### **2.4.2. Fatigue performance of CRMB**

*Linear amplitude sweep test:* Many researchers found drawbacks while investigating the fatigue parameter  $G^* \cdot \sin \delta$  (D Angelo 2009; Johnson et al. 2009). Several researchers from laboratory investigations concluded that the LAS test describes fatigue performance more practically (D Angelo 2009; Dubois et al. 2014; Hintz et al. 2011; Saboo and Kumar 2016; Teymourpour and Bahia 2014). In the LAS test, a broad range of strain levels is subjected to analyse the fatigue behaviour of the asphalt binder (Saboo et al. 2018). According to (Gandhi et al. 2009), the fatigue parameter  $G^* \cdot \sin \delta$  of asphalt binder with WMA additives was least influenced even after short-term aged at different temperatures followed by PAV. The fatigue life of a PMA with sasobit (3%) at a strain amplitude of 6% was found to be increased (Yue et al. 2021). However, CRMB and PMB with WMA additives enhance the fatigue performance after RTFO and PAV aging conditions (Kumar et al. 2020). The long-term performance and durability of modified binder could be enhanced by reducing the mixing temperature as it decreases the initial stage of aging (Copeland et al. 2010; D'Angelo et al. 2008; Fini et al. 2011; Kristjánisdóttir et al. 2007). According to

(Akisetty et al. 2011), CRMB itself shows reduced  $G^* \cdot \sin \delta$  for a long-term aging condition compared to the addition of sasobit. The fatigue parameter  $G^* \cdot \sin \delta$  of recycled WMA binders resulted in lower resistance to fatigue cracking at 25°C intermediate temperature (Lee et al. 2009). For a better fatigue performance of asphalt binder with sasobit, a lower PG grade base binder is required, which decreases the  $G^* \cdot \sin \delta$  by 42% (Kim et al. 2011b; a; Lee et al. 2009).

*Thixotropy test:* The process of disintegrating binder structure and allowing it to rebuild for a given rest period, which is influential to applied shear stress and temperature factors, is known as thixotropy (Barnes and Barnes 1997; Lesueur et al. 1997). During the investigation of fatigue behaviour of the asphalt binder role, the thixotropy phenomenon plays a vital role (Baaq et al. 2005). To understand the fatigue performance, critical information such as binder flows after removal of applied stress will help distinguish between any binders (Lauger 2001). Thixotropy is also one of the main factors causing the hardening of asphalt binders (Petersen 1984). It is the phenomenon of structural breakdown and restoration of binding particles. Asphalt binder was identified as a reversible material under cyclic loading conditions, which can be affected by thixotropic, aging conditions (Di Benedetto et al. 2011; Canestrari et al. 2015; Pérez-Jiménez et al. 2012; Santagata et al. 2013). Here, the rest period during the test represents the traffic flow pattern, which helps in the analysing the thixotropic phenomenon by quantifying the stiffness recovery. And also, it plays a vital role in decreasing the initial stiffness of asphalt binder. Therefore, according to (Micaelo et al. 2015; Pérez-Jiménez et al. 2015), differentiating the thixotropic phenomenon is highly necessary for understanding the fatigue performance of asphalt binder. From the viscometer test result of CRMB analysis, thixotropy was witnessed by changing the shear rate speed from 10 rpm to 100 rpm and when decreased back to 10 rpm order and time gap for higher rubber concentrations (Stroup-Gardiner et al. 1993). Considering the thixotropic phenomenon during testing and evaluation of asphalt binder could perform better than non-thixotropic, which shows low elasticity (Of and Modifiers 1997). According to (Stimilli et al. 2012), the healing of asphalt binder at rest during the time sweep test was mainly associated with visco-elastic and thixotropic properties. The thixotropy phenomenon was assumed to be caused by the



removal of structure formation within the asphalt binders (Traxler.R.N 1936). However, during the development of thixotropy theory, also known as time-dependent behaviour is based on the principle of “making rate” and “breaking rate” of suspension materials (Ross et al. 1973). Moreover, according to (Shan et al. 2011), a study on thixotropic characteristics of asphalt binder indicated that under a  $0.01 \text{ (s}^{-1}\text{)}$ , shear rate viscosity changes exponentially.

## **2.5. MORPHOLOGICAL PROPERTIES OF CRMB**

To analyse the interrelationship between chemical composition and structure of asphalt binder on its rheological properties (Stulirova and Pospisil 2008). According to (Stangl et al. 2006; Stulirova and Pospisil 2008), from the microscopic point of view, the reduction in the size of fibrils indicates the stiffness of asphalt binder. To understand the surface, tiny modification of CRMB and its impact on dynamic mechanism SEM analysis could be employed (Cheng et al. 2006; Kocevski et al. 2012; Wang et al. 2011). SEM technology helps analyse the surface textures such as roughness, a bumpy surface which enhances the adhesive properties of CRMB (Xiao et al. 2018). According to (You et al. 2019), due to the mixing condition of modifiers and asphalt binder, there is a complex connection between amorphous-poly-alpha-olefin (APAO) and asphaltene phase terminal blend asphalt binder. From SEM test results, it indicated that the aggregation of CRMA in asphalt binder is disturbed by the addition of Evotherm-DAT and proves that performance properties of CRMA are not only related to chemical configuration and compositions of binders (Liu et al. 2013). Micrographs obtained from SEM can capture the pores on the surface of CR, which can absorb the light aromatic oil of asphalt binder to make it more compatible with a given base binder (Zheng et al. 2021). According to (Stulirova and Pospisil 2008), handling asphaltene microstructure during the sample preparation is critical as it may get disturbed during preparation or binder type itself.

The microscopical observation of interaction between asphalt binder and rubber particles showed a transfer of carbon black from rubber particles into asphalt binder and appearance of yellowish colour due to the presence of aromatic oils observed by rubber particles (López-Moro et al. 2013).

## 2.6. MODIFICATION IN CHEMICAL BOND OF CRMB

In the context of asphalt binder chemical analysis, the FTIR testing method is basically used to identify the chemical functional groups (Kawahara et al. 1974). The molecules of asphalt binder could be altered at particular frequencies by absorbing the infrared spectra; this principle was implemented during the analysis of functional groups (Jia et al. 2014). During the FTIR data analysis, the width and height of band spectra are considered for determining the bond strength (Yang et al. 2015). The severity of the aging effect would be analyzed using the difference in absorbance of FTIR spectra (Ali et al. 2016; Jia et al. 2014). The two main functional groups that indicate the aging effects were sulfoxide and carbonyl, which is corresponding to 1030  $\text{cm}^{-1}$  and 1700  $\text{cm}^{-1}$  spectral bands (Yao et al. 2016a)

The increased carbonyl group concentration indicates larger molecular sizes (Cortizo et al. 2004; Hamedi and Tahami 2018). The addition of date seed oil into asphalt binder illustrated a high concentration of carbonyl groups, which is directly related to the oxidation of asphalt binder (Foroutan Mirhosseini et al. 2018). The increased viscosity of an short-term and long-term aging condition was mainly associated with increased carbonyl group concentration (Foroutan Mirhosseini et al. 2018). As expected, the FTIR results show a higher aging level for PAV-aged binders than for RTFO-aged binders, followed by the un-aged asphalt binders. The long-term aged asphalt binder indicates a higher level of carbonyl and sulfoxide indices through FTIR test results than short-term aged (Abbas et al. 2013). FTIR results help recognize the presence of modifiers in PMB and its effectiveness in resisting oxidation (Bernier et al. 2012). Aging modified asphalt (MA) binder at 190°C increased oxidization of base binder present in the MA significantly was observed through FTIR results (Ghavibazoo et al. 2015).

FTIR analysis shows that adding an anti-stripping agent (ASA) to CRMB indicates the presence of amine and anhydride functional groups, which enhances the performance of binder thermally and mechanically (Tang et al. 2019). FTIR technique sensitively provides the information related to aliphatic and aromatic alteration in asphalt binder quickly (Doumenq et al. 1991; Lamontagne et al. 2001). According to (Tur Rasool et al. 2017), the characteristics of modified asphalt binder before and after

short-term and long-term aging conditions were characterized using FTIR and SEM techniques, which found some similarity to some extent. However, the FTIR results repeatability and its sensitivity for both functional groups carbonyl and sulfoxide found to be best with a minimum coefficient of variations (Hofko et al. 2017a). Higher the adhesion and stiffness behaviour represents the more chemical transformation due to oxygenated functional groups for long-term aged binders via FTIR test results (Aguiar-Moya et al. 2017).

Through FTIR analysis, the interaction between base binder and PMB was purely physical under the influence of aging characteristics (Singh et al. 2017). FTIR results can show mixing proportion between two different substances such as asphalt binder and WMA additives like sasobit and Deurex, which have a tremendous homogeneous mixing ability and compatibility (Gao et al. 2018). FTIR analysis confirmed that adding guayule resin into CRMB had no liquid phase separation for the sample obtained from the top and bottom portion of the tube (Hemida and Abdelrahman 2020). However, according to (Nivitha et al. 2016), The alteration in molecular weight distribution and functional groups due to the aging conditions of asphalt binder in the presence of sasobit was observable using FTIR (Kheradmand et al. 2015).

## **2.7. SUMMARY**

The selection of working temperature of CRMB in the presence of WMA additives plays a vital role in understanding the visco-elastic properties of the modified binder. This review presents the implementation of test methods on CRMB to evaluate visco-elastic behaviour, rutting, and fatigue properties. However, several studies are available to reduce the working temperature of CRMB using WMA additives and investigate the rutting and fatigue properties, chemical and morphological behaviour based on the laboratory's short-term and long-term aging conditions as shown in Table 2.1. Hence the discussion on behaviour of rheological parameters provides a widespread consideration of the review to resolve the issue of selecting the working temperature.

The first part of the review focused on the working temperature of CRMB. In this section, the influence of higher and lower working temperatures on the physical

and chemical properties of CRMB was included. The operating temperature directly relates to the swelling behaviour of rubber particles, which later guides the rheological properties of CRMB. However, there are no standard protocols to select the short-term aging temperature for any modified asphalt binder. Hence, adopting a suitable methodology in choosing the working temperature will better represent a modified asphalt binder. The second part of the review is focused on the viscosity behaviour of modified and neat asphalt binders concerning increasing temperature in the presence of WMA additives as shown in Table 2.2. The role of viscosity in the selection of working temperature of CRMB in the presence of different types of WMA additives was explored.

The major part of the review focused on the characterisation of rutting and fatigue properties of CRMB using DSR. The main test included in characterising the rutting performance was the frequency sweep test, temperature sweep test, time-temperature superposition (TTS), performance grading test, and Multiple stress creep and recovery tests. Next, to characterise the fatigue behaviour of CRMB, intermediate performance grading, linear amplitude sweep (LAS) test, and thixotropic test. The rutting performance was characterised by conducting the performance grade, MSCR by introducing the different short-term aging temperatures. From this test, researchers identify percent recovery and non-recoverable compliances for the given binders.

Furthermore, a thixotropic methodology was implemented to analyse the impact of short-term and long-term aging temperature on fatigue performance, which shows the tendency to flow even after removing the applied load conditions as shown in Table 2.3. Therefore, the three-stepped flow test is implemented to understand the structural response of modified asphalt binder through the structural building, breaking, and rebuilding pattern. Further, the morphological and chemical structural behaviour were determined using SEM and FTIR techniques, which obtained results comparable with rheological performance. Also, the separation tendency of CRMB with WMA additives shows sensitivity towards the storage temperature and type of WMA additives. Overall, the selection of working temperature of CRMB in the presence of WMA additives controls performance rheologically, morphologically, and chemically.

Table 2.1 Summary on effect of working temperature on rheological properties of CRMB

<b>Researchers</b>	<b>Binder Types</b>	<b>WMA additives</b>	<b>Working Temp (°C)</b>	<b>Findings</b>
(Palit et al. 2004)	CRMB	-	175-180	Significant improvement in Fatigue.
(Wang et al. 2012)	CRMB	Sasobit, RH, Advera	163	Addition of WMA improved resistance to rutting
(Oliveira et al. 2013)	CRMB	Chemical additives	155, 145, 135	Indicated a good efficiency in reducing production temperature
(Li et al. 2017)	CRMB	-	163	At low temperature creep stiffness found to be increased with degradation of CRM
(Ren et al. 2021)	CRMB	SBS	163	CRMB with fully swelled exhibited best rutting and deformation resistance.
(Tang et al. 2016)	CRMB	-	163	MSCR test results indicates that interaction temperature provide more degradation than interaction time.
(Blanchoin and Pollard 1999)	CRMB	-	163	G* increase with particle swelling and $\delta$ decrease by depolymerisation and devulcanization.
(Zanzotto and Kennepohl 1996)	CRMB	-	163	The binder sample after RTFOT, weight loss was found to be more than 1%.
(Huang et al. 2017)	CRMB	-	163	G* value of CRM found to be enhanced at both lower and higher frequencies, and weakened phase angle at lower frequencies as CRM degradation.
(Ghavibazoo and Abdelrahman 2013)	CRMB	-	163	Temperature sensitivity is depended upon type of CRM present in asphalt binder with respect to interaction temperature

Table 2.2 Summary on viscosity test temperature and rheological properties of CRMB

<b>Researchers</b>	<b>Binder Types</b>	<b>WMA additives</b>	<b>Viscosity test temp. (°C)</b>	<b>Findings</b>
(Thodesen et al. 2009)	CRMB	-	135	CRM binder viscosity depends upon the grinding process of scrap binder and base binders viscosity
(Lougheed and Papagiannakis 1996)	CRMB	-	176	Viscosity of CRMB is a function of amount of aromatic oil observation and swelling of rubber particles
(Akisetty et al. 2012)	CRMB	Aspha-min, Sasobit	135	Addition of WMA additives indicates no significant difference in resilient modulus properties at unaged and long-term aged conditions
(Billiter et al. 1997a)	CRMB	-	191	The reason for decreased viscosity of binder was identified as due to reduced size of rubber particles with curing time
(Randy C. West et al. 2006)	CRMB	-	135, 149, 163	Indicated significant difference in viscosity measurement as it depends upon binders sources
(Stroup-Gardiner et al. 1993)	CRMB	-	185	Lower viscosity base binder indicates better reaction with rubber compared to higher viscosity base binder
(Kedarisetty et al. 2016)	CRMB	Reacted & Activated Rubber (RAR)	135, 150, 160, 170, 180	Presence of RAR in base binder showed increased viscosity at higher temperature and reduced viscosity at lower temperature
(Shatanawi et al. 2012)	CRMB	Furfural activated	60	Result indicates that ambient modified binder showed higher viscosity compared to cryogenically modified binder with increasing shear rate
(Xu et al. 2015)	CRMB	Activated Crumb Rubber	130, 140, 150, 160, 170, 180, 190	The viscosity of CRMB was found to be higher compared to Activated CRMB , which provides a binder film thickness while coating the aggregate
(Xu et al. 2016)	CRMB	Elvaloy	135, 150, 165	Showed highest viscosity compared to binder modified with oxidized polyethylene, which demands higher energy for production of asphalt mixture

Table 2.3 Summary on effect of working temperature on rutting and fatigue performance of CRMB

<b>Researchers</b>	<b>Binder Types</b>	<b>WMA additives</b>	<b>Working Temp (°C)</b>	<b>Findings</b>
(Wang et al. 2012)	CRMB	Sasobit, RH Advera	163	Rheological properties tested at 52°C, 58°C, 64°C, 70°C, 76°C, 82°C
(Akisetty et al. 2011)	CRMB	Asphamin, Sasobit	176, 158	The performance characteristics of rubberised warm asphalt mixture and binder properties were compared
(Shatanawi et al. 2009)	CRMB	Water activated	-	Rheological properties of CRMB at high temperature indicated no improvement as hot water removes the light oil fractions in crumb rubber
(Xiao et al. 2012)	PG 64-22	Cecabase, Evotherm, Rediset, Sasobit	163	The failure temperature of asphalt binder found to be depended upon the type of WMA additives
(Lee et al. 2008)	CRMB	-	163	Presence of ambient CRM in asphalt binder indicated improved rutting performance compared to cryogenic CRM, means less susceptible to rutting
(Liu et al. 2009)	CRMB	-	163	With increase in CRM percentage rutting resistance found to be enhanced, which is consistent with softening point trend
(Akisetty et al. 2007)	CRMB	Asphamin, Sasobit	163	It was identified that a significant effect on high failure temperature in CRMB depends upon the type of base binder present in it
(Wasiuddin et al. 2007)	PG 64-22, PG 70-28	Sasobit, Aspha-min	163, 153, 143	Sasobit additive significantly enhanced the performance grade of asphalt binder, which is subjected to reduced working temperature when compared to Aspha-Min.
(Hossain et al. 2012)	PG 64-22	Advera	163, 150, 135	The effect of reduced short-term aging temperature on asphalt binder indicated decreased rutting resistance

(Xiao et al. 2012)	PG 64-22	Cecabase, Sasobit	163	At various frequencies, viscoelastic properties of asphalt binders with WMA additives appeared to be similar for both unaged and RTFO aged conditions
(Biro et al. 2009)	PG 64-22	Sasobit, Aspha-min	163	At any frequency (0.01 to 100 Hz) stiffness of asphalt binder found to be increased in the presence of sasobit compared to Aspha-min
(Kheradmand et al. 2015)	Pen 60/70	Sasobit	163	Asphalt binder in the presence of sasobit showed better elastic performance with lower phase angle and higher complex modulus
(Julaganti et al. 2017)	CRMB	Sasobit	163	Elastic properties of binder were found to be improved due to its increased performance grade
(Edwards et al. 2006)	Pen 160/220	Sasobit, Polyethylene Wax, Poly phosphoric Acid	163	Presence of PW or PPA in binder indicated highest stiffness from temperature between 25°C to 90°C
(Liu et al. 2013)	CRMB	Evotherm-DAT	163	Addition of Evotherm-DAT to CRMB improves high and intermediate temperature properties, except low-temperature properties
(Bouldin et al. 2001)	PG 64-22	-	163	The preliminary test result indicated that $G^*/\sin\delta$ lacks in capturing the accurate viscoelastic performance of binder
(Wasage et al. 2011)	CRMB	-	163	The prediction of non-linear creep compliances of modified binder found to be strongly dependent upon testing temperature
(Zhang et al. 2016)	CRMB	-	163	MSCR test result such as strain response and delayed elasticity analysis are vital in determining the high temperature performances of CRMB



## CHAPTER 3

### MATERIALS AND METHODOLOGY

#### 3.1. MATERIALS

Following sections includes brief information on the basic properties of various materials utilized in this research work.

##### 3.1.1. Asphalt binders

Two unmodified asphalt binders were employed in the present study as VG-30 and VG-40, followed by one crumb rubber modified binder (CRMB-55) were used. VG-30 and CRMB-55 binders were supplied by Mangalore Refinery and Petrochemicals Limited (MRPL). CRMB-55 was modified with 15% dosage of rubber granulates having gradation of 100% passing through 300  $\mu\text{m}$  sieves. VG-40 was provided by the TikiTar Industries, Mangalore (India), and was manufactured through the air blowing process by modifying the control binder (VG-30). These binders' basic properties are summarized in Table 3.1 and Table 3.2. CRMB-55 conforms and specifies the Bureau of Indian Standards specification (IS17079 2019) for modified binders.

Table 3.1 Physical properties of asphalt binder

Sl No.	Characteristics	Test results		Requirements as per IS 73:2013		Methods of test, Ref. to
		VG-30	VG-40	VG-30	VG-40	
i)	Penetration at 25°C, 100g, 5 s, 0.1 mm, <i>Min</i>	46	39	45	35	IS 1203
ii)	Absolute viscosity at 60°C, Poises	2900	3600	2400-3600	3200-4800	IS 1206 (part2)
iii)	Kinematic viscosity at 135°C, cSt, <i>Min</i>	390	490	350	400	IS 1206 (part 3/1)
iv)	Flash point (Cleveland open cup), °C, <i>Min</i>	235	235	220	220	IS 1448 [P:69]
v)	Solubility in trichloroethylene, %, <i>Min</i>	99	99	99	99	IS 1216

vi)	Softening point (R&B), °C, <i>Min</i>	48	54	47	50	IS 1205
	Tests on residue from rolling thin film oven					
vii)	test:	3.2	3.44	4	4	IS 1206 (part 2)
	a) Viscosity ratio at 60°C, <i>Max</i>					
	b) Ductility at 25°C, cm, <i>Min</i>	43	27	40	25	IS1208

Table 3.2 Physical properties of CRMB

Sl No.	Characteristics	Test Results	Requirement as per IS 17079	Methods of test, Ref to
		CRMB-55	CRMB-55	
i)	Penetration at 25°C, 100g, 5 s, 0.1 mm	35	60-30	IS 1203
ii)	Softening point (R&B), °C, <i>Min</i>	59	55	IS 1205
iii)	Flash point, COC, °C, <i>Min</i>	235	220	IS1209
iv)	Complex modulus as (G*/sinδ) at 10 rad/s at a temperature. °C, <i>Min</i>	79	64	IS 15462
vi)	Separation, difference in softening point, R&B, °C, <i>Max</i>	9.5*	4	IS 15462 B
vii)	Viscosity at 150°C, cSt	730	400-800	IS 1206 (part 2)
	Tests on residue from Thin film oven test:			IS 1206 (part 2)
viii)	a) Loss in mass, %, <i>Max</i>	0.87	1.0	IS 1206 (part 2)
	b) Change in Softening point, °C, <i>Max</i>	3	5	IS 1205
	c) Complex Modulus as (G*/Sinδ) at 10 rad/s at a temperature, °C, <i>Min</i>	76	64	IS 15462

\*Results obtained from modified aluminum tube

### 3.1.2. Warm Mix Asphalt Additives

Commercially available WMA additives such as sasobit and rediset were selected to produce the rubberized WMA binders, as shown in Figure 3.1. Rediset is a combination of surface-active agents and organic additives. Surface-active agents improve the wetting of the crumb rubber particles by reducing the surface energy of the asphalt binders and reduce the interfacial frictions between the asphalt and the crumb rubber particles. Table 3.3 shows the basic properties of Sasobit and Rediset. To

achieve laboratory mixing temperature for a rubberized asphalt binder corresponding to viscosity  $170 \pm 20$  cP, the addition of WMA additives is essential. As a result, in the current research, 4% Sasobit and 4% Rediset were blended independently with rubberized asphalt binders at  $150^{\circ}\text{C}$  using a high-speed mechanical agitator. Addition of 4% WMA dosage assist in achieving the  $170 \pm 20$  cP of viscosity which is corresponding to ideal mixing temperature under laboratory condition as per ASTM D6925. Therefore, addition of 3% and 5% of WMA dosage into asphalt binder slightly indicated higher and ideal mixing temperature (similar to 4%), respectively. A study on rheological effects of sasobit on asphalt binder at low temperature performance indicate that 4% of WMA found to be optimal (Edwards et al. 2006).

Table 3.3 Physical properties of WMA additives

Properties	Sasobit	Rediset
Ingredients	Solid saturated Hydrocarbons	Fatty polyamines Non-ionic. component
Physical state	Pastilles, flake	Solid
Colour	Off-white	Brown
Odour	Practically odourless	Amine like
Molecular weight	Approx. 1000	-
Specific gravity	0.9 ( $25^{\circ}\text{C}$ )	-
Ph values	Neutral	-
Flashpoint	$285^{\circ}\text{C}$ (ASTM D92)	$>93.3^{\circ}\text{C}$
Solubility in water	Insoluble	Insoluble in cold water
Melting Point	$106^{\circ}\text{C}$	

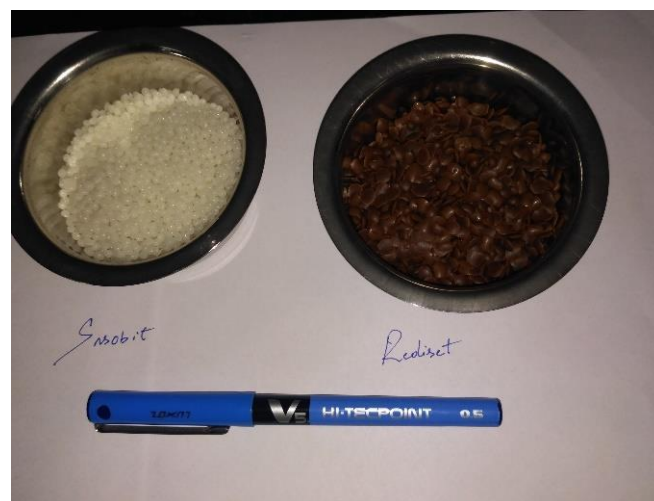


Figure 3.1 Warm mix asphalt additives (WMA); Sasobit and Rediset

### 3.2. ROTATIONAL VISCOMETER

Figure 3.2 illustrates the experimental setup adopted for this study. The aim was to determine the ideal rheological properties of CRMB-55. It was planned to select the short-term aging temperature based on the ideal mixing viscosity requirement (ASTM-D6925-15). During the preliminary viscosity study, 4% of WMA dosage by weight of asphalt binder provided the required working temperature compared to 3% and 5%. The material combination such as CRMB-55 with sasobit (4%) and rediset (4%) are named as CR-55-S-4% and CR-55-R-4%, respectively. Along with these two blends, two conventional binders, such as VG-30 and VG-40, were subjected to rotational viscometer test (ASTM D-4402), as shown in Figure 3.3. The temperature corresponding to an ideal mixing viscosity was determined for VG-30, VG-40; CR-55; CR-55-S-4% and CR-55-R-4%.

VG-30 asphalt binder was used to understand its role during short-term and long-term aging and was compared with the CRMB-55 binder. The effect of aging on CRMB-55 in the presence of WMA additives was also analyzed. In this study, 4% of WMA additives such as sasobit (S) and rediset (R), as shown in Figure 3.1, were mixed with CRMB-55 at 150°C for 15 mins using a mechanical agitator.



Figure 3.2 Rotational viscometer apparatus



Figure 3.3 Determining the viscosity of CRMB using spindle no. 27

### 3.3. THE SHORT-TERM AND LONG-TERM AGING PROCESS

The temperature corresponding to this ideal viscosity was chosen for short-term aging using a rolling thin film oven (RTFO) for all these binders, along with the standard

aging temperature as per ASTM D2872, as shown in Figure 3.4. In Figure 3.5 a horizontal cooling rack is used to hold cylindrical glass container with binder's samples, which can be rotated horizontally after pouring the sample. This test was intended to measure the effect of heat and air on a moving film at 163°C, 177°C, and 195°C temperatures, which simulate the mixing of asphalt mixture at hot mix asphalt plants.

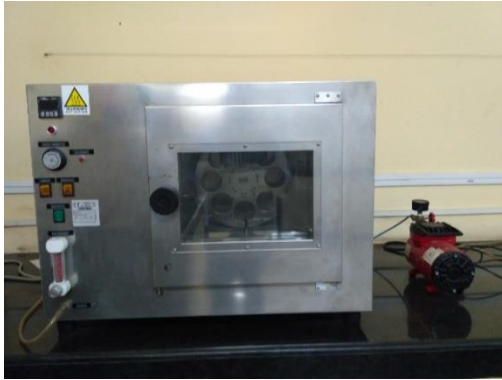


Figure 3.4 RTFO Apparatus



Figure 3.5 Samples placed on a cooling rack after short-term aging

### 3.4. DYNAMIC SHEAR RHEOMETER

The visco-elastic properties of these short-term aged binders were determined using dynamic shear rheometer (DSR) MCR-502 as per (ASTM D7175), as shown in Figure 3.6. The samples were prepared as per ASTM D7175 using silicon mould, as shown in Figure 3.7. The test was conducted using parallel plate geometry with 25 mm diameter at 1 mm gap for all the binders, as shown in Figure 3.8.



Figure 3.6 DSR Apparatus (MCR-502)



Figure 3.7 Silicon mould holding 25mm dia. sample

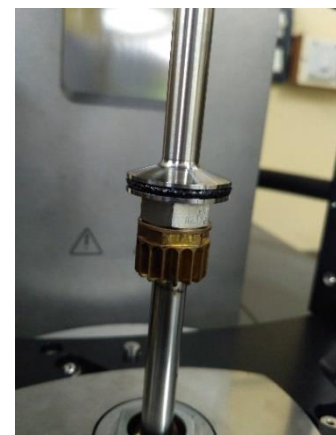


Figure 3.8. 25mm dia. parallel plate geometry

The rheological properties of VG-30 and CRMB-55 with WMA additives were conducted using an Anton Paar MCR 502 dynamic shear rheometer. A rolling thin film oven (RTFO) is used as per ASTM D2872 to simulate the short-term aging effect, which is caused during mixing and placing asphalt mixture in the field. To simulate the short-term aged effect, three different aging temperatures are 163°C, 177°C, and 195°C for 85 minutes. Similarly, pressure aging vessel (PAV) at 100°C for 20 hours of time duration with 2.1 MPa air pressure was used as per ASTM D6521 to simulate the long-term aging effect as shown in Figure 3.9, which reflects the aging of in-service pavement for many years.



Figure 3.9 PAV apparatus and samples

#### 3.4.1. Frequency Sweep Test

Frequency sweep tests were also carried out from 100 rad/s to 0.1 rad/s. The test temperature was fixed at 60°C. The complex shear modulus ( $G^*$ ) and the phase angle ( $\delta$ ) parameters were then used to evaluate the rheological properties.  $G^*$  is a measure of the total resistance to deformation of the asphalt binder; it is a ratio of maximum shear stress to maximum shear strain. The amount of phase shift ( $\delta$ ) is the gap between the applied strain and the stress responses during a test and is a measure of the viscoelastic behaviour of the material. Typically, a frequency of 10 rad/s simulates the shearing action corresponding to a traffic speed of about 88 km/h (Akisetty et al. 2010).

### 3.4.2. Temperature Sweep test

Temperature sweep tests from 44 °C to 88 °C, were performed at a heating rate of 1°C/min at a fixed angular frequency ( $\omega$ ) of 10 rad/s with an applied sinusoidal strain linear viscoelastic region (within the LVER region).

### 3.4.3. Time-Temperature Superposition Test

The effect of short-term aging is better understood by conducting the time-temperature superposition (TTS) test and its rheological response at a wide range of applied frequencies to plot a master curve for the rubberized asphalt binder containing the WMA additives. In the present experimental work, the modified asphalt binder was tested over a wide range of temperature (20°C, 30°C, 40°C, 50°C, 60°C, 70°C, and 80°C) and frequency (100, 63.1, 39.8, 25.1, 15.8, 10, 6.31, 3.98, 2.51, 1.58, 1, 0.63, 0.39, 0.25, 0.15, and 0.1 rad/sec). Further, the master curve was for a reference temperature of 30°C. The reduced angular frequency was determined by using the shift factors according to the William, Landel, and Ferry (WLF) method, as expressed in Eq. 3.1

$$\log a_T = \frac{C_1(T - T_0)}{C_2 + (T - T_0)} \quad \text{Eq. 3.1}$$

Where  $a_T$  – is the shift factor,  $C_1$  and  $C_2$  remain equation coefficients, which depend on the aging effect of material properties and reference temperature ( $T_0$ ), and  $T$  is the test temperature in (°C) from which the shift factor is determined.  $C_1$  and  $C_2$  are empirical constants adjusted to fit the values of the parameter at shift factor,  $G_g$  is glass modulus assumed equal to 1 GPa. The master curve for the complex shear modulus ( $G^*$ ) according to the Christensen, Anderson, and Marasteanu (CAM) model as shown in Eq. 3.2 was plotted

$$|G^*| = G_g \left[ 1 + \left( \frac{\omega_c}{\omega} \right)^v \right]^{-\frac{\omega}{\omega_c}} \quad \text{Eq. 3.2}$$

where  $G^*$  is the complex shear modulus,  $G_g$  is the glass modulus,  $\omega_c$  is the cross-over frequency, and  $v$  and  $\omega$  represent shape parameters for the master curve

The time-temperature superposition was done according to William Landel Ferry equation, in which the master curve for  $G^*$  was calculated manually at 30°C reference temperature.

#### 3.4.4. Performance Grade Test

The Superpave rutting parameter,  $G^*/\sin\delta$ , was used to evaluate high-temperature PG of VG-30 and CRMB-55 binders. The failure temperature corresponding to 1 kPa and 2.2 kPa for unaged and RTFO aged binder were determined. The rutting parameters of all the binders was measured at various temperature (46°C, 52°C, 58°C, 64°C, 70°C, 76°C, 82°C, and 88°C). The test was conducted using a 25 mm diameter parallel plate with 1 mm gap thickness subjecting strain within the LVER at 10 rad/s as per AASHTO T 315.

#### 3.4.5. Multiple Stress Creep Recovery Test

The MSCR test measures the rutting performance of a binder by measuring percent recovery (%R) and non-recoverable creep compliance ( $J_{nr}$ ). This test involves 10 loading and unloading cycles with a creep load for 1s followed by a recovery period of 9s under 0.1 kPa and 3.2 kPa stress levels. In the present study, the MSCR tests were conducted on VG-30, CRMB-55 with and without WMA additives (sasobit and rediset) which were subjected to short-term aging at 163°C, 177°C, and 195°C temperatures and tested at 64°C using 25 mm diameter sample with 1 mm thickness as per ASTM D7405. The %R commonly used indicates elastic recovery of modified binders after removing the applied stress or unloading condition. Higher the %R, lesser the deformation of a pavement, lesser the  $J_{nr}$  value, better the rutting resistance of a binder. The strain values recorded during the MSCR test were used to determine R(%) and  $J_{nr}$  parameter, respectively, as follows:

$$R(\%) = \frac{(\epsilon^1 - \epsilon^{10})}{\epsilon^1} \times 100 \quad \text{Eq. 3.3}$$

$$J_{nr} = \frac{\epsilon^{nr}}{\sigma} \quad \text{Eq. 3.4}$$



Where,  $R(\%)$  =percent recovery;  $\epsilon^1$ =strain recorded at the end of 1s;  $\epsilon^{10}$ =strain recorded at end of the 10-s creep phase;  $J_{nr}$ =nonrecoverable creep compliance ( $\text{kPa}^{-1}$ );  $\epsilon^{nr}$  = nonrecoverable strain value recorded at the end of the rest period; and  $\sigma$  =applied stress level (kPa) applied during the creep loading phase.

Stress Sensitivity can be calculated as follows:

$$J_{nr\_diff}(\%) = \frac{J_{nr\_3.2} - J_{nr\_0.1}}{J_{nr\_0.1}} \times 100 \quad \text{Eq. 3.5}$$

Where,  $J_{nr\_diff}$  = difference in nonrecoverable creep compliance between 0.1 and 3.2 kPa;  $J_{nr\_3.2}$  and  $J_{nr\_0.1}$  represents the nonrecoverable creep compliance value corresponding to 3.2 and 0.1 kPa stress level, respectively.

#### 3.4.6. Linear Amplitude Sweep Test

LAS test is conducted to understand the fatigue performance of asphalt binder in a shorter duration using viscoelastic continuum damage (VECD) principle at intermediate temperature. To estimate the fatigue performance, the samples were subjected to frequency sweep from 0.1 to 30 Hz followed by a linear increase in load amplitude from 1% to 30% with an increasing rate of 1% per round to determine undamaged and accumulated damage property, respectively. LAS test procedure was followed as per AASHTO TP101 specification using DSR with 8 mm diameter parallel plate for 2 mm gap thickness.

The following is a brief of how the fatigue performance of the binders was predicted using LAS test results and the VECD model.

To determine damaged parameter  $\alpha$ , a material constant, which is dependent, is calculated by converting dynamic modulus  $[|G^*(\omega)|]$  and phase angle  $[\delta(\omega)]$  for each frequency from the frequency sweep test into storage modulus as shown in Eq. 3.6,  $G'(\omega)$

$$G'(w) = |G^*(\omega)| \times \cos \delta (\omega) \quad \text{Eq. 3.6}$$

A best-fit straight line is applied between  $\log \omega$  and  $\log G'(\omega)$  as shown in Eq. 3.7, which is the form of

$$\log G'(\omega) = m(\log \omega) + b \quad \text{Eq. 3.7}$$

Using  $m$  value  $\alpha$  is obtained by converting the following transformation as shown in Eq. 3.8:

$$\alpha = 1/m \quad \text{Eq. 3.8}$$

The damage accumulation in the sample is calculated using the below summation Eq. 3.9

$$D(t) = \sum_{i=1}^N [\pi\gamma_0^2 (C_{i-1} - C_i)]^{\alpha/1+\alpha} (t_i - t_{i-1})^{1/1+\alpha} \quad \text{Eq. 3.9}$$

Where:

$$C(t) = \frac{|G^*(t)|}{|G^*|_{initial}} \quad \text{Eq. 3.10}$$

$|G^*|_{initial}$  is the initial undamaged value of  $|G^*|$

$\gamma_0$  is an applied strain for a given data point

$|G^*|$  is complex shear modulus, MPa

$\alpha$  is a material constant

$t$  is testing time

Relationship between  $C(t)$  and  $D(t)$  can be fitted using Eq. 3.11 the below power law

$$C(t) = C_0 - C_1(D(t))^{C_2} \quad \text{Eq. 3.11}$$

Where:

$C_0=1$

$C_1 C_2$  is curve fitting coefficient

Damage accumulation at failure, ( $D_f$ ) as shown in Eq. 3.12

$$D_f = \left( \frac{C \text{ at Peak}}{C_1} \right)^{1/C_2} \quad \text{Eq. 3.12}$$

Binder fatigue performance can be calculated as shown below Eq. 3.13

$$N_f = A_{35}(\gamma_{max})^{-B} \quad \text{Eq. 3.13}$$

Where:

$\gamma_{max}$ =the maximum expected binder strain (%)

In which parameter A and B can be calculated as below Eq. 3.14

$A_{35}$ : 35% reduction in integrity parameter as the failure point

$$A = \frac{f(D_f)^k}{k(\pi I_D C_1 C_2)^\alpha} \quad \text{Eq. 3.14}$$

Where:

$f = \text{loading frequency (10 Hz)}$

$$k = 1 + (1 - C_2)\alpha \quad \text{Eq. 3.15}$$

And

$$B = 2\alpha \quad \text{Eq. 3.16}$$

### 3.4.7. Thixotropy Test

The experimental procedure was developed from previous studies (Mouillet et al. 2012). The selected binder types subjected to thixotropic test protocol were VG-30 as per (IS: 73 2013) and CRMB-55 binders (IS15462 2004). The experimental device used is a dynamic shear rheometer MCR-502, an environmental chamber using a parallel plate geometry (diameter 8 mm, gap 2 mm) as the sensor system. This parallel plate geometry was chosen to provide a similar effect caused by vehicle movements on the long-termed aged roads. The thixotropic behavior of binders is studied in dynamic mode using a rotational stress application, versus time at a relatively lower stress level to permanent destruction at 25°C test temperature. First, the experimental procedure consists of short-term and long term aged samples and measuring the viscosity in three different stepped shear rate in a nonlinear domain. Then, a shear rate from 0.1 to 1(s<sup>-1</sup>) is applied aimed at disturbing or destructuring the sample in a sensitive way and finally the recovery is presumed to be linked to the re-arranging of disturbed sample as monitored in the linear viscoelastic domain.

The detailed experimental protocol is as follows:

1. The shear rate at 0.1(s<sup>-1</sup>) for 90 sec allows the sample's viscosity to gradually increase to the constant value in such a way that sample molecules are accumulated like a long chain.
2. Shear rate increases from 0.1 to 1 (s<sup>-1</sup>) for 5 sec to cause a sensitive destructuring of the selected samples.
3. In step three shear rate is decreased to 0.1 (s<sup>-1</sup>), same as step-1 to monitor the viscosity recovery for 90 sec.

It is worth noting that the viscosity curves X-axis exhibit durations expressed in seconds, as there is a structural formation in the first part of the curve. Figure 3.10 represents the stepwise application of the shear rate to analyze the thixotropic behavior. The second part of the curve destructuring is induced by increasing the shear rate from 0.1 to 1 ( $s^{-1}$ ) and in the final part of the curve, restructuring was build-up by maintaining the shear rate back to 0.1 ( $s^{-1}$ ) versus the time. The viscosity parameter has a clear mechanical meaning only with the sensible shear rate and test temperature. Also, the selection of a higher shear rate, which destructs sample molecules, is required to describe the behavior of the recovery phenomenon as it informs about the evolution of the overall material stiffness during the rest period.

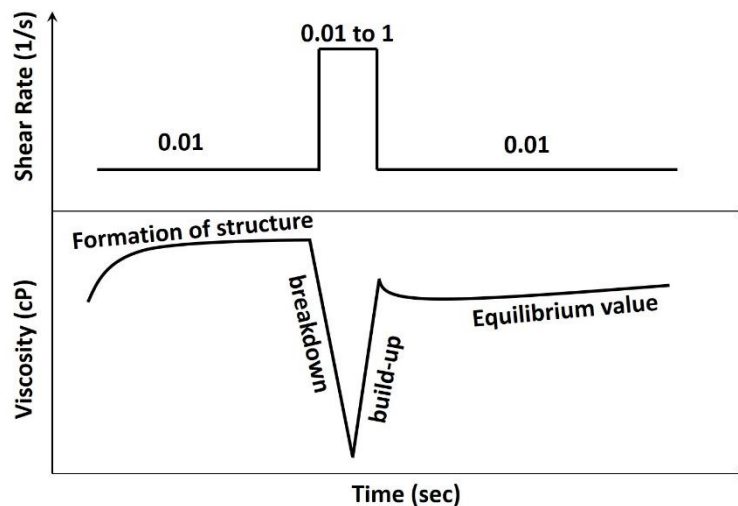


Figure 3.10 The characteristic curve of asphalt binder's thixotropic behavior in dynamic mode (Barnes and Barnes 1997)

### 3.4.8. Storage Stability Test

A significant problem with CRMB is phase separation, which causes the settlement of CR particles in any high-temperature storage conditions. Settlement leads to improper dispersion of rubber particles in CRMB, and, due to this, the quality of the modified binder becomes inferior, which cannot be ignored. To investigate this, a storage stability test was conducted using an aluminum tube as shown in Figure 3.11 with a 25-mm diameter and a 126-mm height as per ASTM D7173 (ASTM 2015a). In this test, a 50 gm CRMB sample with and without WMA additives was placed in the

aluminum tube and kept at a constant 163°C, 177°C, and 195°C for 48 h, and it was then kept in a freezer at -5°C for a minimum period of 4 hours.

Finally, the aluminum tube was cut into three equal parts, and a softening point was determined on CRMB samples taken from the top and the bottom portion of the tube. A CRMB selection was considered stable if the softening point difference between these two portions was less than 2.2°C.

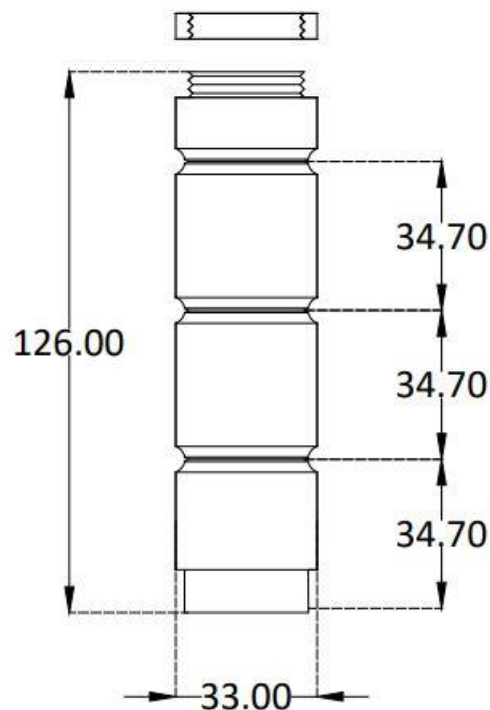


Figure 3.11 Aluminum tube used for storage stability test

### 3.4.9. Short and long-term aging simulation of asphalt binder

Asphalt binders are aged during blending and agitation in the hot mixing facility and during the placement of asphalt mixtures because of the high temperature and airflow involved in the process. This form of aging is called short-term aging. The RTFO procedure is used to simulate short-term aging. After asphalt pavement is constructed, aging continues, but the oxidation mechanism dominates because of the relatively moderate temperatures of the environment. The PAV is used to simulate years of in-service aging in a pavement called long-term aging. Different aging levels of

asphalt were simulated in the lab using the RTFO test and the PAV test. Except for the aging temperature, the RTFO test procedures were conducted according to ASTM D2872 (ASTM 2012). Three different aging temperatures of the RTFO test were set, 163°C, 177°C, and 195°C, and the test time was 85 min. The PAV test was consistent with ASTM D6521 (ASTM 2018); the sample was aged 20 h in a vessel with 2.10-MPa air pressure and 100°C aging temperature. After acquiring asphalt of different aging levels, the DSR and the FTIR tests with attenuated total absorbance (ATR) were used to analyze the aging process.

### 3.4.10. Scanning Electronic Microscopic and Fourier transform infrared spectroscopy Test

Surface morphology and elemental composition of the thin film, as shown in Figure 3.12, were analysed using a scanning electron microscope (Carl Zeiss FE-SEM) with a linked electron dispersion X-ray (EDX) detector operating at an accelerating voltage of 5 kV. Samples were observed at room temperature using various magnification levels such as 15K X and 1K X.



Figure 3.12 SEM Specimens prepared without slanting slide



Figure 3.13 FTIR Specimens

The RTFO and PAV aged CRMB binders' surface morphology was analyzed using a scanning electron microscope (Carl Zeiss FE-SEM) with a linked electron dispersion X-ray (EDX) detector operating at an accelerating voltage of 5 kV. A small drop of the CRMB binder was placed on the top of the cover glass size of 50 mm X 50 mm and kept in a hot oven with 150°C temperature for 5 mins in a slanting position

(Yue et al. 2021) as shown in Figure 3.14. The morphologies of unaged CRMB and PAV aged CRMB binder with and without WMA additives were investigated by determining the dispersed state of the asphaltene-like structure in the CRMB binder. All the samples were coated with a gold sputtering.



Figure 3.14 Specimens for SEM image analysis

FTIR spectroscopy is utilized to determine the changes in the chemical composition of asphalt binders, which are subjected to a different level of short-term aging temperature. In this study, the FTIR test was conducted using a Bruker (Alpha) ATR spectroscopy having a wavenumber range from 500 to 7500  $\text{cm}^{-1}$ . The binder specimens were spread on a cover glass with a thickness of around 0.1 mm, as shown in Figure 3.13. The test was conducted for VG-30 and CRMB-55 aged at 163°C, 195°C, followed by CR-55-S-4% and CR-55-R-4%. Therefore to understand the evolution of bonding structure due to short-term aging at high temperature.

Also, Fourier Transform Infrared Spectroscopy (FTIR) analysis was conducted to characterize the effect of RTFO and PAV aging temperature of CRMB with WMA additives and compare with VG-30 binder. Due to the material's unique light-absorbing characteristics, a chemical functional group could be identified. A small piece of aged CRMB binders was placed onto the ATR diamond crystal of an FTIR spectrometer (Bruker Alpha) and measured consequently. The outline of the test plan is displayed in Figure 3.15. In addition, presence of 3% of WMA additives to CRMB-55 binder exhibited higher viscosity at high temperature i.e., it intersected with 170±20 cP viscosity line at higher working temperature. Whereas, effect of 5% of WMA dosage

on working temperature of CRMB-55 binder were found to be same as addition of 4% of WMA dosage.

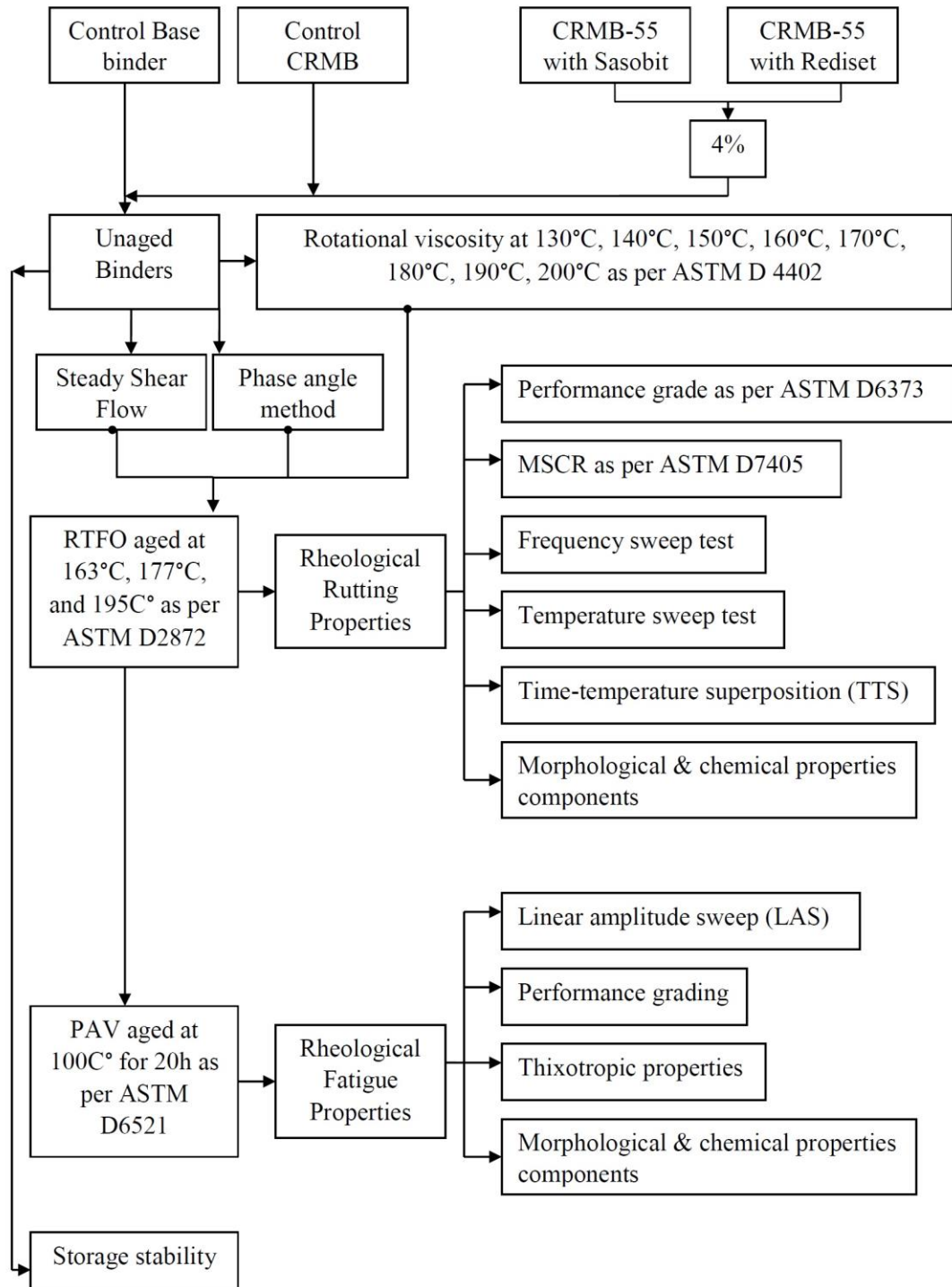


Figure 3.15 Experimental flow chart



## **CHAPTER 4**

### **SELECTION OF OPTIMUM WORKING TEMPERATURE OF CRMB**

#### **4.1. GENERAL**

This chapter explains the method of selecting suitable working temperatures under laboratory conditions for base binders and modified asphalt binders. Working temperature is a temperature implemented during the production of hot-mixed asphalt mixtures (150°C-200°C), transportation, and in paving stages. This chapter aimed at determining the working temperature of asphalt binder by following approaches, (a) Equiviscous Temperature method using rotational viscometer; (b) Steady Shear Flow method and; (c) Phase angle method using a dynamic shear rheometer. To evaluate the effect of these three methods on selecting the working temperature of base binder (VG-30, VG-40) and modified asphalt binder (CRMB-55) for unaged conditions were considered. Viscoelastic properties such as the master curve of CRMB with WMA additives were further determined from the temperature and frequency sweep test. Working temperatures determined by each method are analysed and selected for short-term aging under laboratory conditions using rolling thin film oven test as per (ASTM D 2872-12 2012). Further, the effect of these selected working temperatures on mass loss (volatility of asphalt) was evaluated and correlated with softening point for the short-term aging binders.

#### **4.2. LABORATORY EXPERIMENTAL PLAN**

This study also aimed at determining the working temperature of base and modified asphalt binder with WMA additives concerning its mass loss during short-term aging conditions. It is common to carry out the short-term aging process in the laboratory to simulate the approximate changes in rheological properties of binders that occurred during conventional hot-mixing asphalt plant. A rotational viscometer (RV) test was

carried out at various temperatures from 135°C to 195°C as per (ASTM-D4402 2015). The temperature corresponding to 170±20 cP viscosity was chosen as the optimum working temperature [MS-2 Asphalt Institute 1996a]. Spindle no. SC4-21 and SC4-27 were used to determine the viscosity of the base and modified asphalt binder, respectively. It consists of a rotational viscometer, which can measure the torque required (should be between 10 to 98%) to rotate the spindle. A temperature-controlled thermal chamber heater is used to maintain the temperature of the asphalt binder stored in the sample chamber, which is reusable. The procedure followed in determining mixing temperature using equiviscous method is given below.

1. The viscosity of unaged VG-30, CRMB-55 and CRMB-55 with different WMA additives (with 4% dosages) was measured over a wide range of temperatures (135°C–200°C at 5°C intervals) using a Brookfield viscometer [ASTM D4402].
2. A binder sample CRMB-55 of 10.5 g was tested with a spindle no. 27 in the rotational viscometer at 140°C initially.
3. Whereas, base binder VG-30 was tested by weighing 8.5 g sample using spindle no. 21 in a rotational viscometer at 135°C initially.
4. While testing the binder samples using Brookfield viscometer, shear rates were applied ranging between 6.8 s<sup>-1</sup> to 93 s<sup>-1</sup>, with corresponding RPM from 20 to 100. Therefore, spindle speed is selected in such a way that it develops resistance torque between 10 and 98%.
5. The mixing temperature, which indicates workability of hot mix asphalt mixture in the plant, was determined corresponding to viscosity 0.17±0.02 Pa.s.

Dynamic shear rheometer (DSR) steady shear flow test was carried out with 25mm diameter parallel plate at 1 mm gap for 76°C, 82°C, and 88°C (West et al. 2010). The viscosity of the binders was recorded over a range of shear stress. Using a log-log temperature-viscosity analysis, the viscosity corresponding to 500 Pa shear stress were plotted and extrapolated to 180°C. As per the equiviscous principle, the temperature corresponding to viscosity 170±2 cP was found to be a suitable working temperature.

The phase angle method developed by Casola (West et al. 2010) consists of performing frequency sweep from 0.1 to 100 rad/s with 16 points per decade at 50°C, 60°C, 70°C, and 80°C maintaining shear strain at 12% using DSR. Phase angle master curve was developed at 80°C reference temperature using modified Williams-Landel –Ferry (WLF) equations Eq. 4.1 and Arrhenius functions shown in equation Eq. 4.2

$$\log a(T) = \frac{-19(T - T_d)}{92 + T - T_d} \quad \text{Eq. 4.1}$$

Where,

$\log a(T)$  = Shift factor (Williams-Landel-Ferry equation) for ( $T > T_d$ )

T = Temperature (°C)

$T_d$  = Defining temperature

$$\log a(T) = 13016.07 \left( \frac{1}{T} - \frac{1}{T_d} \right) \quad \text{Eq. 4.2}$$

Where,

$\log a(T)$  = Shift factor (Arrhenius function) for ( $T < T_d$ )

T = Temperature (°C)

$T_d$  = Defining temperature

The region between 90° and 85° of phase angle master curve indicates the transition from viscous to viscoelastic behaviour of asphalt binder. A power law regression was fitted between frequency and mixing temperature by Casola. The frequency corresponding to 86° was considered a reasonable method to determine mixing temperature using the frequency-temperature relationship as shown in Eq. 4.3.

$$\text{Mixing Temperature } (^\circ\text{F}) = 325 \omega^{-0.0135} \quad \text{Eq. 4.3}$$

Where,

$\omega$  = frequency (radians/sec.)

Therefore, the above methods helped select the base's appropriate working temperature and modified the asphalt binder in the presence of WMA additives. The

flow chart for the experimental research plan of selection of working temperature is shown in Figure 4.1. In this research work, three different test methods (equiviscous temperature, Steady shear flow and phase angle method) were carried out on base and modified asphalt binder. Further, the effect of selected working temperature on asphalt volatility is analysing the changes in mass loss of both base and modified asphalt binder and correlating the mass loss behavior concerning softening point after short-term aging at selected working temperature.

Therefore, selecting the appropriate working temperature helps investigate the experimental laboratory results such as rheological, morphological, and chemical structural changes in base and modified asphalt binder before approval of asphalt binder. Though determining the mixing and compaction temperature of asphalt binder originated from the equiviscous concept for many decades, implementing this concept on the modified binder and applying the same temperature during the laboratory investigation is needed for clear understanding.

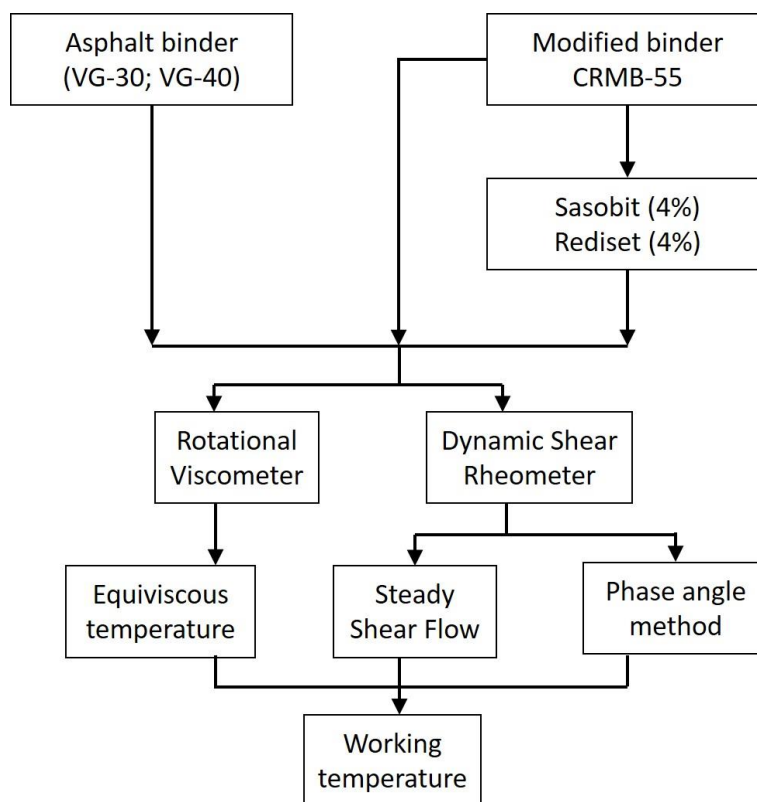


Figure 4.1 Flowchart for experimental research plan of working temperature

### **4.3. RESULTS AND DISCUSSIONS**

The results and discussions of the present investigations are discussed in the following sections.

#### **4.3.1. Equiviscous temperature Method**

Various researchers have reported this test method for different asphalt binders, which helped determine the mixing and compaction temperature through traditional equiviscous temperatures. As per the viscosity reduction with temperature, the dosage of Sasobit (S) and Rediset (R) was found to be 4% (by weight of CRMB-55). The results of the rotational viscometer test on base and modified asphalt binder are presented in Figure 4.2. The curves of viscosity versus temperature from the equiviscous temperature method have been plotted for base binders (VG-30, VG-40), modified binder (CRMB-55), and CRMB-55 with Sasobit and Rediset (CRMB-55+S; CRMB-55+R).

It is clear from the plot that as the temperature increased, the viscosity value decreases for the type of binders irrespective of modification and the presence of WMA additives in binders. For example, the viscosity value of CRMB-55 can be observed to be highest by approximately 1.4, 1.6, and 3.0 times than CRMB-55+R, CRMB-55+S, and base binder (VG-30 and VG-40) respectively at 140°C. While comparing the working temperature of all the binders corresponding to 170 cP viscosity, CRMB-55 was observed to be highest compared to binders with WMA additives and base binder. This comparison was made due to the presence of WMA additives in CRMB. The increase in viscosity of CRMB-55 was due to the fact of CRM particles.

Moreover, it is also noted that the viscosity of CRMB-55+S and CRMB-55+R decreases the working temperature by 18°C compared to the CRMB-55 binder only based on the equiviscous temperature method. Such a response indicates the temperature used during the short-term aging process of CRMB-55 binders needs to be investigated. This result is essential in the sense that the selection of working temperature under laboratory conditions in the presence of WMA additives must be increased by 14°C, i.e., 177°C, compared to standard short-term aging temperature 163°C. It can be further seen that the working temperature of base binder (VG-30 and

VG-40), CRMB-55 with sasobit and rediset additives, and CRMB-55 was found to be 160°C, 177°C, and 195°C, respectively. However, the working temperature is evaluated in the following section using the steady shear flow and phase angle method. The results are in line with the findings reported by (Dondi et al. 2016; Yildirim et al. 2006), where viscosity was sensitive to the subject temperature for all the types of asphalt binder.

Various model parameters that fit the binders' viscosity curve were obtained from the exponential decay function through non-linear fit analysis. The different model parameters obtained from the exponential function for all the binders are presented in Table 4.1.

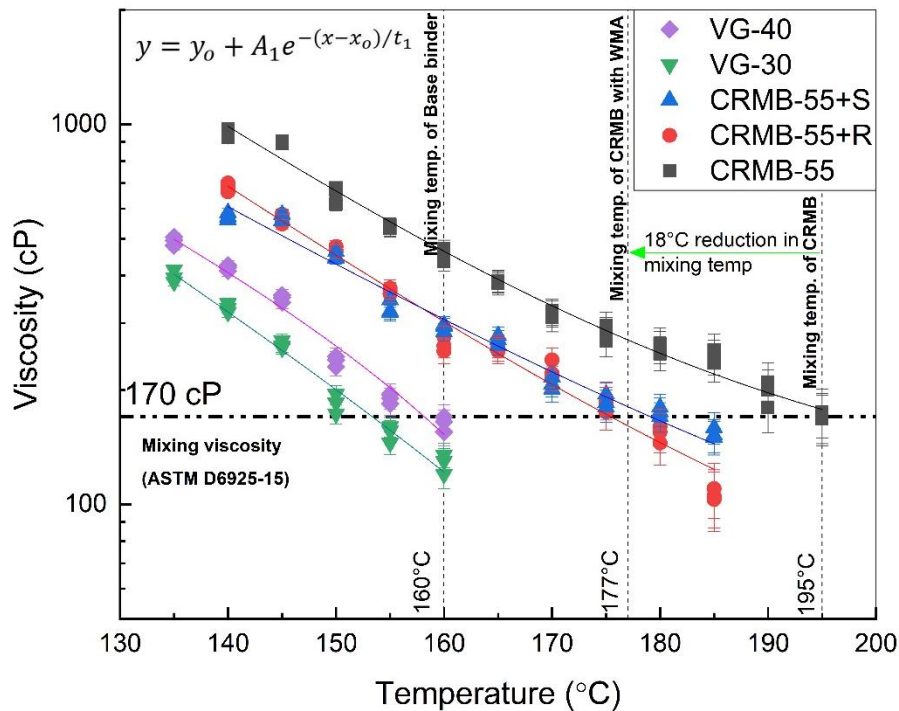


Figure 4.2 Equiviscous temperature test results

Table 4.1 Non-linear curve fit parameters

Binder Type	$y_0$	$x_0$	$A_1$	$t_1$	$R^2$	$F$ -value	$p$ -value
CRMB-55	115.1	140.5	874.21	21.21	0.986	812.36	< 0.001 (Y)
CRMB-55+R	4.69	141.03	647.45	24.88	0.991	1067	<0.001 (Y)
CRMB-55+S	50.81	142.22	515.88	24.95	0.975	492.26	<0.001 (Y)
VG-30	-19.22	138.58	359.45	23.2	0.979	447.99	0.002 (Y)
VG-40	-164.47	143.38	519.58	33.4	0.961	245.87	0.004 (Y)

Table 4.2 depicts the results of One-Way ANOVA test for all the computed viscosity parameters of VG-30, VG-40, CRMB-55 and CRMB-55 with WMA additives. Computed  $F$ -values are indicated for each compared experimental dataset. Moreover, ‘Y’ in the brackets depicts ‘Yes, the difference is statistically significant. In the case of binder CRMB-55+S the transition of temperature from 140°C to 195°C significantly affected the viscosity. Furthermore, at all the temperatures, each individual binder was observed to impart a statistically significant effect on viscosity. The  $p$ -value can alternatively be interpreted as the susceptibility of all types of binders to undergo the change in the measured viscosity parameter as a function of applied temperature. Hence, statistically significant test results will represent a role of viscosity parameter in the selection of mixing temperature. Based on such a method of analysis, it can be observed that the viscosity of base binder and CRMB will be less susceptible by addition of WMA additives caused due to application of high temperature.

Table 4.2 One-Way ANOVA significance test results viscosity

Parameter	One-Way ANOVA		
	Binder Type	F-value	p-value
Viscosity (cP) behaviour	CRMB-55	250.673	<0.001(Y)
	CRMB-55+R	322.203	<0.001(Y)
	CRMB-55+S	185.729	<0.001(Y)
	VG-30	381.024	<0.001(Y)
	VG-40	499.389	<0.001(Y)

#### 4.3.2. Steady Shear Flow Method

Based on the outcome obtained from the steady shear flow test method as discussed earlier, continuous shear flow viscosity measurement was carried by applying series of shear stress levels from 0.33 Pa to 500 Pa. further the viscosities corresponding to 500 Pa shear stress for 76°C, 82°C, 88°C, and 94°C temperatures were plotted between a log viscosity and log temperature chart as shown in Figure 4.3. The data were extrapolated to obtain the working temperature corresponding to 170 cP.

Asphalt binder VG-30, VG-40, CRMB-55 and CRMB-55 with WMA additives such as sasobit and Rediset viscosity test results are shown in Fig 4.3. At 500Pa stress level, the viscosity of CRMB-55 at 76°C, 82°C, 88°C, and 94°C found to be highest followed by CRMB-55+S, CRMB-55+R, VG-40 and VG-30, respectively. Using these

experimental data, viscosity value can be extrapolated at higher temperature. However, after extrapolation an inflection point in viscosities were observed at 110°C test temperature for binders, CRMB-55+S, CRMB-55+R, and VG-40. At 170 cP viscosity of CRMB-55+S, CRMB-55+R, and VG-40 intersect at 152°C, 158°C, and 163°C mixing temperature, respectively. The difference in the mixing temperature of CRMB-55+S, CRMB-55+R with equiviscous were found to be 25°C, and 19°C, respectively. Therefore, the difference in the viscosity result exists primarily for CRMB-55 with WMA additives and unmodified binders, where steady shear flow methods generally yield lower mixing temperature.

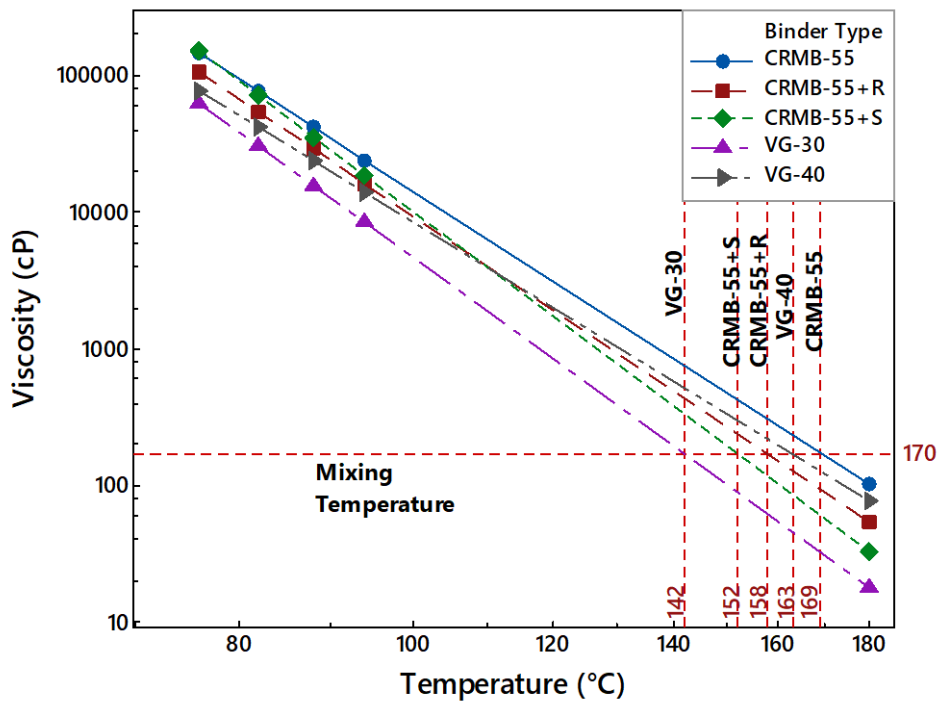


Figure 4.3 Steady shear Flow test results

The working temperature was substantially lower than the equiviscous temperature method. There was a more significant difference between modified binders, i.e., CRMB-55 binder, which shows a shear-thinning effect due to higher shear rates. The steady shear flow methods indicated that it yields lower working temperatures for CRMB-55, CRMB-55 with sasobit and rediset additives, and base binder by 20°C compared to the equiviscous temperature method.



### 4.3.3. Phase Angle Method

The mixing temperature determined using the phase angle method for CRMB-55 is shown in Figure 4.4. The frequency corresponding to 86° phase angle was found to be 5.96 rad/s. For modified binder CRMB-55, the working temperature using the phase angle method was substantially lower than the equiviscous method. The working temperature of CRMB-55 was 158.4°C, which is 36.6°C lower than the equiviscous temperature method. Similarly, in Figure 4.5, CRMB-55+S showed 163.9°C, 13.1°C lower than the equiviscous method.

Furthermore, from Figure 4.6, CRMB-55+R illustrates 163.9°C, which is similar to the previous case. However, the frequency corresponding to 86°C for both CRMB-55+S and CRMB-55+R failed to intersect the master curve at 80°C reference temperature. These illustrate that the phase angle method, i.e., the Casola model, lacks the ideal working temperature compared to the equiviscous and steady-state flow method. However, steady shear flow and phase angle methods are conducted at lower temperatures than actual mixing temperatures. Hence, the fundamental changes of modified binders at higher temperatures cannot be evaluated. Therefore, this study focuses on the equiviscous, i.e., higher temperature viscosity method as it is affected by actual mixing temperature. The interaction plot of working temperature with different techniques and binder types, as shown in Figure 4.7, represents that CRMB-55 has the highest working temperature for equiviscous temperature, steady shear flow method when compared to the phase angle method. Overall, the equiviscous method showed higher working temperature, which is more practical as in field condition than steady shear flow and phase angle method.

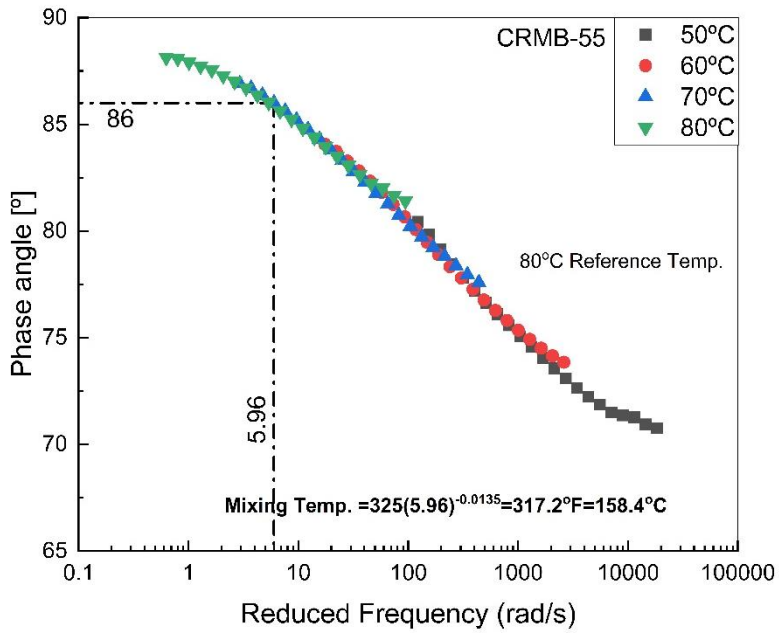


Figure 4.4 Phase angle method test results of CRMB-55

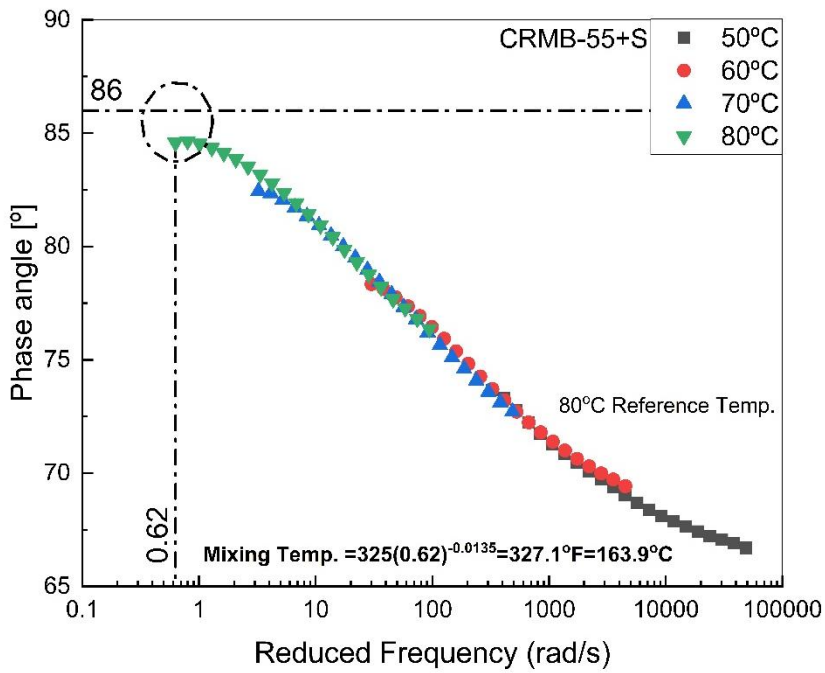


Figure 4.5 Phase angle method test results of CRMB-55+S

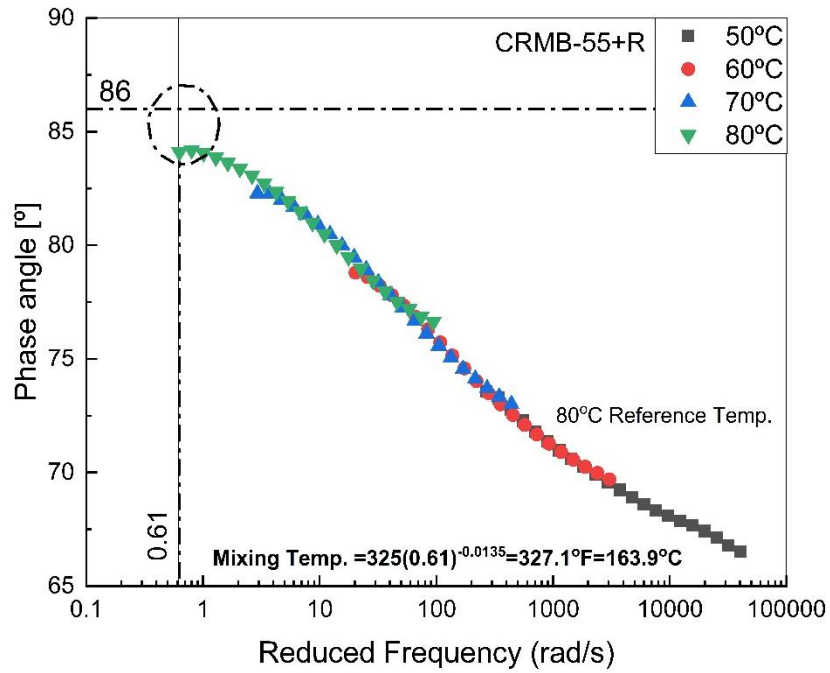


Figure 4.6 Phase angle method test results of CRMB-55+R

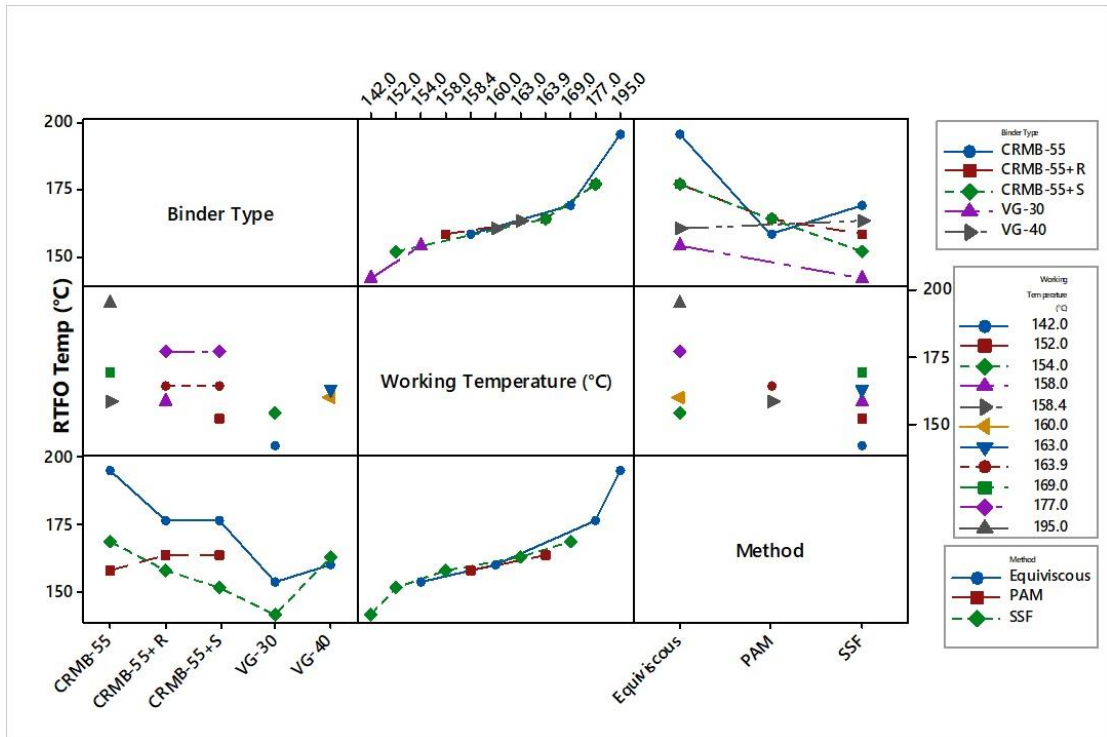


Figure 4.7 Interaction plot of working temperature with type of binders and methods

#### 4.3.4. Effect of working temperature on Mass Loss of asphalt binder

Figure 4.8 to Figure 4.12 depicts the relative change in the value of the percentage mass loss when the binder is subjected to the different short-term aging temperatures. In this study, the different short-term aging temperatures were selected from equiviscous methods such as 163°C, 177°C, and 195°C for base binder, WMA additives with CRMB-55 only, respectively. Figure 4.8 shows that the percentage mass loss of VG-30 increases with increase working temperature from 163°C to 195°C with a linear trend. VG-30 is subjected to RTFO test at 195°C mixing temperature by assuming the hypothesis that if such a binder is used in the preparation of CRMB-55 modified binder. In that case if CRMB-55 is subjected to such a high working temperature may provide insight information related to behaviour of rheological properties of two factors i.e. dependence upon base binder (liquid phase) present in it and presence of rubber particles. VG-40 binder, as shown in Figure 4.9, represents the absence of asphalt volatility as it offers a decreasing trend with the lowest percent mass loss.

Furthermore, binder CRMB-55 as shown in Figure 4.10, indicates more % mass loss but with a constant trend with increased working temperature. Exp3P2 fit is an exponential function whose exponent is a 2<sup>nd</sup> order polynomial as shown in Figure 4.9 to Figure 4.10. However, modified binder CRMB-55+R and CRMB-55+S, as shown in Figure 4.11 and Figure 4.12, respectively represented an increasing trend, i.e., mass loss increases exponentially with increased working temperature. However, Figure 4.12 clearly illustrated that the asphalt volatility is conserved in CRMB-55+S initially from 163°C working temperature compared to CRMB-55+R binder.

This may lead to an inappropriate short-term aging effect on asphalt binder during its rheological property investigation. Therefore, these initial findings demonstrate that selecting the short-term aging temperature impacts asphalt volatility through percentage mass loss of all the binders, which is also supported by the softening point in the following sections.

Using the statistical analysis tools, analysis of various binders is conducted using the Minitab application to plot the interaction effects. The combination of experimental

data such as, RTFO aging temperature, binder type, and percentage mass loss (%) is sorted. By setting the single interaction parameter ‘percentage mass loss’ and assigning the factors affecting the behaviour of the parameter such as binder types and mixing temperatures, the presence of interaction is determined. In an interaction plot one of the factors such as percentage change in mass loss is held constant to determine the response of second factors, such as binder types, and mixing temperatures.

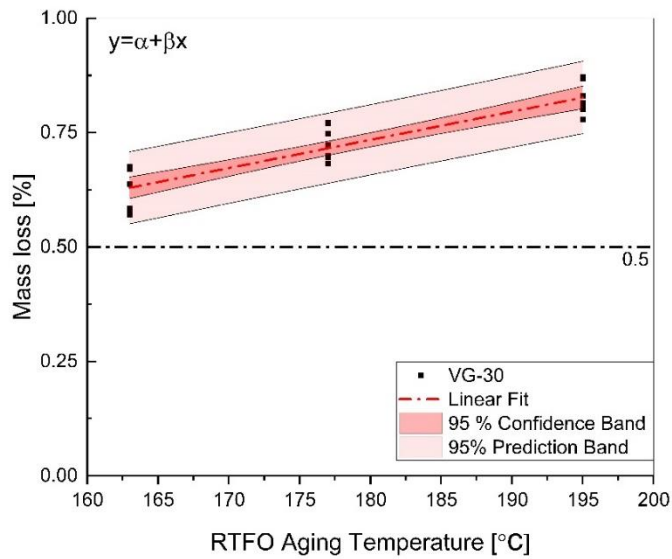


Figure 4.8 Mass loss of VG-30

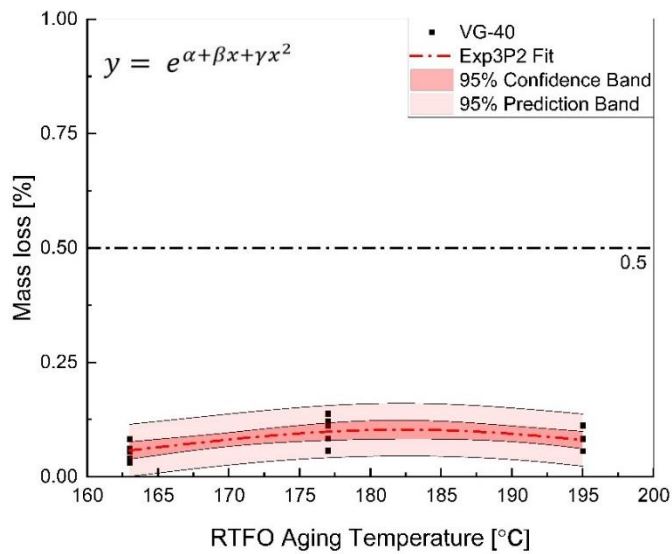


Figure 4.9 Mass loss of VG-40

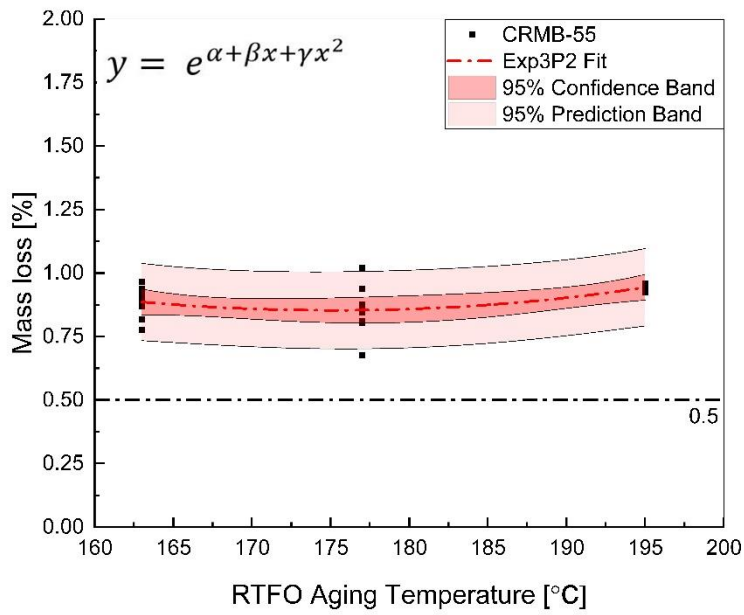


Figure 4.10 Mass loss of CRMB-55

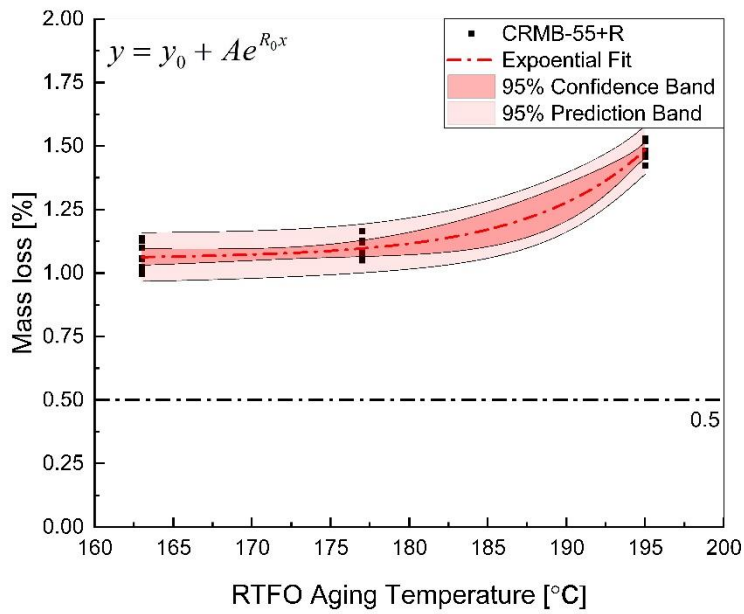


Figure 4.11 Mass loss of CRMB-55+R

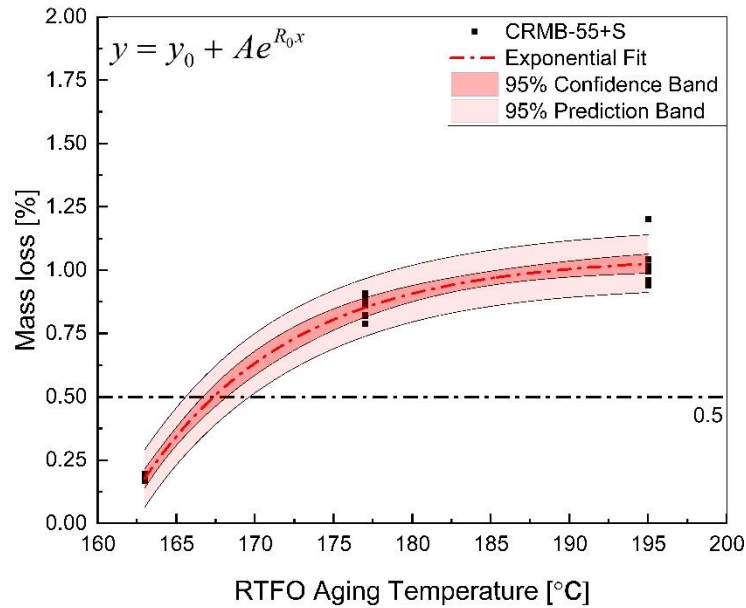


Figure 4.12 Mass loss of CRMB-55+S

Table 4.3 depicts the results of One-Way ANOVA test for all the computed percentage mass loss parameters of VG-30, VG-40, CRMB-55 and CRMB-55 with WMA additives. In the case of binder VG-30, CRMB-55+R, and CRMB-55+S with respect to RTFO aging temperatures from 163°C, 177°C, and 195°C significantly affected the percentage mass loss. Whereas, at all the temperature, binders such as VG-40 and CRMB-55 were observed to impart statistically not significant effect on percentage mass loss (%). The  $p$ -value of binders VG-40 and CRMB-55 implies that they are not susceptible to change in RTFO aging temperatures. Hence, observation of statistical analysis results of percentage change in mass loss (%) parameter is very vital.

Table 4.3 One-Way ANOVA significance test results of % mass loss.

Parameter	One-Way ANOVA		
	Binder Type	$F$ -value	$p$ -value
Percentage change in Mass loss (%)	VG-30	43.026	<0.060(Y)
	VG-40	0.270	<0.960(N)
	CRMB-55	44.355	<0.243(N)
	CRMB-55+R	25.801	<0.044(Y)
	CRMB-55+S	32.699	<0.001(Y)

From figure 4.13, it was observed that base binder VG-30 and VG-40 have less percentage loss than modified binders. Finally, the interaction plot of percentage mass loss as shown in Figure 4.13, represents that higher working temperature has more impact on all the binders, reducing the volatility and increasing the stiffness compared to the 177°C and 163°C. Moreover, when CRMB-55+S is subjected to 163°C working temperature, as observed in Figure 4.13, it shows lesser mass change, which means the binder failed to release the volatile content compared to 177°C and 195°C working temperature.

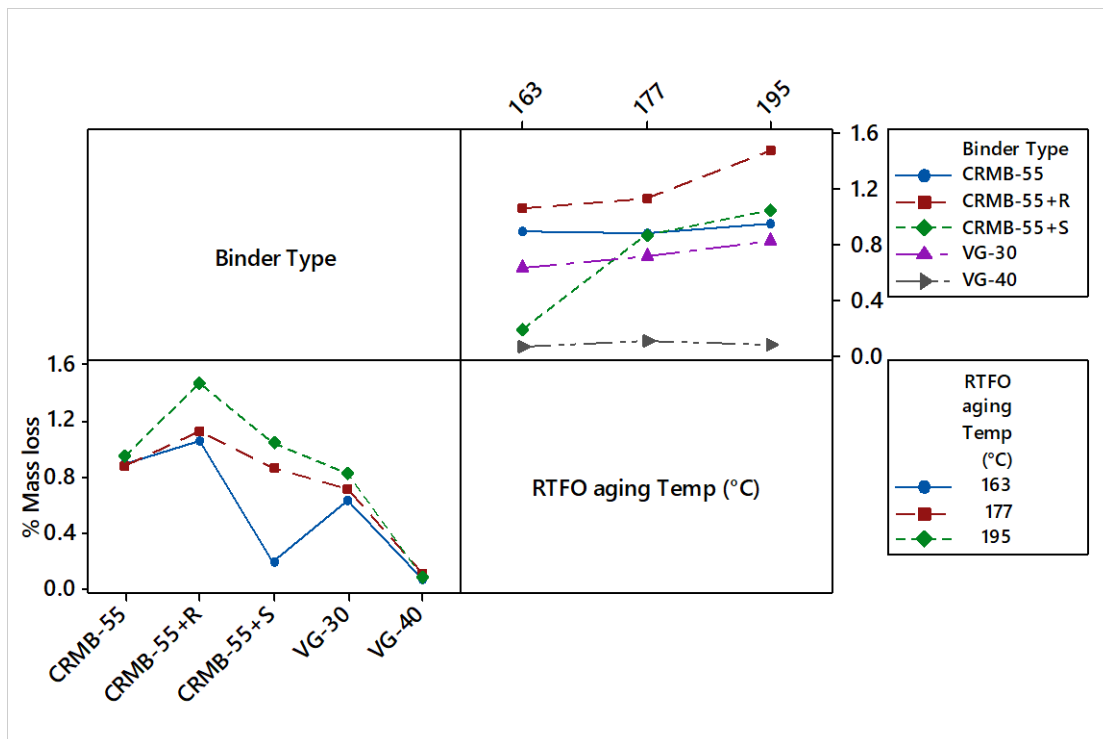


Figure 4.13 Interaction plot of percentage mass loss with RTFO aging temperature and type of binders

#### 4.3.5. Correlation Study

To understand the variation of percentage mass loss and softening point as a function of working temperature, wherein change in percent mass change and softening point were caused due to asphalt volatility, a correlation study was conducted. Figure 4.14 to Figure 4.18 illustrate the obtained correlation between percentage mass loss and softening point of VG-30, VG-40, CRMB-55, and CRMB-55 with sasobit and rediset, respectively, as a function of working temperature.



As discussed in prior sections, % mass loss increases with increased short-term aging temperature, decreasing the asphalt volatility due to advanced aging temperature. The  $R^2$  ranging from 0.89 to 0.95 represents a ‘good to the excellent correlation between % mass loss and softening point for all the binders. However, Figure 4.15 indicates that VG-40 has a poor correlation, which may be due to low volatile content prior short-term aging process. Therefore, the binder can be arranged in the following order from the good to poor correlation point: VG-30, CRMB-55+R, CRMB-55+S, CRMB-55, and VG-40. Hence, percentage mass loss and softening point provide the effect of laboratory aging conditions on viscoelastic properties. Therefore, caution should be taken while selecting temperature during the short-term aging process under laboratory conditions. A comprehensive chemical study is recommended, which is aimed at addressing the above concerns.

To describe the correlation between the percentage mass loss (Y) and softening point (x) after short-term aging at 163°C, 177°C, and 195°C temperatures, linear, exponential, and power models have been proposed, the following Eq. 4.4, Eq. 4.5, Eq. 4.6 describes, respectively, and a and b are the regression constants.

$$Y = a + bx \quad \text{Eq. 4.4}$$

$$Y = e^{a+bx} \quad \text{Eq. 4.5}$$

$$Y = ax^b \quad \text{Eq. 4.6}$$

Furthermore, Table 4.4 summarises the measured parameter values and  $R^2$  achieved for linear, exponential, and power models. It can be observed that for VG-30 and CRMB-55+R, all the three linear, exponential, and power models were observed to represent ‘good’ fitting to the experimental results. However, for CRMB-55 and CRMB-55+S, ‘fair fitting’ was observed based on three models. While, all models was observed to depict ‘poor’ fit for VG-40 binder, which is subjected to short-term aging 163°C, 177°C, and 195°C. Overall, it can be concluded that linear, exponential, and power models can be adopted for predicting the mass loss (%) as a function of softening

point for short-term aged binders VG-30, CRMB-55, CRMB-55+R, and CRMB-55+S with a ‘fair’ to ‘good’ strength. The interaction plot of softening point with binder types and different working temperatures, as shown in Figure 4.19, describes that CRMB-55+S was stiffer than the rest of the binders.

Table 4.4 Regression constant and coefficient of determination for linear, exponential, and power models

Binder Types	Linear Model						
	a	Std.Error	b	Std.Error	R <sup>2</sup>	F-value	P-Value
VG-30	-1.2600	0.4344	0.033	0.0071	0.75	21.03	0.002
VG-40	-0.2280	0.5629	0.005	0.0089	0.04	0.308	0.595
CRMB-55	0.1619	0.2595	0.010	0.0037	0.52	7.447	0.029
CRMB-55+S	-22.990	8.7798	0.264	0.0981	0.51	7.278	0.030
CRMB-55+R	-2.6780	0.8182	0.052	0.0110	0.76	22.57	0.002
Exponential							
VG-30	-2.9360	0.5862	0.043	0.0096	0.73	937.44	0.001
VG-40	-5.4000	6.7418	0.046	0.1062	0.03	20.406	0.002
CRMB-55	-0.9890	0.3064	0.012	0.0044	0.53	1690.9	0.0001
CRMB-55+S	-30.170	12.616	0.332	0.1399	0.47	26.81	0.0012
CRMB-55+R	-3.1140	0.6363	0.044	0.0085	0.79	670.4	0.001
Power Model							
VG-30	1.3E-05	0.0001	2.65	0.5830	0.74	953.38	0.001
VG-40	2.8E-07	0.0001	3.04	6.7211	0.04	20.466	0.002
CRMB-55	2.7E-02	0.0349	0.818	0.3035	0.51	1635.7	0.001
CRMB-55+S	9.5E-71	0.0001	35.8	13.512	0.46	25.92	0.001
CRMB-55+R	8.1E-07	0.001	3.3	0.6451	0.78	645.7	0.001

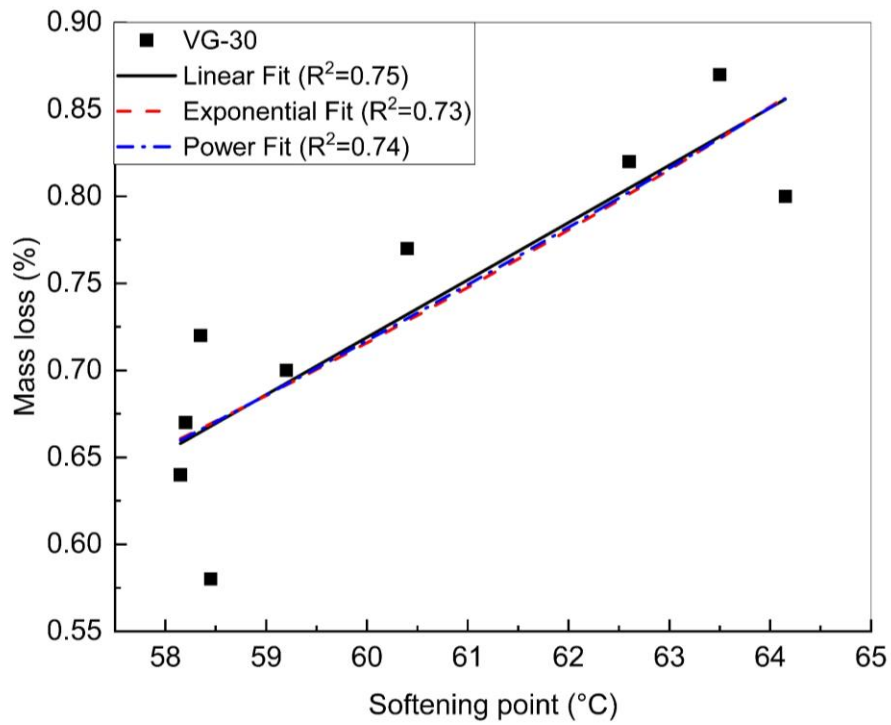


Figure 4.14 Correlation between mass loss and softening point of VG-30

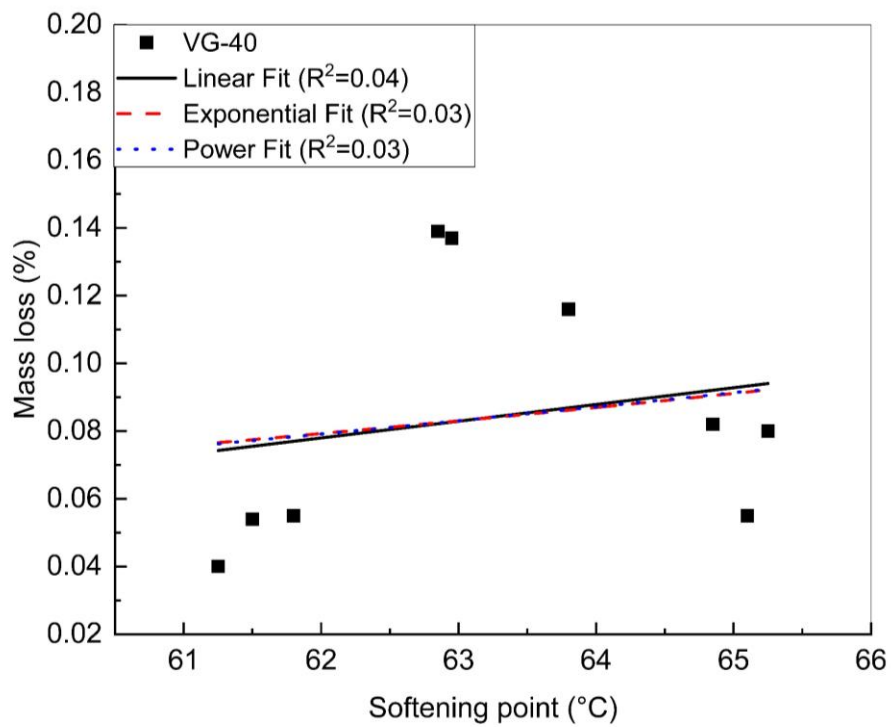


Figure 4.15 Correlation between mass loss and softening point of VG-40

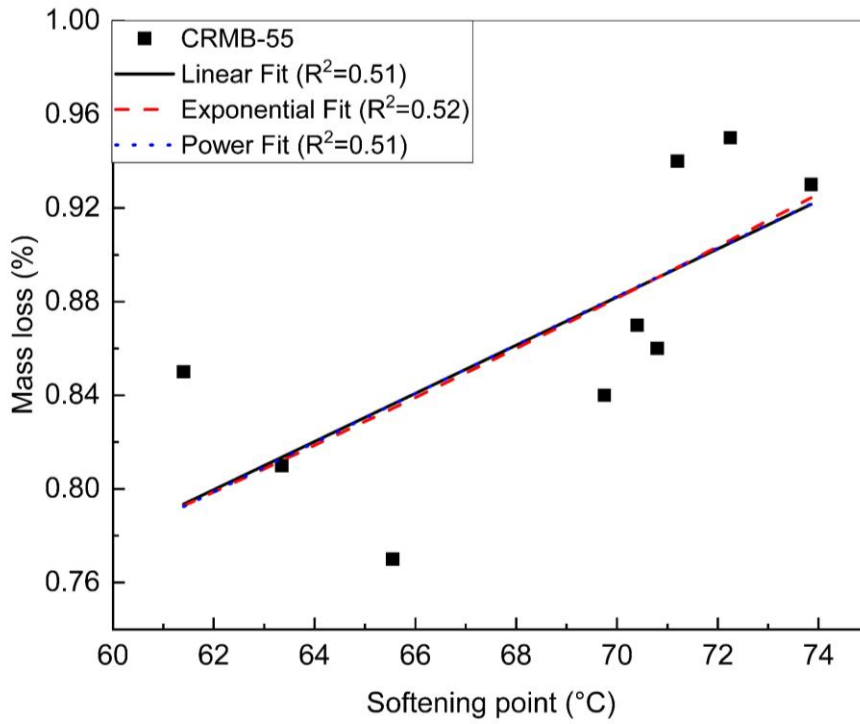


Figure 4.16 Correlation between mass loss and softening point of CRMB-55

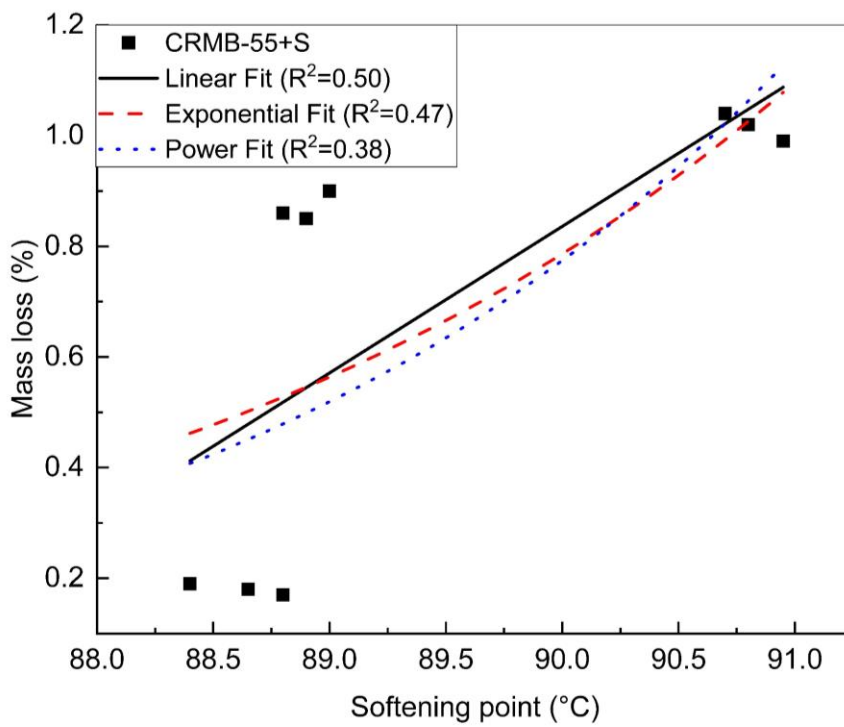


Figure 4.17 Correlation between mass loss and softening point of CRMB-55+S

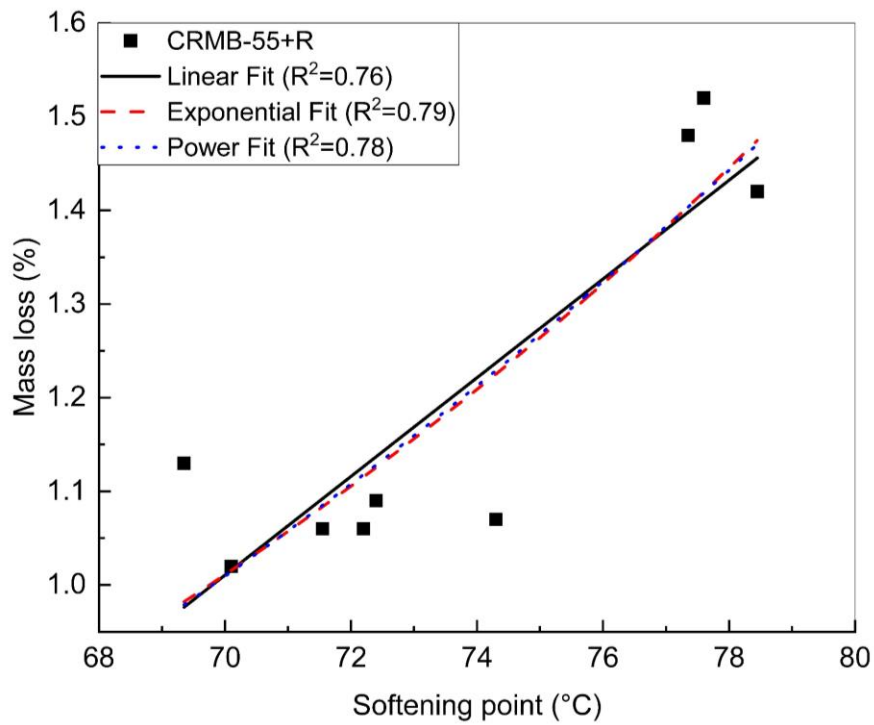


Figure 4.18 Correlation between mass loss and softening point of CRMB-55+R

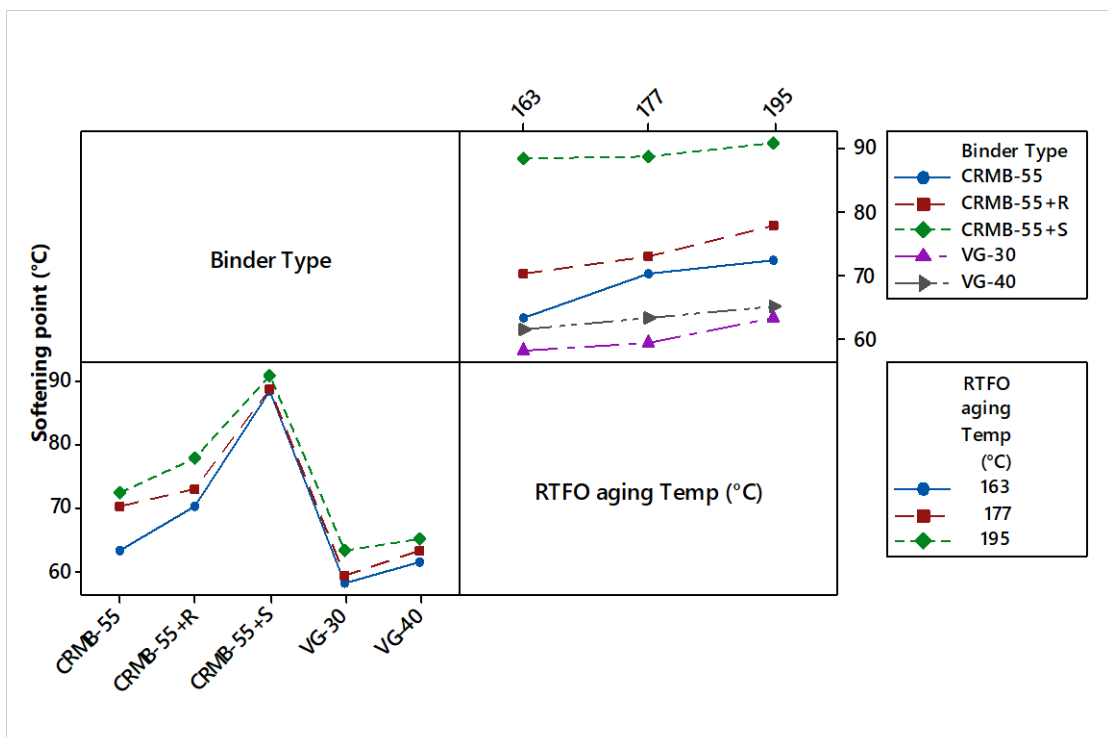


Figure 4.19 Interaction plot of softening point with RTFO aging temperature and type of binders

#### 4.4. SUMMARY

This chapter investigated the method of determining the working temperature based on the appropriated mixing viscosity as per ASTM D2403 in estimation of mixing temperature. Developing the temperature–viscosity relationship for a given asphalt binder and establishing the temperature corresponding to viscosity range  $170\pm 20$  cP for mixing. Subsequently, temperature ranges were established for all type of binders that exhibit Newtonian fluid characteristics at high temperature. The method used to determine the mixing temperature were, equiviscous temperature method using rotational viscometer, steady shear flow and phase angle methods using DSR, respectively. The determined working temperature for VG-30, VG-40, CRMB-55 and CRMB-55 with WMA additives under laboratory conditions mass loss of each binders were investigated. Based on the test results, the following have been obtained.

1. Working temperature corresponding to steady shear flow and phase angle methods found to be lower than equiviscous test method for VG-30, VG-40 and CRMB-55 (with and without WMA additives) binders, which is practically form a concern during the coating of aggregates.
2. Comparing the mass loss data of all binders clearly indicates that with increase in working temperature mass loss increases due to the evaporation of volatility of the binders. However, mass loss of VG-40 binder observed to be least among the other binders.
3. The correlation study between mass loss and softening point indicated that with increase in loss of volatility of binder it increases its softening point, which becomes stiffer in nature.

## **CHAPTER 5**

# **INFLUENCE OF WORKING TEMPERATURE ON RUTTING PERFORMANCE OF CRMB WITH WMA ADDITIVES**

### **5.1. GENERAL**

This chapter aims to assess and analyze the rutting performance of CRMB-55 with WMA additives such as sasobit and rediset at different aged working temperatures. To determine the visco-elastic and rutting behaviour such as complex shear modulus ( $G^*$ ) and phase angle ( $\delta$ ) of CRMB-55 with different working temperatures, frequency sweep test, temperature sweep test, and time-temperature superposition (TTS) were conducted. To determine rutting performance of asphalt binders, multiple stress creep recovery test ( $J_{nr}$ , %R) and high-performance grade test ( $G^*/\sin\delta$ ) were conducted. In this study, the analysis of visco-elastic test results focused at 60°C for different frequency and temperature sweeps. The test was conducted to understand the frequency and temperature susceptibility of CRMB-55 and base binders. Also, to examine the stress sensitivity for different working temperatures, %R and  $J_{nr}$  were calculated. In addition to the rutting performance evaluation of CRMB-55, surface morphological and storage stability were analysed using SEM images and aluminum tubes.

### **5.2. EXPERIMENTAL PLAN FOR RUTTING PERFORMANCE OF CRMB**

A rolling thin film oven test (RTFO) was initially conducted at three different aged working temperatures, 163°C, 177°C, and 195°C, to understand the viscoelastic response and rutting performance behaviour of base and modified binder with WMA additives. Subsequently, surface morphology and storage stability tests were carried out for different short-term aging and storing conditions, respectively, as shown in Figure 5.1. The test matrix adopted for the rutting performance study are presented in Table 5.1. Typically, frequency of 10 rad/s simulates the shearing action effects in asphalt

mixture corresponding to traffic speed of approximately 55 mph / 88 Kmph (Xiao et al. 2012). The frequency sweep test reflects the condition of pavements affected by the traffic speed at 60°C temperature. The rheological properties of asphalt binder vary in a specific pattern as a function of both temperature and loading time particularly below 60°C. Therefore, measuring the rheological properties above this temperature cannot adequately be extrapolated to describe the behaviour of asphalt binder below 60°C temperature.

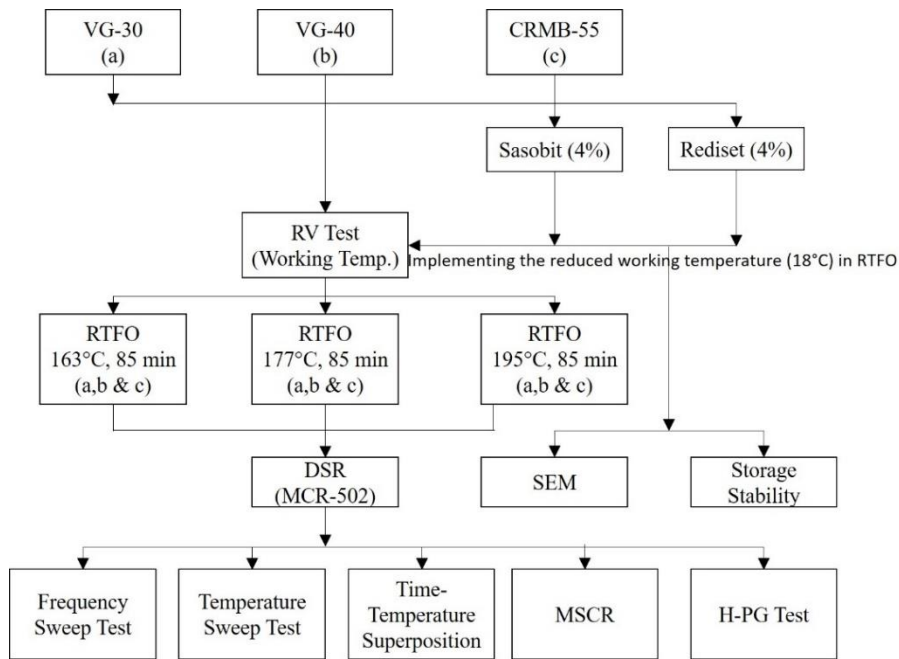


Figure 5.1 Flowchart for an experimental plan of visco-elastic and rutting studies on modified binders

Further, the modified binder's surface morphology and storage stability were analysed for different aged working temperatures, 163°C, 177°C, and 195°C and different storing temperatures, respectively.

Table 5.1 Details on different binder's matrix for the rutting performance study

Test type	Temperature (°C)	Frequency (rad/s)	Strain (%)	Binder types	No. specimens
Temperature sweep test	44 - 88	10	LVER	5	5x3x3
Frequency sweep test	60	0.1 to 100	LVER	5	5x3x3
TTS	20 - 80	10	LVER	3	3x3x3



MSCR	64	-	0.1 & 3.2 kPa stress level	5	5x3x3
H-PG	46 – 88	10	LVER	5	5x3x3

### 5.3. RESULTS AND DISCUSSION

The results and discussion of the present investigation are discussed in the following sections.

#### 5.3.1. Frequency Sweep Test

Using the complex shear modulus ( $G^*$ ) and the phase angle ( $\delta$ ) of the CRMB-55 in comparison with the base binder (VG-30 and VG-40), the effect of short term aging temperature at 163 °C, 177 °C, and 195 °C were evaluated. The influence on  $G^*$  for frequency sweep at high temperatures was found to be highly dependent on the short-term aging temperatures, in addition to binder type and rubber concentration. The RTFO aging temperature for the base binders and CRMB-55 appears to have the most significant effect. The results of the frequency sweep test at 60 °C are shown from Figure 5.2 to Figure 5.7. The variation of  $G^*$  and  $\delta$  with frequency by using the different short-term aging temperatures of 163 °C, 177 °C and 195 °C for VG-30, VG-40, and CRMB-55 binders are shown in Figure 5.3, Figure 5.4, and Figure 5.5, respectively. According to Figure 5.2,  $G^*$  of CRMB-55 were found to be improved with increase of frequency compared to VG-30 and VG-40 base binders. Furthermore, in the case of RTFO aging at 163 °C, the  $G^*$  for CRMB-55 still appeared to dominate compared with the base binder VG-30 and VG-40 in the overall frequency.

Fig 5.2 shows the structural response of VG-30, VG-40 and CRMB-55 for unaged conditions subjected to a range of frequencies.  $G^*$  and  $\delta$  of VG-30, VG-40 and CRMB-55 binders found at different frequencies. At all frequencies, at unaged conditions CRMB-55 showed enhanced complex shear modulus ( $G^*$ ) i.e., elastic and viscous properties were improved at both low and high frequencies compared to VG-30 and VG-40 binders. High frequencies simulate higher traffic conditions and vice-versa (Julaganti et al. 2017). This indicates that CRMB-55 resists rutting performance due to the swelling nature of rubber particles, which depends upon the availability of light oil fractions in the binders (Airey et al. 2004; Wang et al. 2020).

At 163°C aged working temperature as shown in Fig 5.3, indicates that there is increase in  $G^*$  value of CRMB-55, VG-30, and VG-40 compared to their unaged conditions, respectively. This clearly proves that with application of working temperature on any binders there is an alteration in light oil fractions, which may or may not enhance the viscoelastic properties depending upon the presence of type of modifiers for a given range of frequencies. However, the stiffness difference between CRMB-55 and VG-30, VG-40 observed to be decreased in terms of  $G^*$  and  $\delta$  phase with introduction of working temperature along the range of frequencies.

However, for the RTFO aging at 177 °C, as shown in Figure 5.4, it was observed that the  $G^*$  behaviour for the CRMB-55 and VG-30 and VG-40 base binders was getting close to each other throughout the frequency sweep. In other words, it represents optimum RTFO aging temperature in which the base binder and the rubber particles show a relative contribution of stiffness at the time of mixing and pavement performance without getting much damage. By increasing the aging temperature to 195 °C using RTFO, the  $G^*$  of the CRMB-55 and the VG-30 and VG-40 overlapped each other, showing a vastly changed structure of the CRMB-55 as well as of the base binder (VG-30 and VG-40) as shown in Figure 5.5.

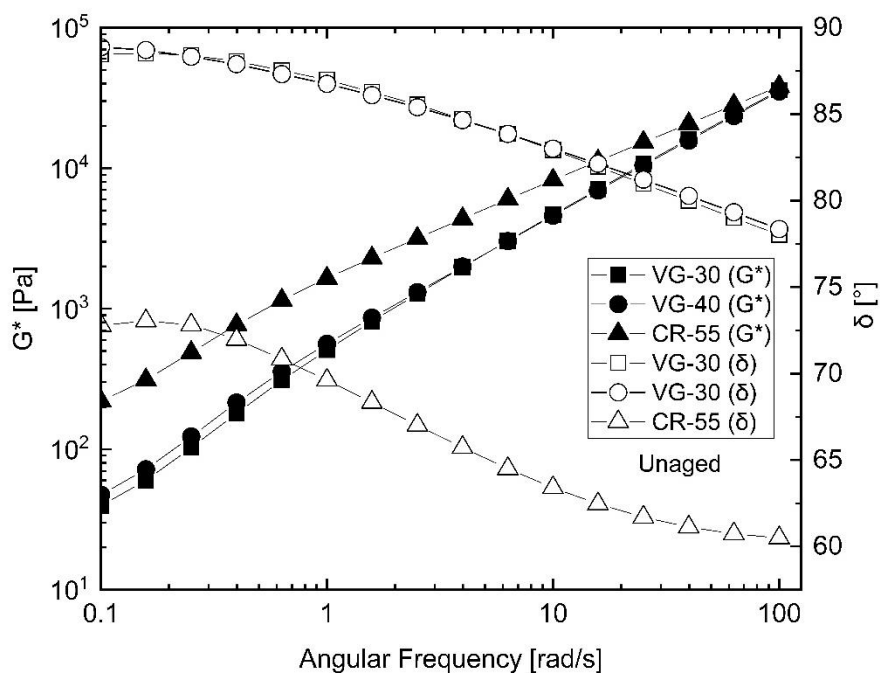


Figure 5.2 Effect of frequency on  $G^*$  and  $\delta$  for unaged conditions

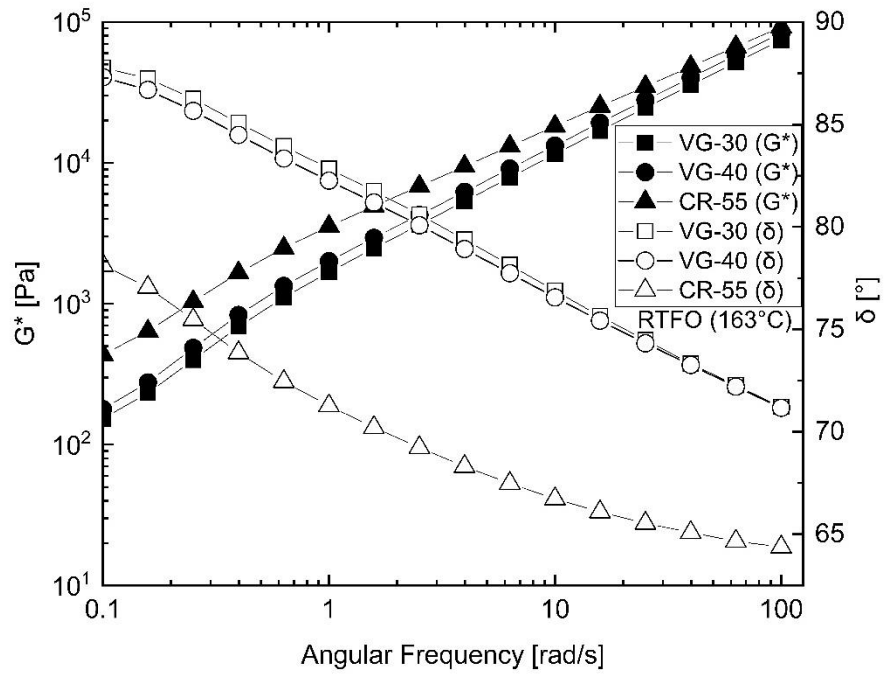


Figure 5.3 Effect of frequency on  $G^*$  and  $\delta$  for 163°C RTFO aging conditions

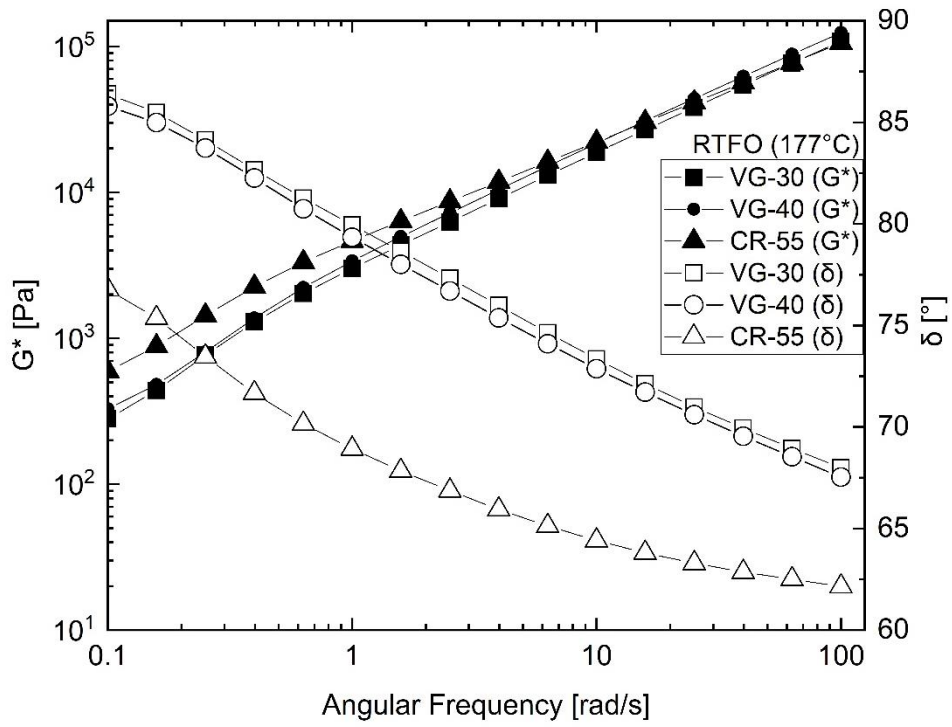


Figure 5.4 Effect of frequency on  $G^*$  and  $\delta$  for 177°C RTFO aging conditions

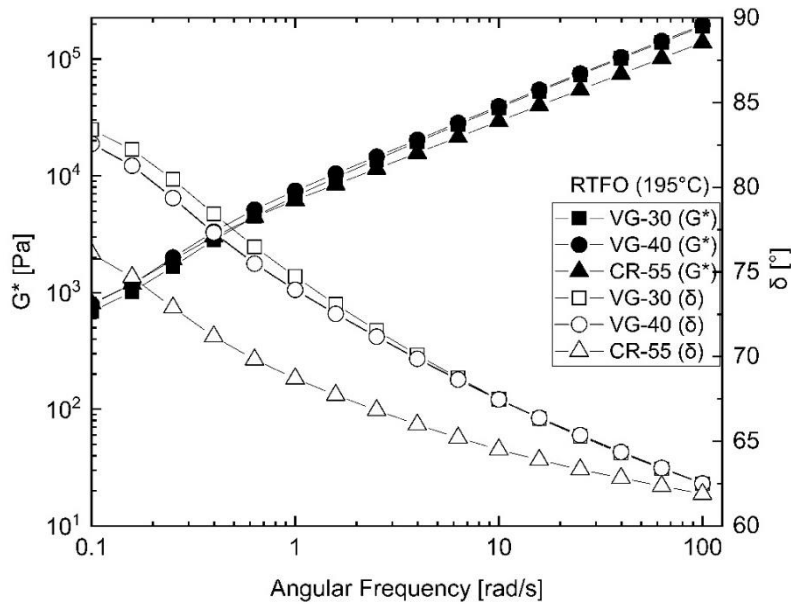


Figure 5.5 Effect of frequency on  $G^*$  and  $\delta$  for 195°C RTFO aging conditions

The reason for CRMB binder indicating lower  $G^*$  for RTFO aging temperature at 195°C is mainly due to the mechanism of swelling in rubber particles. The interaction of light oil fractions and rubber particles can make a substantial increase in elastic energy, which may help rubber particles to dissolve, swell, and decentralize (Meng and Yiqiu 2013). As already mentioned the viscosity of CRMB at 195°C was found to be 170 cP, which indicates ideal mixing viscosity. During this stage rubber particles may swell without degradation (devulcanization or depolymerisation), which may form a gel-like structure adjacent to the asphalt-rubber interface. Also, the main reason for the formation of gel-like structure may be due to diffusion of maltene into the rubber networks (Wang et al. 2019).

Similarly, Figure 5.6 describes the performance of  $G^*$  and  $\delta$  of CRMB-55+S and CRMB-55+R binders, which is subjected to 163°C working temperature, respectively. However, as shown in Figure 5.7 CRMB-55+S binder exhibited better performance under working temperature 177°C compared to CRMB-55+R and CRMB-55, which are aged at 177°C and 195°C, respectively. The obtained results for  $G^*$  and  $\delta$  indicate that the binders aged at 163 °C consist of less stiffness than those aged at 177 °C, particularly for Sasobit additives. Therefore to evaluate the more reliable

rheological properties in the laboratory condition, it is essential to simulate the optimum aging condition and suggest the best compatible base binder with rubber modifiers. Interaction plots for the results of the frequency sweep test for the aging conditions and binder types are shown in Figure 5.8. From the plot, it can be concluded that the binder exhibits higher  $G^*$  value at a higher frequency. At 177°C aged working temperature, CRMB-55 with sasobit additives was stiffer than other binders at 60°C.

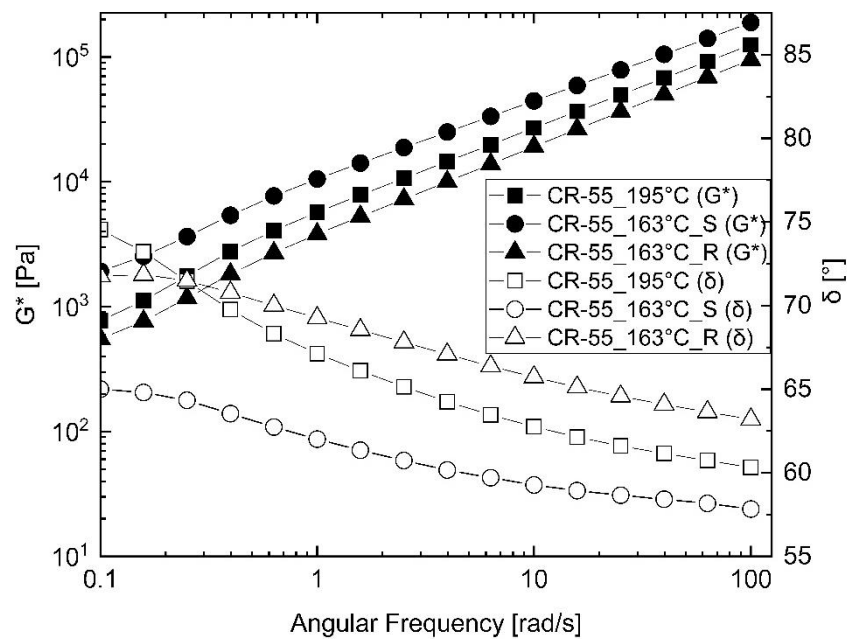


Figure 5.6 Comparison of frequency effect on  $G^*$  and  $\delta$  between 163°C of CRMB with rediset and sasobit with 195°C RTFO aging conditions

Moreover, as shown in Fig 5.4, with increase in working temperature from 163°C to 177°C,  $G^*$  of CRMB-55, VG-30, and VG-40 observed to merge along the given range of frequencies. This mechanism indicates that there is a reduction of fluid phase in all asphalt binders, which shows that binders tend to become hard and increase their rutting resistance performance with increase in frequencies. Similarly, as shown in Fig 5.5, at 195°C working temperature, the  $G^*$  trend increases and merges for all the binders were observed.

At all frequencies complex shear modulus ( $G^*$ ) and phase angle ( $\delta$ ) of CRMB-55 were enhanced in the presence of WMA additives Sasobit (S) for 163°C working temperature compared to CRMB-55 with Rediset additives and CRMB-55 itself when subjected to 195°C working temperature. This indicates that resistance to permanent

deformation became more pronounced in the presence of sasobit in CRMB-55, which may be interfacial interaction between sasobit, rubber particles and working temperature. Moreover, by the application of ideal working temperature 177°C indicates an efficient method of optimizing the swelling mechanism of rubber particles in the presence of Sasobit additives, which is more resistive against rutting particularly at lower frequencies as shown in Fig 5.7.

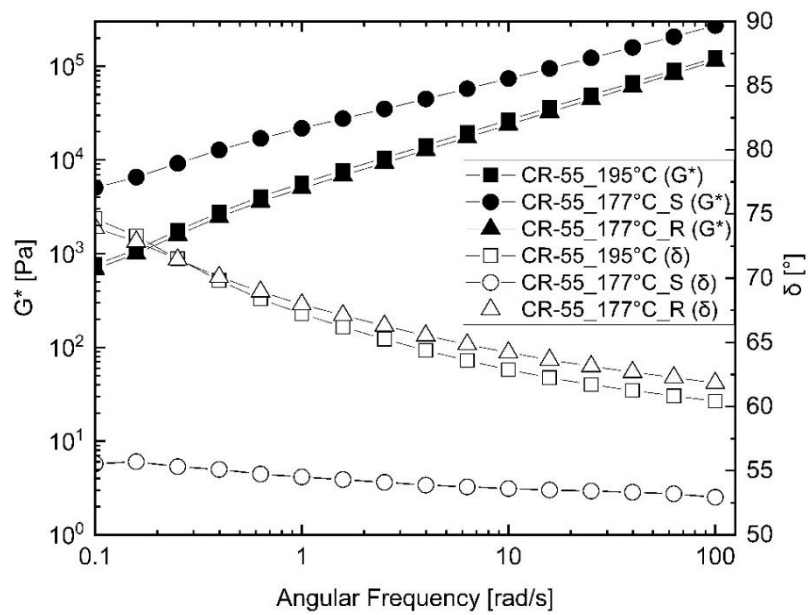


Figure 5.7 Comparison of frequency effect on  $G^*$  and  $\delta$  between 177°C of CRMB with rediset and sasobit with 195°C RTFO aging conditions

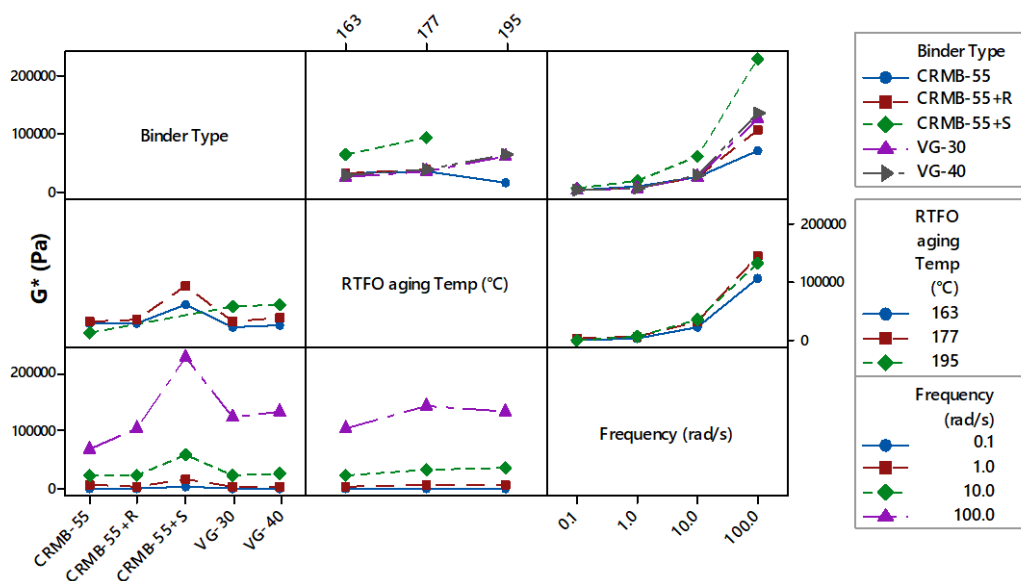


Figure 5.8 Interaction plot of  $G^*$  with working temperature and type of binders

### 5.3.2. Temperature Sweep Test

The effect of working temperature on the rheological parameters using the temperature sweep method, including  $G^*$  and  $\delta$ , is shown in Figure 5.9 to Figure 5.14. As seen in Figure 5.9 for all the unaged binders, the  $G^*$  is reduced by increasing the temperature.  $G^*$  of the CRMB-55 indicates more resistance towards deformation when exposed to repeated cycles of shear strain, i.e., within the LVER region compared with the other two base binders (VG-30 and VG-40) for the entire temperature sweep from 46 °C to 88 °C.

According to Figure 5.10, the curve of the CRMB-55 overlapped with those of the two base binders (VG-30 and VG-40) from 46 °C to 60 °C, indicate similar resistance towards deformation until 60 °C. However, beyond 60 °C, the CRMB-55 appears to be more rigid with less viscoelastic than VG-30 and VG-40, which may lead to the segregation of the rubber particles from its base binder. The effect of short-term aging at 177 °C temperature as shown in Figure 5.11 on  $G^*$  and  $\delta$  indicates that the compatibility of the CR with base binders such as VG-30 and VG-40 can be extended upto 70 °C during the temperature sweep test, and to reduce the segregation between the CR and its base binder used during the manufacturing of the crumb rubber modified binder. But still not fully compatible with the base binder at 177 °C upto 88 °C in the temperature sweep test. As shown in Figure 5.12, the CRMB-55 is completely overlapped by the two base binders VG-30 and VG-40 throughout the temperature sweep from 46 °C to 88 °C, probably due to the presence of ideal viscosity as shown in the previous section at 195 °C for CRMB-55. Furthermore, the interaction plot shown in Figure 5.15 represents that CRMB-55 with sasobit additives showed high complex shear modulus when aged at 177°C, equivalent to VG-30 and VG-40 for 195°C at 60°C test temperature.

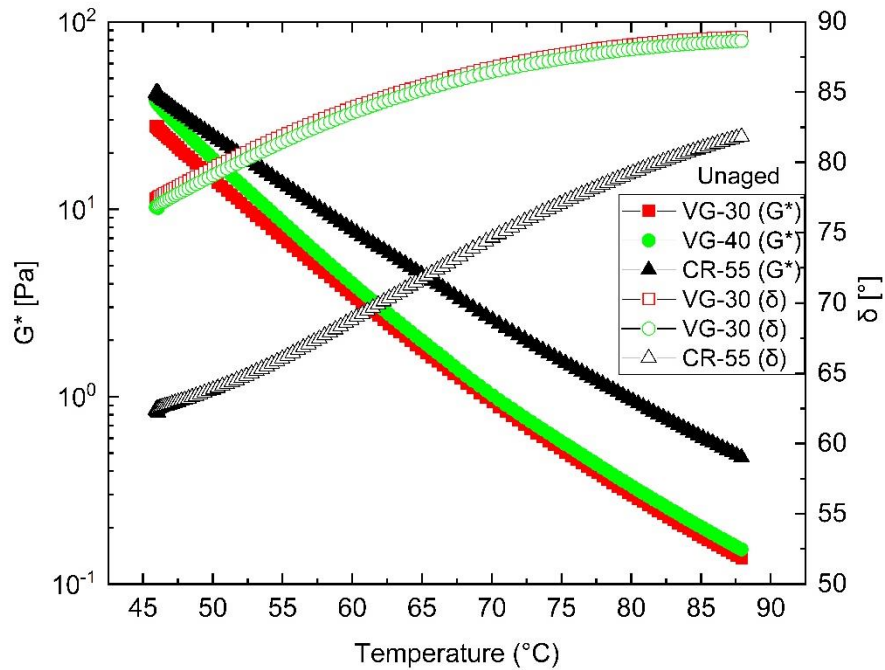


Figure 5.9 Effect of temperature sweep on  $G^*$  and  $\delta$  for unaged

Fig 5.14 shows the effects of working temperature and WMA additives Sasobit and Rediset on complex shear modulus ( $G^*$ ) and phase angle ( $\delta$ ) of the CRMB-55. It can be seen that CRMB-55 with Sasobit additives exhibits higher  $G^*$  at 177°C working temperature compared to CRMB-55 and CRMB-55 with Rediset, which is subjected to 195°C and 177°C working temperature, respectively. It may be attributed to the proper selection of working temperature, WMA additives and complex interaction between rubber particles and asphalt binder phase in CRMB.



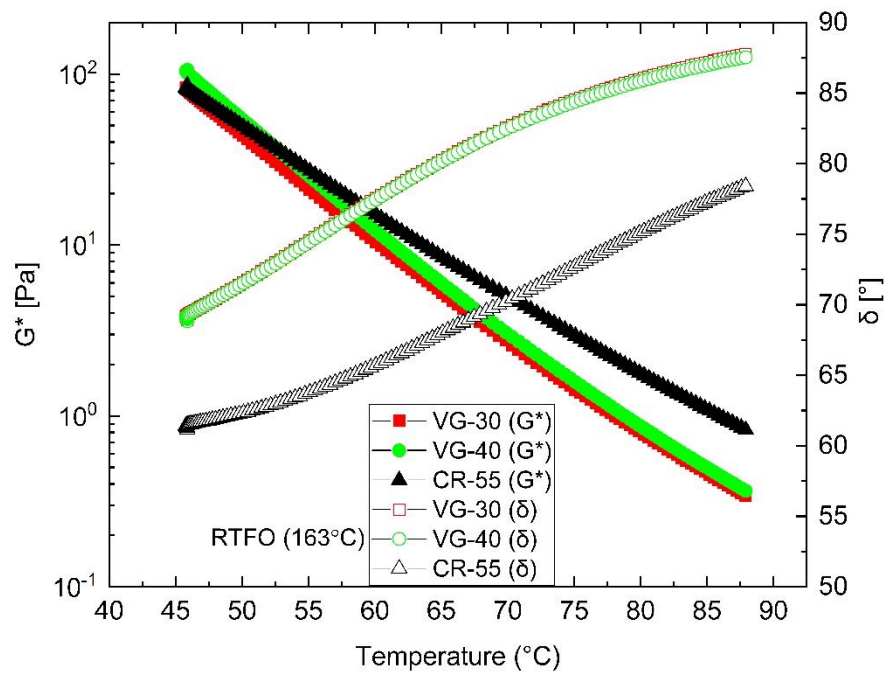


Figure 5.10 Effect of temperature sweep on  $G^*$  and  $\delta$  for 163°C RTFO aging conditions

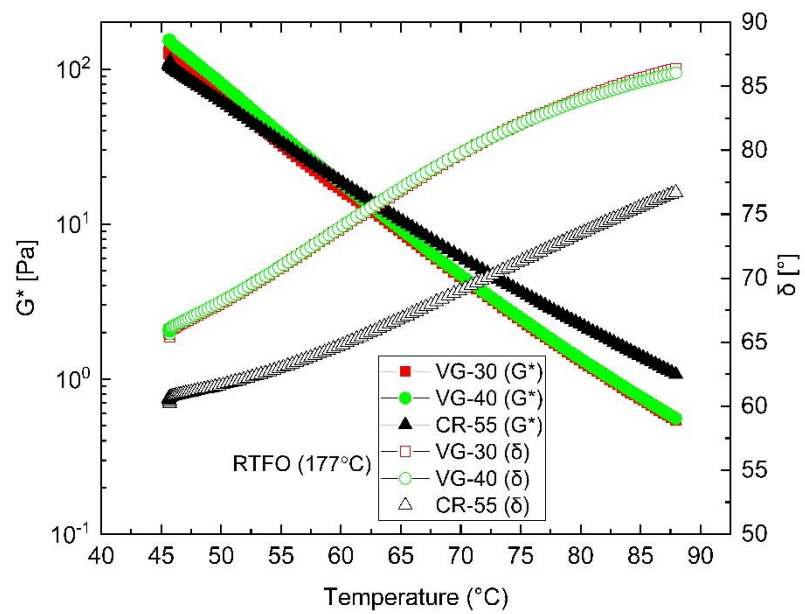


Figure 5.11 Effect of temperature sweep on  $G^*$  and  $\delta$  for 177°C RTFO aging conditions

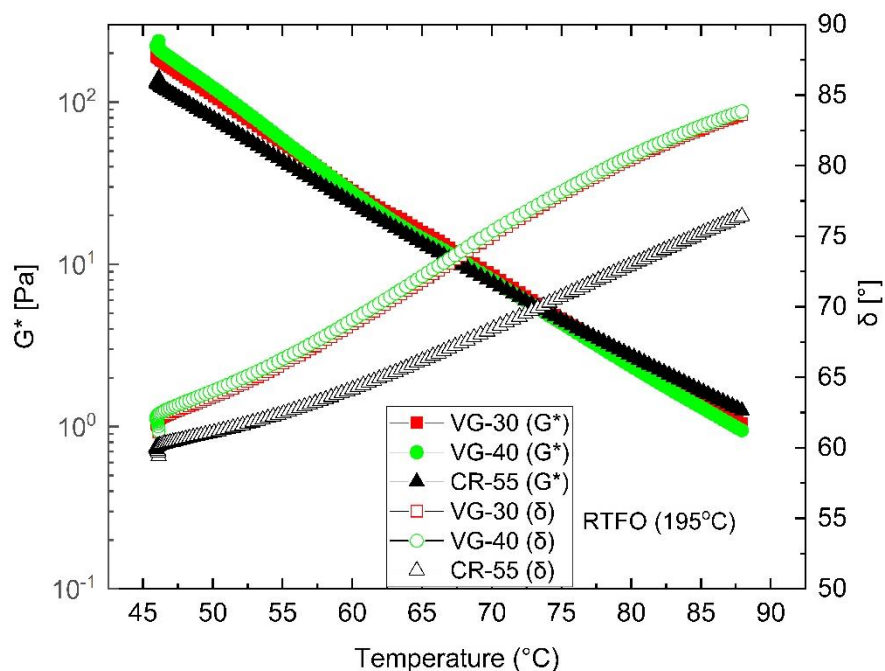


Figure 5.12 Effect of temperature sweep on  $G^*$  and  $\delta$  for 195°C aging conditions

By optimising the working temperature, the process of converting a nonaromatic ring into an aromatic ring known as aromatization and the process by which hydrogen is removed from an organic compound known as dehydrogenation of asphaltene will be under control (Ghavibazoo et al. 2015; Siddiqui and Ali 1999). This exhibit an enhanced performance in terms of  $G^*$  and  $\delta$  in the presence of sasobit under varying test temperature. Therefore, the complex interaction between parts of aromatic, resin and asphaltene in asphalt binder is totally dependent upon working temperature (Liu et al. 1998).

An inflection point were observed in  $G^*$  curves at 77°C temperature for CRMB-55+S and CRMB-55 binders, which were subjected to 163°C working temperature as shown in Figure 5.13. Moreover,  $G^*$  curve of CRMB-55 were found to be slightly stiffer compared to CRMB-55+S beyond inflection point i.e. 77°C. On the other hand, the  $G^*$  of the CRMB-55 with Rediset (R) was much lower than the Sasobit additives throughout the temperature range. Similar behaviour was observed with the phase angle parameter ( $\delta$ ). However, for the combination of CRMB-55 and Rediset, the  $G^*$  value was much lower than that of CRMB-55, similar to the previous case as mentioned in Figure 5.13. Moreover, the phase angle for the combination of the CRMB-55 and

Sasobit was ranging between 70° and 72° at 88 °C when aged at 177 °C, whereas for Rediset WMA additives, it showed between 77° and 88° at 88 °C when aged at 163 °C.

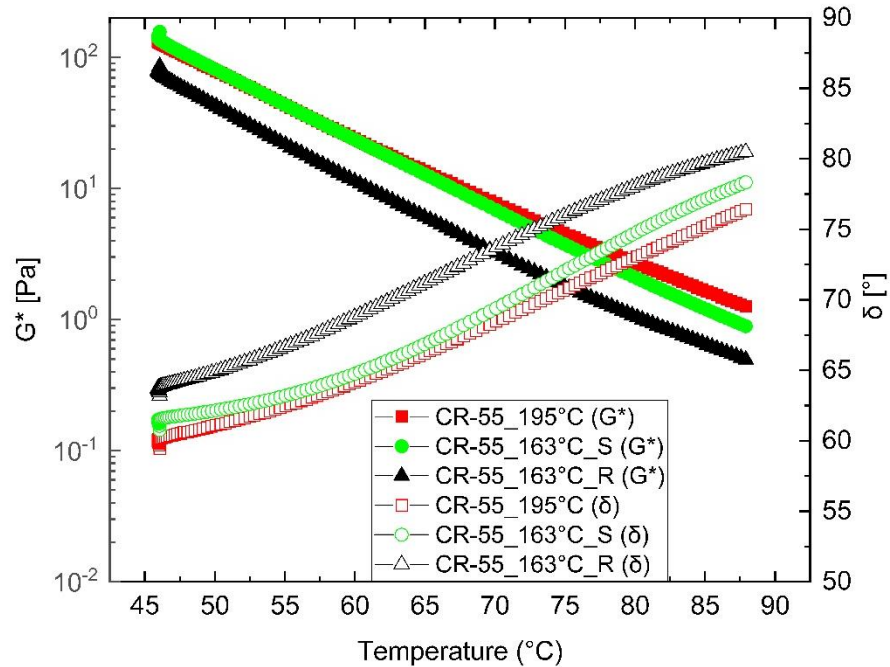


Figure 5.13 Effect of temperature on  $G^*$  and  $\delta$  for CRMB-55+S and CRMB-55+R at 163°C and 195°C RTFO aging conditions

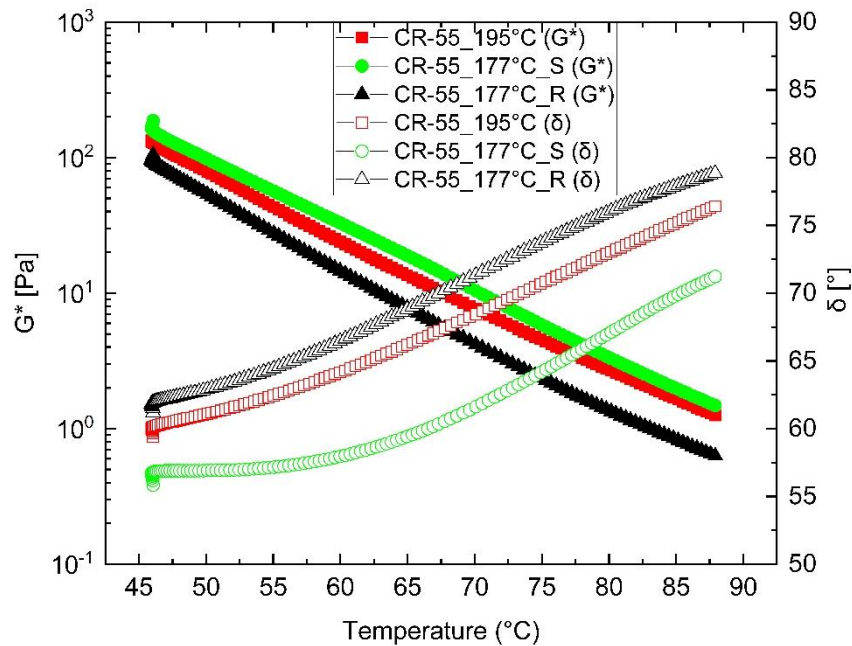


Figure 5.14 Effect of temperature on  $G^*$  and  $\delta$  for CRMB-55+S and CRMB-55+R at 177°C and 195°C RTFO aging conditions

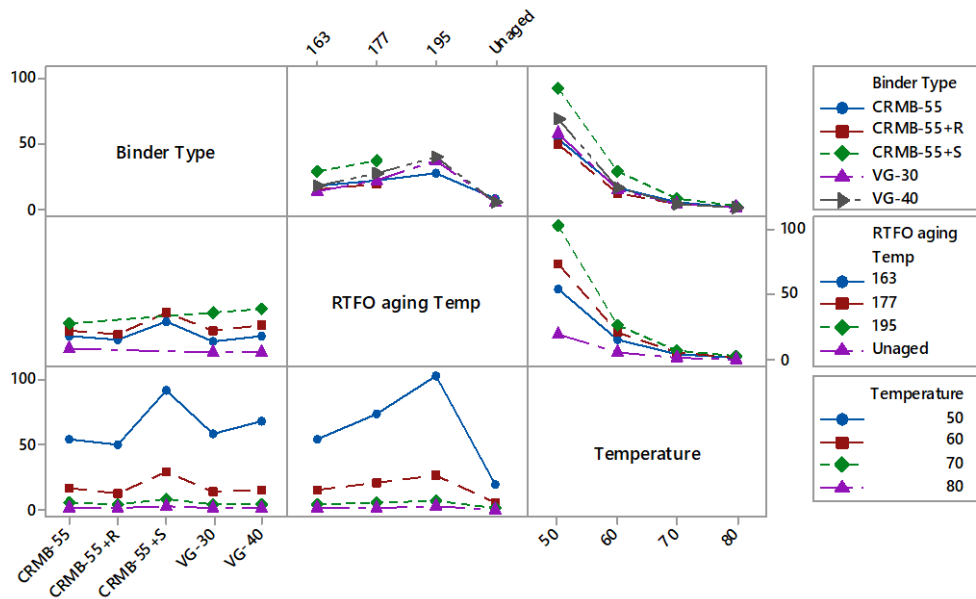


Figure 5.15 Interaction plot between  $G^*$  and working temperature, binder type, test temperature

### 5.3.3. Time-Temperature Superposition Test

TTSP is primarily used to correlate the equivalency between frequency (time) between temperature to obtain a master curve (Yusoff et al. 2011). This thermorheological simplicity tool benefits in evaluating the rheological properties. Figure 5.16 shows the master curve of the CRMB-55 with and without Sasobit, which is short-termed aged at 163 °C. As seen from Figure 5.16, the  $G^*$  curve is flattened and overlapping at a higher frequency range with CRMB-55, aged at 195 °C, but slightly higher at a lower frequency. Again, it indicates less contribution to the rutting performance. Figure 5.17 shows the master curve of the CRMB-55 with and without Sasobit, which is short-termed aged at 177 °C. As seen in Figure 5.17, the  $G^*$  curve is more flattened and above the CRMB-55, which is aged at 195 °C throughout the frequency, which indicates more resistance towards the rutting performance at both higher and lower frequency ranges.

Moreover, the aged CRMB-55 binder at 177°C working temperature as shown in Fig 5.17 with Sasobit has the highest complex shear modulus ( $G^*$ ), which indicates that sasobit has the low restoring effect at 30°C reference temperature compared to CRMB-

55 binder aged at working temperature 195°C and 163°C, respectively. The rheological measurements as shown in Fig 5.17 indicates that, CRMB-55 with sasobit at low frequencies, there is a slight increase in complex shear modulus ( $G^*$ ) and therefore a more elastic response, which may be combined effects of rubber swelling and presence of asphaltenes structure. At 30°C pavement service temperature, CRMB-55+S binder shows viscoelastic solid behavior. The reduced frequency defines the characteristic nature of the viscoelastic response as complex shear modulus is dependent on frequency.

Figure 5.18 and Figure 5.19 show the master curve of the CRMB-55 with Rediset and without Rediset, which is short-termed aged at 163 °C and 177 °C, respectively. As seen in Figure 5.18 and Figure 5.19, the  $G^*$  curve is entirely overlapped by CRMB-55, aged at 195 °C throughout the frequency range, thus indicating that it contributes less towards the rutting performance

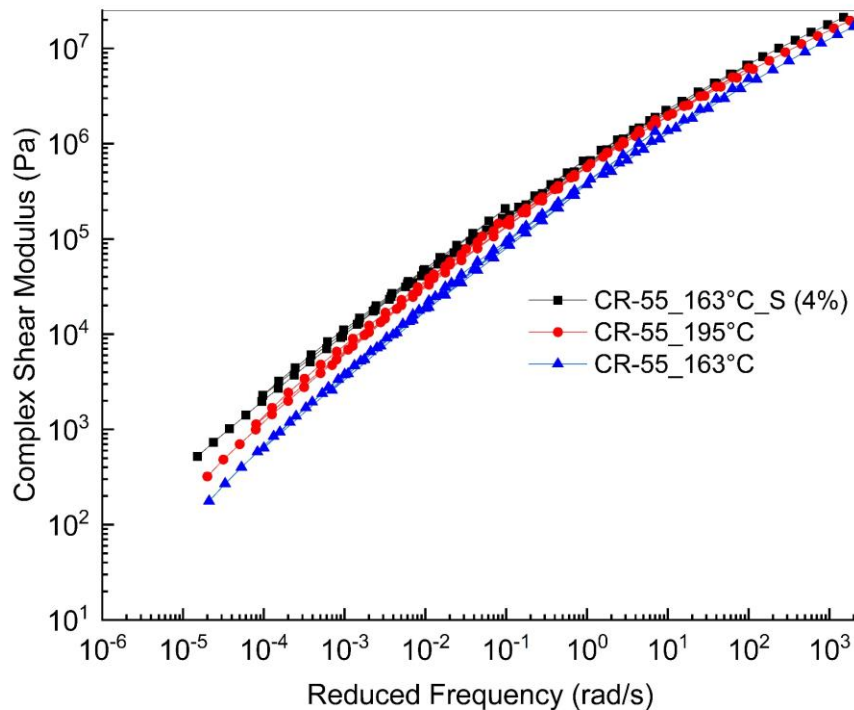


Figure 5.16 Comparison of TTS effect on  $G^*$  master curve data at a 30°C reference temperature between CRMB-55 with sasobit and CRMB-55 at 163°C, 195°C

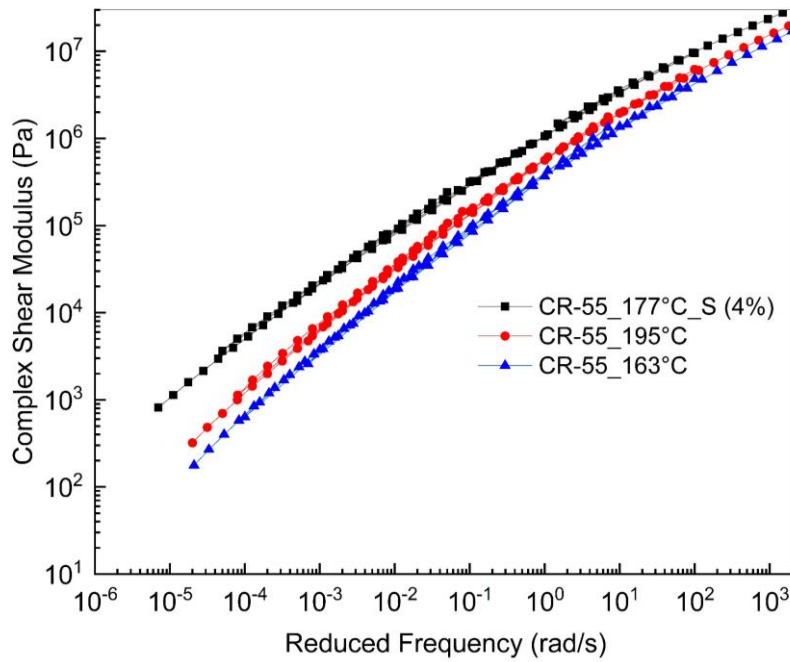


Figure 5.17 Comparison of TTS effect on  $G^*$  master curve data at a 30°C reference temperature between CRMB-55 with sasobit and CRMB-55 at 177°C, 195°C

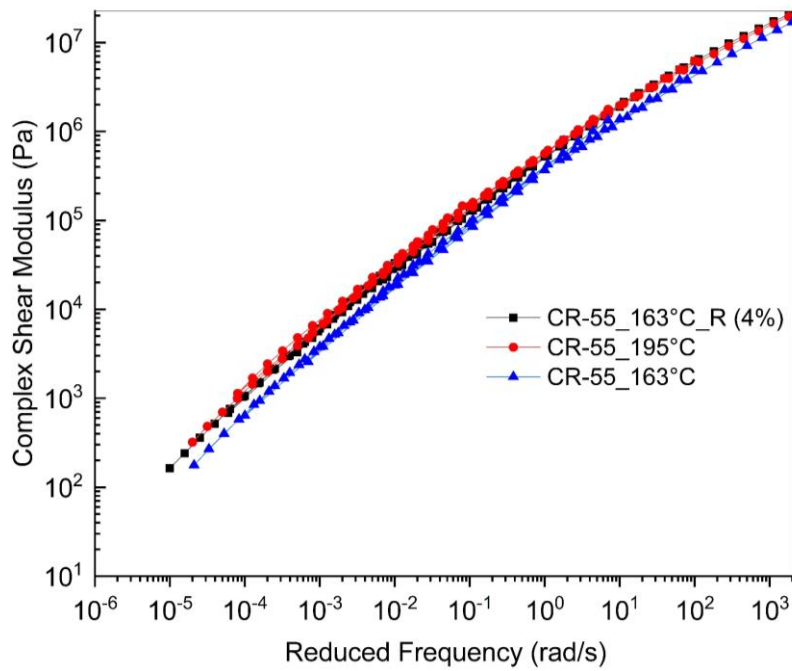


Figure 5.18 Comparison of TTS effect on  $G^*$  master curve data at a 30°C reference temperature between CRMB-55 with rediset and CRMB-55 at 163°C, 195°C

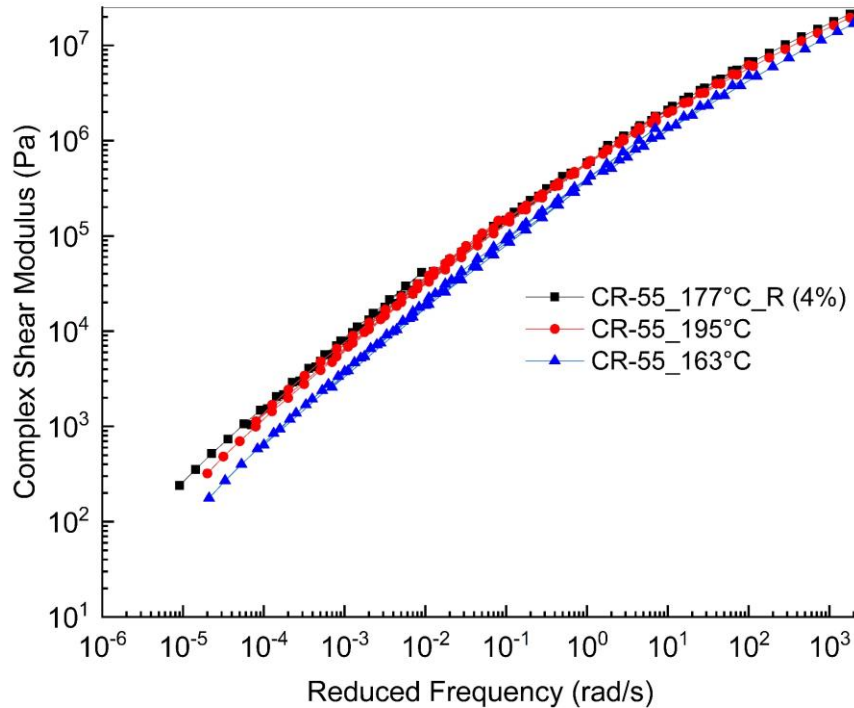


Figure 5.19 Comparison of TTS effect on  $G^*$  master curve data at a 30°C reference temperature between CRMB-55 with sasobit and CRMB-55 at 177°C, 195°C

#### 5.3.4. High-Temperature Performance Test

Figure 5.20 to Figure 5.24 shows Superpave rutting parameter  $G^*/\sin\delta$  values for VG-30, CRMB-55 with and without WMA additives for various short-term aging temperatures. The results show that an increase in short-term aging temperature increases  $G^*/\sin\delta$  value, indicating higher rut resistance for VG-30, CRMB-55 with and without WMA additives. For example,  $G^*/\sin\delta$  value of 2.2 kPa for CRMB-55 binder was achieved at 79.1°C, 81.5°C and 84.9°C for the short-term aging temperature at 163°C, 177°C, and 195°C, respectively, compared to 71.6°C, 72.3°C, and 76.3°C for VG-30 binder. Behl et al. (2012) reported that the presence of wax in Sasobit creates crystalline structure, resulting in enhanced stiffness of a binder; a similar trend can be seen in the present study (Singh and Kataware 2016).

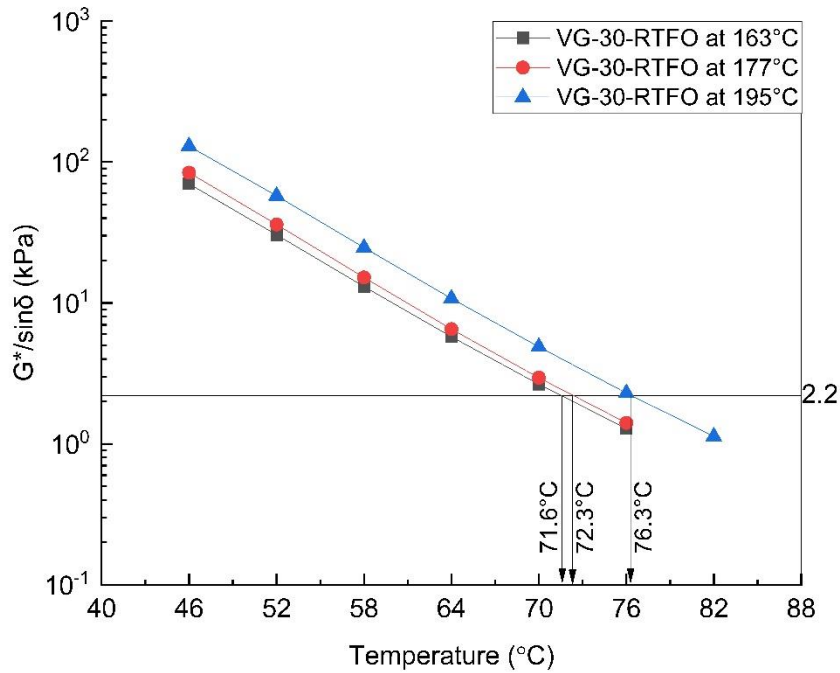


Figure 5.20  $G^*/\sin\delta$  value of VG-30 for 163°C, 177°C, and 195°C RTFO aging conditions

The percentage rate of change in  $G^*/\sin\delta$  value increases up to 195°C of RTFO aging temperature for CRMB-55 with Sasobit content (i.e., 3.83 % increase compared to 163°C of RTFO aging) and then slight increase for 177°C of RTFO aging temperature (i.e., 1.45% increase compared to 163°C of short-term aging temperature). Since the maximum rise in  $G^*/\sin\delta$  can be seen for all the binders, i.e. when RTFO aging temperature increased from 177°C and 195°C, it may be considered that with increase in short-term aging temperature, an optimum temperature could be determined.

Fig 5.24 shows the changes in rheological properties of CRMB-55 binder with Sasobit additives as a function of change in working temperature. It shows that the rutting parameter of CRMB-55+S deteriorates once the test temperature crosses 83.3°C when subjected to 177°C working temperature. This indicates that rubber particles and asphaltene play a dominant role in defining the mechanical properties of binders during selection of working temperature. Also by selecting the appropriate working temperature there may be release of rubber components into the binder, which interact with age hardening mechanisms (Ghavibazoo et al. 2015).



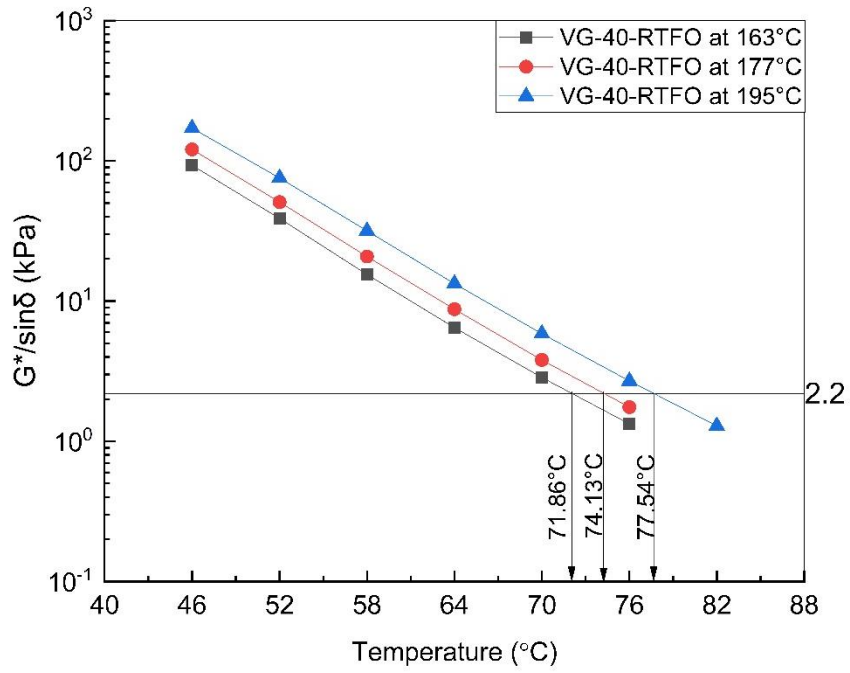


Figure 5.21  $G^*/\sin\delta$  value of VG-40 for 163°C, 177°C, and 195°C RTFO aging conditions

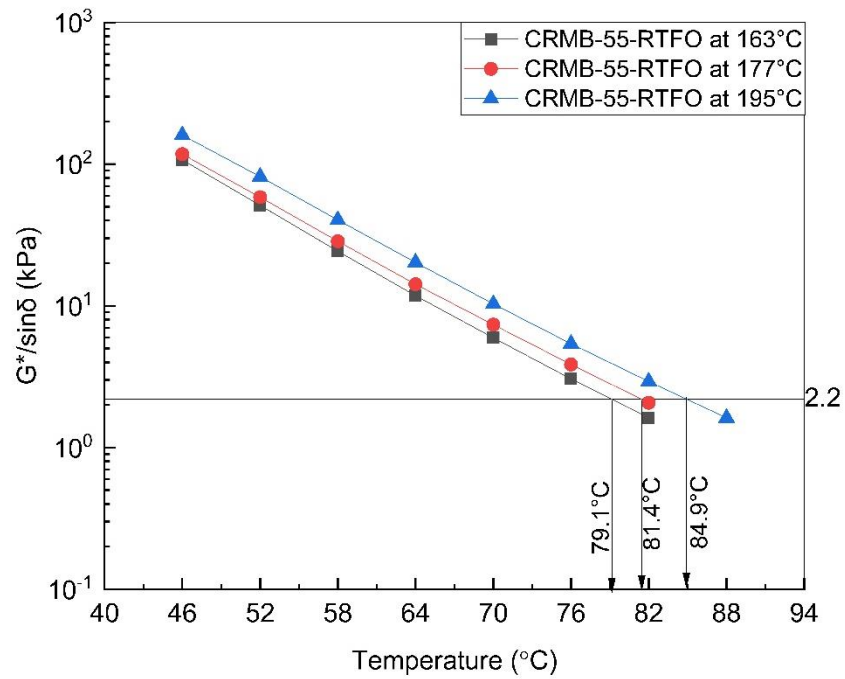


Figure 5.22  $G^*/\sin\delta$  value of CRMB-55 for 163°C, 177°C, and 195°C RTFO aging conditions

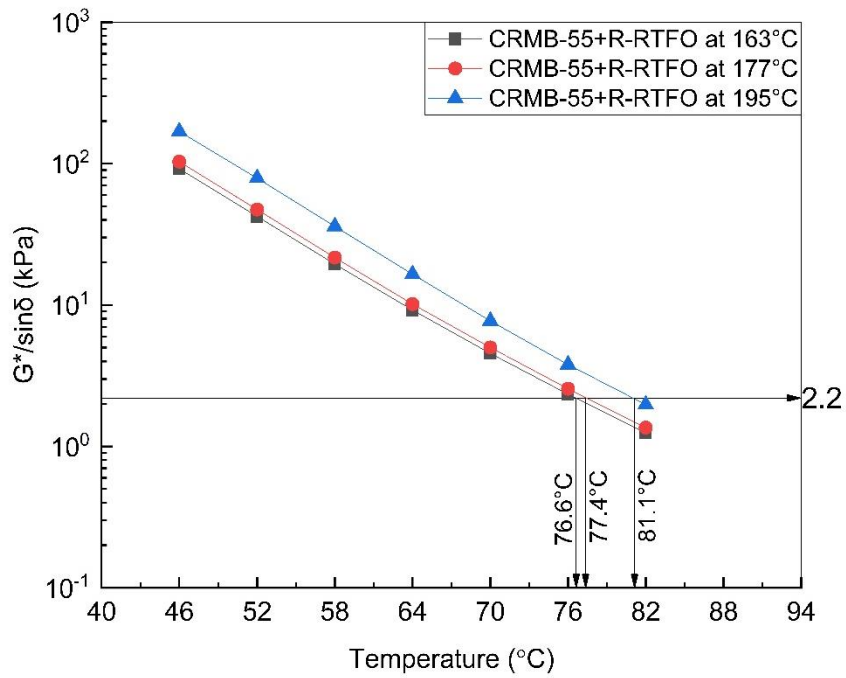


Figure 5.23  $G^*/\sin\delta$  value of CRMB-55+R for 163°C, 177°C, and 195°C RTFO aging conditions

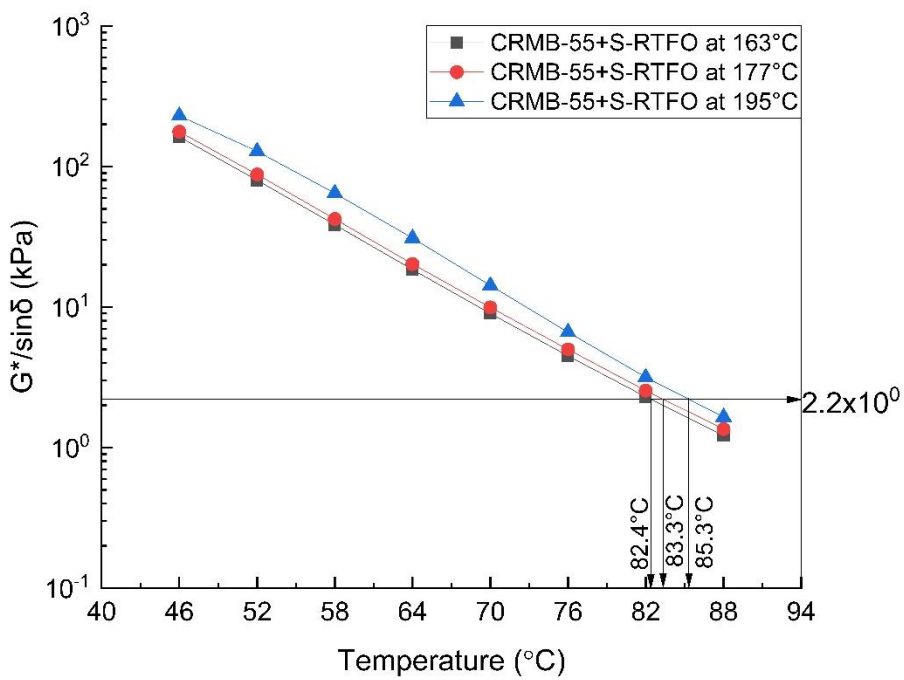


Figure 5.24  $G^*/\sin\delta$  value of CRMB-55+S for 163°C, 177°C, and 195°C RTFO aging conditions

### 5.3.5. Multiple Stress Creep Recovery Test

According to (Subhy et al. 2016), non-recoverable creep compliance ( $J_{nr}$ ) has been recommended as an alternative to the current SHRP parameter  $|G^*|/\sin \delta$  when assessing the permanent deformation performance of different bitumens (D'Angelo et al. 2007).  $J_{nr}$  can predict the improvement imparted by modification. It is also more sensitive to the stress dependence of modified binders, making it suitable for specification purposes for both neat and modified bitumen (Dangelo 2009; Nejad 2016). Measuring the  $J_{nr}$  of binders at high stresses and outside the LVE region is also conceivably more appropriate when considering the rutting behaviour of asphalt mixtures as the strains in binder films on aggregate surfaces can be several hundred times greater than the overall average strain of the mixture (Subhy et al. 2015). Figure 5.25 shows the results of  $J_{nr}$  (average value for the 10 creep and recovery cycles) with a stress level of 3.2 kPa at a test temperature of 64°C.

The results highlight the significance of stress dependency in short-term aging temperatures, overall RTFO aging temperature being more apparent in VG-30 followed by CRMB-55 with rediset content. The CRMB-55 with sasobit content for 195°C and 177°C short-term aging temperature were less dependent on the stress with values of  $J_{nr}$  being relatively stable up to a stress level of 3.2kPa, after which there is evidence of an inflection point in the material response and the presence of non-linearity at 177°C RTFO aging temperature. The  $J_{nr}$  values also captured the effects of WMA additives with the varying short-term aging temperature at 163°C, 177°C, and 195°C, all CRMB-55 binders performing very well as indicated by their low  $J_{nr}$  values compared to VG-30 binder. A similar results were also observed for RTFO aging temperature at 163°C, 177°C, and 195°C.

The higher  $J_{nr}$  values of the VG-30 and CRMB-55 with rediset content produced at various RTFO aging temperatures (163°C, 177°C, and 195°C) indicated that all these conditions lead to some breaking of the cross-linking asphaltene and rubber (polymer) network utilizing short term aging condition. The binder with lower colloidal system indicates a connected network structure (Loeber et al. 1998), in which at higher RTFO aging temperature i.e., 195°C may alter the colloidal structure and also avoid formation of dense and gel-like structure. Therefore, presence of higher colloidal asphalt binder

indicates an increase in asphaltene contents, which favours asphalt to be denser and gel-like structure. At the other extreme, higher  $J_{nr}$  values at lower RTFO aging temperature (163°C) suggest an incomplete interaction (insufficient swelling) between CRM and its base binder.

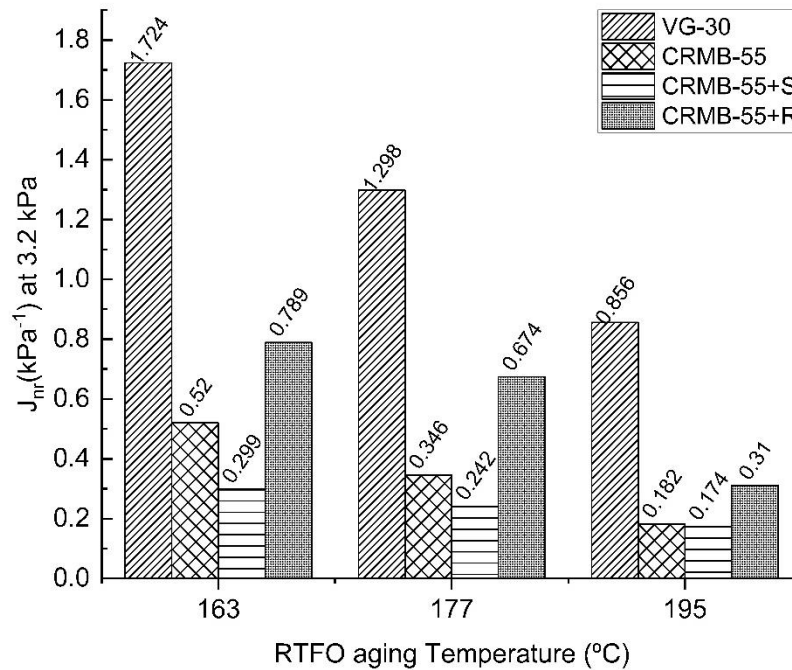


Figure 5.25 Effect of working temperature on  $J_{nr}$  values at 64°C

Providing information about elastic recovery in addition to the non-recoverable compliance, stress sensitivity, and non-linearity behaviour of modified bitumens is another advantage of performing the MSCR test (Subhy et al. 2016). The average percentage recovery of 10 cycles at stress levels (3.2 kPa) is presented in Figure 5.26. The results show that CRMB-55 and CRMB-55 with rediset short-term aged at 177°C and 195°C have the highest elastic response compared to other binders with similar short-term aging conditions. Additionally, these conditions maintained a high elastic recovery across all the stress levels (Subhy et al. 2016). It can be seen that as the RTFO aging temperature increases, the difference in recovery response of the CRMB-55 with and without WMA additives becomes more significant.

The effect of base binder used in the manufacture of CRMB may guide the high and low elastic response at the higher stresses under different short-term aging temperatures. A limit of 15% reduction in the percentage of recovery from 0.1 to 3.2

kPa is considered acceptable for modified bitumen that has an excellent elastomeric response (Subhy et al. 2016). Thus, all the binders with and without WMA additives short-term aged at 163°C, 177°C, and 195°C exceeded the 15% maximum specification, which may not be translated into a better rutting resistance. The results also highlight that characterizing the material within only the LVE region is insufficient for an appropriate material ranking (Subhy et al. 2016).

Figure 5.27 is used by AASHTO TP 70–13 to indicate the presence of an acceptable elastomeric polymer. The average percent recovery at 3.2 kPa, versus the average non-recoverable creep compliance at 3.2 kPa, was plotted on the graph. All the CRMB-55 binders with WMA additives for all RTFO aging temperatures fell below the line, indicating a below criterion elastomeric polymer apart from those RTFO aging temperatures.

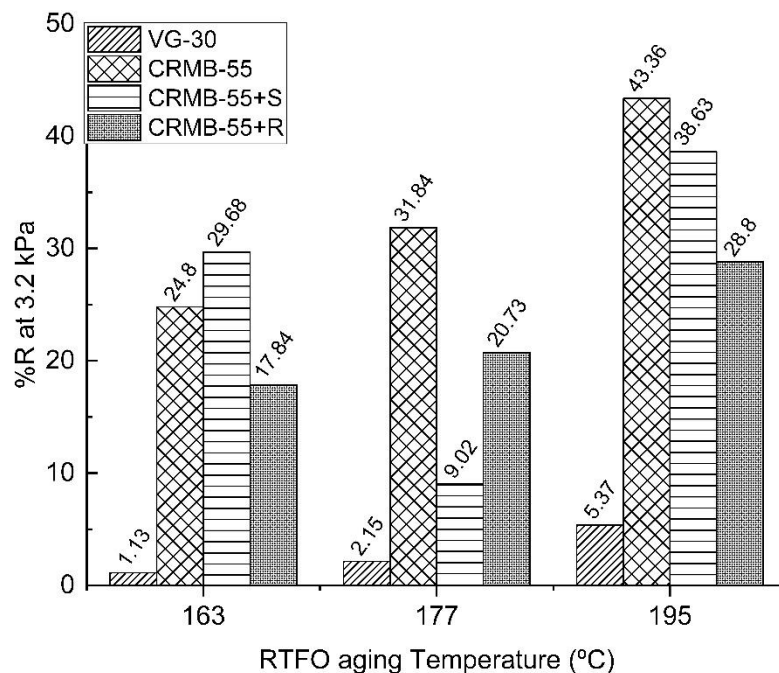


Figure 5.26 Effect of working temperature on %R values at 64°C

MSCR is being developed to measure rutting susceptibility of modified binder.  $J_{nr}$  is considered to have better correlation with rutting performance of asphalt mixes compared to  $G^*/\sin\delta$ . At 177°C working temperature CRMB-55+S showed low  $J_{nr}$  value at 3.2 kPa stress level indicating the presence of a high amount of asphaltene particles,

which is seemingly a solid arrangement in asphalt binder (Loeber et al. 1998). Therefore, by regulating the working temperature, the asphaltene concentration could be increased or decreased, which may lead to a more dense gel-like structure or solid-like structure. Hence, increased asphaltene concentration represents a more flocculated system, which increases the bond between the particles.

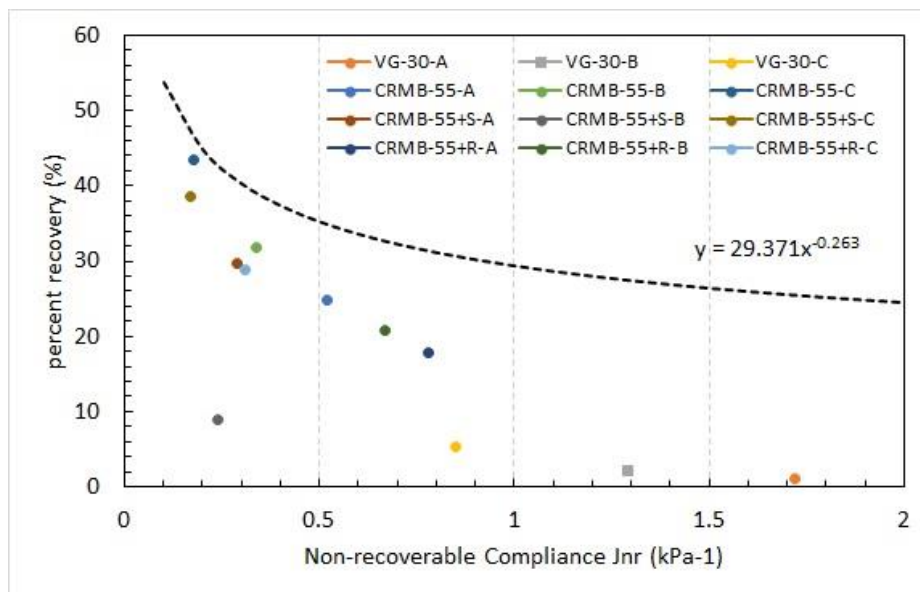


Figure 5.27 The plot between Jnr and %R for asphalt binders

### 5.3.6. Scanning electron micrographs

Using SEM images analysis technique, structural observation of asphalt binder is conducted using various magnification levels (500X to 300KX) to capture high level resolution (20µm to 100nm) images. The images were captured within the working distance (WD) of 3mm in a prepared sample on covering glass. Using a high-voltage generator, an electron high tension (EHT) of 5kV is applied on a sample. Based on investigation of different types of asphalt binder they concluded that the formation of bee-shaped micro-structures can be related to the presence of asphaltenes (Pauli et al. 2001).

Several studies attributed the “bee-like” appearance which is used to characterize the asphalt surface to the asphaltene (Jäger et al. 2004; Loeber et al. 1996). However, in the SEM image Fig 5.28 there is a flat background in which another wave pattern is dispersed. These phases include an elongated structure characterised by succession of

pale and dark lines, which is also known as bee-like structures. By contrast to Fig 5.28, the bee-like structures are not independent of one another. According to (Li et al. 2016), the correlation between bee-like structure and asphaltene has been made. In which, SARA fractionation of base binder proved the presence of asphaltene. Furthermore, in the topographic domain the stiffness properties of asphalt binder were measured using Atomic force microscope (AFM). The peak in the bee-like structure indicated the highest stiffness value and reported that structure containing asphaltene and resins showed highest stiffness, whereas structure with aromatic and saturates showed lower stiffness. Therefore, the appearance of “bee-like” structures were caused by the asphaltene in asphalt binder.

The compatibility effect between the base binder (VG-30) and the rubber particles, also in the presence of WMA additives (sasobit and rediset) in terms of their asphaltenes structure, distribution, and its damages, were identified and analyzed using the SEM. The base binder (VG-30) was compared with the standard RTFO aged temperature at 163 °C with 195 °C, as shown in Figure 5.28 to Figure 5.29. Similarly with CRMB-55 was compared with RTFO aging at 163 °C with 195 °C as shown in Figure 5.31 to Figure 5.32. Finally, the CRMB-55 with WMA additives sasobit and rediset aged at 177 °C was compared with 195 °C aged CRMB-55 alone, as shown in Figure 5.33 and Figure 5.34. In the present study, the SEM images were chosen from 15,000 to 20,000 magnifications for VG-30 and CRMB-55.

However, for the explicit representation of the asphaltenes, all the binder samples with a magnification structure upto 15,000 times for aged conditions are shown here to compare the structures with consistency. Magnification level at 1000 and 2000 for CRMB-55 with sasobit and rediset WMA additives as shown in Figure 5.33 and Figure 5.34 indicates the images of CRMB-55 binders with the two WMA additives sasobit and rediset at 177 °C aging conditions.

The formation of uniform disperse of bee-like structures known as asphaltenes at 163 °C aging conditions can be seen in Figure 5.28. At 195 °C aging condition, destruction of asphaltenes was observed, as shown in Figure 5.29. The destruction of asphaltenes becomes more accessible as the aging temperature is increased to 195 °C.

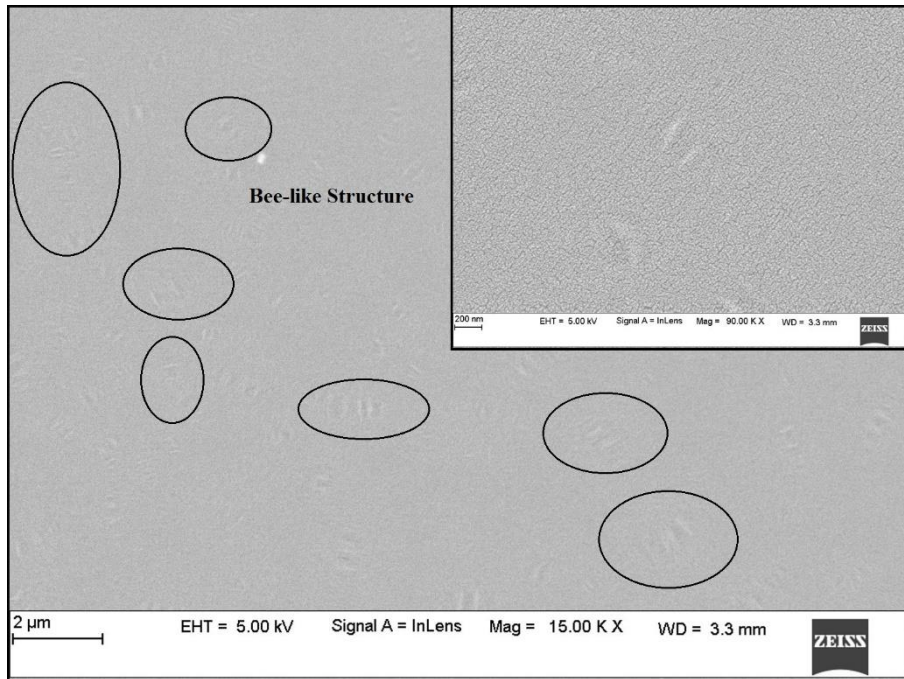


Figure 5.28 SEM image of VG-30 for RTFO aged at 163°C.

EDAX spectra confirm N, C, O, and S in the VG-30 binder after short-term aging conditions, as shown in Figure 5.30. Similarly, CRMB-55 without WMA additive, as shown in Figure 5.31 and Figure 5.32, shows that the asphaltenes had already destructed during the manufacturing process of the CRMB-55. However, at 195°C working temperature the possibility of asphaltene destruction found to be more, and it almost disappears when observed at 2 μm resolution. This can be due to the higher aging temperature during the early manufacturing and laboratory investigation stages. It is noticeable that the morphological changes in the CRMB-55 are were mainly dependent upon short-termed aging conditions (Loeber et al. 1996; Redelius 2009).



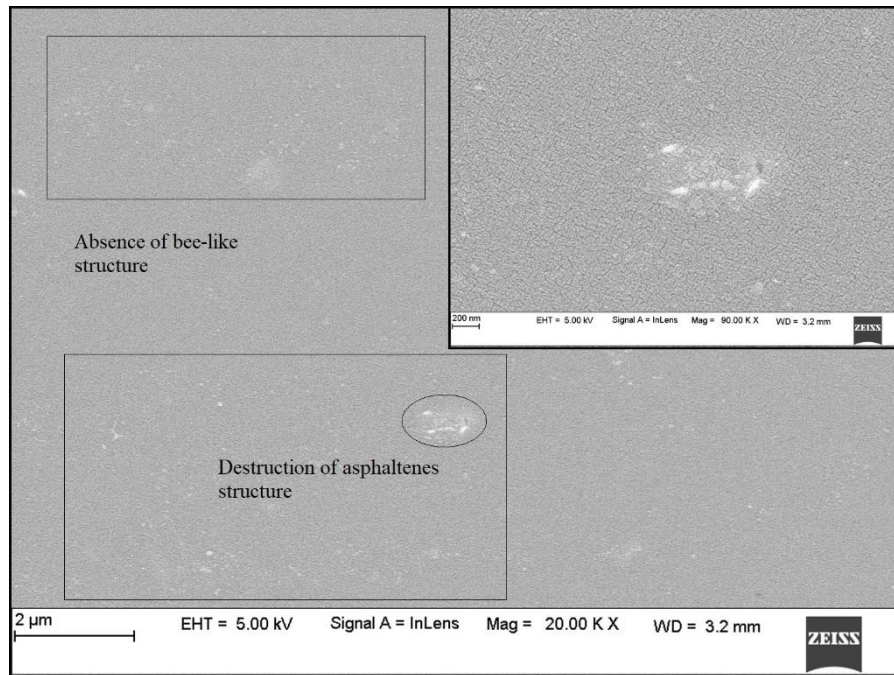


Figure 5.29 SEM image of VG-30 for RTFO aged at 195°C

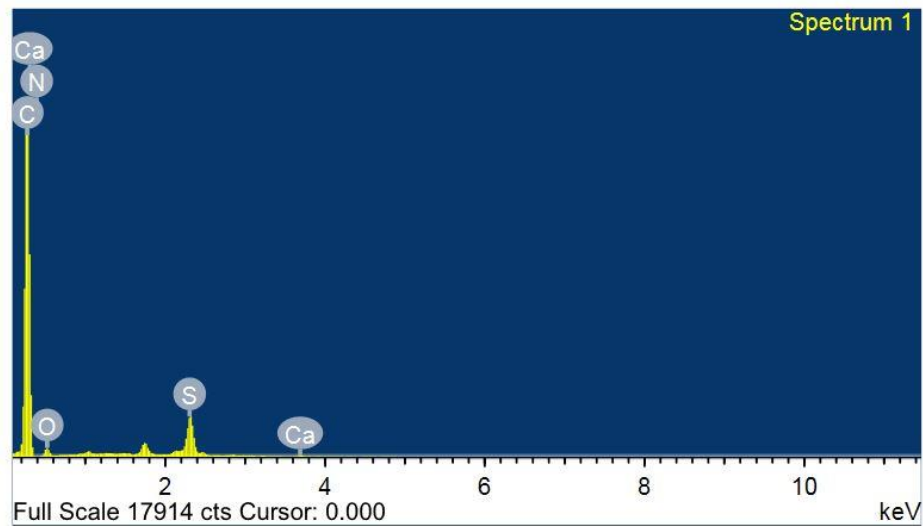


Figure 5.30 EDAX analysis of VG-30 elemental mapping

These changes can be optimized by controlling the RTFO aging temperature at 177 °C with the combination of WMA additives, as shown in Figure 5.33 and Figure 5.34, where a smooth coating of the binder appears around the rubber particles with

sasobit as a WMA additive as seen in Figure 5.33. Similarly, in the case of Rediset WMA additives, a floating of rubber particles in the binder phase is identified in Figure 5.34.

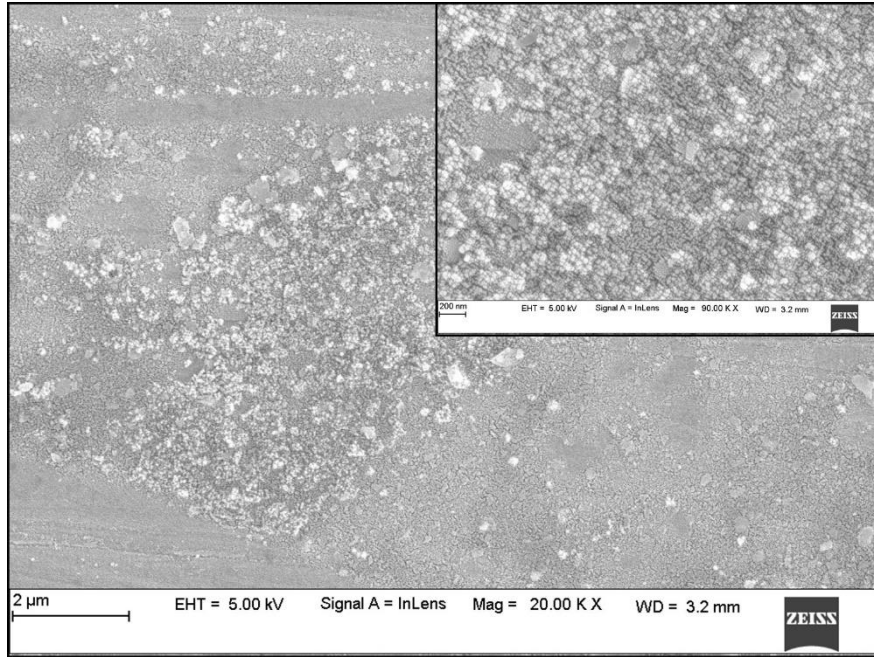


Figure 5.31 SEM image of CRMB-55 for RTFO aged at 163°C

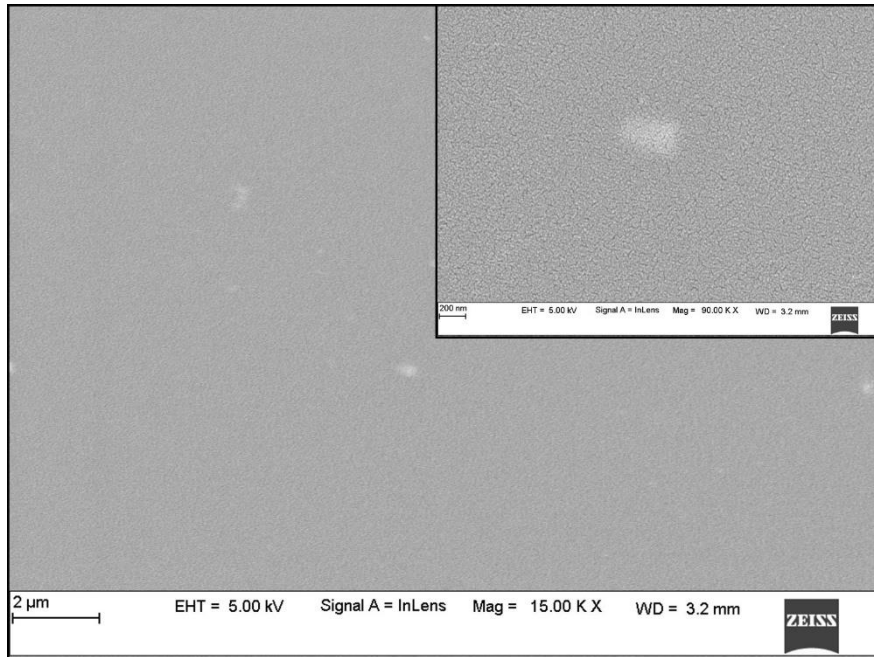


Figure 5.32 SEM image of CRMB-55 for RTFO aged at 195°C

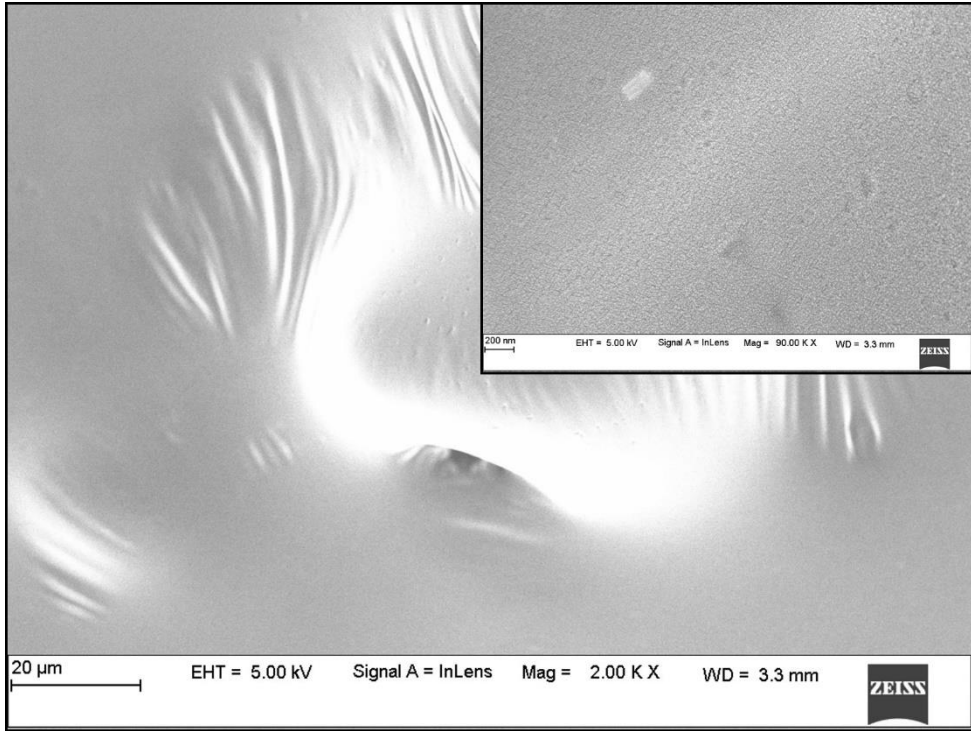


Figure 5.33 SEM image of CRMB-55+S for RTFO aged at 177°C

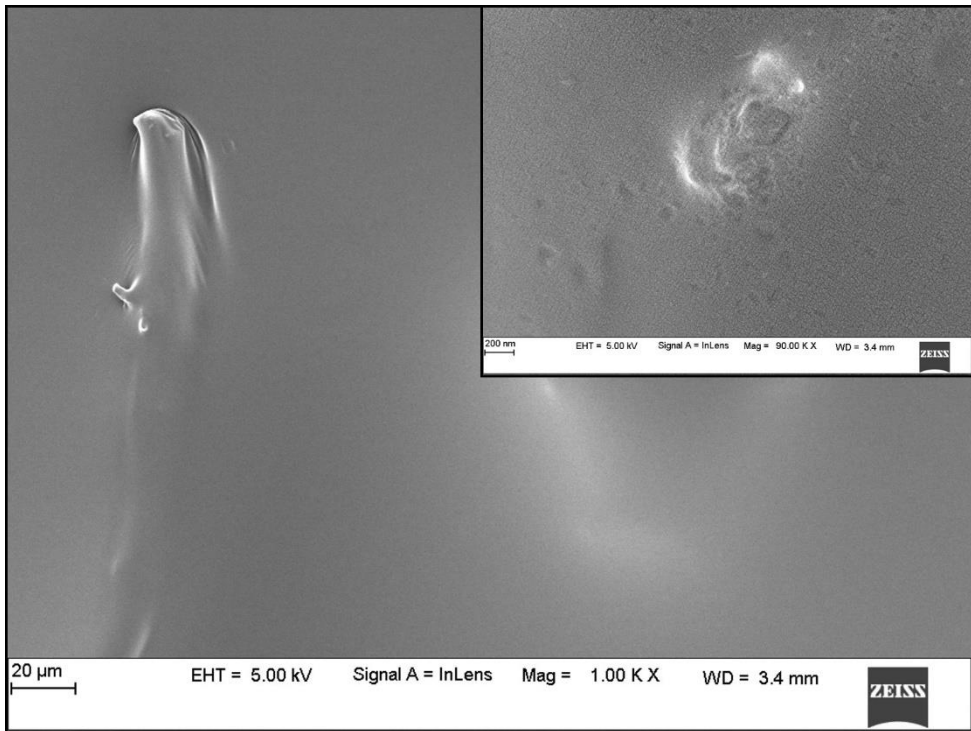


Figure 5.34 SEM image of CRMB-55+R for RTFO aged at 177°C

### 5.3.7. Storage Stability test

The effect of storage temperature, i.e., at 163°C and WMA additives on CRMB-55 binder are presented in Figure 5.35. Separation tubes were used to determine the impact of storage temperature and WMA additives on the overall separation of crumb rubber particles from the asphalt binder. The softening point difference of CRMB-55, CRMB-55+R, and CRMB-55+S between top and bottom indicated more than 2.5°C. Similarly, in 177°C storage temperature, the softening point difference between the top and bottom portion of the tube for CRMB-55 and CRMB-55+S was also greater than 2.5°C expect CRMB-55+R binder where the difference was found to be lesser than 2.5°C as shown in Figure 5.35. Eventually, when all binders were stored at 195°C temperature, the difference in softening point between the top and bottom portion of the aluminum tube was found to be more than 9°C, as shown in Figure 5.35. This implies that storage temperature and WMA additives play a vital role in the suspension of rubber particles in a binder medium, as explained in the image analysis.

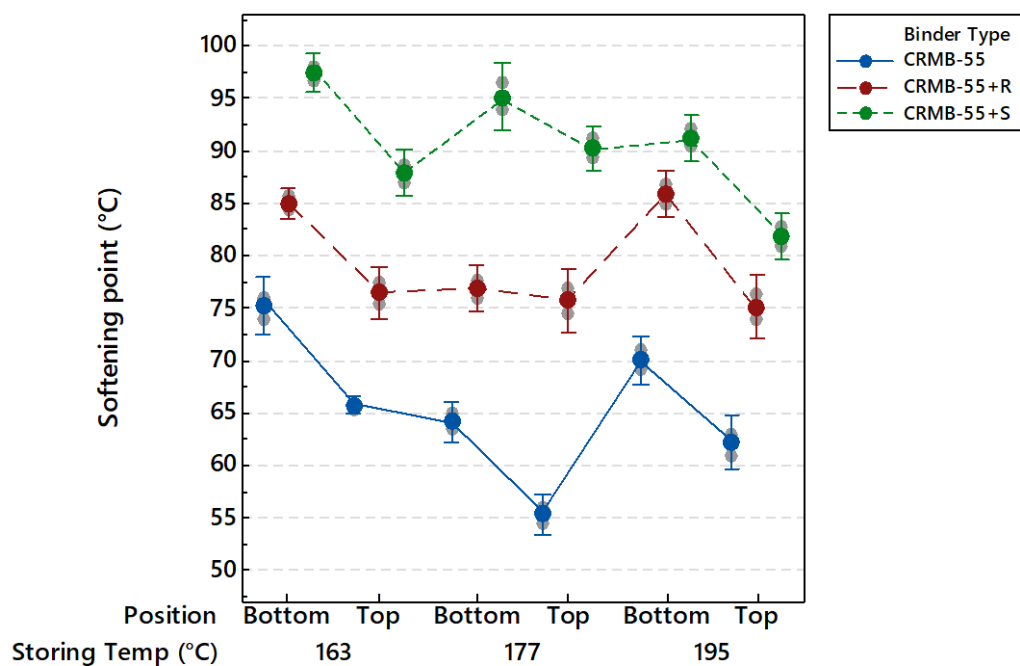


Figure 5.35 Comparison between softening point of one-third top and bottom of aluminum tube

#### 5.4. SUMMARY

This chapter investigated the influence of working temperature on the rheological properties of asphalt binder using rutting related parameters. Rheological tests such as frequency sweep test, temperature sweep test, and time-temperature superposition test, followed by multiple shear creep recovery (MSCR) and performance grade test were conducted to characterize and compare the high-temperature performance, temperature sensitivity of the all binders. Based on the test results, the following findings have been obtained:

1. With increase in working temperature,  $G^*$  of all binders exhibits similar behaviour with increase in frequencies at  $60^\circ\text{C}$ . With the addition of WMA additives into CRMB-55, Sasobit enhanced the  $G^*$  throughout the frequency range 0.1 rad/s to 100 rad/s compared to rediset additives for the binder subjected to  $177^\circ\text{C}$  working temperature.
2. Similarly, CRMB-55+S binder subjected  $177^\circ\text{C}$  working temperature enhanced the  $G^*$  throughout the temperature sweep ranging from  $46^\circ\text{C}$  to  $88^\circ\text{C}$  compared to Rediset additives and rest of the binders.
3. TTS test results evidenced that  $G^*$  of CRMB-55+S at extreme low frequency was high compared to Rediset additives, which is subjected to  $177^\circ\text{C}$  working temperature.
4. Performance grade test indicated that by considering the working temperature  $177^\circ\text{C}$ , CRMB-55+S exhibited highest failure temperature corresponding to 2.2 kPa compare to Rediset additive.
5. However, MSCR test indicated that there is concern in percent recovery of CRMB-55+S, which is subjected to  $177^\circ\text{C}$  working temperature, even though it exhibited lower  $J_{nr}$  value. In this case in terms of % recovery and non-recoverable creep compliances CRMB-55 appeared to be best in resistance to the rutting performance.
6. SEM images analysis showed that the proof of existence of asphaltene in CRMB-55 binder with WMA additives Sasobit and Rediset found to low except

in VG-30 at 163°C working temperature. However, this gives the inferences that volatility of the CRMB-55 binder in the presence of WMA additives is protected at 177°C working temperature.

7. The storage stability test was conducted for the CRMB-55 at 163°C, 177°C, and 195°C storage temperature. the results showed that softening point difference of CRMB-55+R found to be less than 4°C at 177°C storing temperature, means it remains stable by being equilibrium between asphalt binder and rubber particles compared.

## CHAPTER 6

### INFLUENCE OF WORKING TEMPERATURE ON FATIGUE PERFORMANCE OF CRMB

#### 6.1. GENERAL

The main aim of this chapter is to study and analyse the fatigue performance parameters, using intermediate performance grading, linear amplitude sweep (LAS) test, and thixotropic behaviour at 25°C for the short-term aging condition at 163°C, 177°C, and 195°C working temperature and followed by PAV aging. In addition, the binder's surface morphology and chemical structural behaviour were analysed using SEM and FTIR tests. Furthermore, the effect of working temperature and long-term aging conditions were summarized.

#### 6.2. EXPERIMENTAL PLAN FOR STUDIES ON FATIGUE PERFORMANCE OF CRMB

The short-term aging was initially conducted at three different working temperatures, 163°C, 177°C, and 195°C for VG-30 and CRMB-55 binders, as shown in the experimental plan in Figure 6.1. Further, the test matrix adopted to determine fatigue performance parameter for three different working temperature and PAV aging conditions were presented in Table 6.1.

Table 6.1 Details on different matrix for analysing the fatigue performance study

Test type	RTFO (°C)	PAV (°C)	Frequency (rad/s)	Strain (%)	Temp.(°C)	Shear Rate (s <sup>-1</sup> )	No. of Specimens
PG test		100	10	1	25		4x3x3
LAS	163, 177, 195	100	10	0.1 to 30	25		4x3x3
Thixotropy		100	-	-	25	0.1 to 1	4x3x3

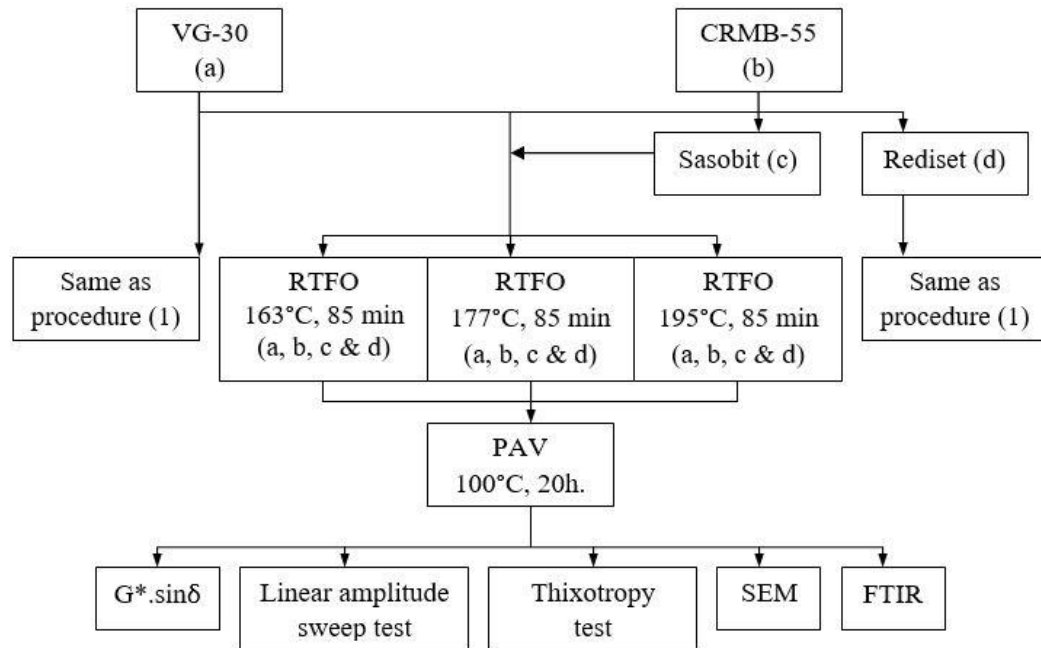


Figure 6.1 Flowchart for experimental plan of fatigue performance of CRMB-55 with WMA additives

### 6.3. RESULTS AND DISCUSSION

The results and discussions of the present investigations are discussed in the following sections.

#### 6.3.1. Intermediate Performance grade test

Figure 6.2 shows the relationship between the fatigue criterion ( $G^* \cdot \sin \delta$ ) and temperatures for all binders, indicating that, with a decrease in temperature, the fatigue factor of all binders proportionally increases, and the threshold temperatures of all binders are less than 25 °C. The temperature at which fatigue property ( $G^* \cdot \sin \delta$ ) is equal to 5000 kPa is critical temperature. For CRMB-55, asphalt binders without WMA additives, with higher RTFO aging temperature, i.e., 195°C and PAV aged, can reduce the fatigue factor, corresponding to higher fatigue resistance. Compared to the VG-30 binder, which is RTFO aged at 163°C, the fatigue factor value of CRMB-55 increases at approximately 8.85% and 15.25% when short-term aged at 163°C and 195°C, respectively, at 22 °C test temperature.

However, CRMB-55 binder with rediset content observed an enhanced fatigue behaviour with the short-term aging temperature at 177°C followed by PAV aging



condition. Moreover, it seems to exhibit a similar behaviour compared to VG-30 binder, which is short-term aged at 163°C and PAV aged. Therefore, it can be concluded that CRMB-55 binder with rediset content can improve the fatigue performance compared to sasobit additives as shown in Figure 6.2, as lower fatigue failure temperature indicates the better fatigue resistance behaviour.

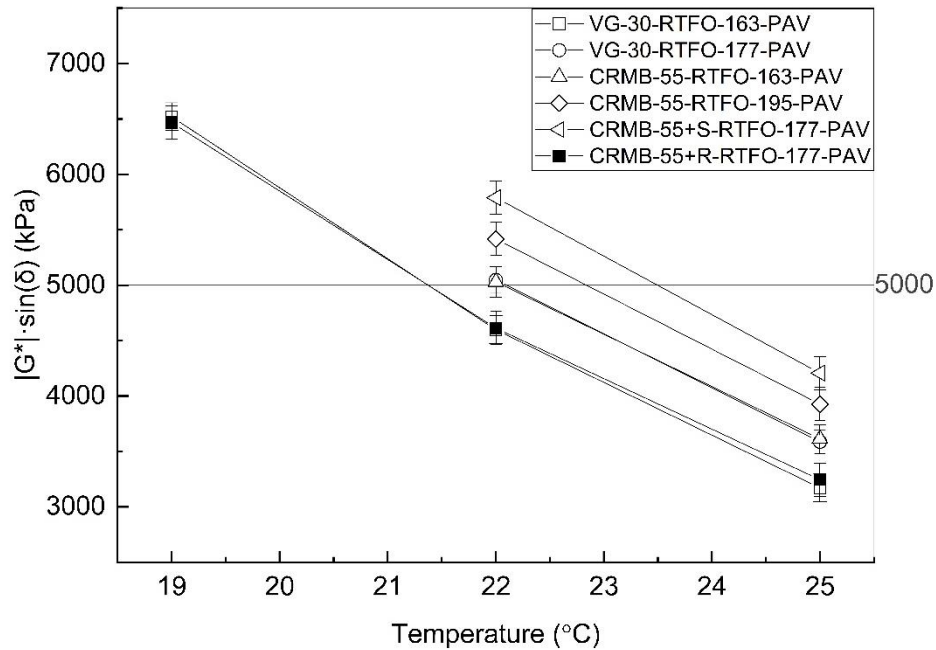


Figure 6.2 Performance grade at intermediate service temperature

### 6.3.2. Linear Amplitude Sweep test

Figure 6.3 to Figure 6.5 represents the plot of effective shear stress versus effective shear strain obtained from the amplitude strain sweep test under strain-controlled conditions. All binder combinations results showed considerable damage at a higher amplitude strain level, which is similar to Ashish et al. (2017) discussion on LAS test results. Also, the maximum shear stress value increased with an increase in short-term aging temperature, indicating a decrease in load carrying capacity under shear action with the addition of WMA additives sasobit compared to rediset into CRMB-55 binder. The maximum shear stress value can be observed at the applied amplitude strain level of 5% for VG-30 and CRMB-55 binder. Still, it sharply decreases, indicating sudden failure after 5% of strain-level with an increase in short-term aging temperature. However, CRMB-55 with sasobit content shows a higher shear

stress-strain pattern followed by CRMB-55 and CRMB-55 with rediset beyond amplitude strain level of 5%, indicating interesting behaviour of amplitude sweep testing beyond this strain level as evident from Figure 6.4. Considering the rate of damage in the post-peak region with an increasing amplitude strain level, the binder VG-30 content exhibited the highest rate of damage followed by CRMB-55, CRMB-55 with sasobit (4%) and rediset (4%), for RTFO aged at 163°C, 177°C, and 195°C, respectively. This may be attributed to the increase in short-term aging temperature, which increases the stiffness value of VG-30, CRMB-55, along with WMA additives.

A particular value of “C” represents the level of material integrity at any instant of time. A value of “C” equal to 1 represents the material with highest integrity level with no damage, whereas a material with “C” equal to 0 represents the complete damage to it.

As per AASHTO TP 101-14, damage (D) to the binder at any time (t) can be expressed as

$$D(t) = \sum_{i=1}^N [\pi\gamma_0^2 (C_{i-1} - C_i)]^{\alpha/1+\alpha} (t_i - t_{i-1})^{1/1+\alpha} \quad (6.1)$$

Where,  $C(t) = G^*(t)/G^*$  (Initial) = integrity parameter;  $\gamma_0 = \text{applied strain}$ ;  $G^* = \text{complex shear modulus (Mpa)}$ ;  $t = \text{testing time (s)}$

The power law model has been used to develop the relationship between damage to the integrity parameter as follows:

$$C(t) = C_0 - C_1 D^{C_2} \quad (6.2)$$

Where,  $C_1$  and  $C_2 = \text{coefficient of curve-fitting equations}$ .

.The damage value at failure point is calculated. According to Johnson (2010) considered a 35% reduction in integrity parameter as the failure point, whereas, Bahia et al. (2013) considered the peak shear stress as the failure point. AASHTO TP 101-14 suggests the use of peak shear stress as the failure point, and the same was considered for evaluating the fatigue life in the current research work.

Figure 6.6 to Figure 6.8 shows the relationship between damage intensity (D) and integrity parameter (C) for VG-30, CRMB-55 with WMA additives sasobit, and rediset obtained from the LAS test. Value of C equals 1 represents the highest integrity

with no damage, while C equal to zero shows the complete failure of a material (Singh et al. 2017). Figure 6.6 to Figure 6.8 shows that the rate of decrease in C increases with the increase of short-term aging temperature and addition of WMA additives to CRMB-55, indicating rapid damage to the performance of VG-30 at 163°C, 177°C, and 195°C short-term aged temperature compared to CRMB-55 binder with WMA additives.

Fig 6.3 to Fig 6.5, represents the effect of working temperature on variation of effective shear stress at different amplitude strain levels during amplitude sweep in the LAS test. These plots describe the strain dependence and damage to asphalt binder during shear loading. The binder with broader peak represents the less dependence on applied strain during shear loading case as a result of variation in its structural components. Similarly, the sharp peak of CRMB-55+R shows that the strain dependency increases with increase in working temperature, which is comparable to VG-30 binders. Therefore, with a help of stress-strain behaviour the effect of working temperature would be observed. Similarly, as shown in Fig 6.6 to Fig 6.8 the plot of integrity parameter (C) versus damage intensity (D) represents the level of material integrity for any given instant of time. Binder CRMB-55 indicates a better fatigue performance, in which  $C_1$  and  $C_2$  remain unchanged with increase in working temperature followed by CRMB-55+R, CRMB-55+S and VG-30.

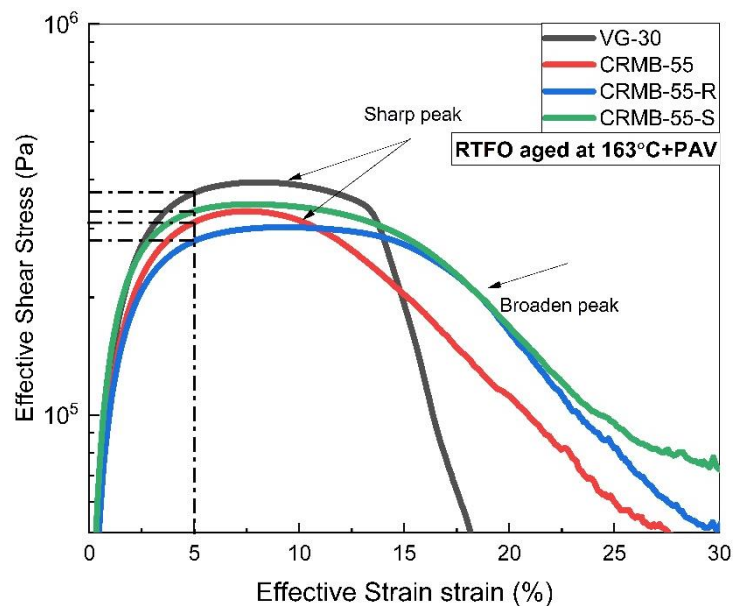


Figure 6.3 Effective shear stress versus strain response of binders RTFO aged at 163°C and PAV aged

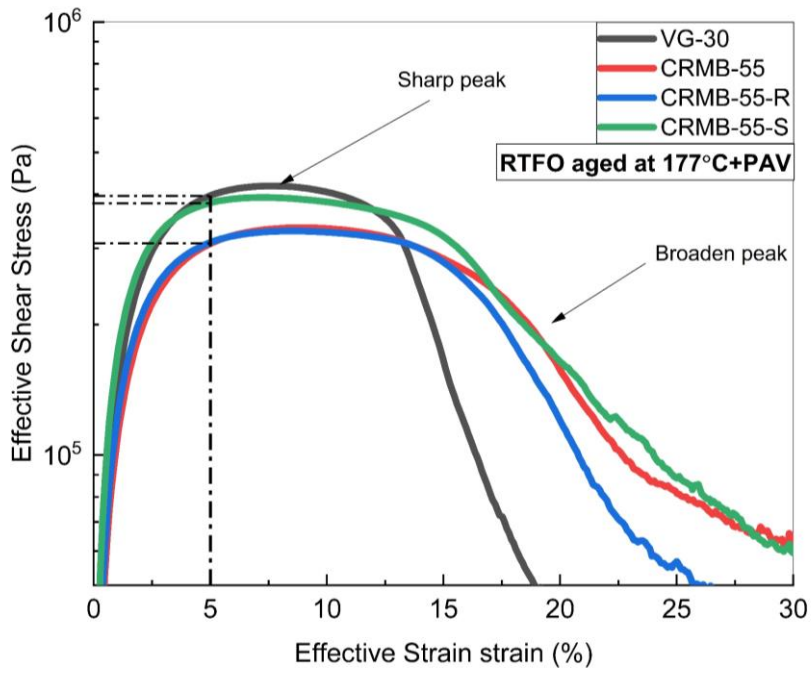


Figure 6.4 Effective shear stress versus strain response of binders RTFO aged at 177°C and PAV aged

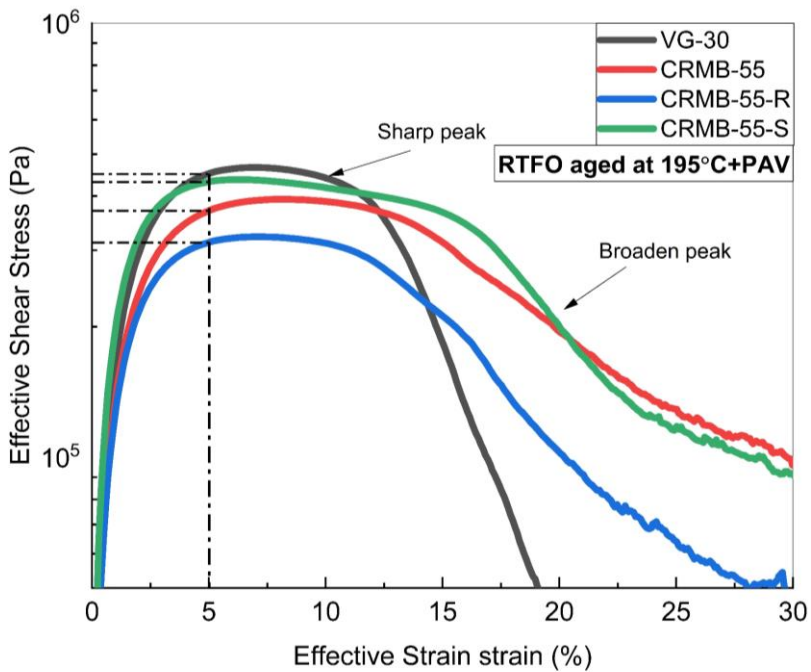


Figure 6.5 Effective shear stress versus strain response of binders RTFO aged at 195°C and PAV aged

The CRMB-55 with 4% sasobit shows high effective shear stress after VG-30 compared to control CRMB-55 and with rediset for the short-term aged temperature, which indicates brittle nature binder and contributes to the short-term aging temperature to rapid damage. For any particular level of D, C is the highest for control VG-30 binder, followed by CRMB-55 with sasobit (4%), CRMB-55, and CRMB-55 with rediset (4%).

As discussed in Chapter-3, VECD principles is used in estimating the fatigue performance of binders Table 6.2 shows the values of fatigue damage parameters obtained from the LAS test. The  $C_0$  parameter for all the binder types was 1, representing the highest integrity with no damage. Parameters  $\alpha$  and A were determined after carrying out damage analysis of CRMB-55 with and without WMA additives from an amplitude sweep test, whereas B signifies the undamaged material property. Number of load cycle to fatigue failure ( $N_f$ ) is directly proportional to parameter A as discussed in Chapter-2. Moreover, the fatigue life of asphalt is sensible to the value of  $\alpha$  and A, where the  $\alpha$  value indicates the rate of reduction in fatigue life with an increase in strain amplitude. Parameter A is fatigue law coefficient that depend on material characteristics, which is determined using viscoelastic continuum damage theory (VECD). Thus a lower value of  $\alpha$  and a higher value of A is desirable for superior performance against fatigue.

A decrease in A can be seen with an increase of RTFO aging temperature from 163°C to 177°C and increases with a further increase of RTFO aging temperature to 195°C, which ultimately increases the fatigue life of CRMB-55 with WMA additive Table 6.2. Similarly, an increase in  $\alpha$  of the CRMB-55 with rediset binder was observed with an increase in RTFO aging temperature from 177°C to 195°C Table 6.2, indicating higher strain susceptibility at intermediate temperature. Furthermore, the  $\tau_{max}$  value of CRMB-55 with rediset increased from 302 to 329 kPa as shown in Table 6.2 with the addition of rediset (4%), showing an increase in shear stress carrying capacity of CRMB binder after increasing the RTFO aging temperature. Thus the increase of short-term aging temperature may be beneficial to resist early fatigue failure. Figure 6.6 to Figure 6.8 shows that the rate of increase of integrity level of CRMB-55 increased with the increase in RTFO aging temperature. At any particular level of integrity, the damage to

the CRMB-55 binder was lowest in the case of RTFO aging temperature at 163°C, 177°C, and 195°C and highest for CRMB-55 with sasobit additives (4%).

Table 6.2 Different coefficients obtained from VECD Analysis

RTFO aged	Sample code	A	B	$\alpha$	$\tau_{in}$	$\tau_{max}$	$C_o$	$C_1$	$C_2$
163°C	VG-30	1.180E+05	-3.895	1.947	8.07E+03	3.79E+05	1.000	0.109	0.401
	CRMB-55	1.529E+05	-4.160	2.080	7.32E+03	3.32E+05	1.000	0.124	0.371
	CRMB-55+R	7.308E+04	-4.089	2.044	7.25E+03	3.02E+05	1.000	0.155	0.324
	CRMB-55+S	4.345E+04	-4.476	2.238	8.50E+03	3.46E+05	1.000	0.188	0.296
177°C	VG-30	1.287E+05	-4.007	2.003	8.40E+03	4.18E+05	1.000	0.112	0.398
	CRMB-55	1.856E+05	-4.220	2.110	7.26E+03	3.35E+05	1.000	0.131	0.352
	CRMB-55+R	7.127E+04	-4.173	2.087	7.80E+03	3.29E+05	1.000	0.156	0.328
	CRMB-55+S	4.755E+04	-4.634	2.317	9.12E+03	3.93E+05	1.000	0.190	0.296
195°C	VG-30	1.672E+05	-4.251	2.126	8.95E+03	4.66E+05	1.000	0.116	0.394
	CRMB-55	2.102E+05	-4.466	2.233	8.15E+03	3.93E+05	1.000	0.140	0.343
	CRMB-55+R	2.997E+05	-4.887	2.443	7.84E+03	3.22E+05	1.000	0.143	0.347
	CRMB-55+S	1.164E+05	-5.159	2.580	9.55E+03	4.36E+05	1.000	0.188	0.296

<sup>a</sup>  $C_1$ ,  $C_2$  are curve fitting coefficients,  $\tau_{in}$  and  $\tau_{max}$  are initial and peak shear stress in Pa

<sup>b</sup> represents average values

The LAS test gives results regarding the number of load repetitions of ESAL ( $N_f$ ) to failure versus applied shear strain (Singh et al. 2017). The  $N_f$  obtained from the calculation was normalized to 1 million ESALs and plotted in Figure 6.9 and Figure 6.10. It can be seen that the addition of 4% of sasobit shows a significant reduction in  $N_f$  at all levels of strain, which can be linked to the stiffer nature of binders as evident from  $G^*/\sin\delta$  and  $J_{nr}$  parameters, discussed in previous sections. However, VG-30 shows better behavior than CRMB-55, CRMB-55 with 4% of sasobit, and rediset at a 2.5% strain level. The  $N_f$  for CRMB-55 is the highest followed by CRMB-55 + 4% rediset, CRMB-55 + 4% sasobit. Overall, the addition of sasobit results in lower fatigue life of the CRMB-55 binder. Many reported that incorporating sasobit to rubber modified binder made the mixtures stiff and prone to reflective cracking (Vahidi et al. 2014).

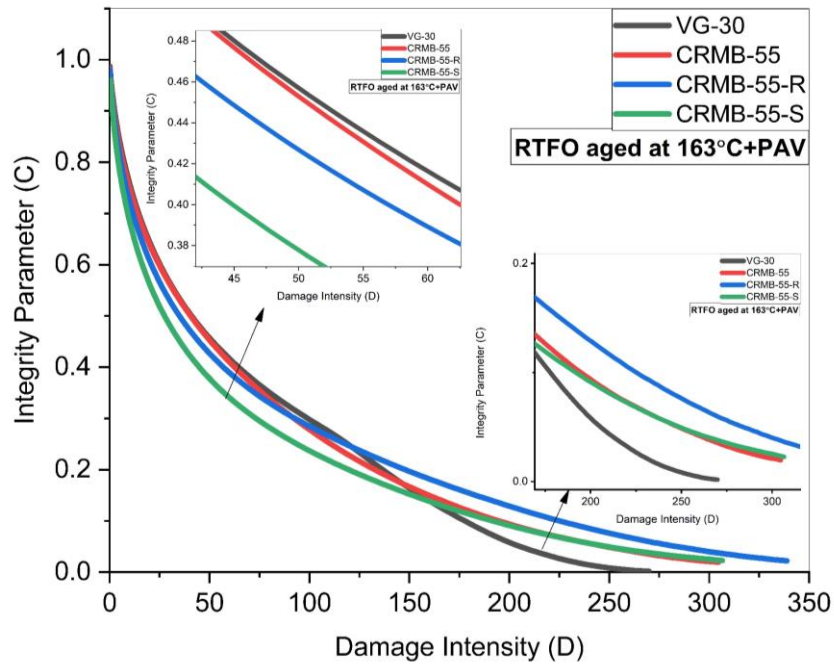


Figure 6.6 Variation of integrity parameter with damage intensity of binders RTFO aged at 163°C and PAV aged

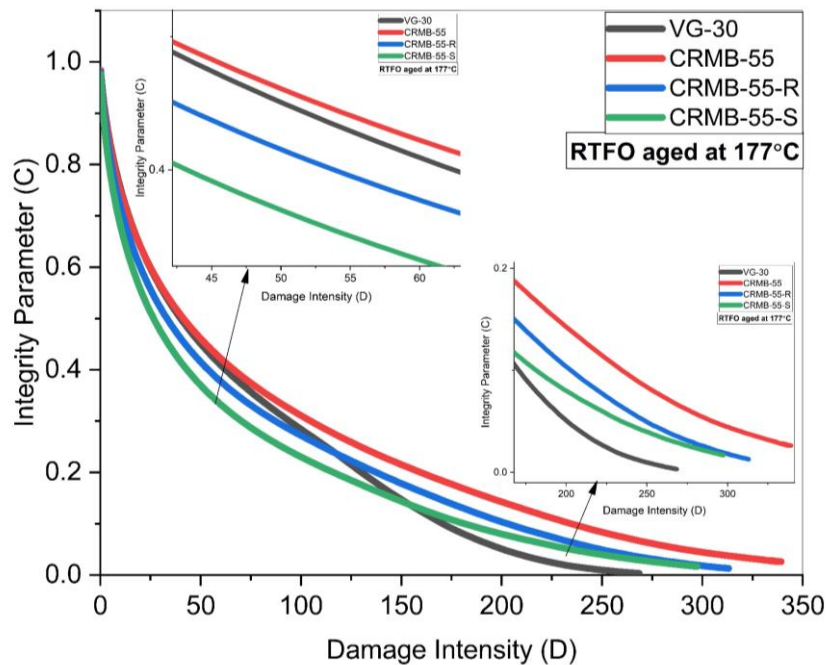


Figure 6.7 Variation of integrity parameter with damage intensity of binders RTFO aged at 177°C and PAV aged

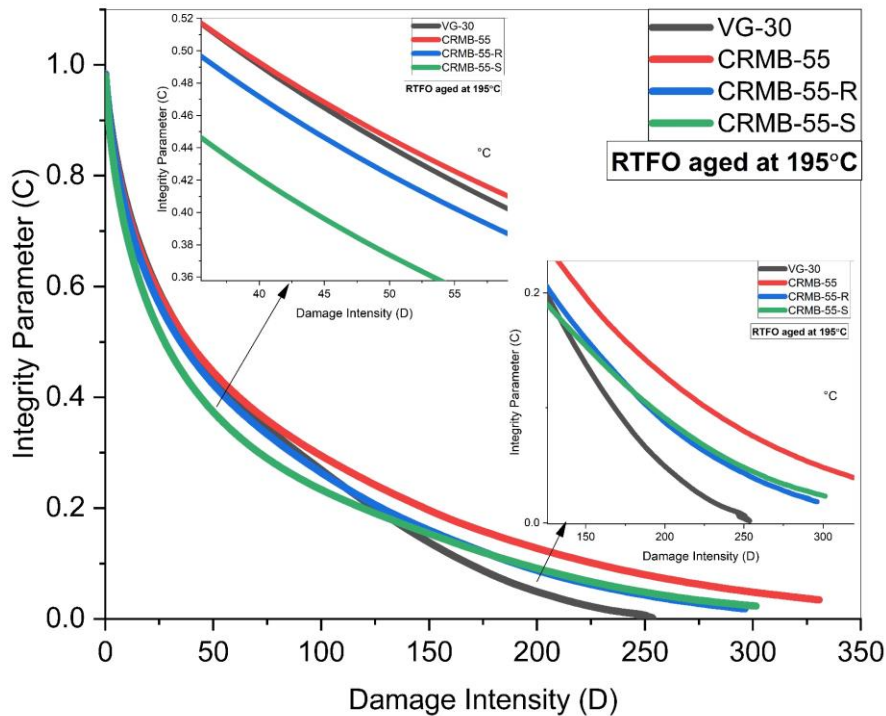


Figure 6.8 Variation of integrity parameter with damage intensity of binders RTFO aged at 195°C and PAV aged

Figure 6.9 and Figure 6.10 show the variation of several load cycles to failure against applied amplitude strain level. It offers significant improvement in fatigue life of CRMB-55 for short-term aged at 195°C with the addition of rediset, particularly in lower applied strain levels. For example, at the strain level of 2.5%, the load cycles to failures increased from 1742.5 to 3427 when the short-term aging temperature increased from 163°C to 195°C for the binder containing rediset, indicating an increase in fatigue life by almost two times. It can be seen that at the higher strain level, the effects of RTFO temperature on the fatigue behaviour of CRMB-55 modified binder play a vital role. Similar, improvement in fatigue life depends upon the short-term aging temperature has been reported in the literature based upon different parameters used for fatigue life assessment of rubber modified binder.



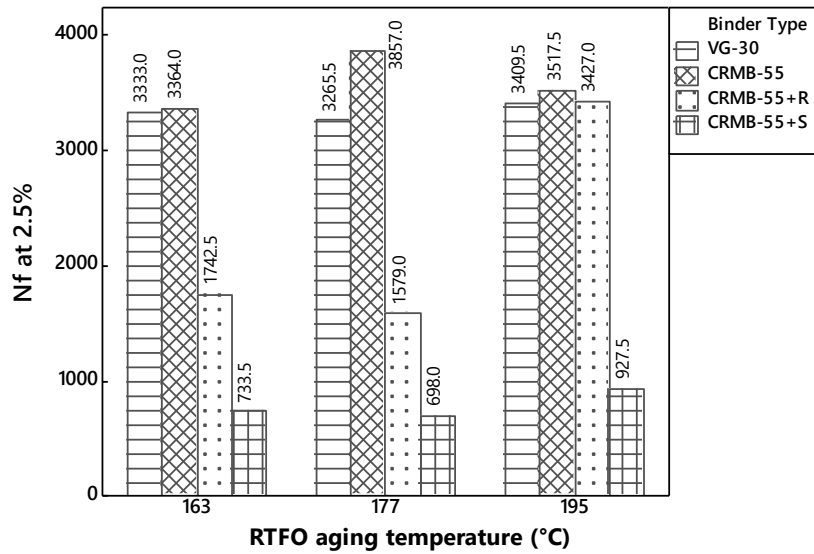


Figure 6.9 Fatigue Life of binders RTFO aged at 163°C, 177°C, 195°C and PAV aged for 2.5% stress level

Earlier, a hypothesis was made regarding improvement in fatigue life of CRMB-55 with the increase in RTFO aging temperature from 163°C to 177°C upon a decrease in Jnr and increase in %R value obtained through the MSCR test as shown in MSCR test results in the previous chapter. This hypothesis is true for CRMB-55 binder short-term aged at 177°C exhibited the high %R value and highest number of cycles to fatigue failures as shown in Figure 6.9 and Figure 6.1.

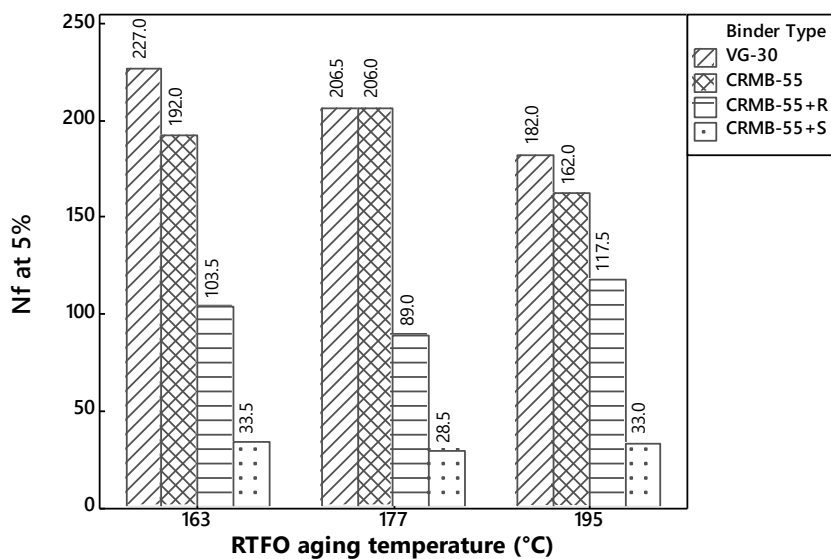


Figure 6.10 Fatigue Life of binders RTFO aged at 163°C, 177°C, 195°C and PAV aged for 5% stress level

### 6.3.3. Thixotropic behaviour

The thixotropic behavior of the VG-30 binder was studied at two different short-term aging temperatures (163°C and 177°C) and subjected to PAV for a given shear rate of 0.1(s<sup>-1</sup>) and 1 (s<sup>-1</sup>) as shown in Figure 6.11 to Figure 6.12. Similarly, for CRMB-55 (163°C & 195°C), CRMB-55+S and CRMB-55+R binders were short-term aged at 177°C, respectively and followed by PAV aging process before applying shear rate at 25°C test temperature as shown in Figure 6.13 to Figure 6.16.

At 25°C test temperature, the viscosity of VG-30, which is short-term aged at 177°C, was observed to be increased in the first step compared to 163°C short-term aging temperature. Whereas, in the third step, the increase in recovery after subjecting the higher shear rate to sample was found to be more in the case of 177°C short-term aging than 163°C temperature, as shown in Figure 6.11. Figure 6.12 and Figure 6.12. Similarly, in the sample CRMB-55, the viscosity was found to be increased in the first step of the curve, which is due to an increase in short-term aging temperature from 163°C to 177°C. In this case, the CRMB-55 binder RTFO aged at 163°C has more tendency to recover in the third step than RTFO aging temperature at 195°C, as shown in Figure 6.13 and Figure 6.14. However, CRMB-55 in the presence of WMA additives sasobit showed higher viscosity and rate of recovery in the first and third curve, respectively when compared to rediset additives, which indicates that rediset additives soften the modified binder even after short-term aging at 177°C and long-term aging but at the same time it leads to a weaker destructuring state.

Figure 6.17 shows the viscosity curve (structural formation or build-up) for RTFO and PAV aged asphalt binder, respectively. A non-linear regression analysis model was developed from the experimental data analysis to fit the formation and relaxation curves generated in the first step and third step of the curve at 0.1 (s<sup>-1</sup>), respectively. For this purpose, the exponential and Biguassian function was implemented to fit the desired expressions as shown in equations Eq. 6.3 & Eq. 6.4 on viscosity curves, respectively.

As shown in Figure 6.17, an increase in short-term aging temperature (RTFO aging at 195°C) for CRMB-55 results in increased viscosity at a constant shear rate of

0.1 ( $s^{-1}$ ) for 90 sec of time duration. Similarly, CRMB-55 in the presence of sasobit RTFO aged at 177°C, followed by CRMB-55 and VG-30 RTFO aged at 163°C and 177°C, respectively. However, the lowest viscosity was exhibited in VG-30 and CRMB-55 in the presence of rediset when RTFO aged at 163°C and 177°C, respectively. The effect of short-term aging temperature shows favorable trends of changes at 0.1 ( $s^{-1}$ ) shear rate for the 90-sec duration. These changes indicate an increase in viscosity by a build-up of internal structures, which results in poor fatigue resistance. The viscosity of CRMB-55 in the presence of rediset after RTFO aged at 177°C indicated a similar behaviour as of VG-30, which is short-term aged at 163°C and found to be significantly improved in fatigue property at 25°C test temperature. Table 6.3 shows the exponential curve fit model parameters for all the binders, which helps predict the viscosity behaviour in the process of understanding the thixotropic behaviour.

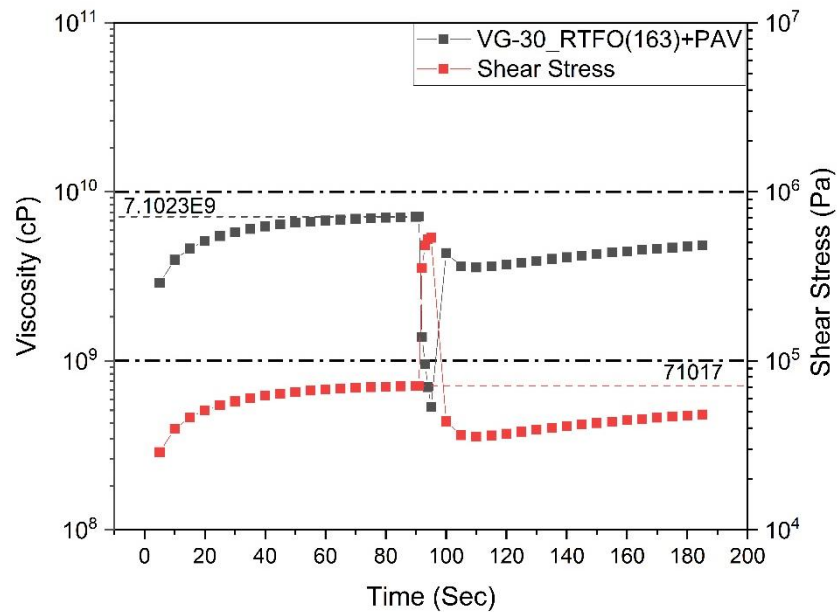


Figure 6.11 Thixotropic behaviour of VG-30 for RTFO aged at 163°C and PAV aged

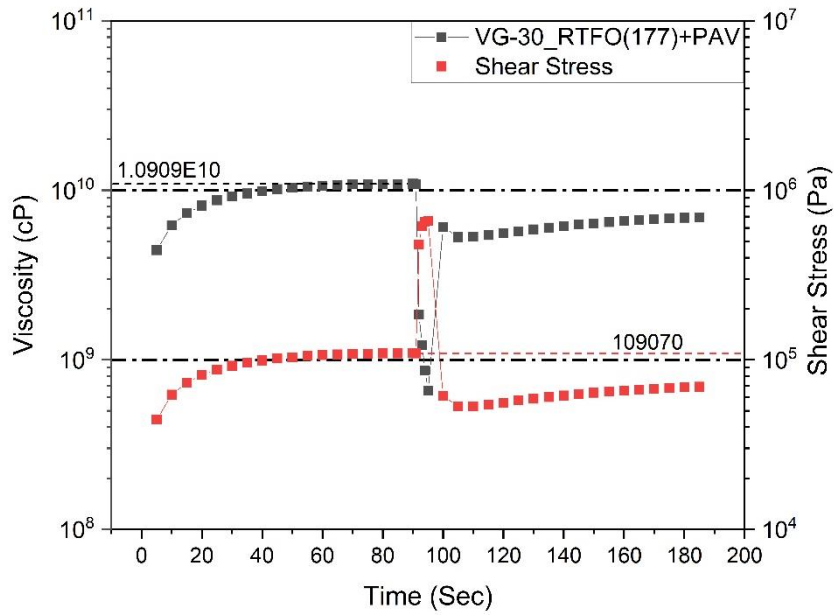


Figure 6.12 Thixotropic behaviour of VG-30 for RTFO aged at 177°C and PAV aged

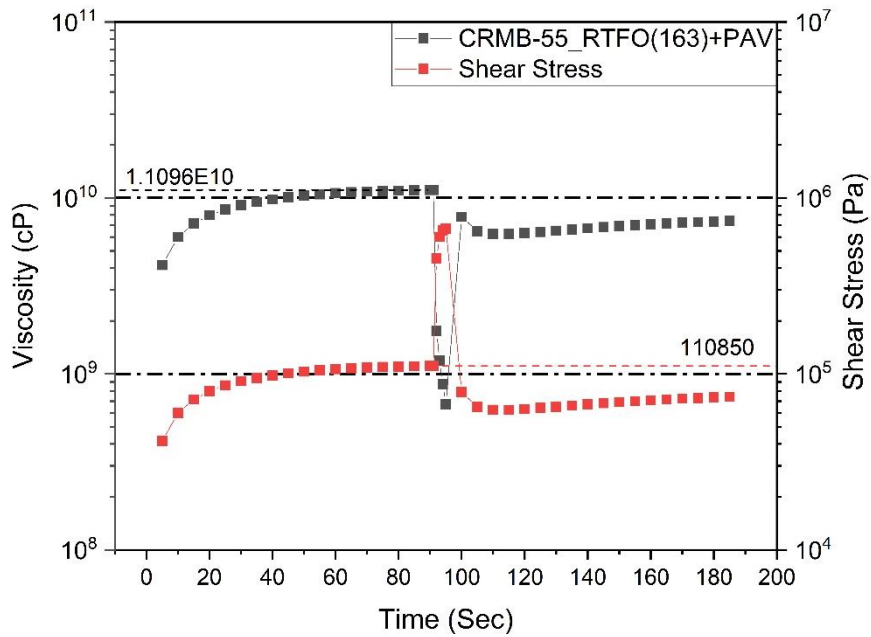


Figure 6.13 Thixotropic behaviour of CRMB-55 for RTFO aged at 163°C and PAV aged

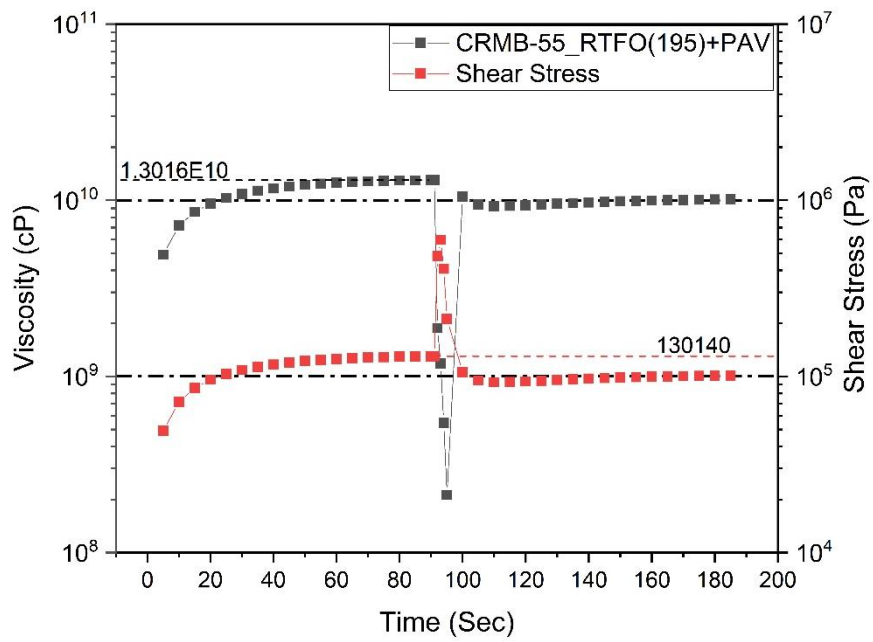


Figure 6.14 Thixotropic behaviour of CRMB-55 for RTFO aged at 195°C and PAV aged

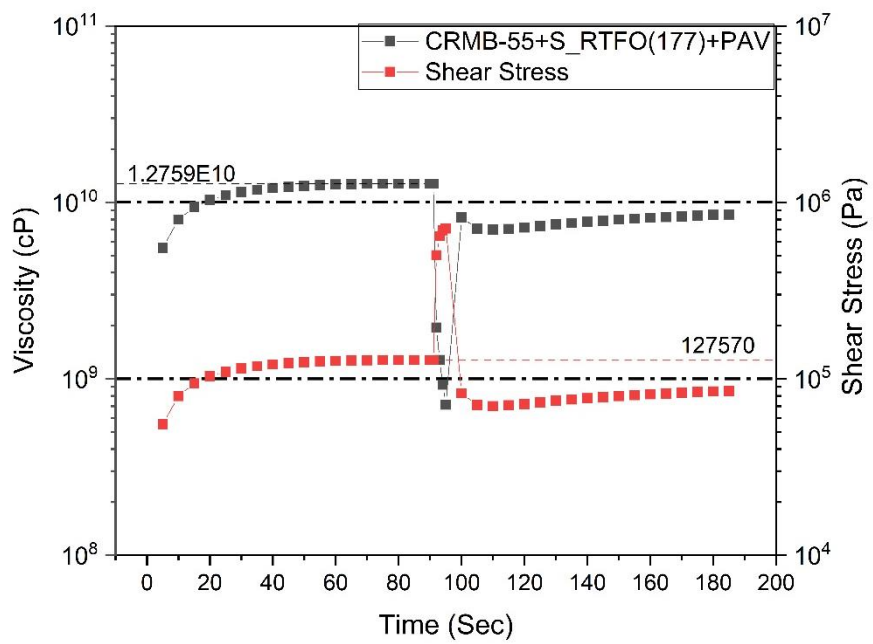


Figure 6.15 Thixotropic behaviour of CRMB-55+S for RTFO aged at 177°C and PAV aged

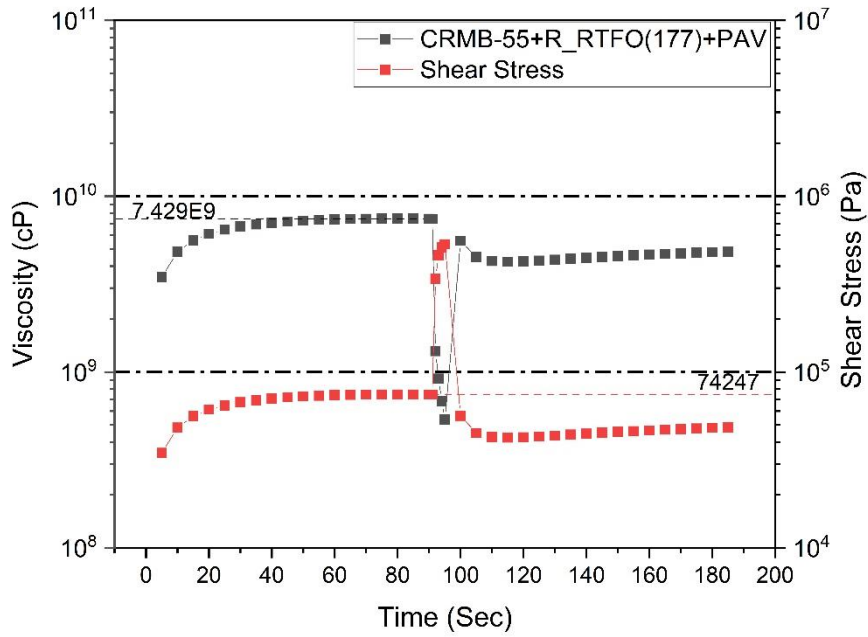


Figure 6.16 Thixotropic behaviour of CRMB-55+R for RTFO aged at 177°C and PAV aged

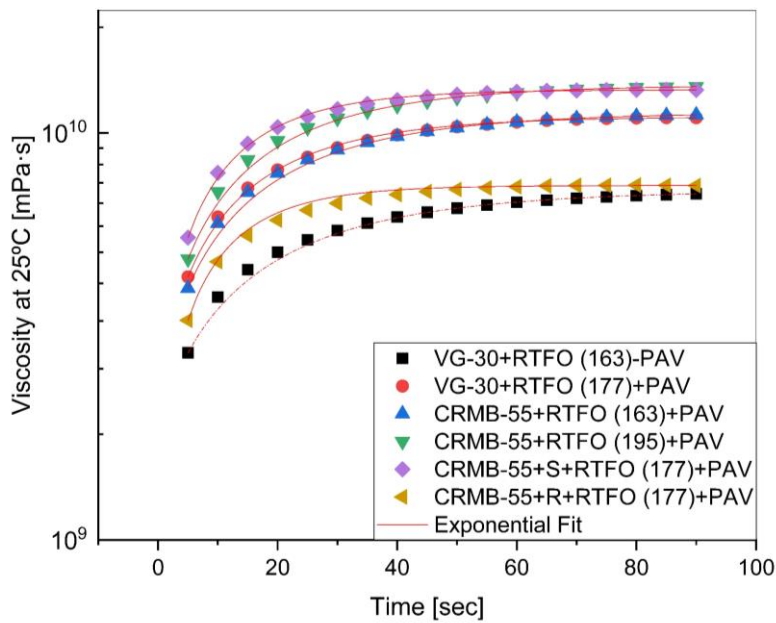


Figure 6.17 Exponential fit model for the first part of the thixotropic curve “formation of the structure” at 0.1 (s-1) shear rate of binders

$$y = y_0 + A \cdot e^{(R_0 \cdot x)} \quad \text{Eq. 6.3}$$

Where  $y$  is the viscosity after RTFO and PAV aged,  $y_0$ ,  $A$ , and  $R_0$  exponential model fitting parameters at a given time ‘ $x$ .’

Table 6.3 Exponential fit parameters values of the first part of the curve for different short-term aging temperatures

Binder Type	VG-30		CRMB-55		CRMB-55+S	CRMB-55+R
	163°C	177°C	163°C	195°C	177°C	177°C
$y_0$	$7.1E9 \pm 3.8E7$	$1E10 \pm 3.8E7$	$1.1E10 \pm 5.3E7$	$1.3E10 \pm 5.7E7$	$1.2E10 \pm 3.7E7$	$7.43E9 \pm 2.05E7$
A	$-5.1E9 \pm 8E7$	$-8.31E9 \pm 1E8$	$-8.6E9 \pm 1.3E8$	$-1.03E10 \pm 1.6E8$	$-1E10 \pm 1.7E8$	$-5.54E9 \pm 9.78E7$
$R_0$	$-0.04 \pm 0.0016$	$-0.05 \pm 0.001$	$-0.04 \pm 0.0015$	$-0.05 \pm 0.001$	$-0.07 \pm 0.0019$	$-0.07 \pm 0.0019$
Adj. R-Square	0.996	0.998	0.997	0.997	0.997	0.997

To simulate the third part of the recovery curve, Bigaussian fit was used to model the thixotropic behaviour in which the shear rate is changed from  $1 \text{ (s}^{-1}\text{)}$  to  $0.1 \text{ (s}^{-1}\text{)}$  for 90 sec. Due to the decrease in applied shear rate or stress relaxation, the microstructure is recognized to be recovered to its new steady-state level, as shown in Figure 6.18. The combination of a sudden increase in shear rate followed by fast relaxation with a gradual increase in viscosity of all binders is shown in Figure 6.18, which shows that the general form of response is thixotropic behaviour (Mewis and Wagner 2009). Table 6.4 shows the Bigaussian fit parameters for the third step curve, which indicates the recovery of the molecular structure by an increase in viscosity.

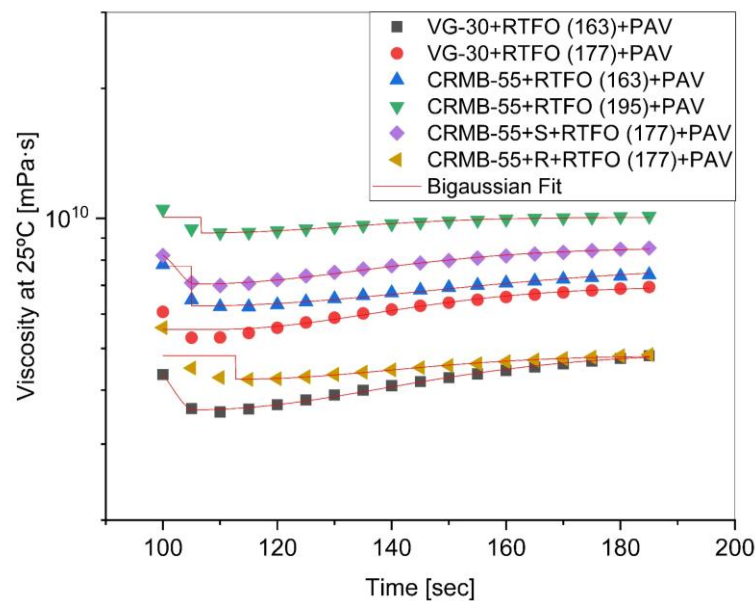


Figure 6.18 Exponential fit model for the first part of the thixotropic curve “formation of the structure” at  $0.1 \text{ (s}^{-1}\text{)}$  shear rate of binders

$$y = y_0 + H \cdot e^{-0.5\left(\frac{x-x_c}{w_1}\right)^2} \quad \text{Eq. 6.4}$$

$$(x < x_c)$$

Where  $y$  is the recovering viscosity, and  $y_0$ ,  $H$ ,  $x_c$ ,  $w_1$  are Bigaussian model fitting parameters at a given time (s).

Table 6.4 Bigaussian fit parameters values of the third part of the thixotropic curve for different short-term aging temperatures.

Binder Type	VG-30	VG-30	CRMB-55	CRMB-55	CRMB-55+S	CRMB-55+R
RTFO	163°C	177°C	163°C	195°C	177°C	177°C
$Y_0$	4.87E9 ± 4.06E7	6.9E9 ± 2E8	7.7E9 ± 4.7E7	1E10 ± 1E8	8.5E9 ± 3.6E7	4.8E9 ± 1.4E8
$x_c$	105.51 ± 0.54	108.7 ± 10.4	105 ± 4.86	106 ± 24	105.6 ± 0.36	112.7 ± 42.9
$H$	-1.27E9 ± 3.69E7	-1.41E9 ± 2.4E8	-1.48E9 ± 7.4E7	-8E8 ± 2.9E8	-1.48E9 ± 3.49E7	-5.68E8 ± 3.22E8
$w_1$	4.1 ± 0.39	6.4E9 ± 0	0.02 ± 0.68	0	3.2 ± 0.24	2.08E-8
$w_2$	36.07 ± 1.54	30.16 ± 10.97	44 ± 3.7	24.9 ± 16.6	30.7 ± 1.19	28.0 ± 30.76
Adj. R-Square	0.994	0.887	0.988	0.993	0.623	0.253

#### 6.3.4. Scanning Electronic Microscopic (SEM) test

Figure 6.19 displays the FE-SEM images of the CRMB (unaged) and from Figure 6.20 CRMB short-term aged at 163°C and PAV aged in the presences of sasobit and rediset, at the same magnification level of 1 K X as shown in Figure 6.24 and Figure 6.25. From Figure 6.19, it can be seen that the crumb rubber particles are entirely covered by asphalt binder with a bee-like structure appearance when viewed at 100 nm scale and magnified at 10 K X, which indicates the existence of asphaltene micelles in CRMB-55 at the unaged condition. However, Figure 6.20 has no bee-like structure for the CRMB-55 binder, which is subjected to short-term aging conditions at 163°C and PAV aged when viewed at the same scale and magnification. The presence of sasobit additives consists of “fibrils” like structure with 1µm length and 0.2µm wide, which indicates the presence of resin and asphaltene phases as shown in Figure 6.24. Whereas,



in the presence of rediset additives, it is observed that the asphaltene structure consisted of smaller-sized fibrils compared to sasobit additives, as shown in Figure 6.25.

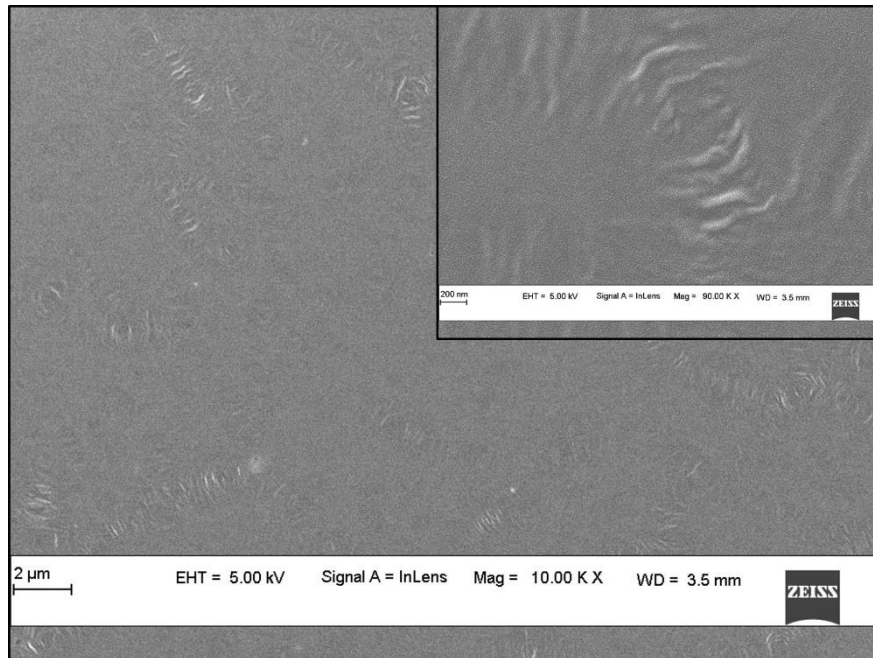


Figure 6.19 FE-SEM images of CRMB-55 for unaged conditions

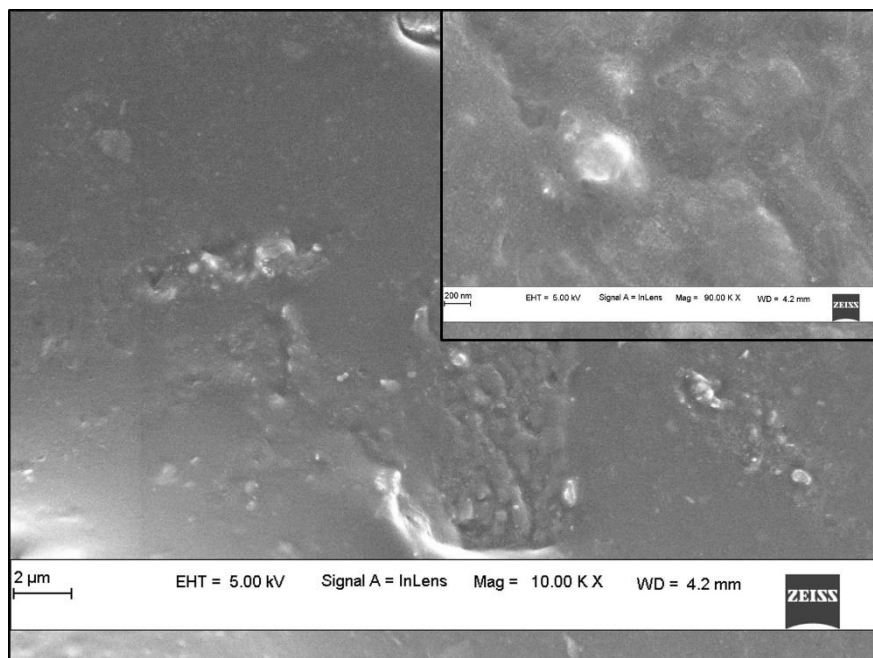


Figure 6.20 FE-SEM images of CRMB-55 for 163°C RTFO aging followed by PAV conditions

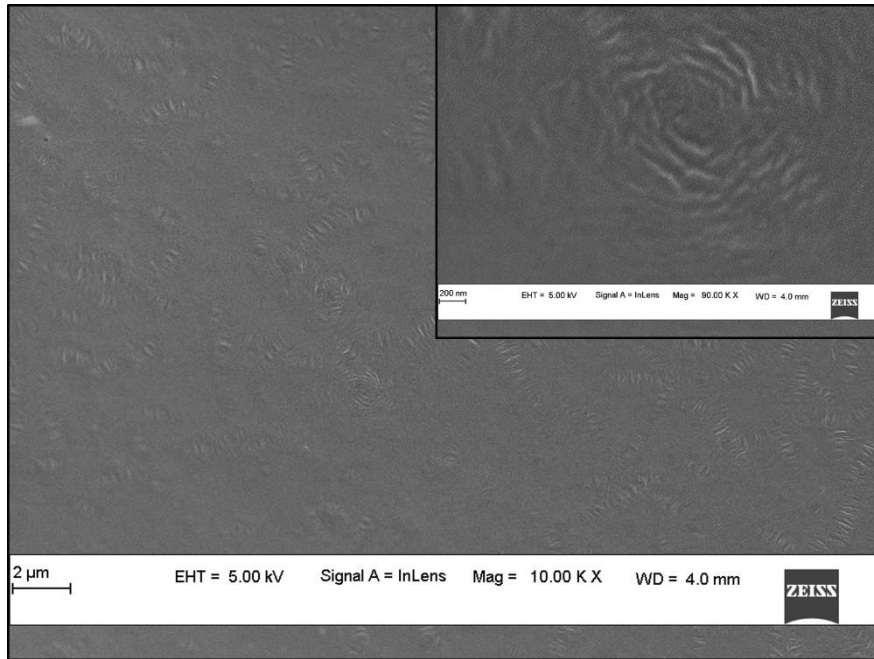


Figure 6.21 FE-SEM images of CRMB-55 for 177°C RTFO aging followed by PAV conditions

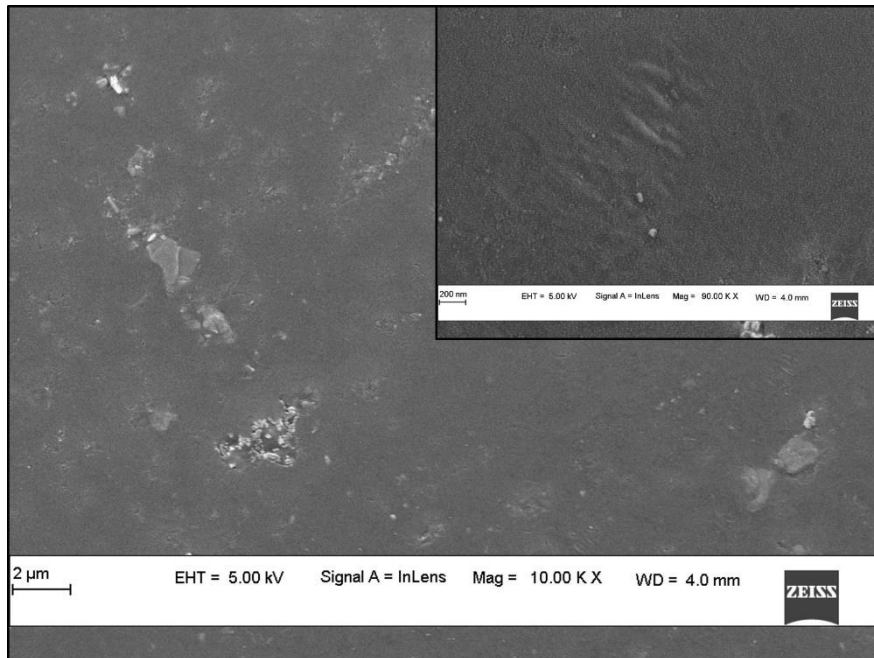


Figure 6.22 FE-SEM images of CRMB-55 for 195°C RTFO aging followed by PAV conditions

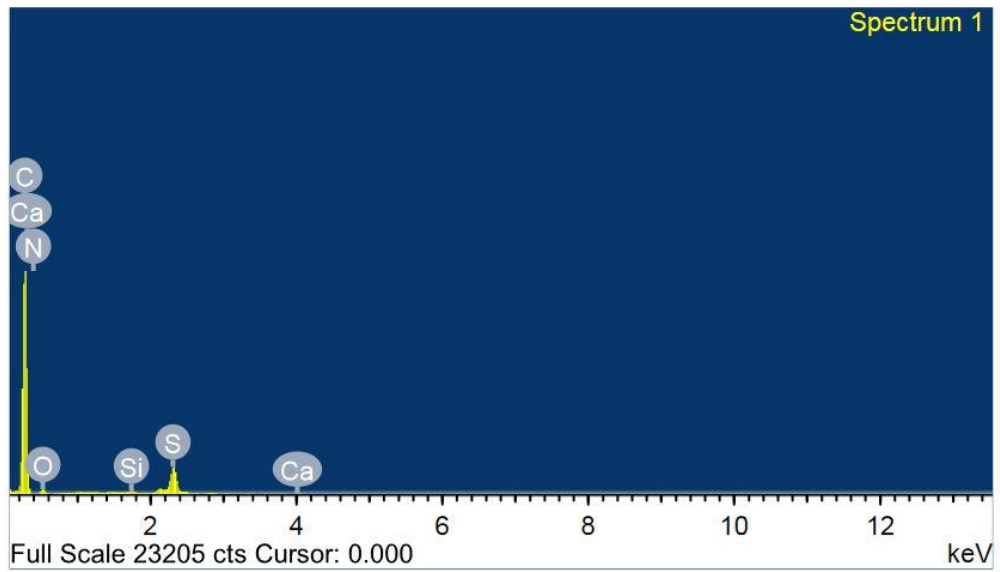


Figure 6.23 EDAX analysis of CRMB-55 elemental mapping for RTFO and PAV aging conditions

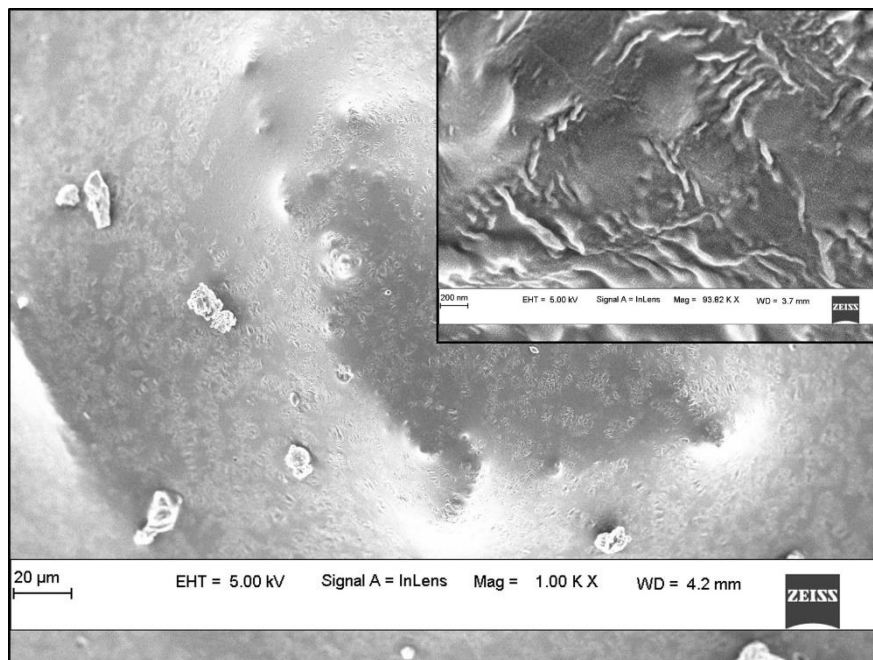


Figure 6.24 FE-SEM images of CRMB-55+S for 163°C RTFO aging followed by PAV conditions

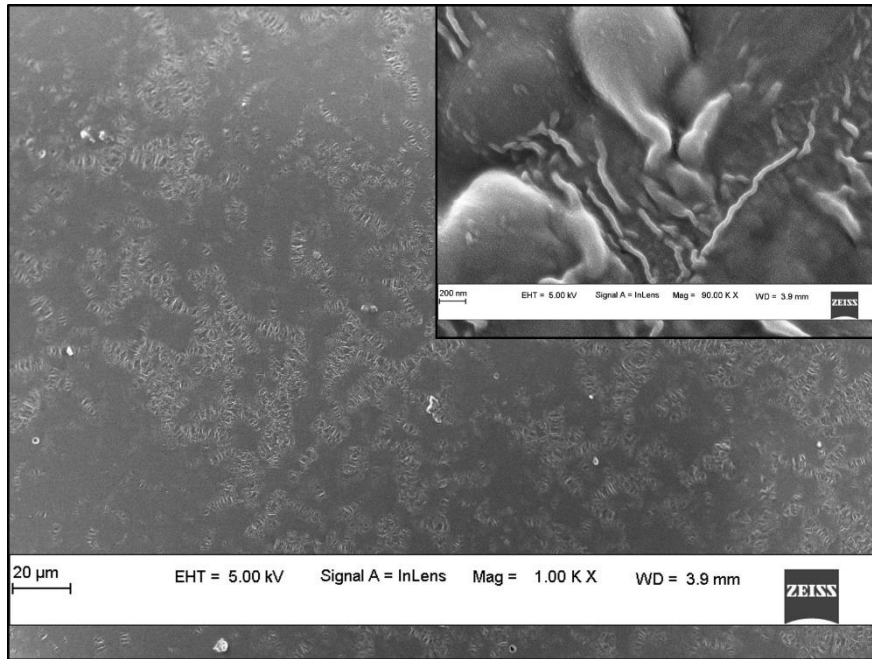


Figure 6.25 FE-SEM images of CRMB-55+R for 163°C RTFO aging followed by PAV conditions

Similarly, as shown in Figure 6.21, asphaltene appears in CRMB-55, which is merely extruded from the asphalt surface when short-term aged at 177°C and PAV aged compared to 163°C short-termed aged. Whereas, in the presence of sasobit additives conditioned at 177°C and PAV aged, there is an appearance of broken fibrils in a cluster form as shown in Figure 6.26 compared to 163°C aging conditions. However, in the presence of rediset additives, as shown in Figure 6.27, the appearance of fibrils is the same as previous short-term aging conditions, i.e., at 163°C temperature.

Under short-term aging conditions at 195°C, as shown in Figure 6.22, CRMB-55 evidenced the presence of an asphaltene-like structure as compared to 177°C, and it also shows the disintegration of rubber particles. Whereas, in the presence of sasobit, thin fibrils are stacked on each other in a maltene fraction, as shown in Figure 6.28. However, rediset additives at 195°C short-term aging conditions indicated interconnected fibrils' appearance with slightly wider size as shown in Figure 6.29 compared to 177°C short-term aging conditions.

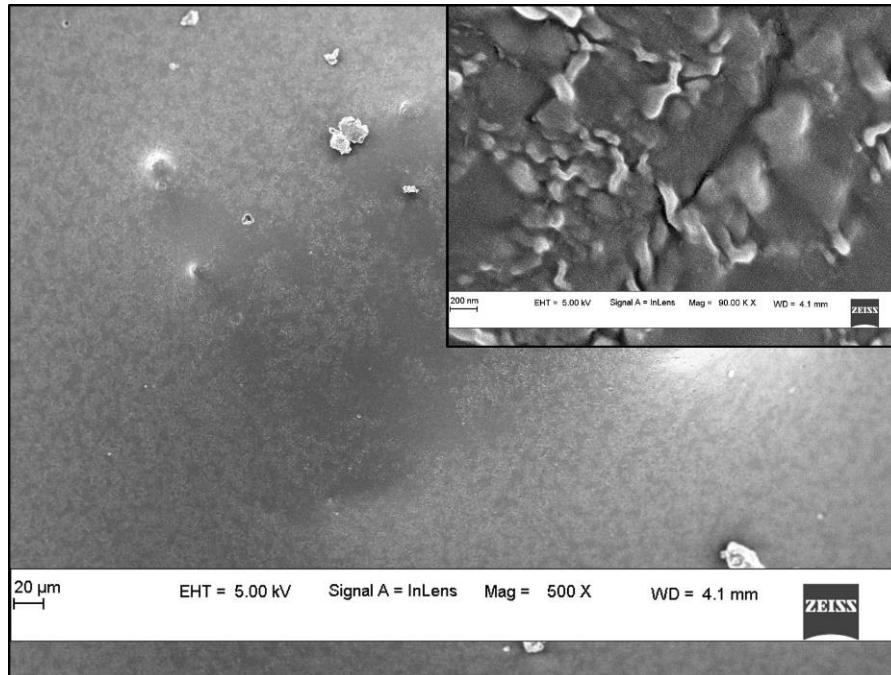


Figure 6.26 FE-SEM images of CRMB-55+S for 177°C RTFO aging followed by PAV conditions

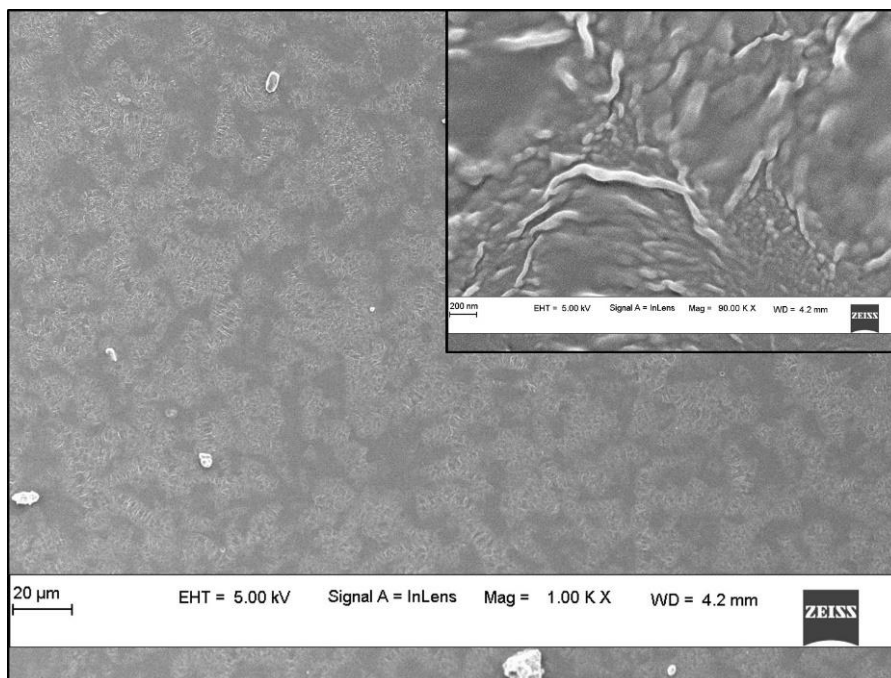


Figure 6.27 FE-SEM images of CRMB-55+R for 177°C RTFO aging followed by PAV conditions

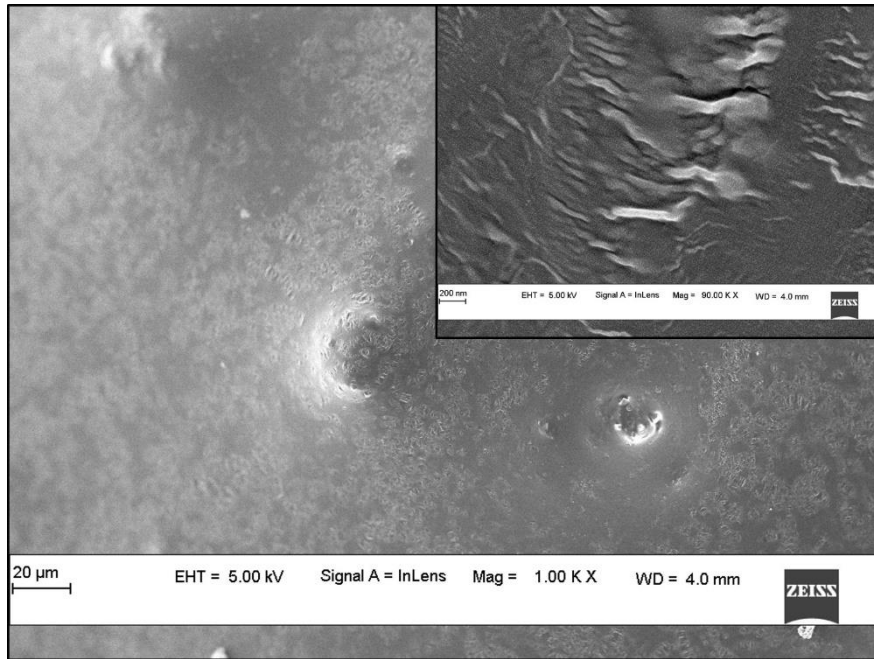


Figure 6.28 FE-SEM images of CRMB-55+S for 195°C RTFO aging followed by PAV conditions

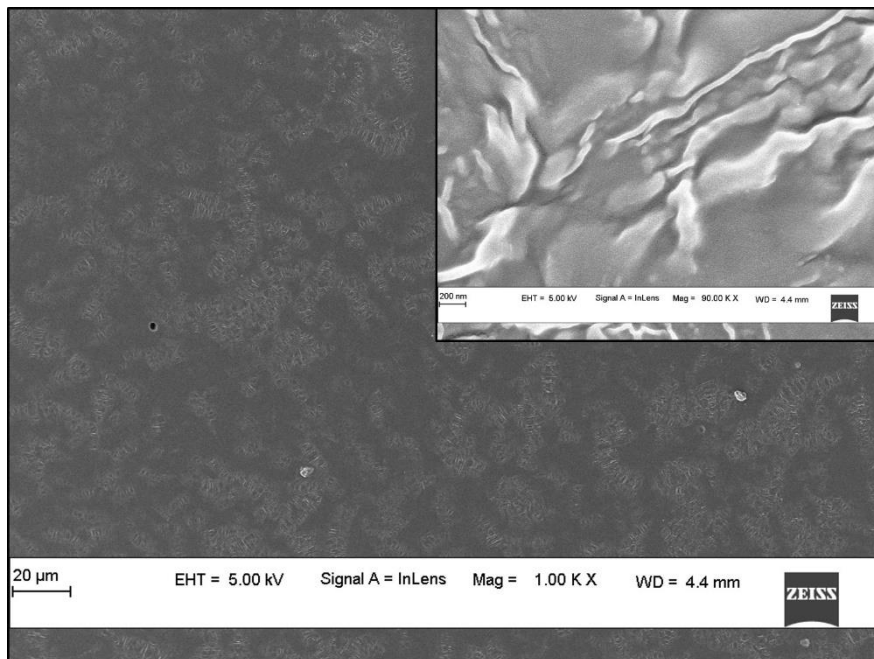


Figure 6.29 FE-SEM images of CRMB-55+R for 195°C RTFO aging followed by PAV conditions

### 6.3.5. Fourier Transform Infrared Spectroscopy (FTIR) test

FTIR spectrometry was primarily conducted to investigate the effect of different working temperature and difference between RTFO and PAV aging conditions on base

and rubber modified asphalt binder. The FTIR spectra of base and CRMB-55, which are subjected to short and long-term aging are shown from Fig 6.30 to Fig 6.33. This indicates that the transmittance of FTIR spectra RTFO and PAV aged decreased compared to RTFO aging condition only. Furthermore, change in working temperature (RTFO) followed by PAV aging condition generates chemical structure between rubber particles and asphalt binder. This is within our expectation that the change in working temperature is carried into PAV aging conditions, which alter the chemical structure of CRMB. Spectral bands at different wavenumbers replicate absorbance of various molecular structures as given below in Table 6.5 (Feng et al. 2016b).

Table 6.5 The characteristics of molecular structures at different wavenumbers

Wavenumber (cm <sup>-1</sup> )	Absorbance of molecular structures
2918	Asymmetric stretching vibration of C-H in methylene (-CH <sub>2</sub> -)
2853	Symmetric stretching vibration of C-H in methylene (-CH <sub>2</sub> -)
1700	Stretching vibration of carbonyl (C=O)
1591	Breathing vibration of asymmetric substituted benzene
1454	Scissoring vibration of methylene (-CH <sub>2</sub> -)
1372	Umbrella vibration of methyl (-CH <sub>3</sub> )
1023	Stretching vibration of sulphoxide (S=O)

Among these functional structures, the evolution of carbonyl (1700 cm<sup>-1</sup>) and sulphoxide (1032cm<sup>-1</sup>) is regularly applied to evaluate the aging extent of CRMB-55 during different working temperature processes. Furthermore the changes in the molecular structure such as (benzene, methylene, and methyl) can also show the chemical modification of CRMB-55. In order to determine the functional structures of the CRMB-55 quantitatively, the branched aliphatic index ( $I_B$ ), aromatic index ( $I_{AR}$ ), carbonyl index ( $I_{C=O}$ ) and sulphoxide index ( $I_{S=O}$ ) are defined as follows.

$$I_B = A_{1372} / (A_{1454} + A_{1372} + A_{723})$$

$$I_{Ar} = A_{1591} / \sum A$$

$$I_{C=O} = A_{1709} / \sum A$$

$$I_{S=O} = A_{1023} / \sum A$$

$$\sum A = A_{1372} + A_{1454} + A_{1372} + A_{1591} + A_{1709} + A_{1023}$$

Where,  $A$  is the area of corresponding spectral band, which can be obtained using the Origin software. The value of  $I_B$  and  $I_{AR}$  can reflect the changes of aliphatic structure and aromatic structure, respectively. The value of  $I_{C=O}$  and  $I_{S=O}$  can reflect the changes of oxygen-containing functioning groups (Feng et al. 2013, 2016).

The FTIR spectroscopy is used mainly to determine the chemical functional groups of VG-30, CRMB-55, and CRMB-55 with Sasobit (4%), and Rediset (4%) additives, which reveals the influence of short-termed aging at 163 °C, 177 °C, and 195 °C on the modified asphalts with WMA additives. FTIR analysis of the VG-30 and CRMB-55 was conducted to justify the optimum working temperature for CRMB-55 with the WMA additives and to observe the oxidation of the base binder such as VG-30 asphalts components. The infrared spectra for VG-30 short-term aged at 163 °C and PAV aged are shown in Figure 6.30. The functional group peak position of the VG-30 at 163 °C of the RTFO aging and 195 °C varied drastically in the region of C–H, S = O, and C = O.

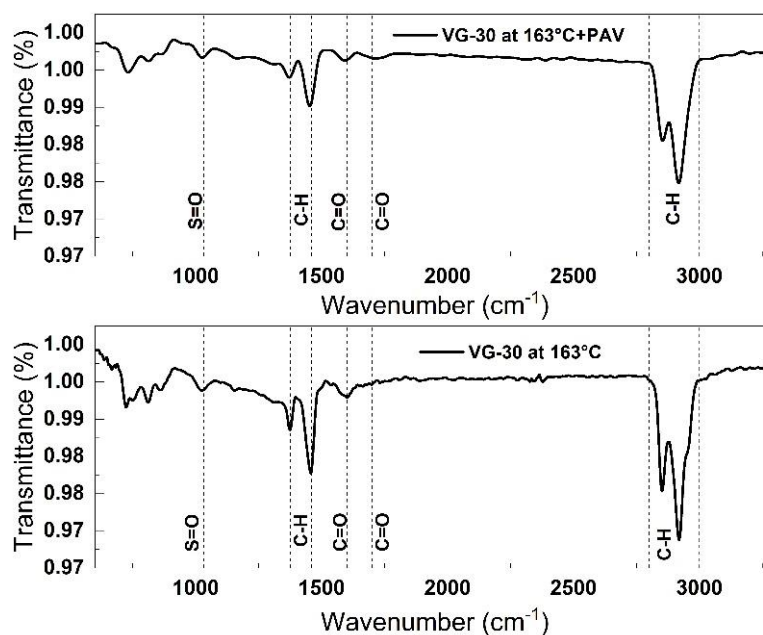


Figure 6.30 Observation of FTIR spectra of VG-30 for RTFO (163°C) and PAV aging conditions

The two different WMA additives modified binder (sasobit and rediset) with CRMB-55 display different FTIR spectra compared to the VG-30 binder, which



indicates that the altering short-term aging temperature generates new chemical structures in asphalt binder due to chemical reaction occurring between the WMA and CRMB-55 binder. This is within our expectation that altering the short-term aging temperature in the presence of WMA additives can enhance the rutting and fatigue properties by structural behaviour. The FTIR spectrum of the VG-30 RTFOT aged at 163 °C is given in Figure 6.30. The solid peak in the region of 2800–2900  $\text{cm}^{-1}$  is recognized as typical C–H stretching vibrations in the asphaltenes structure. The peak at 1600  $\text{cm}^{-1}$  is known as C=O stretching vibrations in the asphaltenes structure of the asphalt molecules. The short-term aging at 195 °C of the VG-30 has two specific peaks, one between 2800 and 2900  $\text{cm}^{-1}$  and the other at 1600  $\text{cm}^{-1}$ , which are higher than the aging at 163 °C and higher sulfoxide function S=O, respectively.

The carbonyl peak's presence indicates a series of oxidation reactions during RTFO aging at 195°C for VG-30 and CRMB-55, which can generate carboxylic acids containing the carbonyl peak. The higher sulfoxide peak indicates the oxidation of sulphur also present during the RTFO aging process at 195 °C, and it may be a significant influence on the base binder used in the manufacturing process of the CRMB-55, as shown in Figure 6.31.

It can be observed that the behaviour of CRMB-55 with sasobit and rediset, which is aged at 177 °C, respectively from Figure 6.32 and Figure 6.33, such that C–H, C=O, and S=O appear lesser than CRMB-55 alone, which is short-termed aged at 195 °C. In the short-term aging process at 195 °C for the VG-30 and CRMB-55 binders, initially, the carbon chain of the VG-30 asphalt will be broken. Then in the presence of oxidation reactions, the carbonyl groups will be formed, and the sulphur converted will convert into sulfoxide in the presence of oxygen and heat. This reduced short-termed aging process from temperature 195°C to 177°C indicates little hydrocarbons, sulfoxide, and carbonyl groups, sufficient to serve the pavement life for an extended period.

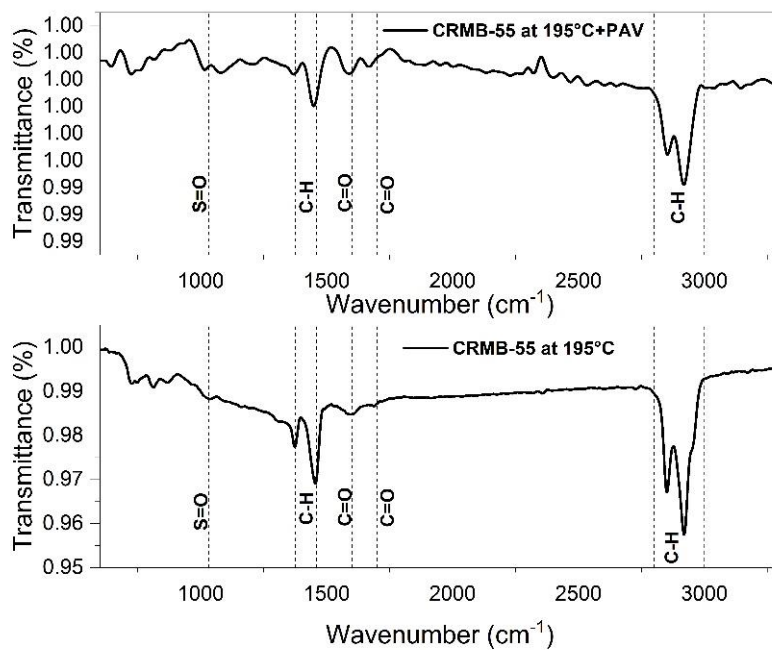


Figure 6.31 Observation of FTIR spectra of CRMB-55 for RTFO (195°C) followed by PAV aging conditions

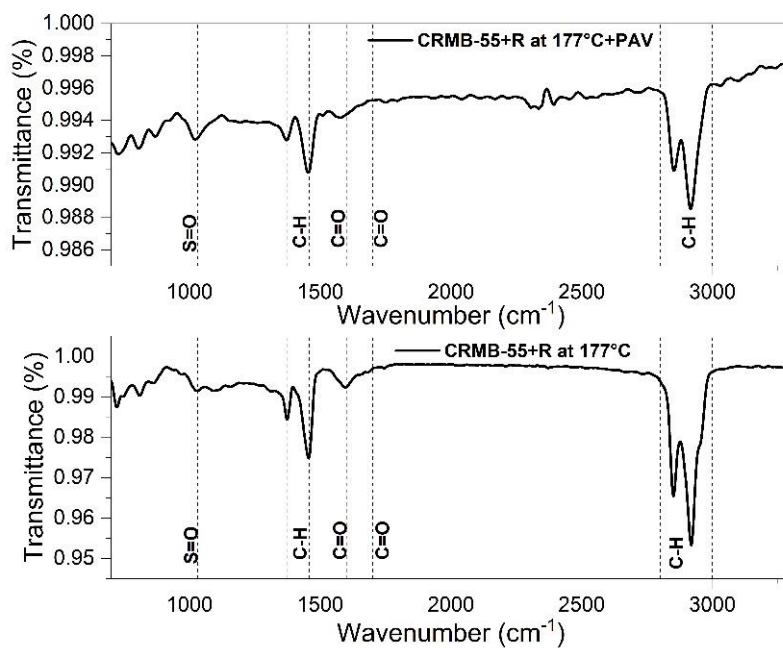


Figure 6.32 Observation of FTIR spectra of CRMB-55+R for RTFO (177°C) followed by PAV aging conditions

From Figure 6.32 and Figure 6.33, the typical spectral bands of the CRMB-55 with two WMA additives, sasobit and rediset, are seen because of the altering the short-term aging temperature (177°C).

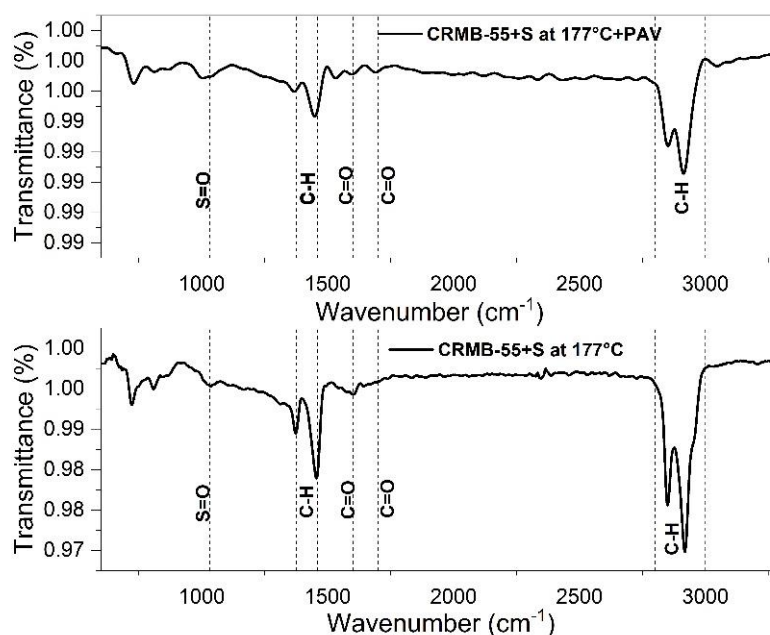


Figure 6.33 Observation of FTIR spectra of CRMB-55+S for RTFO (177°C) followed by PAV aging conditions

However, the FTIR spectra for the CRMB-55 binder in the presence of WMA additives differ in the intensity of each spectral band as can be illustrated by the area or height of the spectral band. Figure 6.30 and Figure 6.31 show the FTIR spectra of RTFO and PAV aged binders. The spectral band at 1700  $\text{cm}^{-1}$  appears for the VG-30 binder after the RTFO aging temperature at 163°C, indicating that the VG-30 binder suffers from oxidation during the short-term and long-term aging process and generates the oxygen-containing products in a binder. Besides, the intensity of other spectral bands also changes to some extent, which will be quantitatively compared via the structural indexes below Table 6.6. Compared with the VG-30 binder, the CRMB-55+S modified binder seem to exhibit no noticeable difference in the curves of FTIR spectra after the RTFO aging at 177°C and PAV aging, as shown in Table 6.6. The FTIR spectra of the CRMB-55+S (sasobit) and CRMB-55+R (rediset) RTFO aged at 177°C and PAV aged binders are displayed in Figure 6.32 and Figure 6.33. After RTFO and PAV aging, the

FTIR spectra of the CRMB-55+S sample display a U-shaped infrared peak at  $1700\text{ cm}^{-1}$  and  $1032\text{ cm}^{-1}$ , indicating that the oxidation is comparatively more minor VG-30 binder. However, the spectral band at  $1700\text{ cm}^{-1}$ , CRMB-55+R, displayed no peak for RTFO aged at  $177^\circ\text{C}$  and PAV aged, but the peak was shown at  $1032\text{ cm}^{-1}$ , which implies the presence of sulphoxide.

The variation of structural indexes (structural index of VG-30 after RTFO aging at  $163^\circ\text{C}$  and PAV aged – structural index of rest of samples at corresponding aging temperature) is calculated to quantitatively evaluate the influence of WMA additives (sasobit, rediset) on structural changes of asphalt binder during aging as shown in Table 6.6. The  $\Delta I_{\text{C=O}}$ , and  $\Delta I_{\text{S=O}}$  values of the CRMB-55 and CRMB-55+S, RTFO aged at  $195^\circ\text{C}$ ,  $177^\circ\text{C}$  respectively and PAV aged are found to be decreased and increased, respectively. Which indicates that the carbonyl decreased and sulphoxide increased during the short-term and long-term aging. Whereas CRMB-55+R RTFO aged at  $177^\circ\text{C}$  and PAV aged were found to be improved. The results also show that  $\Delta I_{\text{B}}$  and  $\Delta I_{\text{AR}}$  for CRMB-55 binder after RTFO aged at  $195^\circ\text{C}$  and PAV aged, which was found to be decreased and increased, respectively. Whereas, in CRMB-55+S binder, both structural bond was been reduced, and for CRMB-55+R binder  $\Delta I_{\text{B}}$  was increased and  $\Delta I_{\text{AR}}$  was decreased, respectively.

However, the aliphatic structures of the CRMB-55 and CRMB-55+S RTFO aged at  $195^\circ\text{C}$  and  $177^\circ\text{C}$ , respectively, and PAV aged are reduced as revealed by decreased  $\Delta I_{\text{B}}$  values, which shows the chemical structure are restrained during the short-term aging and long-term aging. However, the CRMB-55+R binder RTFO aged at  $177^\circ\text{C}$  and PAV aged increased  $\Delta I_{\text{B}}$  value, which indicates the degradation of chemical structure. Similarly, the aromatic structure ( $I_{\text{AR}}$ ) values of the CRMB-55 RTFO aged at  $195^\circ\text{C}$  and PAV are positive compared to CRMB-55+R and CRMB-55+S RTFO aged at  $177^\circ\text{C}$  and PAV aged, which indicates the process of polymer formation of small molecules which are fragmented.

Structural indexes of VG-30, CRMB-55, CRMB-55+S, and CRMB-55+R subjected to RTFO and PAV are shown in Table 6.6. According to (Singh et al. 2017), aliphatic ( $I_{\text{B}}$ ) and aromatic ( $I_{\text{AR}}$ ) indexes are directly related to each other. From the

observation, CRMB-55 with rediset additives RTFO aged at 177°C followed by PAV showed lesser aromatic formation than CRMB itself and the rest of the binders. According to (Petersen 2009), lack of aromaticity, formation decreases the mechanism of naphthenic and perhydroaromatic rings, which leads to lesser stability by reducing the viscosity (Nivitha et al. 2016). However, the carbonyl and sulphoxide index increases along with this behavior, which has a lesser effect on the binder's viscosity (Petersen and Harnsberger 1998). The variation of structural indexes of CRMB-55 with WMA additives concerning VG-30 as shown in Table 6.6 indicates the importance of selecting working temperature, which may affect the base binder in any modified asphalt binder.

The structural indexes of the CRMB-55 and CRMB-55 with WMA additives after short-term and long term aging conditions is shown in Table 6.7. The  $I_b$  values of CRMB-55 short-term aged at 195°C followed by long-term aging were lower than CRMB-55+S, and CRMB-55+R, which were subjected to short-term aging at 177°C and long-term aged. This indicates that change in working temperature has influenced the branched aliphatic structure of CRMB-55 in the presence of WMA additives. With respect to  $I_{Ar}$ , the CRMB-55 binder with WMA additives showed smaller values than the CRMB-55 for similar aging conditions. This implies that the aromatic structure of CRMB-55 binder with WMA additives decreased with change in working temperature, which ascribed reduction in carbon, hydrogen and sulphur content indicating decreased elastic performance of CRMB-55 binder with WMA additives. Similarly, structural indexes of CRMB-55+S for 177°C working temperature followed by PAV aging conditions are lower than VG-30 binder for 163°C RTFO aging followed by PAV aging condition. This indicates that the CRMB-55+S binder exhibits lower elastic performance than VG-30 binder under long term aging conditions.

Table 6.6 Structural indexes of the CRMB-55 with and without WMA additives

Samples	Structural indexes			
	$I_b$	$I_{Ar}$	$I_{C=O}$	$I_{S=O}$
VG-30 at 163°C+PAV	0.152	0.029	0.039	0.033
CRMB-55 at 195°C+PAV	0.116	0.078	0.037	0.035
CRMB-55+S at 177°C+PAV	0.124	0.015	0.017	0.085
CRMB-55+R at 177°C+PAV	0.213	0.006	0.120	0.302

Table 6.7 Variation of structural indexes of the CRMB-55 with and without WMA additives after aging in comparison with VG-30.

Samples	Variation of structural indexes			
	$\Delta I_B$	$\Delta I_{Ar}$	$\Delta I_{C=O}$	$\Delta I_{S=O}$
CRMB-55 at 195°C	-0.036	0.049	-0.002	0.002
CRMB-55+S at 177°C	-0.028	-0.014	-0.022	0.052
CRMB-55+R at 177°C	0.061	-0.023	0.081	0.269

Structural indices of VG-30, CRMB-55, CRMB-55+S, and CRMB-55+R were investigated to determine the impact of working temperature on base binder VG-30, which may also be a part of CRMB binder too. In CRMB, liquid phase represents the base binder and gel/elastic phase indicates rubber particles. In order to analyse these structural indices with respect to working temperature, binders subjected to selected working temperature were tested. The significance of data presented in table 6.8 showed no effect was observed on selected binders.

Table 6.8. One -Way Anova significance test results structural indexes

Parameter	Binder Types	Working Temperature (°C)	One-Way ANOVA	
			<i>F</i> -value	<i>p</i> -value
$\Delta I_B$	CRMB-55	177, 195	0.463	0.620 (N)
$\Delta I_{Ar}$	CRMB-55+S		75	0.073 (N)
$\Delta I_{C=O}$	CRMB-55+R		0.124	0.772 (N)
$\Delta I_{S=O}$			0.711	0.533 (N)

#### 6.4. SUMMARY

1. The LAS showed that fatigue damage rate of CRMB-55 and VG-30 binder remained almost same for all the three working temperature 163°C, 177°C, and 195°C with highest effective shear stress. The *N<sub>f</sub>* for CRMB- 55 was found to be the highest followed by VG-30, CRMB-55+R, and CRMB-55+S. Overall it could be concluded that, as expected, the binder with volatility content and addition of Rediset in CRMB-55 resulted in higher fatigue life.
2. Fatigue performance of VG-30 and CRMB-55+R showed lower fatigue failure temperature, when subjected to 163°C and 177°C, respectively.

3. Thixotropic phenomena test results indicated that viscosity behaviour VG-30 binder were similar to CRMB-55+R subjected to 163°C and 177°C, respectively. The low viscosity describe the presence of volatility in both binders even after PAV aging.
4. Using SEM image, morphological analysis of CRMB-55+R binders indicated presence of more fibrils like structure arranged compactly stacked compared to CRMB-55+S, when subjected 177°C working temperature.
5. The high carbonyl and sulfoxide indices in CRMB-55+R indicates higher stiffness and elastic-like behaviour in presence of Rediset and when subjected 177°C working temperature.





## CHAPTER 7

### CONCLUSIONS AND RECOMMENDATIONS

#### 7.1. CONCLUSIONS

From the present study, the following conclusions are made.

##### 7.1.1. The working temperature of CRMB

The unmodified and modified asphalt binder's working temperature was investigated as per AASHTO T312 and NCHRP-648 recommendations. The effect of WMA additives on viscosity behaviour of CRMB-55 were evaluated by conducting an equiviscous temperature test, higher shear rate flow test, and phase angle method using rotational viscometer and DSR. Results were compared with base binders through the viscosity-temperature curve, extrapolating the high shear rate viscosity and phase angle master curve. The role of suitable working temperature on mass loss of base and modified binders were also investigated. They established the relationship between the mass loss and softening point of binders, subjected to three different short-term aging temperatures. The findings from this study are based on identifying the better method in determining the working temperature of rubberized WMA asphalt binder and correlating the mass loss with the softening point of CRMB. The same findings are summarized below.

- Performing the rotational viscosity test for CRMB-55, equiviscous temperature was found to be higher (195°C) compared with the presence of sasobit and rediset additives (177°C), which is 14°C higher than base binders (163°C).
- Findings of the Steady shear flow method on CRMB-55 showed a much lower working temperature, 169°C compare to the equiviscous method (195°C), which lacks practicality due to extrapolating the viscosity till 180°C.

- In most cases, the phase angle method showed that the master curve at 80°C reference temperature failed to intersect the 86° phase angle line while determining the frequency ( $\omega$ ).
- The working temperature concerning these three methods indicated that equiviscous temperature was highest, followed by the steady shear flow and the phase angle method.
- Mass loss results of CRMB-55 with and without WMA additives, VG-30 found to be increasing with increase in short-term aging temperature except for VG-40 binders. CRMB-55 with rediset additives showed the highest mass loss with all aging temperatures.
- Linear, exponential, and power regression fit indicated a positive correlation between softening point and mass loss with an increase in short-term aging temperature for the binders except for VG-40.

### **7.1.2. Rutting behaviour of CRMB**

The rutting and viscoelastic performance of CRMB-55 with WMA additives sasobit and rediset were evaluated at three different short-term aging temperatures (163°C, 177°C, and 195°C). And compared with based binder performance by conducting Frequency sweep test, Temperature sweep test, time-temperature superposition (TTS), performance grade test, multiple stress creep recovery (MSCR), SEM images analysis, and storage stability test. Based on the detailed, rheological investigation of CRMB-55 with WMA additives in comparison with a base binder in the laboratory, the following conclusive remarks are summarized below:

- $G^*$  value obtained from frequency sweep test at 60°C test temperature for 0.1, 1, 10, and 100 rad/s indicated that CRMB-55 with Sasobit showed more stiffness for all the frequencies when short-term aged 177°C compared to the rest of binders and aging temperatures. This represents better rutting performance is dependent upon the short-term aging temperature.
- From temperature sweep test results,  $G^*$  value of CRMB-55 with sasobit indicated to be higher throughout temperature sweep from 44°C to 88°C for

short-term aged at 177°C, which is equivalent to 195°C short-term aging temperature in particular at 60°C test temperature. This indicates CRMB-55+S performs better rutting performance compared to the rest of binders and aging conditions.

- TTSP data for 30°C reference temperature showed that the addition of sasobit to CRMB enhanced the stiffness by indicating higher  $G^*$  value at the lower reduced frequency when short-term aged at 177°C temperature compared to rediset additives and aged at 163°C and 195°C. This reveals the better rutting performance even at lower traffic flow conditions.
- $G^*/\sin\delta$  value was observed to increase with the increase in working temperature 163°C, 177°C, and 195°C, for CRMB-55 with and without WMA additives, and base binder as well. Such an increase was attributed to the occurrence of a high oxidation process. However, CRMB-55 with sasobit content illustrated higher performance than rediset additives, CRMB-55, and base binders when short-term aged at 177°C.
- $J_{nr}$  value showed decreasing with increased working temperature, indicating better rut resistance irrespective of WMA additives and binders. CRMB-55 with sasobit aged at 177°C represented a better  $J_{nr}$  value compared to rediset additives. However, CRMB-55 with sasobit showed a lesser %R value compare to Rediset additive, indicating a negative impact on rutting performance at 64°C test temperature, which was further demonstrated by the ratio of %R and  $J_{nr}$ .
- The morphological evaluation showed that the CRMB-55 binder with sasobit had a smooth coating around the crumb rubber particles. In contrast, the rediset modified CRMB-55 binders were almost floating in the base binder phase at 177°C working temperature. More importantly, for the VG-30 at 163°C RTFO aging condition at 2 mm magnification, the asphaltenes structured like “bee” could be noticed. However, at 195°C RTFO aging condition, all the bee-like structures had almost disappeared. Therefore,

WMA additives have better compatibility with the base binder and with the CRM modified binder only at optimized RTFO aging conditions, which could help improve the rheological properties.

- Storage stability is detected by measuring the softening point difference between the top and bottom of the aluminum tube stored at different temperatures. CRMB with rediset additives showed a lesser softening point difference ( $<2.5^{\circ}\text{C}$ ), indicating better CRM particles' dispersion at  $177^{\circ}\text{C}$  temperature. Whereas CRMB itself shows an apparent phase separation at all the storing temperatures, indicating poor storage stability.

### **7.1.3. Fatigue performance of CRMB**

Base binder and CRMB with and without WMA additives were subjected to different short-term aging conditions, followed by long-term aging in which fatigue performance was characterized using laboratory performance tests. Laboratory tests consist of performance grading tests at intermediate temperatures, linear amplitude sweep test, thixotropy test, SEM, and FTIR test. Based on the results and discussion presented in this section, the following conclusion can be drawn:

- In general, the CRMB-55 with rediset, short-term aging at  $177^{\circ}\text{C}$  temperature and long term aged indicated lower  $G^* \cdot \sin\delta$  value, which was similar to VG-30, meaning that the short-term aging temperature could result in binders being more resistant to fatigue cracking at intermediate temperatures.
- The effective stress-strain response, material integrity value, and fatigue life ( $N_f$ ) from the LAS test showed that the addition of WMA additives to CRMB-55 varies its strain dependency concerning short-term aging temperature followed by long-term aging. It was found that CRMB with rediset additives showed better fatigue performance when subjected to  $177^{\circ}\text{C}$  short-term aging temperature.
- Thixotropic tendencies of CRMB-55 depend upon a type of WMA additives and applied maximum shear rate because the viscosity of the binders under three

stepped shear rates changes according to a general exponential function concerning short-term aging temperature. In the presence of Rediset additives, the viscosity was low compared to Sasobit content, which indicates a better fatigue performance under intermediate service temperature as it regains its broken-down structure.

- The SEM images show that the asphaltene structure is confirmed to be a “bee-like” structure, which changes with aging conditions. Any changes in its structure will affect the viscosity of the asphalt binder, mainly at intermediate temperatures. In this case, the structure of asphaltene in CRMB-55 with Rediset was in better condition at 177°C short-term aging, followed by PAV, compared to the rest of the binders.
- The influence of the short-term aging process was observed for the CRMB-55 with WMA additives, which indicated a decrease in carbonyl and an increase in sulfoxide index from FTIR results. This shows that how the original microstructure can evolve during the laboratory aging process. This also advises that one cannot have a fixed RTFO aging temperature for different modified binders.

## **7.2. RECOMMENDATIONS AND LIMITATIONS**

This section provides recommendations for selecting the working temperature of modified binders rather than implementing the standard short-term aging temperature to assess the rheological properties of CRMB and base binders during the selection of binders in road constructions. This approach helps in understanding the current field scenarios before the construction of roads. Following recommendations are made based on rheological, morphological, and chemical investigations on CRMB.

While investigating the viscoelastic properties of CRMB, it is essential to note that the results of frequency sweep test, temperature sweep test, TTS, performance grading, MSCR, selection of short-term aging temperature matters. The physical and chemical properties significantly altered under laboratory aging conditions. The selection of binders specially modified binders becomes a big challenging task for road construction. Aging at higher working temperature for modified binders such as CRMB

may degrade the binder phase in it. Overall, the working temperature of each binder has its specific equiviscous temperature to perform against rutting and fatigue distress.

- This dissertation on the working temperature of CRMB in the presence of WMA additives makes a good contribution during the modified asphalt mixture production. Implementation of actual working temperature based on ideal viscosity, i.e., equiviscous temperature, which is 14°C greater than standard short-term aging temperature 163°C, i.e., 177°C that enhanced the rheological, morphological and chemical structural properties in the place of 163°C and 195°C short-term aging temperature.

The presence of WMA additives in CRMB affects rutting and fatigue performance significantly.

- The study showed that adding sasobit to CRMB-55 and RTFO aged at 177°C showed a better rutting performance than rediset additives.
- Moreover, rediset additive to CRMB-55 and RTFO aged at 177°C followed by PAV aging conditions showed better fatigue performance than sasobit.
- Therefore, it is recommended that selecting the combination of WMA additives and working temperature helps in selecting appropriate binders for road constructions.
- However, the selection of working temperature greatly impacts the asphaltene structure and chemical components when examined through SEM images and FTIR analysis as it is directly related to the viscosity behaviour of CRMB-55.
- To evaluate the storage stability of CRMB in the presence of WMA additives, suitable storing temperature, type of WMA additives, and design of the aluminum tube are required.

However, the limitation of the study is that the type of CRM, CRMB production temperature, and type of base binder used in manufacture plant needs to confirmed. In addition, rheological performance needs to be related to swelling phenomenon of rubber particles under the different working temperature conditions in this research. Nevertheless, considering the presence of asphaltene in asphalt binder, the dependency

of asphaltene on CRMB and sources, further research on changes in these parameters is recommended.

### **7.3. SUGGESTIONS FOR FUTURE RESEARCH**

The conclusion and recommendation presented in the previous sections are based on extensive research work under laboratory aging conditions carried out on CRMB-55 with WMA additives. The following suggestions need to be addressed in future studies.

- The present research work can be implemented to different types of modified binders, base binders and evaluate the effect of appropriate working temperature on visco-elastic, rutting, and fatigue properties.
- There is a need to evaluate the impact of selected working temperatures on rubber-modified asphalt mixture in the presence of WMA additives.
- To evaluate the low-temperature properties of CRMB with WMA additives subjected to suitable working temperature followed by PAV aging condition Bending Beam Rheometer (BBR) should be conducted.
- There is a need to evaluate rutting performance through MSCR test for different stress levels and test temperature for selected short-term aging temperature for a given modified binder.
- The rheological, morphological and chemical component behaviour of top and bottom portion of modified aluminium tube can be evaluated for the selected storing temperature.





## References

- Abbas, A. R., Mannan, U. A., and Dessouky, S. (2013). "Effect of recycled asphalt shingles on physical and chemical properties of virgin asphalt binders." *Constr. Build. Mater.*, 45, 162–172.
- Abdelrahman, M. (2006). "Controlling Performance of Crumb Rubber-Modified Binders through Addition of Polymer Modifiers." *Transp. Res. Rec.*, 1962(1), 64–70.
- Abdelrahman, M., and Carpenter, S. (1999). "Mechanism of interaction of asphalt cement with crumb rubber modifier." *Transp. Res. Rec. J. Transp. Res. Board*, (1661), 106–113.
- Aguiar-Moya, J. P., Salazar-Delgado, J., García, A., Baldi-Sevilla, A., Bonilla-Mora, V., and Loría-Salazar, L. G. (2017). "Effect of ageing on micromechanical properties of bitumen by means of atomic force microscopy." *Road Mater. Pavement Des.*, 18, 203–215.
- Airey, G. D. (2002). "Use of Black Diagrams to Identify Inconsistencies in Rheological Data." *Road Mater. Pavement Des.*, 3(4), 403–424.
- Airey, G. D., and Mohammed, M. H. (2008). "Rheological properties of polyacrylates used as synthetic road binders." *Rheol. Acta*, 47(7), 751–763.
- Airey, G. D., Rahman, M. M., and Collop, A. C. (2007). "Absorption of Bitumen into Crumb Rubber Using the Basket Drainage Method." *Int. J. Pavement Eng.*, 4(2), 105–119.
- Airey, G. D., Singleton, T. M., and Collop, A. C. (2002). "Properties of Polymer Modified Bitumen after Rubber-Bitumen Interaction." *J. Mater. Civ. Eng.*, 14(4), 344–354.
- Airey, G., Rahman, M., and Collop, A. C. (2004). "Crumb Rubber and Bitumen Interaction as a Function of Crude Source and Bitumen Viscosity." *Road Mater. Pavement Des.*, 5(4), 453–475.

Akisetty, C. K., Gandhi, T., Lee, S.-J., and Amirkhanian, S. N. (2010). "Analysis of rheological properties of rubberized binders containing warm asphalt additives." *Can. J. Civ. Eng.*, 37(5), 763–771.

Akisetty, C. K., Lee, S.-J., and Amirkhanian, S. N. (2007). "High temperature properties of rubberized binders containing warm asphalt additives." *Constr. Build. Mater.*, 23(1), 565–573.

Akisetty, C. K., Lee, S., Rogers, W., and Amirkhanian, S. N. (2012). "Evaluation of Engineering Properties of Rubberized Laboratory Mixes Containing Warm Mix Additives." *J. Test. Eval. ASTM*, 38(1), 1–8.

Akisetty, C., Xiao, F., Gandhi, T., and Amirkhanian, S. (2011). "Estimating correlations between rheological and engineering properties of rubberized asphalt concrete mixtures containing warm mix asphalt additive." *Constr. Build. Mater.*, 25(2), 950–956.

Ali, A. W., Mehta, Y. A., Nolan, A., Purdy, C., and Bennert, T. (2016). "Investigation of the impacts of aging and RAP percentages on effectiveness of asphalt binder rejuvenators." *Constr. Build. Mater.*, 110, 211–217.

Anderson, D. A., Christensen, D. W., Bahia, H. U., Dongree, R., Sharma, M. G., Antle, C. E., and Button, J. (1994). "Binder Characterization and Evaluation. SHRP A-369." *Washington, DC Transp. Res. Board*.

Anderson, D. A., and Kennedy, T. W. (1993). "Development of SHRP binder specification (with discussion)." *J. Assoc. Asph. Paving Technol.*, 62.

Andriescu, A., and Hesp, S. A. M. M. (2009). "Time-temperature superposition in rheology and ductile failure of asphalt binders." *Int. J. Pavement Eng.*, 10(4), 229–240.

Arega, Z., Bhasin, A., Motamed, A., and Turner, F. (2011). "Influence of Warm-Mix Additives and Reduced Aging on the Rheology of Asphalt Binders with Different Natural Wax Contents." *J. Mater. Civ. Eng.*, 23(October), 1453–1459.

Asphalt Institute. (1994). *Performance graded asphalt binder specification and testing*. Asphalt Institute.

ASTM-D4402. (2015). “Standard test method for viscosity determination of asphalt at elevated temperatures using a rotational viscometer.” *Am. Soc. Test. Mater.*

ASTM D2872-12. (2012). “Standard Test Method for Effect of Heat and Air on a Moving Film of Asphalt (Rolling Thin-Film Oven Test).” *Annu. B. ASTM Stand.*, i(C), 1–6.

Attia, M., and Abdelrahman, M. (2009). “Enhancing the performance of crumb rubber-modified binders through varying the interaction conditions.” *Int. J. Pavement Eng.*, 10(6), 423–434.

Baaj, H., Benedetto, H. Di, and Chaverot, P. (2005). “Effect of binder characteristics on fatigue of asphalt pavement using an intrinsic damage approach.” *Road Mater. Pavement Des.*, 6(2), 147–174.

Bahia, H., Perdomo, D., and Turner, P. (1997). “Applicability of superpave binder testing protocols to modified binders.” *Transp. Res. Rec. J. Transp. Res. Board*, 1586(971313), 16–23.

Bahia, H. U., and Davies, R. (1994). “Effect of crumb rubber modifiers (CRM) on performance related properties of asphalt binders.” *Asph. paving Technol.*, 63, 414.

Bahia, H. U., and Davies, R. (1995). “Factors controlling the effect of crumb rubber on critical properties of asphalt binders (with discussion).” *J. Assoc. Asph. paving Technol.*, 64.

Bahia, H. U., Hanson, D. I., Zeng, M., Zhai, H., Khatri, M. A., and Anderson, R. M. (2001a). *NCHRP Report 459: Characterization of modified asphalt binders in Superpave Mix Design. TRB, Natl. Res. Council. Washington, DC.*

Bahia, H. U., Hanson, D. I., Zeng, M., Zhai, H., Khatri, M. A., Anderson, R. M., and NCHRP-459. (2001c). “Characterization of modified asphalt binders in superpave mix design.” NCHRP Report 459.

Banerjee, A., Fortier, A. De, and Prozzi, J. A. (2012). “The effect of long-term aging on the rheology of warm mix asphalt binders.” *Fuel*, 97, 603–611.

Barnes, H. H. a., and Barnes, A. (1997). “Thixotropy - A review.” *J. non-Newtonian*

*fluid Mech.*, 70(97), 1–33.

Benedetto, H. Di, Nguyen, Q. T., and Sauzéat, C. (2011). “Nonlinearity, heating, fatigue and thixotropy during cyclic loading of asphalt mixtures.” *Road Mater. Pavement Des.*, 12(1), 129–158.

Bernier, A., Zofka, A., and Yut, I. (2012). “Laboratory evaluation of rutting susceptibility of polymer-modified asphalt mixtures containing recycled pavements.” *Constr. Build. Mater.*, 31, 58–66.

Billiter, T. C., Chun, J. S., Davison, R. R., Glover, C. J., and Bullin, J. A. (1997a). “Investigation of the curing variables of asphalt-rubber binder.” *Pet. Sci. Technol.*, 15(5–6), 445–469.

Billiter, T. C., Davison, R. R., Glover, C. J., and Bullin, J. A. (1997b). “Production of Asphalt-Rubber Binders by High-Cure Conditions.” *Transp. Res. Rec.*, (970717), 50–56.

Billiter, T. C., Davison, R. R., Glover, C. J., and Bullin, J. A. (1997c). “Physical properties of asphalt-rubber binder.” *Pet. Sci. Technol.*, 15(3–4), 205–236.

Biro, S., Gandhi, T., and Amirhanian, S. (2009). “Midrange temperature rheological properties of warm asphalt binders.” *J. Mater. Civ. Eng.*, 21(7), 316–323.

Blanchoin, L., and Pollard, T. D. (1999). “Mechanism of Interaction of.” *Biochemistry*, 274(22), 15538–15546.

Bocoum, A., Hosseinezhad, S., and Fini, E. H. (2014). “Investigating effect of amine based additives on asphalt rubber rheological properties.” *Asph. Pavements*, CRC Press, 945–956.

Bouldin, M. G., Dongré, R., and D’ Angelo, J. (2001). “Proposed refinement of Superpave high-temperature specification parameter for performance-graded binders.” *Transp. Res. Rec.*, 1766(1), 40–47.

Branthaver, J. F., Petersen, J. C., Robertson, R. E., Duvall, J. J., Kim, S. S., Harnsberger, P. M., Mill, T., Ensley, E. K., Barbour, F. A., and Scharbron, J. F. (1993). *Binder characterization and evaluation. Volume 2: Chemistry.*

- Canestrari, F., Virgili, A., Graziani, A., and Stimilli, A. (2015). "Modeling and assessment of self-healing and thixotropy properties for modified binders." *Int. J. Fatigue*, 70, 351–360.
- Cao, D., and Ji, J. (2011). "Evaluation of the Long-term Properties of Sasobit Modified Asphalt." 4(6), 384–391.
- Celik, O. N., and Atis, C. D. (2008). "Compactibility of hot bituminous mixtures made with crumb rubber-modified binders." *Constr. Build. Mater.*, 22(6), 1143–1147.
- Chehovits, J. D., Dunning, R. L., and Morris, G. E. (1982). "Characteristics of asphalt-rubber by the sliding plate microviscometer." *Proceedings, Assoc. Asph. Paving Technol.*, 240–261.
- Cheng, C., Liye, Z., and Zhan, R.-J. (2006). "Surface modification of polymer fibre by the new atmospheric pressure cold plasma jet." *Surf. Coatings Technol.*, 200(24), 6659–6665.
- Cheng, G., Shen, B., and Zhang, J. (2011). "A study on the performance and storage stability of crumb rubber-modified asphalts." *Pet. Sci. Technol.*, 29(2), 192–200.
- Ching, W. C. (2007). "Effect of crumb rubber modifiers on high temperature susceptibility of wearing course mixtures." *Constr. Build. Mater.*, 21, 1741–1745.
- Ching, W. C., and Wing-gun, W. (2007). "Effect of crumb rubber modifiers on high temperature susceptibility of wearing course mixtures." 21, 1741–1745.
- Copeland, A., D'Angelo, J., Dongre, R., Belagutti, S., and Sholar, G. (2010). "Field evaluation of high reclaimed asphalt pavement–warm-mix asphalt project in Florida: Case study." *Transp. Res. Rec.*, 2179(1), 93–101.
- Corps, U. (2000). "Hot-Mix Asphalt Paving Handbook." *USA US Army Corps Eng.*
- Cortizo, M. S., Larsen, D. O., Bianchetto, H., and Alessandrini, J. L. (2004). "Effect of the thermal degradation of SBS copolymers during the ageing of modified asphalts." *Polym. Degrad. Stab.*, 86(2), 275–282.
- D'Angelo, J. (2009). "Current status of Superpave binder specification." *Road Mater. Pavement Des.*, 10(sup1), 13–24.

D'Angelo, J., and Dongré, R. (2002). "Superpave binder specifications and their performance relationship to modified binders." *Proc. Can. Tech. Asph. Assoc.*, 91–103.

D'Angelo, J., Harm, E., Bartoszek, J., Baumgardner, G., Corrigan, M., Cowsert, J., Harman, T., Jamshidi, M., Jones, W., Newcomb, D., Prowell, B., Sines, R., and Yeaton, B. (2008). *Warm-mix asphalt : European practice*. (I. American Trade Initiatives, ed.).

D Angelo, J. A. (2009). "The relationship of the mscr test to rutting." *Road Mater. Pavement Des.*, 10(2009), 61–80.

Domingos, M. D. I., and Faxina, A. L. (2015). "Rheological behaviour of bitumens modified with PE and PPA at different MSCR creep-recovery times." *Int. J. Pavement Eng.*, 16(9), 771–783.

Dondi, G., Mazzotta, F., Simone, A., Vignali, V., Sangiorgi, C., and Lantieri, C. (2016). "Evaluation of different short term aging procedures with neat , warm and modified binders." *Constr. Build. Mater.*, 106, 282–289.

Doumenq, P., Guiliano, M., Mille, G., and Kister, J. (1991). "Approche méthodologique directe et continue du processus d'oxydation des bitumes par spectroscopie infrarouge à transformée de Fourier." *Anal. Chim. Acta*, 242, 137–141.

Dubois, E., Mehta, D. Y., and Nolan, A. (2014). "Correlation between multiple stress creep recovery (MSCR) results and polymer modification of binder." *Constr. Build. Mater.*, 65, 184–190.

Edwards, Y., and Isacson, U. (2005). "Wax in bitumen: part 1—classifications and general aspects." *Road Mater. pavement Des.*, 6(3), 281–309.

Edwards, Y., Tasdemir, Y., and Isacson, U. (2006b). "Rheological effects of commercial waxes and polyphosphoric acid in bitumen 160/220 - Low temperature performance." *Fuel*, 85(7–8), 989–997.

Feng, Z.-G., Yu, J.-Y., Zhang, H.-L., Kuang, D.-L., and Xue, L.-H. (2013). "Effect of ultraviolet aging on rheology, chemistry and morphology of ultraviolet absorber modified bitumen." *Mater. Struct.*, 46(7), 1123–1132.

Feng, Z., Bian, H., Li, X., and Yu, J. (2016). "FTIR analysis of UV aging on bitumen

and its fractions.” *Mater. Struct.*, 49(4), 1381–1389.

Ferry, J. D. (1980). *Viscoelastic properties of polymers*. John Wiley & Sons.

Fini, E. H., Kalberer, E. W., Shahbazi, A., Basti, M., You, Z., Ozer, H., and Aurangzeb, Q. (2011). “Chemical Characterization of Biobinder from Swine Manure: Sustainable Modifier for Asphalt Binder.” *J. Mater. Civ. Eng.*, 23(11), 1506–1513.

Foroutan Mirhosseini, A., Kavussi, A., Tahami, S. A., and Dessouky, S. (2018). “Characterizing Temperature Performance of Bio-Modified Binders Containing RAP Binder.” *J. Mater. Civ. Eng.*, 30(8), 04018176.

Gallego, J., Rodríguez-Alloza, A., and Giuliani, F. (2016). “Black curves and creep behaviour of crumb rubber modified binders containing warm mix asphalt additives.” *Mech. Time-Dependent Mater.*, 20(3), 389–403.

Gandhi, T., Akisetty, C., and Amirkhanian, S. (2009). “Laboratory evaluation of warm asphalt binder aging characteristics.” *Int. J. Pavement Eng.*, 10(5), 353–359.

Gao, J., Yan, K., He, W., Yang, S., and You, L. (2018). “High temperature performance of asphalt modified with Sasobit and Deurex.” *Constr. Build. Mater.*, 164, 783–791.

Gawel, I., Stepkowski, R., and Czechowski, F. (2006). “Molecular interactions between rubber and asphalt.” *Ind. Eng. Chem. Res.*, 45(9), 3044–3049.

Ghaly, A. M. (1999). “Properties of asphalt rubberized with waste tires crumb.” *J. Solid Waste Technol. Manag.*, 26(1), 45–50.

Ghavibazoo, A., and Abdelrahman, M. (2013). “Composition analysis of crumb rubber during interaction with asphalt and effect on properties of binder.” *Int. J. Pavement Eng.*, 14(5), 517–530.

Ghavibazoo, A., Abdelrahman, M., and Ragab, M. (2013). “Mechanism of Crumb Rubber Modifier Dissolution into Asphalt Matrix and Its Effect on Final Physical Properties of Crumb Rubber – Modified Binder.” *Transp. Res. Board*, 2370(1), 92–101.

Ghavibazoo, A., Abdelrahman, M., and Ragab, M. (2015). “Evaluation of Oxidization of Crumb Rubber–Modified Asphalt During Short-Term Aging.” *Transp. Res. Rec. J. Transp. Res. Board*, 2505, 84–91.

- Girdler, R. B. (1965). "Constitution of asphaltenes and related studies." *Assoc Asph. Paving Technol Proc.*
- Green, E. L., and Tolonen, W. J. (1977). *The Chemical and Physical Properties of Asphalt Rubber Mixtures. Part I. Basic Material Behavior.*
- Habal, A., and Singh, D. (2016). "Moisture susceptibility of a crumb rubber modified binder containing WMA additives using the surface free energy approach." *Geotech. Spec. Publ.*, 245–253.
- Hamedi, G. H., and Tahami, S. A. (2018). "The effect of using anti-stripping additives on moisture damage of hot mix asphalt." *Int. J. Adhes. Adhes.*, 81, 90–97.
- Heitzman, M. (1992a). "State of the practice-design and construction of asphalt paving materials with crumb rubber." *Fed. Highw. Adm. (FHWA), FHWA-SA-92-022, Washington, DC.*
- Heitzman, M. (1992b). "Design and construction of asphalt paving materials with crumb rubber modifier." *Transp. Res. Rec.*, 1339.
- Heitzman, M. A. (1992c). "State of the Practice: Design and Construction of Asphalt Paving Materials with Crumb Rubber Modifier Methods." *Fhwa a-Sa-92-022.*
- Hemida, A., and Abdelrahman, M. (2020). "Monitoring separation tendency of partial asphalt replacement by crumb rubber modifier and guayule resin." *Constr. Build. Mater.*, 251, 118967.
- Hintz, C., Velasquez, R., Johnson, C., and Bahia, H. (2011). "Modification and validation of linear amplitude sweep test for binder fatigue specification." *Transp. Res. Rec. J. Transp. Res. Board*, (2207), 99–106.
- Hofko, B., Alavi, M. Z., Grothe, H., Jones, D., and Harvey, J. (2017a). "Repeatability and sensitivity of FTIR ATR spectral analysis methods for bituminous binders." *Mater. Struct. Constr.*, 50(3), 1–15.
- Hofko, B., Cannone Falchetto, A., Grenfell, J., Huber, L., Lu, X., Porot, L., Poulidakos, L. D., and You, Z. (2017b). "Effect of short-term ageing temperature on bitumen properties." *Road Mater. Pavement Des.*, 18, 108–117.



- Hofko, B., Porot, L., Falchetto Cannone, A., Poulikakos, L., Huber, L., Lu, X., Mollenhauer, K., and Grothe, H. (2018). "FTIR spectral analysis of bituminous binders: reproducibility and impact of ageing temperature." *Mater. Struct. Constr.*, 51(2).
- Hossain, Z., Zaman, M., O'Rear, E. A., and Chen, D. H. (2012). "Effectiveness of water-bearing and anti-stripping additives in warm mix asphalt technology." *Int. J. Pavement Eng.*, 13(5), 424–432.
- Huang, S.-C. (2008). "Rubber Concentrations on Rheology of Aged Asphalt Binders." *J. Mater. Civ. Eng.*, 20(3), 221–229.
- Huang, S. C. (2006). "Rheological characteristics of crumb rubber-modified asphalts with long-term aging." *Road Mater. Pavement Des.*, 7, 37–56.
- Huang, W., Lin, P., Tang, N., Hu, J., and Xiao, F. (2017). "Effect of crumb rubber degradation on components distribution and rheological properties of Terminal Blend rubberized asphalt binder." *Constr. Build. Mater.*, 151, 897–906.
- Hurley, G. C., and Prowell, B. D. (2006). "Evaluation of Evotherm for use in warm mix asphalt." *NCAT Rep.*, 2, 15–35.
- IS: 73. (2013). "Paving bitumen – specification. New Delhi, India." *Bur. Indian Stand.*, (April), 1–4.
- IS15462. (2004). "Polymer and rubber modified bitumen - Specification (IS 15462 : 2004)." *Intian Stand.*, 1–19.
- IS17079. (2019). "Rubber Modified Bitumen (RMB) - Specification." *Bur. Indian Stand. Stand.*, (May), 1–6.
- Jafari, M., Babazadeh, A., and Aflaki, S. (2015). "Effects of stress levels on creep and recovery behavior of modified asphalt binders with the same continuous performance grades." *Transp. Res. Rec.*, 2505(1), 15–23.
- Jamshidi, A., Golchin, B., Othman, M., and Turner, P. (2015). "Selection of type of warm mix asphalt additive based on the rheological properties of asphalt binders." *J. Clean. Prod.*, 100, 89–106.
- Jamshidi, A., Hamzah, M. O., and Aman, M. Y. (2012). "Effects of Sasobit® content

on the rheological characteristics of unaged and aged asphalt binders at high and intermediate temperatures.” *Mater. Res.*, 15(4), 628–638.

Jia, X., Huang, B., Bowers, B. F., and Zhao, S. (2014). “Infrared spectra and rheological properties of asphalt cement containing waste engine oil residues.” *Constr. Build. Mater.*, 50, 683–691.

Johnson, C., Bahia, H., and Wen, H. (2009). “Practical application of viscoelastic continuum damage theory to asphalt binder fatigue characterization.” *Asph. Paving Technol.*, 28, 597.

Jorgenson, L. (2003). “Tires make the road-asphalt rubber pavement construction.” *Public Work.*, 134(1).

Julaganti, A., Choudhary, R., and Kumar, A. (2017). “Rheology of modified binders under varying doses of WMA additive–Sasobit.” *Pet. Sci. Technol.*, 35(10), 975–982.

Julaganti, A., Choudhary, R., and Kumar, A. (2018). “Permanent Deformation Characteristics of Warm Asphalt Binders under Reduced Aging Conditions.” *KSCE J. Civ. Eng.*, 23, 160–172.

Kataware, A. V., and Singh, D. (2017a). “Evaluating effectiveness of WMA additives for SBS modified binder based on viscosity, Superpave PG, rutting and fatigue performance.” *Constr. Build. Mater.*, 146, 436–444.

Kataware, A. V., and Singh, D. (2017b). “A study on rutting susceptibility of asphalt binders at high stresses using MSCR test.” *Innov. Infrastruct. Solut.*, 2(1), 4.

Kataware, A. V., and Singh, D. (2018). “Effects of Wax-Based, Chemical-Based, and Water-Based Warm-Mix Additives on Mechanical Performance of Asphalt Binders.” *J. Mater. Civ. Eng.*, 30(10), 4018237.

Kataware, A. V., and Singh, D. (2017c). “Dynamic mechanical analysis of crumb rubber modified asphalt binder containing warm mix additives.” *Int. J. Pavement Eng.*, 8436, 0.

Kawahara, F. K., Santner, J. F., and Julian, E. C. (1974). “Characterization of heavy residual fuel oils and asphalts by infrared spectrophotometry using statistical

discriminant function analysis.” *Anal. Chem.*, 46(2), 266–273.

Kedarisetty, S., Prapoorna, K., and Sousa, J. B. (2016). “Advanced rheological characterization of Reacted and Activated Rubber ( RAR ) modified asphalt binders.” *Constr. Build. Mater.*, 122, 12–22.

Kheradmand, B., Muniandy, R., Hua, L. T., and Solouki, A. (2015). “A Laboratory Investigation on the Rheological Properties of Aged and Unaged Organic Wax Modified Asphalt Binders.” *Pet. Sci. Technol.*, 6466.

Kim, H., Lee, S.-J., Amirhanian, S. N., and Park, T.-S. (2011a). “Performance evaluation of recycled PMA binders containing warm mix asphalt additives.” *J. Test. Eval.*, 39(4), 728–734.

Kim, H., Lee, S., and Amirhanian, S. N. (2011b). “Rheology of warm mix asphalt binders with aged binders.” *Constr. Build. Mater.*, 25(1), 183–189.

Kim, S., Loh, S.-W., Zhai, H., and Bahia, H. U. (2001a). “Advanced characterization of crumb rubber-modified asphalts, using protocols developed for complex binders.” *Transp. Res. Rec. J. Transp. Res. Board*, 1767(1), 15–24.

Kim, S., Loh, S., Zhai, H., and Bahia, H. U. (2001b). “Advanced Characterization of Crumb Rubber-Modified Asphalts , Using Protocols Developed for Complex Binders.” *Transp. Res. Rec.*, 1767(01), 15–24.

Kocevski, S., Yagneswaran, S., Xiao, F., Punith, V. S., Smith, D. W., and Amirhanian, S. (2012). “Surface modified ground rubber tire by grafting acrylic acid for paving applications.” *Constr. Build. Mater.*, 34, 83–90.

Kristjánisdóttir, Ó., Muench, S. T., Michael, L., and Burke, G. (2007). “Assessing potential for warm-mix asphalt technology adoption.” *Transp. Res. Rec.*, 2040(1), 91–99.

Kuennen, T. (2005). “Science gives asphalt rubber recycling a thumbs-up.” *Better Roads*, 75(10).

Kumar, A., Choudhary, R., Kandhal, P. S., Julaganti, A., Behera, O. P., Singh, A., and Kumar, R. (2020). “Fatigue characterisation of modified asphalt binders containing

warm mix asphalt additives.” *Road Mater. Pavement Des.*, 21(2), 519–541.

Lakshmi Roja, K., Padmarekha, A., and Krishnan, J. M. (2018). “Rheological investigations on warm mix asphalt binders at high and intermediate temperature ranges.” *J. Mater. Civ. Eng.*, 30(4), 1–13.

Lamontagne, J., Dumas, P., Mouillet, V., and Kister, J. (2001). “Comparison by Fourier transform infrared (FTIR) spectroscopy of different ageing techniques: Application to road bitumens.” *Fuel*, 80(4), 483–488.

Lauger, D. J. (2001). *Rheological characterization of the application behavior of sealants. Ant. Paar.*

Lee, S. J., Akisetty, C. K., and Amir Khanian, S. N. (2008). “The effect of crumb rubber modifier (CRM) on the performance properties of rubberized binders in HMA pavements.” *Constr. Build. Mater.*, 22(7), 1368–1376.

Lee, S. J., Amir Khanian, S. N., Park, N. W., and Kim, K. W. (2009). “Characterization of warm mix asphalt binders containing artificially long-term aged binders.” *Constr. Build. Mater.*, 23(6), 2371–2379.

Lesueur, D., Gérard, J.-F., Claudy, P., Létouffé, J.-M., Planche, J.-P., and Martin, D. (1997). “Relationships between the structure and the mechanical properties of paving grade asphalt cements.” *J. Assoc. Asph. Paving Techn.*, 66, 486–507.

Lesueur, D., Gerard, J., Claudy, P., Letoffe, J., Planche, J., and Martin, D. (1996). “A structure-related model to describe asphalt linear viscoelasticity.” *J. Rheol. (N. Y. N. Y.)*, 40(5), 813–836.

Lexington, K. Y. (1993). “Background of SHRP asphalt binder test methods.” *Asph. Inst. Res. Cent.*

Li, B., Huang, W., Tang, N., Hu, J., Lin, P., Guan, W., Xiao, F., and Shan, Z. (2017). “Evolution of components distribution and its effect on low temperature properties of terminal blend rubberized asphalt binder.” *Constr. Build. Mater.*, 136, 598–608.

Li, P., Jiang, X., Ding, Z., Zhao, J., and Shen, M. (2018). “Analysis of viscosity and composition properties for crumb rubber modified asphalt.” *Constr. Build. Mater.*, 169,

638–647.

Liu, J., Asce, M., Saboundjian, S., Li, P., Asce, S. M., Connor, B., and Brunette, B. (2011). “Laboratory Evaluation of Sasobit-Modified Warm-Mix Asphalt for Alaskan Conditions.” *J. Mater. Civ. Eng. ASCE*, 23(11), 1498–1505.

Liu, S., Cao, W., Fang, J., and Shang, S. (2009). “Variance analysis and performance evaluation of different crumb rubber modified (CRM) asphalt.” *Constr. Build. Mater.*, 23(7), 2701–2708.

Liu, Z., Asce, S. M., Yu, X., and Asce, M. (2013). “Investigation of the Rheological Modification Mechanism of Warm-Mix Additives on Crumb-Rubber-Modified Asphalt.” *J. Mater. Civ. Eng.*, 27(September), 1239–1247.

López-Moro, F. J., Moro, M. C., Hernández-Olivares, F., Witoszek-Schultz, B., and Alonso-Fernández, M. (2013). “Microscopic analysis of the interaction between crumb rubber and bitumen in asphalt mixtures using the dry process.” *Constr. Build. Mater.*, 48, 691–699.

Lougheed, T. J., & Papagiannakis, A. T. (1996). “Viscosity characteristics of rubber-modified asphalts.” *J. Mater. Civ. Eng.*, 8(August), 153–156.

Lougheed, T. J., and Papagiannakis, A. T. (1996). “Viscosity Characteristics of Rubber-Modified Asphalts.” *J. Mater. Civ. Eng.*, 8(3), 153–156.

Lu, X., and Isacsson, U. (2002). “Effect of ageing on bitumen chemistry and rheology.” *Constr. Build. Mater.*, 16(1), 15–22.

Macleod, D., Ho, S., Wirth, R., and Zanzotto, L. (2007). “Study of crumb rubber materials as paving asphalt modifiers.” *Can. J. Civ. Eng.*, 1288, 1276–1288.

Mark, J. E., Erman, B., and Roland, M. (2013). *The science and technology of rubber*. Academic press.

Masad, E. A., Huang, C.-W., D'Angelo, J., and Little, D. N. (2009). “Characterization of asphalt binder resistance to permanent deformation based on nonlinear viscoelastic analysis of multiple stress creep recovery (MSCR) test.” *J. Assoc. Asph. Paving Technol.*, 78.

McGennis, R. B. (1995a). "Evaluation of Physical Properties of Fine Crumb Rubber-Modified Asphalt Binders." *Transp. Res. Rec.*, (1488), 62–71.

McGennis, R. B. (1995b). "Evaluation of physical properties of fine crumb rubber-modified asphalt binders." *Transp. Res. Rec.*, (1488), 62–71.

Mehta, Y., Jahan, K., Laicovsky, J., Miller, L., Parikh, D., and Lozano, A. L. (2004). "Evaluation of the effect of coarse and fine rubber particles on laboratory rutting performance of asphalt concrete mixtures." *J. Solid Waste Technol. Manag.*, 30(2), 112–120.

Meng, G., and Yiqiu, T. (2013). "Effects of various modifiers on rheological property of asphalt." *Multi-Scale Model. Charact. Infrastruct. Mater.*, Springer, 343–356.

Micaelo, R., Pereira, A., Quaresma, L., and Cidade, M. T. (2015). "Fatigue resistance of asphalt binders: Assessment of the analysis methods in strain-controlled tests." *Constr. Build. Mater.*, 98, 703–712.

Mishra, V., and Singh, D. (2019). "Impact of short-term aging temperatures of asphalt binder and aggregate roughness levels on bond strength." *Constr. Build. Mater.*, 218, 295–307.

Mohammadlouay, N., and Gravesphilip, S. (1994). "Louisiana Experience with Crumb Rubber-Modified Hot-Mix Asphalt Pavement Effect of Fine Aggregate Angularity on Compaction and Shearing Resistance of Asphalt Mixtures."

Mouillet, V., la Roche, C. De, Chailleux, E., and Coussot, P. (2012). "Thixotropic Behavior of Paving-Grade Bitumens under Dynamic Shear." *J. Mater. Civ. Eng.*, 24(1), 23–31.

Natu, G. S., and Tayebali, A. A. (2000). "Viscoelastic behavior of crumb rubber modified asphalt binders." *Road Mater. Pavement Des.*, 1(1–2), 119–129.

Navarro, F. J., Partal, P., Martínez-Boza, F., and Gallegos, C. (2005). "Influence of crumb rubber concentration on the rheological behavior of a crumb rubber modified bitumen." *Energy and Fuels*, 19(5), 1984–1990.

Navarro, F. J., Partal, P., Martinez-Boza, F., and Gallegos, C. (2004). "Thermo-

rheological behaviour and storage stability of ground tire rubber-modified bitumens.” *Fuel*, 83(14–15), 2041–2049.

Nivitha, M. R., and Krishnan, J. M. (2018). “Rheological characterisation of unmodified and modified bitumen in the 90 – 200 ° C temperature regime.” *Road Mater. Pavement Des.*, 1(18).

Nivitha, M. R., Krishnan, J. M., and Rajagopal, K. R. (2018). “Viscoelastic transitions exhibited by modified and unmodified bitumen.” *Int. J. Pavement Eng.*, 0(0), 1–15.

Nivitha, M. R., Prasad, E., and Krishnan, J. M. (2016). “Ageing in modified bitumen using FTIR spectroscopy.” *Int. J. Pavement Eng.*, 17(7), 565–577.

Oliveira, J. R. M., Silva, H. M. R. D., Abreu, L. P. F., and Fernandes, S. R. M. (2013). “Use of a warm mix asphalt additive to reduce the production temperatures and to improve the performance of asphalt rubber mixtures.” *J. Clean. Prod.*, 41, 15–22.

Palade, L. I., Attané, P., and Camaro, S. (2000). “Linear viscoelastic behavior of asphalt and asphalt based mastic.” *Rheol. Acta*, 39(2), 180–190.

Palit, S. K., Reddy, K. S., and Pandey, B. B. (2004). “Laboratory Evaluation of Crumb Rubber Modified Asphalt Mixes.” *J. Mater. Civ. Eng.*, 16(1), 45–53.

Pang, L., Liu, K., Wu, S., Lei, M., and Chen, Z. (2014). “Effect of LDHs on the aging resistance of crumb rubber modified asphalt.” *Constr. Build. Mater.*, 67(PART B), 239–243.

Pavlovich, R. D., Shuler, T. S., and Rosner, J. C. (1979). *Chemical & Physical Properties Of Asphalt Rubber Mixtures--Phase II Product Specifications And Test Procedures*.

Pérez-Jiménez, F. E., Botella, R., and Miró, R. (2012). “Differentiating between damage and thixotropy in asphalt binder’s fatigue tests.” *Constr. Build. Mater.*, 31, 212–219.

Pérez-Jiménez, F. E., Botella, R., Miró, R., and Martínez, A. H. (2015). “Analysis of the thixotropic behavior and the deterioration process of bitumen in fatigue tests.” *Constr. Build. Mater.*, 101, 277–286.

Petersen, J. C. (1984). "Chemical Composition of Asphalt as Related to Asphalt Durability : State of the Art." *Transp. Res. Rec.*, (999), 13–30.

Petersen, J. C. (2009). "A review of the fundamentals of asphalt oxidation: chemical, physicochemical, physical property, and durability relationships." *Transp. Res. Circ.*, (E-C140).

Petersen, J. C., and Harnsberger, P. M. (1998). "Asphalt aging: dual oxidation mechanism and its interrelationships with asphalt composition and oxidative age hardening." *Transp. Res. Rec.*, 1638(1), 47–55.

Planche, J. P., Martin, D., LESUEUR, D., and King, G. N. (1996). *Evaluation of elastomer modified bitumens using SHRP binder specifications*.

Putman, B. J., and Amirkhanian, S. N. (2010). "Characterization of the Interaction Effect of Crumb Rubber Modified Binders Using HP-GPC." *J. Mater. Civ. Eng.*, 22(2), 153–159.

Ragab, M., Abdelrahman, M., and Ghavibazoo, A. (2013). "Performance Enhancement of Crumb Rubber – Modified Asphalts Through Control of the Developed Internal Network Structure." *Transp. Res. Rec. J. Transp. Res. Board*, (2371), 96–104.

Ragni, D., Ferrotti, G., Lu, X., and Canestrari, F. (2018). "Effect of temperature and chemical additives on the short-term ageing of polymer modified bitumen for WMA." *Mater. Des.*, 160, 514–526.

Randy C. West, Page, G. C., Veilleux, J. G., and Choubane, B. (2006). "Effect of Tire Rubber Grinding Method on Asphalt-Rubber Binder Characteristics." *Transportation Res. Rec.*, 1638(98), 134–140.

Ren, S., Liu, X., Xu, J., and Lin, P. (2021). "Investigating the role of swelling-degradation degree of crumb rubber on CR / SBS modified porous asphalt binder and mixture." *Constr. Build. Mater.*, 300, 124048.

Roberts, F. L., Kandhal, P. S., Brown, E. R., and Dunning, R. L. (1989). "Investigation and evaluation of ground tire rubber in hot mix asphalt." *NCAT Rep.*, 83–89.

Roberts, F. L., Kandhal, P. S., Brown, E. R., Lee, D.-Y., and Kennedy, T. W. (1991).



*Hot mix asphalt materials, mixture design and construction.*

Rodríguez-Alloza, A. M., Gallego, J., Giuliani, F., Rodríguez-Alloza, A. M., Gallego, J., and Giuliani, F. (2017). “Complex shear modulus and phase angle of crumb rubber modified binders containing organic warm mix asphalt additives.” *Mater. Struct.*, 50(1), 77.

Rodríguez-Alloza, A. M., Gallego, J., and Pérez, I. (2013). “Study of the effect of four warm mix asphalt additives on bitumen modified with 15% crumb rubber.” *Constr. Build. Mater.*, 43, 300–308.

Ross, R. A., Weymann, H. D., and Chuang, M. C. (1973). “Structure of thixotropic suspensions in shear flow: II. Optical properties.” *Phys. Fluids*, 16(6), 784–789.

Ruan, Y., Davison, R. R., and Glover, C. J. (2003). “Oxidation and viscosity hardening of polymer-modified asphalts.” *Energy and Fuels*, 17(4), 991–998.

Rühl, R., Musanke, U., Kolmsee, K., Prieß, R., and Breuer, D. (2007). “Bitumen emissions on workplaces in Germany.” *J. Occup. Environ. Hyg.*, 4(S1), 77–86.

Saboo, N., and Kumar, P. (2016). “Analysis of Different Test Methods for Quantifying Rutting Susceptibility of Asphalt Binders.” *J. Mater. Civ. Eng.*, 28(January), 1–8.

Saboo, N., Kumar, R., Kumar, P., and Gupta, A. (2018). “Ranking the Rheological Response of SBS- and EVA-Modified Bitumen Using MSCR and LAS Tests.” 30(8).

Santagata, E., Baglieri, O., Tsantilis, L., and Dalmazzo, D. (2013). “Evaluation of self healing properties of bituminous binders taking into account steric hardening effects.” *Constr. Build. Mater.*, 41, 60–67.

Shan, L., Tan, Y., Underwood, B. S., Kim, Y. R., `Shan, L., Tan, Y., Underwood, B. S., and Kim, Y. R. (2011). “Thixotropic Characteristics of Asphalt Binder.” *J. Mater. Civ. Eng.*, 23(12), 1681–1686.

Shatanawi, K., Biro, S., Thodesen, C., and Amirkhanian, S. (2009). “Effects of water activation of crumb rubber on the properties of crumb rubber-modified binders.” *Int. J. Pavement Eng.*, 10(4), 289–297.

Shatanawi, K. M., Biro, S., Geiger, A., and Amirkhanian, S. N. (2012). “Effects of

furfural activated crumb rubber on the properties of rubberized asphalt.” *Constr. Build. Mater.*, 28(1), 96–103.

Shatanawi, K. M., Biro, S., Naser, M., and Amir Khanian, S. N. (2013). “Improving the rheological properties of crumb rubber modified binder using hydrogen peroxide.” *Road Mater. Pavement Des.*, 14(3), 723–734.

Shen, J., Amir Khanian, S., Xiao, F., and Tang, B. (2009). “Influence of surface area and size of crumb rubber on high temperature properties of crumb rubber modified binders.” *Constr. Build. Mater.*, 23(1), 304–310.

Shen, Z., Zhao, Z. G., and Wang, G. T. (2012). “Colloid and surface chemistry.” *Chinese Chem. Industry Press. Beijing*, 213–236.

Shenoy, A. (2001). “Refinement of the Superpave specification parameter for performance grading of asphalt.” *J. Transp. Eng.*, 127(5), 357–362.

Shiva Kumar, G., and Suresha, S. N. (2017). “Evaluation of properties of nonfoaming warm mix asphalt mixtures at lower working temperatures.” *J. Mater. Civ. Eng.*, 29(11), 4017229.

Shrum, E. D. (2010). “Evaluation of moisture damage in warm mix asphalt containing recycled asphalt pavement.”

Shuler, T. S., Pavlovich, R. D., Epps, J. A., and Adams, K. C. (1986). *Investigation of materials and structural properties of asphalt rubber paving mixtures*.

Siddiqui, M. N., and Ali, M. F. (1999). “Studies on the aging behavior of the Arabian asphalts.” *Fuel*, 78(January), 1005–1015.

Singh, B., Saboo, N., and Kumar, P. (2017). “Use of Fourier transform infrared spectroscopy to study ageing characteristics of asphalt binders.” *Pet. Sci. Techn.*, 6466(35:16), 1648–1654.

Stangl, K., Jäger, A., and Lackner, R. (2006). “Microstructure-based identification of bitumen performance.” *Road Mater. Pavement Des.*, 7, 111–142.

Stienss, M., Mejlun, L., and Judycki, J. (2018). “Influence of selected WMA additives on viscoelastic behaviour of asphalt mixes and pavements.” *Int. J. Pavement Eng.*,

8436, 0.

Stimilli, A., Hintz, C., Li, Z., Velasquez, R., and Bahia, H. U. (2012). "Effect of Healing on Fatigue Law Parameters of Asphalt Binders." *Transp. iResearch Board*, 1, 96–105.

Stroup-Gardiner, M., Newcomb, D. E., and Tanquist, B. (1993). "Asphalt-rubber interactions." *Transp. Res. Rec.*, 1417, 99.

Stulirova, J., and Pospisil, K. (2008). "Observation of bitumen microstructure changes using scanning electron microscopy." *Road Mater. pavement Des.*, 9(4), 745–754.

Sun, D. Q., and Li, L. H. (2010). "Factors affecting the viscosity of crumb rubber–modified asphalt." *Pet. Sci. Technol.*, 28(15), 1555–1566.

Suresha, S. N., and Kumar, G. S. (2018). "Evaluation of workability and mechanical properties of nonfoaming warm mix asphalt mixtures." *Adv. Civ. Eng. Mater.*, 7(1), 132–157.

Tang, J., Zhu, C., Zhang, H., Xu, G., Xiao, F., and Amirkhanian, S. (2019). "Effect of liquid ASAs on the rheological properties of crumb rubber modified asphalt." *Constr. Build. Mater.*, 194, 238–246.

Tang, N., Huang, W., and Xiao, F. (2016). "Chemical and rheological investigation of high-cured crumb rubber-modified asphalt." *Constr. Build. Mater.*, 123, 847–854.

Tayebali, A. A., Vyas, B. B., &, and Malpass, G. A. (1997). "Effect of crumb rubber particle size and concentration on performance grading of rubber modified asphalt binders." *ASTM Int.*, 30–47.

Teymourpour, P., and Bahia, H. (2014). "Linear amplitude sweep test: Binder grading specification and field validation." *Bind. Expert Task Gr. Meet.*

Thodesen, C., Shatanawi, K., and Amirkhanian, S. (2009). "Effect of crumb rubber characteristics on crumb rubber modified (CRM) binder viscosity." *Constr. Build. Mater.*, 23(1), 295–303.

Traxler, R. N. (1936). "The Physical Chemistry of Asphaltic Bitumen." *Chem. Rev.*, 19(2), 119–143.

- Tur Rasool, R., Wang, S., Zhang, Y., Li, Y., and Zhang, G. (2017). "Improving the aging resistance of SBS modified asphalt with the addition of highly reclaimed rubber." *Constr. Build. Mater.*, 145, 126–134.
- Wang, H., Dang, Z., You, Z., and Cao, D. (2012). "Effect of warm mixture asphalt (WMA) additives on high failure temperature properties for crumb rubber modified (CRM) binders." *Constr. Build. Mater.*, 35, 281–288.
- Wang, H., Liu, X., Apostolidis, P., Erkens, S., and Scarpas, T. (2019). "Numerical investigation of rubber swelling in bitumen." *Constr. Build. Mater.*, 214, 506–515.
- Wang, H., Liu, X., Apostolidis, P., Ven, M. van de, Erkens, S., and Skarpas, A. (2020a). "Effect of laboratory aging on chemistry and rheology of crumb rubber modified bitumen." *Mater. Struct.*, 53(2), 26.
- Wang, H., Liu, X., Erkens, S., and Skarpas, A. (2020b). "Experimental characterization of storage stability of crumb rubber modified bitumen with warm-mix additives." *Constr. Build. Mater.*, 249, 118840.
- Wang, L., Chang, C., and Xing, Y. (2011). "Creep characteristics of crumb rubber modified asphalt binder." *J. Wuhan Univ. Technol. Sci. Ed.*, 26(1), 118–120.
- Wang, S., Cheng, D., and Xiao, F. (2017). "Recent developments in the application of chemical approaches to rubberized asphalt." *Constr. Build. Mater.*, 131, 101–113.
- Wasage, T. L. J., Stastna, J., and Zanzotto, L. (2011). "Rheological analysis of multi-stress creep recovery (MSCR) test." *Int. J. Pavement Eng.*, 12(6), 561–568.
- Wasiuddin, N. M., Selvamohan, S., Zaman, M. M., Louise, M., and Anne, T. (2007). "Comparative Laboratory Study of Sasobit and Aspha-Min Additives in Warm-Mix Asphalt." *Transportation Res. Rec.*, (1998), 82–88.
- Wasiuddin, N., Saltibus, N., and Mohammad, L. (2011). "Effects of a wax-based warm mix additive on cohesive strengths of asphalt binders." *Transp. Dev. Inst. Congr. 2011 Integr. Transp. Dev. a Better Tomorrow*, 528–537.
- West, R. C., Watson, D. E., Turner, P. A., and Casola, J. R. (2010a). *Mixing and compaction temperatures of asphalt binders in hot-mix asphalt*.

- West, R., Page, G., Veilleux, J., and Choubane, B. (1998). "Effect of tire rubber grinding method on asphalt-rubber binder characteristics." *Transp. Res. Rec. J. Transp. Res. Board*, (1638), 134–140.
- West, R., Watson, D. E., and Casola, J. R. (2010b). "NCHRP Report 648: Mixing and Compaction Temperature of Asphalt Binders in Hot-Mix Asphalt." *TRB, Natl. Res. Counc. Washington, DC*, 157.
- Wu, S. peng, Pang, L., Mo, L. tong, Chen, Y. chun, and Zhu, G. jun. (2009). "Influence of aging on the evolution of structure, morphology and rheology of base and SBS modified bitumen." *Constr. Build. Mater.*, 23(2), 1005–1010.
- Xiang, L., Cheng, J., and Que, G. (2009). "Microstructure and performance of crumb rubber modified asphalt." *Constr. Build. Mater.*, 23(12), 3586–3590.
- Xiao, F., and Amirkhanian, S. N. (2010). "Laboratory investigation of utilizing high percentage of RAP in rubberized asphalt mixture." *Mater. Struct.*, 43(1–2), 223–233.
- Xiao, F., Amirkhanian, S. N., Asce, M., and Zhang, R. (2012). "Influence of Short-Term Aging on Rheological Characteristics of Non-Foaming WMA Binders." *J. Mater. Civ. Eng.*, 26(April), 145–152.
- Xiao, F., Yao, S., Wang, J., Wei, J., and Amirkhanian, S. (2018). "Physical and chemical properties of plasma treated crumb rubbers and high temperature characteristics of their rubberised asphalt binders." *Road Mater. Pavement Des.*, 0(0), 1–20.
- Xu, M., Liu, J., Li, W., and Duan, W. (2015). "Novel method to prepare activated crumb rubber used for synthesis of activated crumb rubber modified asphalt." *J. Mater. Civ. Eng.*, 27(5), 4014173.
- Xu, O., Xiao, F., Han, S., Amirkhanian, S. N., and Wang, Z. (2016). "High temperature rheological properties of crumb rubber modified asphalt binders with various modifiers." *Constr. Build. Mater.*, 112, 49–58.
- Yang, X., You, Z., and Mills-Beale, J. (2015). "Asphalt binders blended with a high percentage of biobinders: Aging mechanism using FTIR and rheology." *J. Mater. Civ.*

*Eng.*, 27(4), 4014157.

Yao, H., Dai, Q., You, Z., Ye, M., and Yap, Y. K. (2016a). "Rheological properties, low-temperature cracking resistance, and optical performance of exfoliated graphite nanoplatelets modified asphalt binder." *Constr. Build. Mater.*, 113, 988–996.

Yao, H., You, Z., Li, L., Goh, S. W., and Dedene, C. (2012). "Evaluation of the master curves for complex shear modulus for nano-modified asphalt binders." *CICTP 2012 Multimodal Transp. Syst. - Conv. Safe, Cost-Effective, Effic. - Proc. 12th COTA Int. Conf. Transp. Prof.*, 3399–3414.

Yao, H., Zhou, S., and Wang, S. (2016b). "Structural evolution of recycled tire rubber in asphalt." *J. Appl. Polym. Sci.*, 133(6), 1–7.

Yildirim, Y. (2007). "Polymer modified asphalt binders." 21, 66–72.

Yildirim, Y., Ideker, J., and Hazlett, D. (2006). "Evaluation of Viscosity Values for Mixing and Compaction Temperatures." *J. Mater. Civ. Eng.*, 18(4), 545–553.

You, L., Yan, K., Wang, D., Ge, D., and Song, X. (2019). "Use of amorphous-poly-alpha-olefin as an additive to improve terminal blend rubberized asphalt." *Constr. Build. Mater.*, 228, 116774.

Yu, X., Leng, Z., and Wei, T. (2014). "Investigation of the Rheological Modification Mechanism of Warm-Mix Additives on Crumb-Rubber-Modified Asphalt." *J. Mater. Civ. Eng.*, 26(2), 312–319.

Yue, M., Yue, J., Wang, R., and Xiong, Y. (2021). "Evaluating the fatigue characteristics and healing potential of asphalt binder modified with Sasobit® and polymers using linear amplitude sweep test." *Constr. Build. Mater.*, 289, 123054.

Zanzotto, L., and Kennepohl, G. (1996a). "Development of rubber and asphalt binders by depolymerization and devulcanization of scrap tires in asphalt." *Transp. Res. Rec. J. Transp. Res. Board*, (1530), 51–58.

Zanzotto, L., and Kennepohl, G. J. (1996b). "Development of rubber and asphalt binders by depolymerization and devulcanization of scrap tires in asphalt." *Transp. Res. Rec.*, 1530(1), 51–58.

Zapata, P., and Gambatese, J. A. (2005). "Energy consumption of asphalt and reinforced concrete pavement materials and construction." *J. Infrastruct. Syst.*, 11(1), 9–20.

Zhang, L., Xing, C., Gao, F., Li, T. shuai, and Tan, Y. qiu. (2016). "Using DSR and MSCR tests to characterize high temperature performance of different rubber modified asphalt." *Constr. Build. Mater.*, 127, 466–474.

Zheng, W., Wang, H., Chen, Y., Ji, J., You, Z., and Zhang, Y. (2021). "A review on compatibility between crumb rubber and asphalt binder." *Constr. Build. Mater.*, 297, 123820.





## BIO-DATA

NAME	HEMANTH KUMAR V	
ADDRESS	HLC 3/B, hutha colony, Newtown, Bhadravathi-577301, Shimoga, Karnataka, India.	
MOBILE NO.	8904958991	
E-MAIL	hemanth.visl@gmail.com	
QUALIFICATION	(Ph.D. in Civil Engineering) Registered : July-2016	National Institute of Technology Karnataka (NITK), Surathkal, Mangalore.
	M.Tech. in Civil Engineering (2012) (Specialization : Highway Technology) DSCE	Dayananda Sagar College of Engineering
	B.E. in Civil Engineering (2010) Visvesvaraya Technological University (VTU).	Rashtreeya Vidyalaya College of Engineering, Bangalore. Karnataka
	2 <sup>nd</sup> P.U.C. (2006), Department of Pre-University Education	Paper Town Independent PU College, Bhadravathi, Shimoga
	S.S.L.C. (2004), Karnataka Secondary Education Examination Board.	St. Charles High School, Bhadravathi, Shimoga.

### LIST OF PUBLICATIONS

Publications based on Ph.D. Research Work

#### Indian Patent

- a) **Hemanth Kumar V**, Suresha Subbarao Nagabhushanarao, “Separation Tube for Investigating Storage Stability of Modified Asphalt Binder.” *Indian patent filed-Application Number: 202241010501*, dated 25-02-2022

#### Articles in SCI journals

- a. Hemanth Kumar, V., & Suresha, S. N. (2019). Investigation of Aging Effect on Asphalt Binders Using Thin Film and Rolling Thin Film Oven Test. *Advances in Civil Engineering Materials*, 8(1), 637–654. <https://doi.org/10.1520/ACEM20190119>
- b. Kumar Veeraiah, H., & Subbarao Nagabhushanarao, S. (2020). Effect of optimized short-term aging temperature on rheological properties of rubberized binders containing warm mix additives. *Construction and Building Materials*, 261, 120019. <https://doi.org/10.1016/j.conbuildmat.2020.120019>

Proceedings

- a) Suresha, S. N., and Kumar, V. H. (2021). "Characterization of asphalt binder using tackiness properties." *Green Intell. Technol. Sustain. Smart Asph. Pavements Proc. 5th Int. Symp. Front. Road Airt. Eng. 12-14 July, 2021, Delft, Netherlands, CRC Press, 62.*

Conferences/Seminars: International

- a. Hemanth Kumar, V., & Suresha, S. N. (2020). Effect of short-term aging temperature on rheological and morphological properties of rubber modified binder. In 7th Conference on Transportation Systems Engineering and Management (p. 80, CTSEM). College of Engineering, Trivandrum.
- b. Suresha, S. N., & Kumar, V. H. (2021b). Effect of WMA additives on thixotropic behaviour of crumb rubber modified asphalt binder. In Transportation Systems engineering and management (p. CTSEM 2021). NIT Calicut.